Perception and responses to strigolactones in arbuscular mycorrhizal fungi

Quentin Taulera

Université Fédérale
Toulouse Midi-Pyrénées

THÈSE

En vue de l'obtention du
DOCTORAT DE L'UNIVERSITÉ DE TOULOUSE
Délivré par l'Université Toulouse 3 - Paul Sabatier

Présentée et soutenue par

Quentin TAULERA

Le 11 mai 2022

Perception et réponses aux strigolactones chez les champignons mycorhiziens à arbuscules

Ecole doctorale : **SEVAB - Sciences Ecologiques, Vétérinaires, Agronomiques et Bioingenieries**

Spécialité : **Developpement des plantes, interactions biotiques et abiotiques**

Unité de recherche :
LRSV - Laboratoire de Recherche en Sciences Végétales

Thèse dirigée par
Soizic ROCHANGE

Jury

Mme Sandrine BONHOMME, Rapporteure
M. Pierre-Emmanuel COURTY, Rapporteur
M. Guillaume BECARD, Examinateur
Mme Soizic ROCHANGE, Directrice de thèse

Résumé

La symbiose mycorhizienne à arbuscules (MA) est une association symbiotique entre les racines de la majorité des espèces végétales terrestres et des champignons du sol du sous-phylum Glomeromycotina. Tandis que le champignon fournit à la plante de l'eau et des minéraux, la plante lui apporte du carbone sous forme de lipides et de glucides. L'initiation de la symbiose MA implique des molécules diffusibles sécrétées par les deux partenaires. Les strigolactones (SLs) sont des dérivés de caroténoïdes produits par les plantes et exsudés dans le sol. Elles sont nécessaires lors de l'initiation de la symbiose et déclenchent chez les champignons MA des réponses cellulaires, métaboliques et développementales telles que la ramification des hyphes. En plus de leur bioactivité sur les champignons MA, les SLs induisent la germination des graines de plantes parasites et jouent un rôle hormonal dans le développement des plantes.

Les diverses SLs naturelles identifiées à ce jour sont composées d'un cycle méthylbuténolide (D) invariable, lié à une partie lactone tricyclique (ABC) variable. Les mécanismes de perception des SLs sont bien documentés chez les plantes : ils impliquent des récepteurs de la famille des alpha/bêta-hydrolases, qui ont la particularité de cliver les SLs et de former une liaison covalente avec le cycle D. L'objectif principal de ma thèse était de mieux comprendre la perception des SLs chez les champignons MA.

Dans une première partie de mon travail, j'ai utilisé des analogues de SLs portant un cycle D modifié. J'ai évalué leurs impacts sur le développement du champignon MA *Rhizophagus irregularis* cultivé *in vitro*, ainsi que leurs capacités à favoriser l'initiation de la symbiose. Un résultat marquant a été qu'un analogue de SL avec un cycle D non méthylé pouvait inhiber la ramification des hyphes tout en augmentant la capacité de *R. irregularis* à coloniser les racines d'une plante hôte. Cette observation a montré pour la première fois que l'initiation de la symbiose MA peut être découplée de la ramification du champignon.

Dans la deuxième partie de mon projet, j'ai cherché à aborder la nature des récepteurs des SLs chez les champignons MA. J'ai observé que deux inhibiteurs connus pour cibler les récepteurs des SLs chez les plantes suppriment également les réponses de *R. irregularis* aux SLs. Cela suggère que les récepteurs fongiques partagent des caractéristiques structurals avec ceux des plantes. Par une approche de modélisation, nous avons identifié huit protéines fongiques de la famille des alpha/bêta-hydrolases présentant une structure tridimensionnelle proche de celle d'un récepteur végétal de SLs. L'analyse phylogénétique a révélé une expansion des gènes codant pour ces protéines et des protéines apparentées chez les Glomeromycotina. La caractérisation *in vitro* de ces protéines a révélé que deux d'entre elles étaient capables de cliver des analogues synthétiques de SL, et que les deux inhibiteurs des récepteurs des SLs de plantes interféraient avec leur activité enzymatique. Collectivement, ces observations soutiennent l'hypothèse selon laquelle les champignons MA ont évolué la capacité de percevoir les SLs par expansion et néo-fonctionnalisation d'alpha/bêta-hydrolases, de façon comparable aux plantes parasites et aux mousses.

Un dernier objectif était d'étudier le transfert de phytohormones d'une plante à une autre via des réseaux mycorhiziens communs. Des protocoles expérimentaux ont été conçus et mis en œuvre, mais les analyses biochimiques n'ont pas permis de fournir des preuves concluantes d'un tel transfert. Néanmoins, il reste important de garder à l'esprit la contribution de ces réseaux aux interactions plante-champignon et plante-plante dans les environnements naturels. L'ensemble de mon projet de thèse met également en évidence le fait que des signaux moléculaires tels que les SL peuvent être perçus, modifiés ou transportés par un certain nombre d'organismes vivants, et peuvent donc jouer des rôles complexes dans les écosystèmes au-delà de leur classification en tant que phytohormones.

M**ots clés** : Mycorhize à arbuscules; Strigolactone; Symbiose; Récepteur; *Rhizophagus*

Mes remerciements sauront être brefs, pour les simples et bonnes raisons que les personnes qui devraient apparaître sur cette page sont déjà au courant de ma reconnaissance pour leur implication lors de ces trois années de thèse.

Cependant, je me dois de remercier chaleureusement Soizic ici. Sans m'étendre sur les raisons qui exposeraient pourquoi j'ai adoré travailler avec toi, ces trois années ont été extrêmement riches et nos discussions m'accompagneront pendant longtemps ! Ta rigueur et ton éthique scientifique, ton combat autour des enjeux climatiques, tes réflexions sur notre société ont été plus que revivifiants.

Dans un deuxième temps, je tiens à remercier Sandrine Bonhomme, Pierre-Emmanuel Courty et Guillaume Bécard. Merci à vous trois pour votre participation à mon jury de thèse et aux discussions qui ont suivi. Je remercie également François-Didier Boyer et Benoît Lefebvre d'avoir pris le temps de m'aiguiller et de me suivre à l'occasion de mes comités de thèse.

Merci aux différentes personnes avec lesquelles j'ai eu l'occasion de travailler :

- L'équipe de Versailles, particulièrement Alexandre De Saint Germain et François-Didier Boyer pour m'avoir accueilli au sein de votre laboratoire, pour nos discussions et la découverte de l'enzymologie. Merci au reste de l'équipe de m'avoir intégré dans votre quotidien les quelques semaines passées avec vous.
- Even though we have not met, I would like to thank our collaborators in New Zealand: Kim Snowden, Bart Janssen and Cyril Hamiaux
- Virginie Durand, Virginie Puech-Pages et Sylvie Fournier de la plateforme Metatoul.
- Aurélie et toute l'équipe microscopie ! Toujours un plaisir !
- Les différentes personnes du service commun qui font tourner le laboratoire, MERCI !
- Toutes les personnes avec qui j'ai travaillé ou que j'ai pu côtoyer au laboratoire.

Et pour finir, merci à toutes les personnes sur lesquelles j'ai pu compter et m'appuyer lorsque c'était nécessaire.

Table of contents

List of illustrations

List of abbreviations

At	*Arabidopsis thaliana*	**Ri**	*Rhizophagus irregularis*
Ph	*Petunia hybrida*	**O.**	*Orobanche*
Gi.	*Gigaspora*	**S.**	*Striga*
Pp	*Physcomitrium patens*	**Os**	*Oryza sativa*
Lj	*Lotus japonicus*	**Pa**	*Phelipanche aegyptiaca*
Ps	*Pisium sativum*	**Sl**	*Solanum lycopersicum*
Mp	*Marchantia paleacea*		

ABA	Abscisic acid	**LBO**	LATERAL BRANCHING OXIDOREDUCTASE
ABH	Alpha/beta-hydrolase	**LYK3**	LysM-RLK-3
AM	Arbuscular mycorrhizal	**MAX1**	MORE AXILLARY GROWTH 1
AMF	Arbuscular mycorrhizal fungi	**MEC**	Minimum effective concentration
AMT2	AMMONIUM TRANSPORTER 2	**MeCLA**	Methyl carlactonoate
AUX	Auxin	**NIN**	NODULE INCEPTION
BF	Branching factor	**NSP**	NODULATION SIGNALING PATHWAY
BR	Brassinosteroids	**PAM**	Peri-arbuscular membrane
BRC1	BRANCHED 1	**PDR1**	PLEIOTROPIC DRUG RESISTANCE 1
BSB	Bryosymbiol	**Pi**	Phosphate
CCD	Carotenoid cleavage dioxygenase	**PPA**	Pre-penetration apparatus
CL	Carlactone	**PT1**	PHOSPHATE TRANSPORTER 1
CLA	Carlactonoic acid	**RAM**	REDUCED ARBUSCULAR MYCORRHIZA
CLIM	Covalently-linked intermediate molecule	**SA**	Salicylic acid
CMN	Common mycorrhizal network	**SABP2**	SA BINDING PROTEIN 2
CO	Chitin oligomers	**SAR**	Structure-activity relationship
CSSP	Common symbiotic signaling pathway	**SCF**	Skp–Cullin–F-box containing complex
DSF	Differential scanning fluorimetry	**SL**	Strigolactone
ET	Ethylene	**SMS**	Shoot multiplication signal
FW	Fresh weight	**SPL**	SQUAMOSA PROMOTER BINDING PROTEIN
GA	Gibberellins	**SUT**	SUCROSE TRANSPORTER
HTL	HYPOSENSITIVE TO LIGHT	**TCP1**	CP DOMAIN PROTEIN 1
HPC	Hypodermal passage cells	TFA	Tolfenamic acid
JA	Jasmonic acid	**Tm**	Melting temperature
KAI	KARRIKIN-INSENSITIVE	**TPL**	TOPLESS
KAR	Karrikin	**TPR**	TOPLESS-RELATED
KL	KAI2-ligand	**YLG**	Yoshimulactone Green
LCO	Lipochitooligosaccharide	**4DO**	4-deoxyorobanchol
LLD	LOTUSLACTONE-DEFECTIVE	**5DS**	5-deoxy-strigol

General Introduction

The following introduction is divided into three parts. The first part is focused on the description of mycorrhizal fungi and on the process of arbuscular mycorrhizal symbiosis. The second part is devoted to strigolactones, a class of molecules that regulate the arbuscular mycorrhizal symbiosis. Finally, the third part will give an overview of the current state of knowledge regarding the mechanisms of strigolactone perception.

I) The arbuscular mycorrhizal symbiosis

I-1) General information about arbuscular mycorrhizal fungi

I-1-A) Classification and origin of the arbuscular mycorrhizal symbiosis

The arbuscular mycorrhizal (AM) symbiosis between most terrestrial plant species and fungi from the Glomeromycotina subphylum of the phylum Mucuromycota is one of the most widespread beneficial associations (Brundrett et al., 2018). AM fungi (AMF) exhibit low host specificity (Klironomos et al., 2000). They provide water and minerals such as phosphate, nitrate and ammonium ions (Smith & Read, 2008), in exchange for carbon in the form of lipids and carbohydrates from the plant (Luginbuehl et al., 2017). Several lines of evidence indicate that AM symbiosis is a very ancient interaction, present since the colonization of the terrestrial environment by plants. The first indication is that some fossils of early land plants dating from about 450 million years ago contain in their cells fungal structures sharing morphological similarities to the current AMF (Redecker et al., 2000; Remy et al., 1994; van der Heijden et al., 2015). The second line of evidence is the identification of genes required for AM symbiosis in the algae closest to terrestrial plants. The function of the associated proteins is also conserved, suggesting that the most recent ancestor of land plants was pre-adapted for AM symbiosis (Delaux et al., 2015). Finally, a large diversity of early diverging land plants are able to interact with AMF (liverworts, hornworts and lycophytes) (Brundrett et al., 2018).

Based on these observations, it has been speculated that AMF have helped plants to adapt to the terrestrial environment, which was challenging with regards to the restricted availability

of water and nutrients (Bonfante & Genre, 2010; Humphreys et al., 2010; Malloch et al., 1980; Raven, 2018). Recently, Rich et al. (2021) reported that like angiosperms, the bryophyte *Marchantia paleacea* is able to biosynthesize lipids and transfer them to AMF during symbiosis. The lipid transfer is regulated by orthologous genetic pathways in bryophytes and in angiosperms, and this pathway is not present in algae. This shows that mutualism with AMF was present in the most recent ancestor of bryophytes and angiosperms, but not in algae. Thus, the authors conclude that arbuscular mycorrhizal symbiosis is a trait that evolved in the first land plants, and facilitated plant terrestrialization.

I-1-B) Arbuscular mycorrhizal fungi are obligate biotrophs

It is generally considered that arbuscular mycorrhizal fungi cannot complete their life cycle without interacting with a host plant. This obligate biotrophy could be due to the dependency of AMF on some essential nutrients, like vitamins and carbon provided by the host plant. In particular, AMF do not possess genes encoding a fatty acid synthase (Kamel et al., 2017; Wewer et al., 2014), which could prevent them from synthesizing some of their lipids. As a result AMF fully rely on carbon supply by their host plants to complete their life cycle. This characteristic makes their study difficult, because the fungus cannot be analyzed independently of its host plant.

I-1-C) Laboratory production of arbuscular mycorrhizal fungi

In order to study AMF, it is necessary to produce sufficient amounts of biological material. Two culture systems have been implemented over the years to produce fungal material and in particular spores. The first method consists of inoculating host plants with AMF to establish symbiosis. After several weeks, the fungus forms new spores which are collected from the substrate. Yet the obtained spores are not exempt of root fragments and other microorganisms. The second method has been developed in axenic conditions. For this purpose, carrot roots were genetically transformed with *Agrobacterium rhizogenes* to allow them to grow indefinitely in the absence of aerial parts. These so-called hairy roots are grown *in vitro* and inoculated with AMF (Bécard & Piché, 1989; St-Arnaud et al., 1996). The inoculated roots are grown in a two-compartment system that allows the fungus only to develop in the second compartment. In these conditions, the fungus produces spores free of any contamination. Recently, major advances have been achieved in the axenic culture of AMF. When fatty acids (palmitoleate or myristate) and a source of organic nitrogen were added to

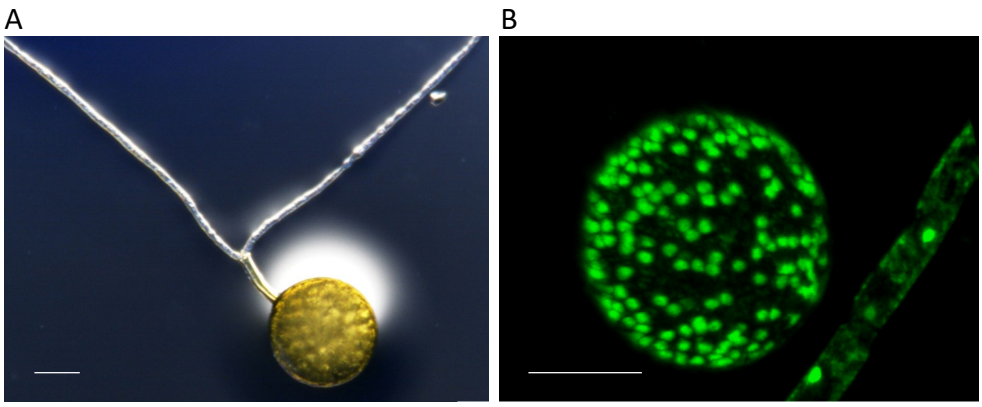

Figure 1. Spores of *Rhizophagus irregularis*

(A) Germinating spore observed under a dissecting microscope. (B) Germinating spore observed in fluorescence microscopy. Nuclei were stained with SytoGreen fluorescent dye. Scale bars = 35 µm. Credit: Aurélie Le Ru.

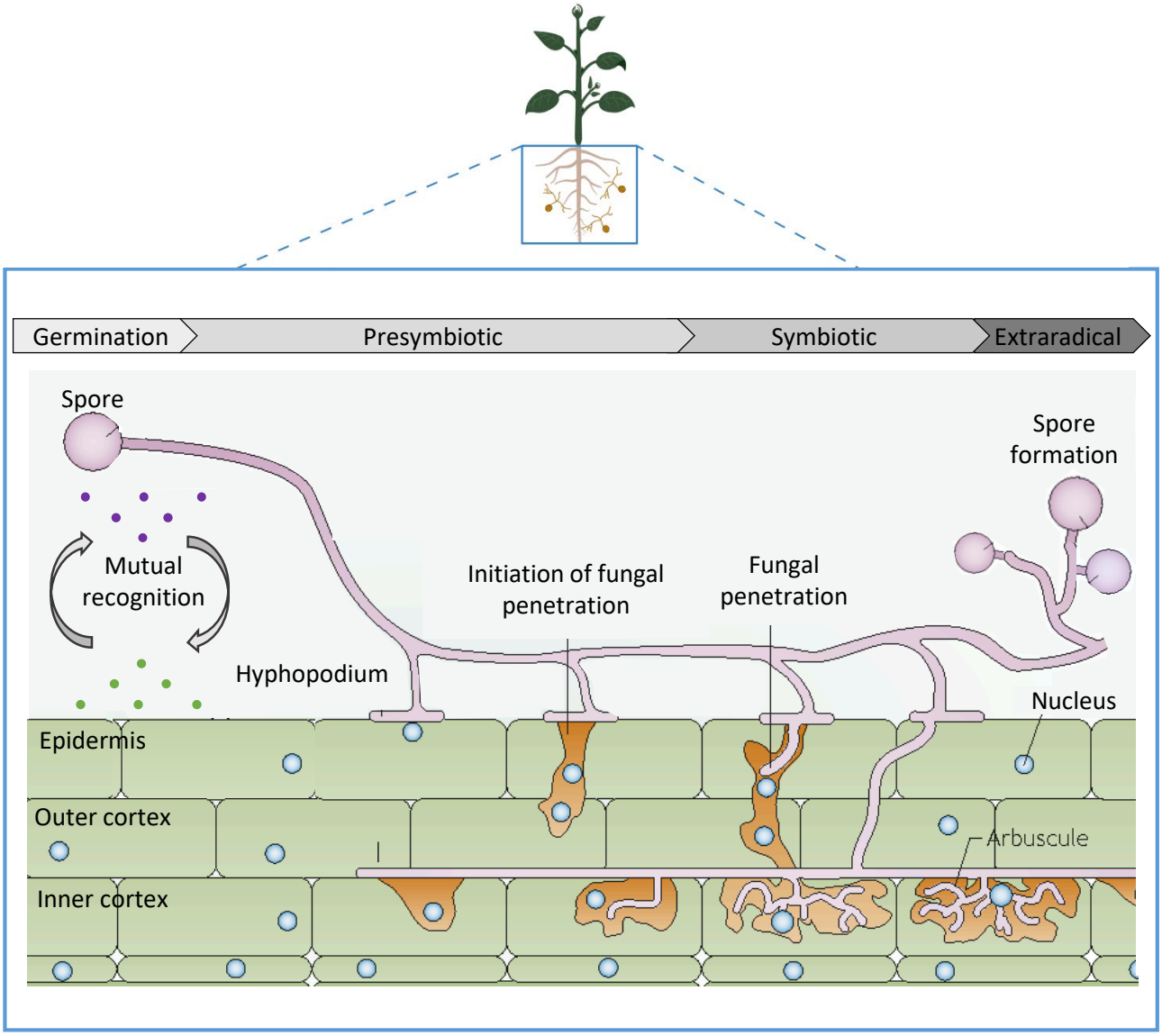

Figure 2. Schematic overview of the different stages of arbuscular mycorrhizal symbiosis

Adapted from Parniske et al., 2008.

the culture medium, AMF could complete a full developmental cycle in the absence of host roots, and produce numerous infectious spores (Kameoka et al., 2019; Sugiura et al., 2020; Tanaka et al., 2022).

I-1-D) Arbuscular mycorrhizal fungi are coenocytic

Arbuscular mycorrhizal fungi are coenocytic organisms, meaning that there is no separation between fungal cells. This cellular organization allows a rapid flow through the hyphae, facilitating the rapid migration of various molecules and organelles. Because of this coenocytic cell organization, AM spores and hyphae contain up to several thousand nuclei (Fig. 1), sharing the same cytoplasm. For example, a unicellular spore can contain up to 35,000 nuclei (Hosny et al., 1998). The different nuclei contained in a spore do not result from the division of one or few founder nuclei during the development of the spore, but rather come from the previous mycelium (Jany & Pawlowska, 2010).

I-1-E) Genetic transformation of arbuscular mycorrhizal fungi

In addition to the difficulties to study AMF because of their obligate biotrophy, several of their characteristics (for which I will not go into details) have prevented the development of stable genetic transformation methods. Nevertheless, fungal genes can be silenced using the Host-Induced Gene Silencing (HIGS) technique. This consists in introducing an RNAi construct targeting a fungal gene of interest into a host plant via genetic transformation. During the symbiotic interaction, intermediate molecules of the RNA interference process can be transferred to the fungal cells, resulting in the silencing of the gene of interest (Helber et al., 2011).

I-2) Establishment of the arbuscular mycorrhizal symbiosis

The establishment of AM symbiosis follows a defined sequence of events which will be detailed later in this introduction. To give a brief overview (Fig. 2), after spore germination the pre-symbiotic phase takes place and involves mutual recognition between the host plant and the fungus. This is mediated by diffusible molecules secreted by both partners. Then, the symbiotic phase starts with the contact between fungal hyphae and the plant root epidermis. Through intracellular accommodation structures made by plant cells, the fungus is guided across root cells. Reaching the cortical cells, the fungus forms specific intracellular exchange structures, referred to as arbuscules. The arbuscules are where nutrients, water and carbon

Figure 3. Hyphal development of a germinating spore of *Rhizophagus irregularis* grown *in vitro*

A straight germ tube emerges from the spore with a strong apical dominance. From the germ tube, ramifications emerge (white arrow). Scale bar = 700 µm.

are exchanged between the host plant and the fungus. As root colonization develops, extraradical hyphae explore the soil from the plant root in search for nutrients and other plant hosts to interact with. Moreover, from the extraradical mycelium AMF develop a new generation of spores, allowing AMF to complete their life cycle. These different steps, well established in time and space, require a fine communication between both partners using a specific molecular dialogue.

In both laboratory and ecological contexts, AM symbiosis can be initiated through different propagules including spores, extra-radical mycelium and living or dead mycorrhizal root fragments (Pepe et al., 2018; Smith & Read, 2008). Depending on AMF taxa, one type of propagule is preferentially used to infect a new plant. For example, *Glomus spp.* preferentially initiate colonization from AM root fragments (Schalamuk & Cabello, 2010), while *Gigaspora* (*Gi*) species preferentially colonize from spores (Klironomos & Hart, 2002). In laboratory studies, plant inoculations are predominantly performed using spore-based inoculum.

I-2-A) Spore germination

From their previous symbiotic cycle, AMF spores store large amounts of carbon, mainly in the form of lipids which enable them to germinate and to grow for a few days until they can colonize a host plant (Sancholle et al., 2001). Spores of AMF are able to germinate in the absence of a host plant in response to favorable environmental conditions such as temperature, moisture, pH, and the presence of nutrients. The spore germination process is activated through several chains of events which lead to the development of the germ tube. Plastid reorganization, cytoskeleton remodeling and biochemical changes have been observed in different AMF species. At the molecular level, the activation of metabolism is reflected by an increase in the synthesis of RNA, proteins, amino acids, mitochondrial DNA, lipids and polysaccharides. Just before germination, nuclei were reported to migrate near the place where the germ tube will emerge (Giovannetti, 2000; Souza, 2015). Germ tubes are described as straight, aseptate hyphae with a strong apical dominance. From these germ tubes, right-angled ramifications emerge (Fig. 3). These ramifications are thinner and often translucent compared to germ tubes. In the absence of a host plant, hyphal growth from spores can only be maintained for a few days. After this period, retraction of hyphal cytoplasm and hyphal septation from the tips to the spore are observed (Mosse, 1988). Then, the spore can switch back to a dormancy state and wait for optimal conditions to germinate again (Logi et al., 1998;

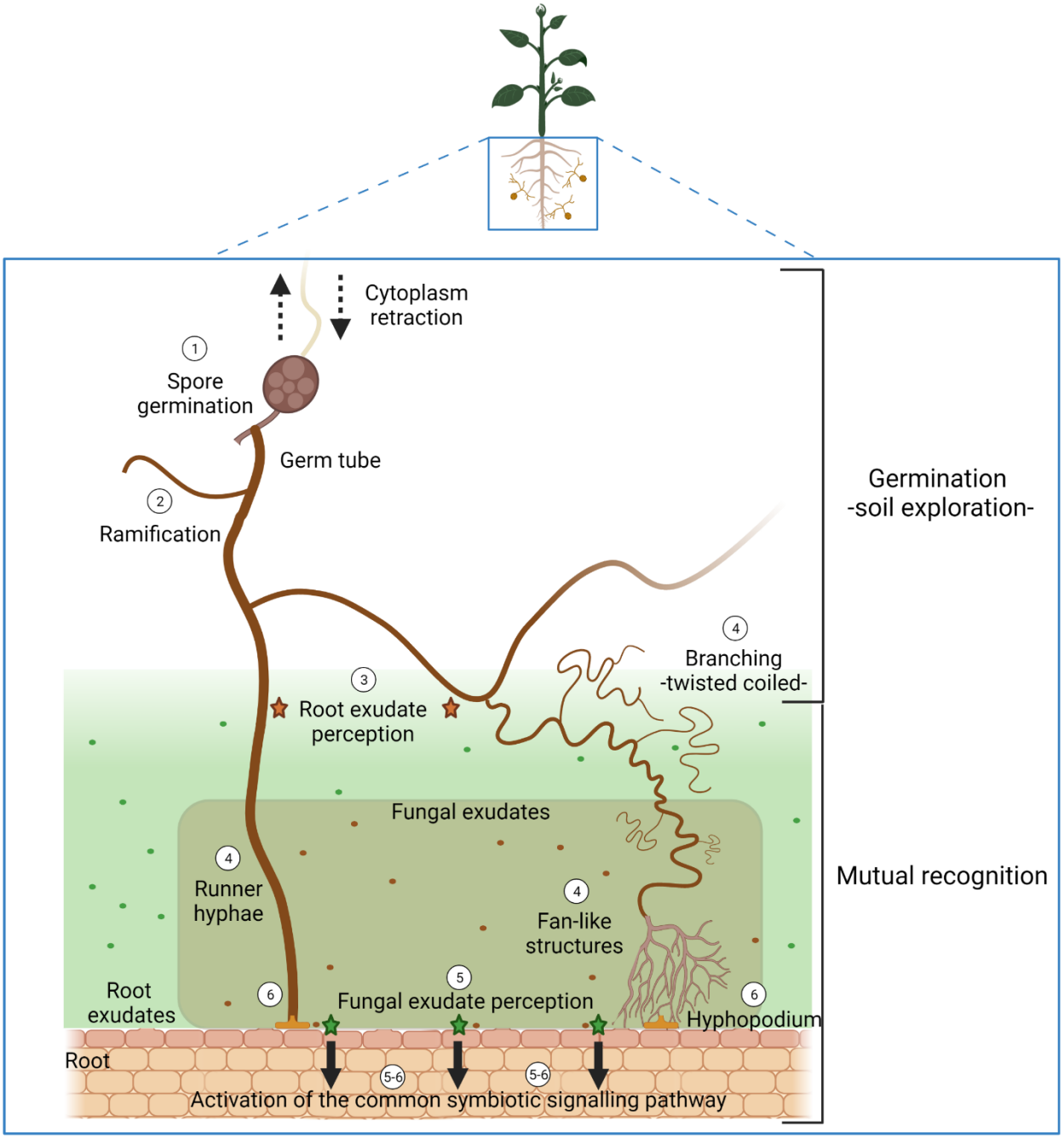

Figure 4. Schematic representation of the early stages of arbuscular mycorrhizal symbiosis

Spores of AMF germinate in response to environmental conditions. Retraction of the hyphal cytoplasm occurs in the absence of a host plant. (2) Right-angle ramifications emerge from the germ tube and explore the soil in search of a host plant. (3) The perception of root exudates by the fungus increases the release of signal molecules and induces extensive hyphal branching. The branched hyphae are thin, transparent, twisted and coiled. (4) As hyphae approach the root, a fan-like structure is formed with small, often septate hyphal clusters. Straight, white, unseptate hyphae, called runner hyphae, also develop. (5) During the pre-symbiotic process, the fungus releases molecular signals. (6) Fungal exudates are perceived by roots, activating the common symbiotic signaling pathway. Both fan-like structures and runner hyphae can colonize the root system through the formation of a particular fungal structure, called the hyphopodium. Created with BioRender.com.

Oehl, 2008). This is considered to be a survival strategy in the absence of a host plant to colonize. On the contrary, in the presence of a host plant, the germinating spore moves on to the pre-symbiotic stage.

I-2-B) Pre-symbiotic stage

I-2-B-a) Plant exudates

Mosse and Hepper (1975) were the first to report that AMF show extensive hyphal ramifications (later referred to as branching) in the vicinity of host roots (Fig. 4). From the spore, the authors described a straight growth of the germ tube exploring the soil, referred to as a runner hypha. When they get closer to the root of a host plant, runner hyphae develop fan-like structures characterized by the formation of small hyphal clusters that are often septate (Fig. 4) (Mosse & Hepper, 1975). Using a system of membranes that physically separate AM hyphae from the plant root but allow molecules to pass through, Giovannetti et al. (1993) were able to observe such fan-like structures. This demonstrated that contact with the host root is not necessary to induce hyphal branching, and highlights the importance of root exudates during the initiation of the symbiotic interaction (Giovannetti et al., 1993).

Following this study, some degree of hyphal branching was observed in the absence of host roots in isolated AMF grown *in vitro* and treated with root exudates. It was hypothesized that hyphal branching reflected a metabolic switch of AMF prior to the establishment of AM symbiosis (Buée et al., 2000; Nagahashi et al., 1996; Nagahashi & Douds, 1999). Buée et al. (2000) observed a hyphal branching pattern similar to that reported by Mosse and Hepper (1975) after application of root exudates, and added that hyphae closest to the site of application were twisted and curled. Hyphae located more than 30 mm away from the site of application exhibited a distinct phenotype with fewer, longer and less twisted/curled branches (Fig. 4) (Buée et al., 2000).

Root-exuded flavonoids have long been known to initiate the symbiotic interaction between rhizobia and legumes, so their effect on AM fungal development was investigated. Application of several flavonoids was shown to enhance germination, hyphal growth or hyphal branching depending on the AMF species used. Thus, they were hypothesized to favor the development of AMF prior contact with a host plant (Vierheilig & Piché, 2002). Nevertheless, maize mutants impacted in flavonoid synthesis were normally colonized by AMF, demonstrating that flavonoids are not essential to establish AM symbiosis (Bécard et al., 1995).

Root exudates from host plant species, but not from non-host plants, were shown to induce hyphal branching of three species of AMF. The compound(s) contained in active fractions of root exudates and responsible for this effect were referred to as branching factors (BFs) (Buée et al., 2000; Nagahashi & Douds, 2000). Root exudates of flavonoid-deficient maize plants could still induce hyphal branching, confirming that flavonoids are not essential for this activity (Buée et al., 2000). Tamasloukht et al. (2003) investigated the metabolic events associated with hyphal ramification in response to BFs. Within a few hours after BF application, the authors reported an induction of the expression of genes related to mitochondrial activity, an increase in respiration rate, and a mitochondrial multiplication and reorganization (Tamasloukht et al., 2003). This suggested that BFs trigger a metabolic switch in AMF prior to the development of hyphal branching, which was supposed to be required for AM symbiosis. Thus, the identification of BFs became a major interest.

In 2005, Akiyama et al. succeeded in isolating a BF from a root exudate fraction of *Lotus japonicus* displaying BF activity. The authors demonstrated that strigolactones (SLs): 5-deoxy-strigol (5DS), sorgolactone and the SL analog (±)-GR24 stimulate hyphal branching of the AM fungus *Gigaspora margarita* at subnanomolar concentrations. A year later, SL branching activity was confirmed on other species of AMF by Besserer et al. (2006) who also investigated the associated cellular responses. The physiological responses of AMF triggered by SL applications will be further detailed later in this introduction.

Hyphal branching has been suggested to increase the chances for the fungus to encounter a host root, although this idea has not been supported by experimental evidence. For instance, it is noteworthy that although hyphal branching was observed in the majority of cases before fungal penetration into the host root, direct colonization through runner hyphae without the formation of ramifications was also described (Fig. 4) (Bécard & Fortin, 1988). This suggests that the symbiotic ability of AMF could be uncoupled from hyphal branching.

Strigolactones are not the only signals produced by plants that are perceived by AMF prior to root colonization. Highly diverse signals such as flavonoids (Bécard et al., 1995; Chabot et al., 1992; Siquiera et al., 1991), hydroxy fatty acids (Nagahashi & Douds, 2011), phytohormones and N-acetylglucosamine (Nadal et al., 2017) have been reported to stimulate AMF either physiologically or at the transcriptomic level. In parallel, application of AMF spore exudates on roots also induces physiological and transcriptomic modifications in the host plant.

I-2-B-b) Fungal exudates

The perception of root exudates by the fungus increases the release of signal molecules that in turn trigger plant responses. Upon application of AM fungal spore exudates, oscillations of Ca^{2+} (Chabaud et al., 2011) and upregulation of the expression of early symbiotic genes have been reported in root epidermal cells (Kosuta et al., 2003). Some of the molecules responsible for these effects have been identified. Chitin oligomers (CO) (Genre et al., 2013) and lipochitooligosaccharides (LCO) (Maillet et al., 2011) were demonstrated to stimulate root development in *Medicago truncatula* and rice, as well as to induce the expression of several genes involved in AM symbiosis (Sun et al., 2015). Moreover, application of COs and LCOs induced oscillations of Ca^{2+} (Genre et al., 2013; Sun et al., 2015) and decreased plant immunity (Feng et al., 2019). In addition, AMF produce a set of small secreted proteins during root colonization (Kamel et al., 2017) which can decrease plant immunity responses allowing the establishment of the interaction (Schmitz et al., 2019).

I-2-B-c) Activation of the common symbiotic signaling pathway

Upon perception of signals from AMF, plant responses are mediated by the activation of the common symbiotic signaling pathway (CSSP). This pathway prepares the plant to be colonized at the cellular level by a foreign organism (AMF or rhizobia). Genes associated with the CSSP were primarily associated with nitrogen-fixing symbiosis. Later, it was reported that plants mutated for CSSP genes were also affected in AM symbiosis. Thus, the idea of a common signaling pathway for both symbiotic interactions emerged (Oldroyd, 2013; Parniske, 2008). A core set of genes are involved in both interactions, and specific sets of genes allow the development of each symbiosis (for review see Maclean et al., 2017; Pimprikar & Gutjahr, 2018). Recently, the common symbiosis signaling pathway has been demonstrated to be conserved in all plants forming intracellular endosymbioses, but lost by species forming exclusively extracellular symbioses (Radhakrishnan et al., 2020).

The mechanisms of perception of fungal signals such as COs and LCOs are not yet fully elucidated. However, several receptors and co-receptors belonging to the LysM receptor-like kinase and receptor-like protein families are required to establish the AM symbiosis. For instance, plants mutated in *LYSM DOMAIN RECEPTOR-LIKE KINASE 3* (*LYK3)* and *DOES NOT MAKE INFECTION* 2 (*DMI2*) genes encoding putative CO/LCO receptors are unable to host the fungus, which remains stuck outside the root epidermis. Interaction between DMI2 and an enzyme called HMG-CoA reductase leads to the production of mevalonate following AM signal

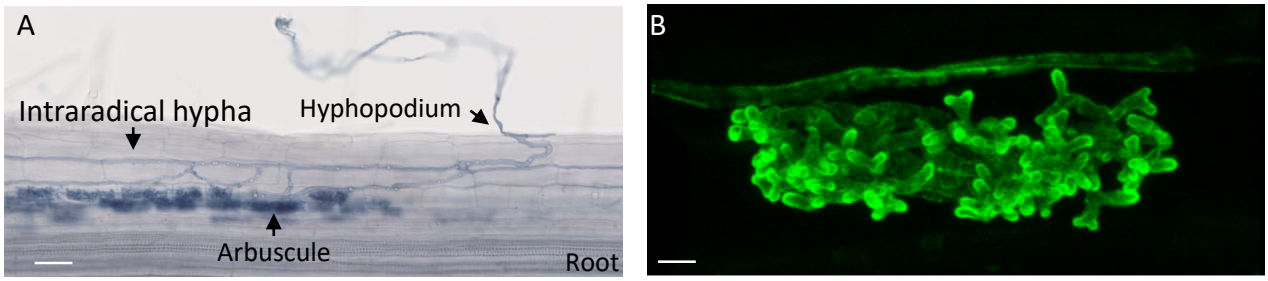

Figure 5. Root colonization of *Medicago truncatula* by *Rhizophagus irregularis*

(A) Root of *M. truncatula* colonized by *R. irregularis* observed under a dissecting microscope. Fungal structures are stained in blue. Scale bar = 100 µm. Credit: Lukas Brichet.

(B) Arbuscule observed in fluorescence microscopy. The fungus was stained with Wheat Germ Agglutin-fluorescein isothiocyanate. Scale bar = 10 µm. Credit: Aurélie Le Ru.

perception. Mevalonate acts as a secondary messenger in signal transmission from the plasma membrane to the nucleus. It is supposed that mevalonate directly interacts with the nuclear cation (K+) channel DMI1 and that this interaction triggers Ca^{2+} oscillations in the nucleus. These oscillations are decoded by a calcium- and calmodulin-dependent kinase (DMI3) which in turn phosphorylates IPD3 proteins. Together, DMI3 and IPD3 interact with GRAS transcription factors such as the DELLA protein REDUCED ARBUSCULAR MYCORRHIZA 1 (RAM1), NODULATION SIGNALING PATHWAY (NSP1-NSP2) and NODULE INCEPTION (NIN) to modulate the expression of symbiotic genes allowing the symbiotic interaction to take place.

I-2-C) Symbiotic stages

I-2-C-a) Root colonization

Activation of the CSSP prepares the root to be penetrated by the fungus. The contact and recognition between the hyphae and the root surface lead to the formation of a particular fungal structure, called the hyphopodium, preparing the fungus to penetrate the root (Fig. 5A). The penetration into root epidermal cells is facilitated by the plant through the formation of a pre-penetration apparatus (PPA), which guides the fungus through the cell. The formation of the PPA requires an important reprogramming of epidermal cells to undergo a series of events such as a restructuring of nuclei, microtubules and endoplasmic reticulum (Genre et al., 2005, 2008). Observations of fungal development in the root cortex led to distinguish two morphological patterns. The most studied is known as Arum-type AM symbiosis, in which intraradical hyphae reach root cortical cells via intercellular spaces to form highly branched fungal structures known as arbuscules (Fig. 5B) (Smith & Smith, 1997). Whereas during Paris-type AM symbiosis, intracellular hyphae develop from one cell to another and form arbuscule-like coiled structures. A given AM fungus can form both types of symbiosis depending on the host plant species (Hong et al., 2012). Conversely, a single host plant species can host both types of AM symbiosis (Cavagnaro et al., 2001).

I-2-C-b) Arbuscule formation

The cortical cells that will host arbuscules undergo a cellular reprogramming similar to the epidermal pre-penetration apparatus (Genre et al., 2008). The fungal hyphae penetrate the cell wall of the cortical cells but do not cross the plasma membrane of the host cell. The plant plasma membrane extends to envelop the hyphae forming the arbuscules (Fig. 5B) and becomes the peri-arbuscular membrane (PAM) that delimits the symbiotic interface (Paszkowski, 2006; Harrison, 2012). This interface is the main site of nutrient exchange

between the two symbionts. Arbuscules can fill the majority of the cell space and can last several days in a cell before degenerating. The plant cell then returns to its previous cell organization, while other arbuscules emerge in the neighboring cells (Kobae & Hata, 2010).

I-2-C-c) Nutrient exchange

The peri-arbuscular membrane harbors a set of specific proteins that ensure exchanges between the plant and the fungus (Banasiak et al., 2021; Wipf et al., 2019). The fungus provides water and mineral nutrients such as phosphate (Pi), nitrogen (NH_4^+/NO_3^-) and micro-nutrients (Lanfranco et al., 2018).

Water transfer during AM symbiosis is thought to be mediated by both plant and fungal aquaporins (Cheng et al., 2021). Plant aquaporin gene expression during mycorrhizal interaction is complex and highly dependent on environmental conditions. In maize, up to 16 out of 36 aquaporins are differentially expressed during AM symbiosis (Bárzana et al., 2014).

Due to the low availability of phosphate to roots, symbiotic phosphate supply plays an important role in plant development. Phosphate is taken up from the soil by the fungal hyphae and transferred into the peri-arbuscular space putatively through Na+/Pi transporters (Garcia et al., 2016). The uptake of phosphate from the fungus is mediated by specific members of the plant PHOSPHATE TRANSPORTER (PT) family. For exemple, the MtPT4 transporter (Harrison et al., 2002) and its homolog OsPT11 in rice (*Orysa sativa*) (Paszkowski et al., 2002) are located at the peri-arbuscular membrane. *Mtpt4* mutants show premature arbuscular degeneration resulting in the loss of symbiosis (Harrison et al., 2002).

Several studies have pointed out the importance of nitrogen transfer during AM symbiosis. Ammonium seems to be the form of nitrogen transferred from the fungus to the plant. Several ammonim transporters have been identified in *R. irregularis* (Calabrese et al., 2016; López-Pedrosa et al., 2006; Pérez-Tienda et al., 2011) and in host plants (Guether et al., 2009; Koegel et al., 2013) where they belong to the AMMONIUM TRANSPORTER (AMT) family. In several plant species, the expression of some members of this family is increased during AM symbiosis (Guether et al., 2009; Kobae et al., 2010). These are located at the peri-arbuscular membrane suggesting their implication during AM symbiosis (Kobae et al., 2010). Yet plants mutated for these genes did not show any alteration in their ability to establish or maintain the symbiotic interaction. Nevertheless, premature arbuscular degeneration observed in *Mtpt4* mutants could be completely suppressed under nitrogen deficiency in *M. truncatula* (Javot et al., 2011)

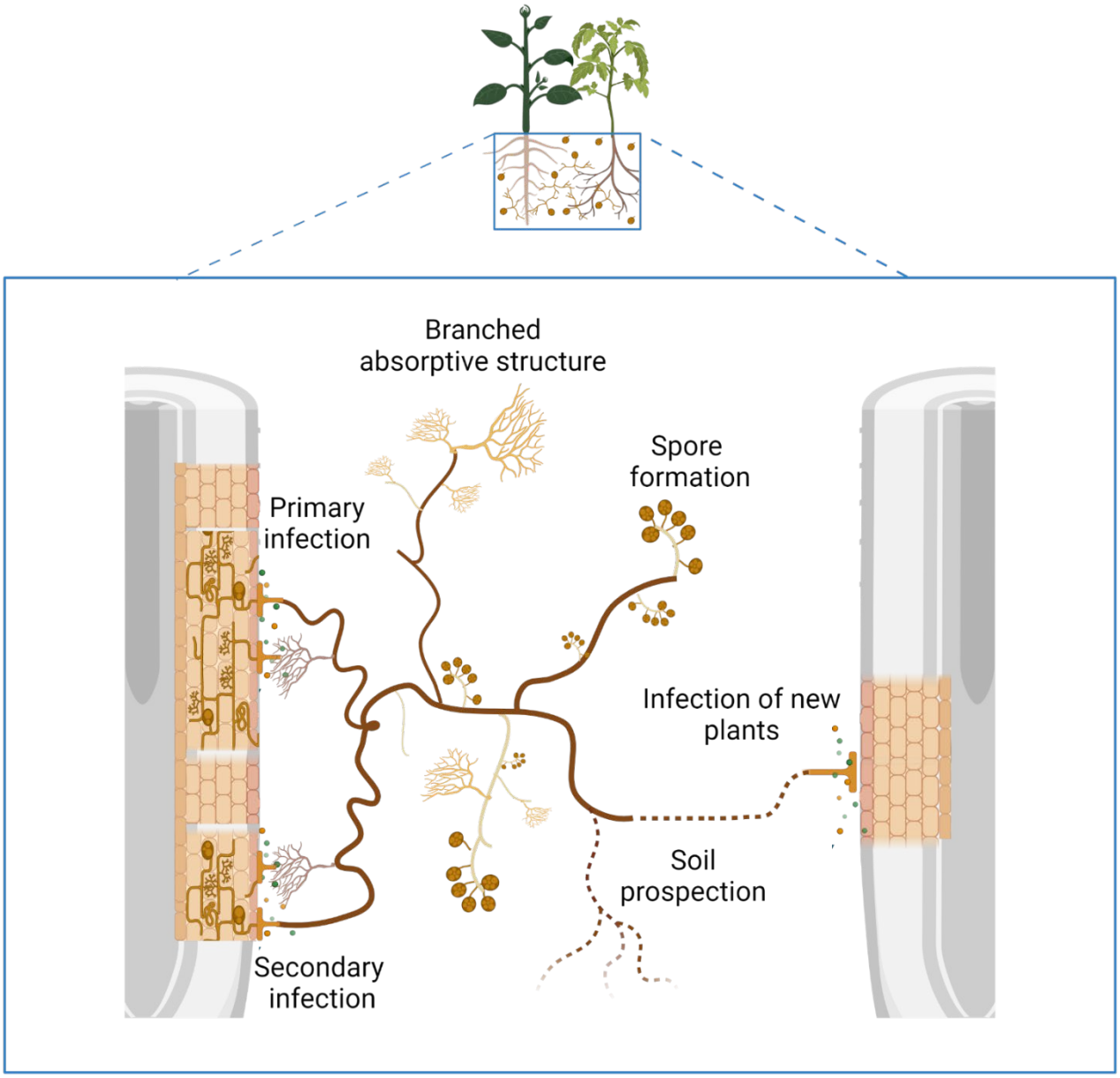

Figure 6. Schematic representation of the late stages of arbuscular mycorrhizal symbiosis

Upon successful symbiotic interaction, a network of extraradical hyphae develops into the soil. Runner hyphae explore the soil in search for nutrients and other plants to colonize. Soil nutrient uptake is thought to be mediated by branched absorptive structures. Secondary infection of the host root can occur through intra- or extra-radical hyphae. Spore formation usually occurs 3 to 4 weeks after colonization of the host plant. Created with BioRender.com.

and this phenomenon is dependent on MtAMT2 (Breuillin-Sessoms et al., 2015). This demonstrates the importance of ammonium transfer during AMF and its relation with phosphate uptake. In addition, a recent study shows that ammonium is not the only form of nitrogen transferred during AM symbiosis. The authors identified a mycorrhiza-specific nitrate transporter in rice, maize and sorghum, named NPF4. Loss-of-function *Osnpf4* mutants are slightly affected in AM colonization and nitrogen content. However, well-developed arbuscules were observed in these mutants suggesting that nitrate transport might not be an essential requirement for arbuscule development (Wang et al., 2020d).

In exchange for the minerals provided by the fungus, the plant provides carbon in different forms (Banasiak et al., 2021). For a long time carbohydrates were considered as the main source of carbon delivered to the fungus during AM symbiosis. The fungal monosaccharide transporter RiMST2 is expressed in arbuscules and was suggested to uptake sugar from the plant (Helber et al., 2011). From a plant point of view several transporters belonging to the SUGARS WILL EVENTUALLY BE EXPORTED TRANSPORTER (SWEET) and SUCROSE TRANSPORTER (SUT) have been proposed as good candidates for symbiotic sugar transfer (Banasiak et al., 2021).

More recently, lipids were shown to be an additional and perhaps most important source of carbon supplied by the host plant. Several studies have reported that mutants in AM-induced lipid biosynthesis plant genes such as *DIS*, *FATM* and *RAM2* harbored stunted arbuscules with reduced colonization. Plants deficient in a half-size ABC transporter gene (STR) displayed the same phenotype, thus STR was proposed to mediate lipid transfer at the peri-arbuscular membrane. More importantly, evidence for direct lipid transfer from the plant to the fungus through the PAM was reported (Jiang et al., 2017; Keymer, 2017; Luginbuehl et al., 2017). A recent study demonstrated that lipid transfer during AM symbiosis is mediated by the same pathway across land plants (Rich et al., 2021), which suggests that it is an ancient trait closely related to the appearance of AM symbiosis.

I-2-D) Development of the extraradical mycelium

Following successful root colonization, AMF develop an extraradical hyphal network serving several functions. First, extraradical hyphae contribute to the extension of host root colonization. They can spread in the soil along the host root to establish new infection points on the same root system (Fig. 6). In addition, hyphae harboring a similar morphology to that

of pre-symbiotic runner hyphae can explore the soil to infect new plants. Another role of extraradical hyphae is the uptake of soil nutrients. Some hyphae develop branched absorptive structures which are characterized by small clusters of dichotomous hyphae and are thought to increase hyphal contact surface to enhance soil nutrient uptake (Bago et al., 1998). Finally, spore formation has been observed emerging from extracellular and extraradical hyphae (Fig. 6). Spore formation usually occurs 3 to 4 weeks after colonization of the host plant, although this depends on the fungal species (Souza, 2015).

Throughout the symbiotic process, each organism produces and perceives signals allowing the initiation, regulation and maintenance of the interaction. Among these signals, phytohormones play an essential role.

I-3) Arbuscular mycorrhizal symbiosis and phytohormone signaling

The content of phytohormones, their biosynthesis and their perception in the host plant are modified throughout the interaction. In addition, exogenous application of phytohormones strongly influences the symbiosis. Nevertheless, different studies have reported contrasting results regarding the role of each class of phytohormones. Several factors may explain these differences: for example, the combination of plant and fungal species, the concentration and the form of hormone that is applied, the method of application or the use of mutants affected at different levels of the hormonal pathways. Moreover, it seems that the regulation of AM symbiosis is very sensitive to a defined spatiotemporal status that may also vary between studies. Thus, apart from a few, it is difficult to clearly define a role for each hormone during AM symbiosis (Das & Gutjahr, 2019; Bedini et al., 2018). Broadly speaking, strigolactones, auxin (AUX), abscisic acid (ABA) and brassinosteroids (BR) are considered as positive regulators of the AM symbiosis while gibberellins (GA) and salicylic acid (SA) are considered as negative regulators. The effects of cytokinins (CK), ethylene (ET) or jasmonic acid (JA) are less clear.

Briefly, the contents of auxin (Etemadi et al., 2014), ABA (Ludwig-Müller, 2010), GA (Martín-Rodríguez et al., 2015), SA (Blilou et al., 2000), JA (Song et al., 2019) and CKs (Cosme et al., 2016) increase in mycorrhizal roots. Exogenous application of AUX, ABA or BR promotes root colonization whereas application of GA, SA or ET precursors decreases root colonization. Application of JA or CK has been reported to either enhance or reduce AM fungal colonization. The phenotypes displayed by hormone perception or biosynthesis mutants point in the same

direction. For example, exogenous application of auxin increases arbuscule abundance and fungal spread (Dutra et al., 1996) while auxin biosynthesis or perception mutants show a reduced AM colonization and arbuscule abundance in several plant species (Etemadi et al., 2014; Foo, 2013).

I-4) Objectives of the Mycormones project

So far phytohormones have been mostly described as internal plant signals, and even in the context of plant-microbe interactions they have been studied from a plant perspective. The ANR project Mycormones which funds my PhD aims to investigate the role of phytohormones from the perspective of the AM fungal partner. This project addresses the production, perception and transport of phytohormones by AMF. More specifically, we are interested in: (I) describing the set of phytohormones that AMF are able to release, (II) assessing the effects of the main classes of phytohormones on AM fungal biology, and (III) describing the underlying perception mechanisms. Last, we have investigated whether phytohormones are transported during plant-plant communication through common mycorrhizal networks (CMN).

I-4-A) Do AM fungi produce phytohormones?

Different species of bacteria and fungi are able to produce phytohormones (Chanclud & Morel, 2016; Egamberdieva et al., 2017). Over the past decades, several studies have reported the presence of phytohormones in spores and hyphae of the AM fungus *R. irregularis*. There is indirect evidence that *R. irregularis* produces molecules with auxin-like and cytokinin-like activity (Barea & Azcón-Aguilar, 1982). In addition, ELISA tests have detected the presence of ABA in spores and hyphae (Esch et al., 1994). Finally, using mass spectrometry, a small amount of auxin was measured in spores of *R. irregularis* (Ludwig-Müller et al., 1997). Recently, using mass spectrometry, a PhD student from the team has detected one cytokinin (isopentenyl adenosine) and one auxin (indole-acetic acid) in *R. irregularis* spore exudates, and one gibberellin (GA_4) in spore extracts (Pons et al., 2020). Thus, AMF are able to release phytohormones. However, because AMF always develop in connection with a host plant, it is possible that these phytohormones have been taken up from the host plant. In the case of ethylene, *de novo* production by germinating spores of *R. irregularis* has been shown using gas chromatography (Pons et al., 2020).

I-4-B) Do AM fungi respond to phytohormones?

One of the challenges in investigating the effects of phytohormones on AMF is that from the early symbiotic stages it is difficult to treat the fungal partner without also affecting the plant. Therefore, it is impossible to distinguish between effects exerted on the fungus, on the plant or on the interaction between them. It is however possible to assess the effect of phytohormones in asymbiotic conditions using isolated AM fungal spores grown *in vitro*. A second possibility is to use double compartment culture systems, where roots colonized by AMF are maintained on one side and the fungal mycelium alone can reach the other compartment. In asymbiotic conditions, application of JA slightly stimulates hyphal growth of *R. irregularis* (Nagata et al., 2016). Exogenous application of ethylene stimulates hyphal growth and spore germination at low concentrations but inhibits them at high concentrations (Ishii et al., 1996). Last, ABA stimulates sporulation of *R. irregularis* in asymbiotic and pre-symbiotic conditions (Liu et al., 2019). The response of AMF to strigolactones will be detailed later in this introduction.

The Mycormones project aims to pursue the characterization of effects of the main classes of phytohormones on AM fungal biology, and to describe the underlying molecular and cellular mechanisms.

I-4-C) How do AM fungi perceive phytohormones ?

In a study focused on histidine kinases (Hérivaux et al., 2017), homologs of plant cytokinin and ethylene receptors have been identified in AMF genomes. These homologs bear the canonical domains and conserved amino acids required for receptor function, which makes them good candidates for the perception of CK and ethylene. Their characterization will be performed by another student in the group.

The main part of my PhD aims to investigate the perception mechanisms that allow AMF to respond to strigolactones. In the following part of this introduction, I will give an overview of the current state of knowledge regarding these compounds.

II) Strigolactones

II-1) Discovery of strigolactones

Strigolactones (SLs) were discovered over 50 years ago, but many questions remain unanswered. To fully understand the complexity of SLs, it is important to take into consideration that SLs are perceived by at least three different kinds of organisms: parasitic weeds, mycorrhizal fungi, and plants. Discoveries of such broad functions result from investigations in historically distinct research fields. In the following part, I will try to provide an overview of the discoveries of SL activities as a germination stimulant, a hyphal branching factor, and an endogenous plant hormone.

II-1-A) Strigolactones as germination stimulants of parasitic weeds

Parasitic weeds are angiosperms that grow at the expense of other plants by attaching themselves to a host and taking up a variable range of resources from this host. There are two main strategies of parasitism. Holoparasitic plants have lost their photosynthetic abilities, so they cannot assimilate carbon on their own. These plants acquire all the nutrients, water and carbon from their host plants to complete their life cycle. This is in contrast to hemiparasitic plants that acquire mineral nutrients and water from their host plant, but have retained the photosynthetic abilities providing them with most of the carbon needed for growth. Both holoparasitic and hemiparasitic plants are obligate biotrophs. In addition, two major groups of parasitic weeds have been distinguished depending on their strategy to infect their host: stem parasites and root parasites. For instance, *Cuscuta* spp known as dodders are part of the stem parasitic weeds. One important group of root parasites is the Orobanchaceae family, which is the largest family of parasitic plants (Heide-Jørgensen, 2008). Within this family the most studied species belong to the genera *Orobanche* and *Phelipanche* (known as broomrapes) or *Striga* (witchweeds). These pests have the ability to affect a wide spectrum of hosts and present a certain degree of host specificity. Hereafter I will use the term “parasitic weeds” to refer to Orobanchaceae.

After germination and contact with a host plant, parasitic weeds are able to penetrate the host root system and to form a physiological bridge between their vasculature and that of their host, through an organ named haustorium. Using this interconnection, parasitic weeds

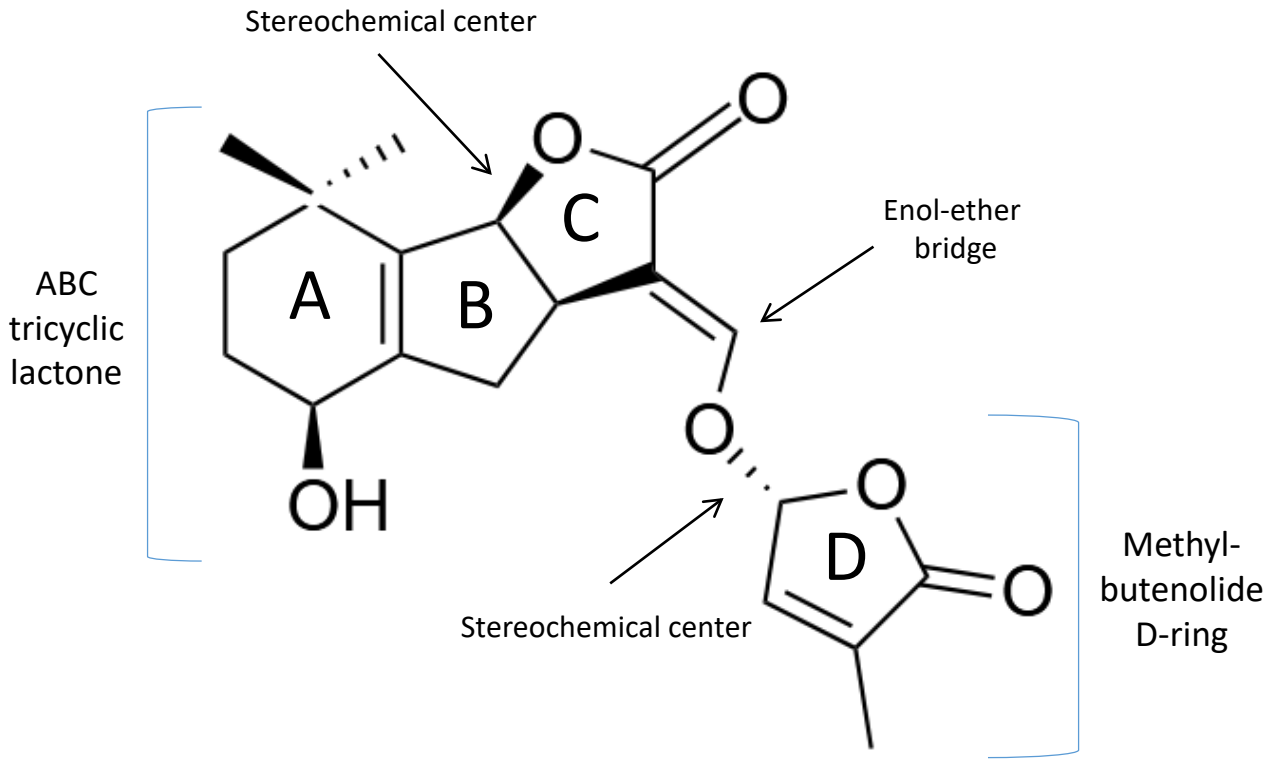

Figure 7. Structure of natural canonical strigolactones

The structure of strigol is shown. Two stereochemical centers exist. The first one is located at the junction of the B- and C-rings, and determines the classification of SLs between strigol (5DS) and oranbanchol (4DO) types. The second one is located at the junction of the D-ring and the enol-ether bridge, giving rise to the 2'S and 2'R configurations. All natural SLs share the same 2'R configuration.

take up from nutrients from their host. While witchweeds only connect their xylem to that of their host, broomrapes establish connections for both the xylem and phloem (Westwood, 2013). Parasitic weeds then develop an aboveground inflorescence within a few weeks. This inflorescence produces up to several thousands of seeds, that can remain dormant and viable in soil for many years (Joel et al., 2013). These seeds contain just enough reserves to survive for a few days after germination and to search for a host plant to parasite. Similar to the germination of non-parasitic plants, germination of parasitic weed relies on the environmental conditions such as light, temperature or humidity. However, their germination has evolved to also rely on plant-derived signals to ensure the proximity of a host plant (Matusova et al., 2004).

Investigations that aimed to identify plant-derived germination stimulants suggested that these molecules were unstable and produced at very low concentrations. In 1966, by using concentrated root exudates from a large number of cotton plants, Cook et al. (1966) isolated a germination stimulant. The first SL was thus identified and designated as strigol. A first strigol structure was proposed from spectral data analysis (Cook et al., 1972), and was later corrected by X-ray diffraction analysis (Fig. 7) (Brooks et al., 1985). Ironically, Cook et al. (1966) pointed out that strigol was biologically active at hormonal concentrations, but its hormonal activity in plants was revealed only forty years later.

By that time, various SLs differing in structure were identified from several plant species, based on their activities as germination stimulants of parasitic weeds (Hauck et al., 1992; Yokota et al., 1998). Given the worldwide emergence of parasitic weeds as a cause of severe crop losses, elucidation of SL biosynthesis became a subject of concern. Strigolactones were first hypothesized to be sesquiterpene lactones. However, in 2005 Matusova et al. hypothesized that SLs derived from the carotenoid pathway, based on their structural resemblance with ABA and other carotenoid-derived compounds. They observed that root exudates of maize carotenoid-deficient mutants and of plants treated with carotenoid biosynthesis inhibitors exhibited impaired germination-stimulant activities. This was consistent with their hypothesis and led the authors to propose that SLs were biosynthesized from the carotenoid pathway and produced by the cleavage of β-carotene (Matusova et al., 2005). As will be detailed below, this assumption was an essential premise to help the discovery of SL hormonal activities in plants (Fig. 8).

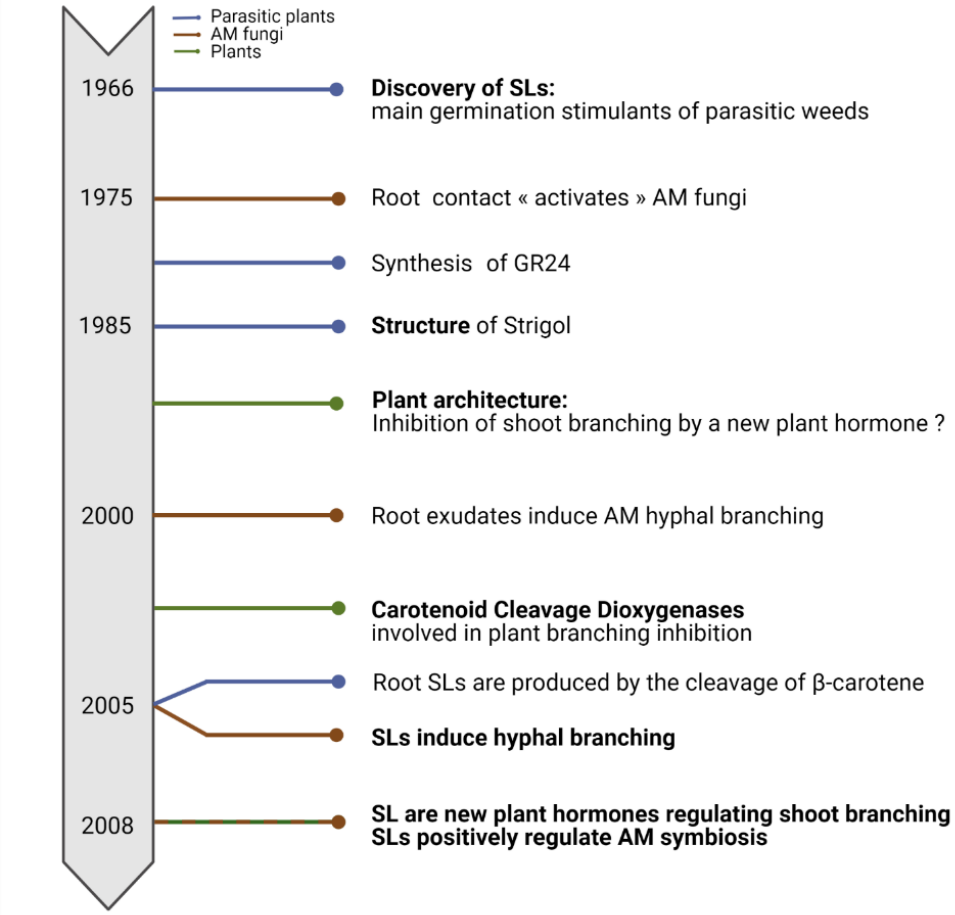

Figure 8. Timeline of important discoveries about strigolactones

Discoveries concerning parasitic weeds are shown in blue, AM fungi in brown and non-parasitic plants in green. Created with BioRender.com.

II-1-B) Strigolactones as branching factors of AM fungi

In parallel, as mentioned earlier in the introduction, research teams working on mycorrhizal fungi were trying to identify plant signals that elicit morphological responses of AMF. In 2005, Akiyama et al. reported the purification and identification of SLs as hyphal branching factors. In parallel, Besserer et al. (2006) hypothesized that BFs were SLs based on two arguments. First, like SLs, BFs were known to be lipophilic molecules with a low molecular weight (Buée et al., 2000) and to be exuded at very low concentrations. Second, similar to parasitic plants, mycorrhizal fungi were described as obligate biotrophs. The authors thus tested the activity of SLs on AM fungal germinated spores. In 2006 they were able to extend the results of Akiyama et al. (2005) by showing SL branching activity on different species of AMF (Fig. 8).

II-1-C) Strigolactones as plant hormones

Meanwhile, plant biologists were looking for a new class of molecules involved in the control of shoot branching. Forward genetic approaches had identified a series of mutants with enhanced shoot branching in several species including pea (*Pisum Sativum* (Ps)), *Arabidopsis thaliana* (At), rice (*Oryza Sativa* (Os)) and *Petunia hybrida* (Ph). Grafting experiments using pea and *Petunia* mutants named *RMS* and *DAD* respectively, revealed the existence of a root-to-shoot mobile signal that was responsible for shoot branching inhibition (Beveridge et al., 1997; Napoli, 1996). This signal was termed SMS (shoot multiplication signal, Beveridge, 2006). Similar graft experiments were performed in *Arabidopsis* with mutants of the *max* series. Together with the previous observations, they allowed to distinguish two groups of highly branched mutants: some seemed to be deficient in the production of SMS, while others appeared to be SMS-insensitive (Booker et al., 2005). The mobility of SMS through plants led these authors to propose that it was a plant hormone (Beveridge et al., 1997; Morris et al., 2001). Moreover, analysis of the hormonal content of shoot branching mutants suggested that SMS was different from auxin and cytokinin (Beveridge et al., 2000; Foo et al., 2001). The chemical nature of SMS thus remained to be identified.

Genes involved in the regulation of shoot branching were identified by positional cloning using *Arabidopsis max* mutants. Two mutations underlying SMS deficiency, *max4* (Sorefan et al., 2003) and *max3* (Booker et al., 2004) affect genes encoding *CAROTENOID CLEAVAGE DIOXYGENASES* (*CCD*). *MAX4* and *MAX3* are referenced as *CCD8* and *CCD7*, respectively. They were reported to be the respective orthologs of *RMS1* and *RMS5* in pea (Johnson et al., 2006;

Sorefan et al., 2003) and *D10* and *D17* in rice (Arite et al., 2007; Zou et al., 2006). AtCCD7 and AtCCD8 were shown to cleave β-carotene and hypothesized to carry out the initial steps of SMS biosynthesis (Schwartz et al., 2004). *Arabidopsis* mutants affected in SMS perception carry a mutation in a gene called *MAX2* encoding an F-box-LRR protein (Stirnberg et al., 2002). Its orthologs in pea and rice are named *RMS4* and *D3*, respectively (Ishikawa et al., 2005; Johnson et al., 2006).

To summarize, in 2008 SLs were known to induce parasitic weed germination and to act as branching factors on AMF (Fig. 8). Interestingly, SLs were detected in both roots and aerial parts of several plant species, including some that do not interact with AMF (Goldwasser et al., 2008; Yoneyama et al., 2007). These observations suggested another role for SLs, independent from AM symbiosis or parasitic weed interactions. In parallel, plant biologists were working on a new putative plant hormone named SMS, which inhibits shoot branching. The key findings that brought these different stories together were linked to biosynthetic pathways: two enzymes belonging to the CCD family were shown to be involved in the production of SMS from carotenoids (Booker et al., 2004; Sorefan et al., 2003), and SLs were proposed to be formed from β-carotene cleavage (Matusova et al., 2005). Together, these findings led two teams in 2008 to hypothesize that the SMS was a SL or closely related compound. Their studies were published in the same issue of *Nature* (Gomez-Roldan et al., 2008; Umehara et al., 2008).

Gomez-Roldan et al. (2008) were looking for mutants in SL synthesis in order to assess the importance of SLs in mycorrhizal symbiosis. Since SLs were supposed to derive from carotenoid cleavage (Matusova et al., 2005), they started with two available pea mutants that were affected in carotenoid cleavage enzymes, CCD7 and CCD8. They showed that root exudates of *ccd7* and *ccd8* mutants were less active on AM hyphal branching and parasitic weed germination, as compared with wild-type exudates. In addition, a lower level of AM fungal colonization was reported in *ccd8* mutants. This encouraged them to investigate whether SL production was reduced in these mutants. Using mass spectrometry, they gathered biochemical evidence that this was the case. Both *ccd7* and *ccd8* mutants were SL-deficient, while *rms4* SMS-insensitive mutants with a similar shoot branching phenotype were able to produce SLs. These observations supported the hypothesis of a tight link between SLs and SMS. To further investigate this possibility, the authors attempted to rescue the shoot branching phenotypes of pea *rms* mutants through exogenous application of SLs. Because SMS

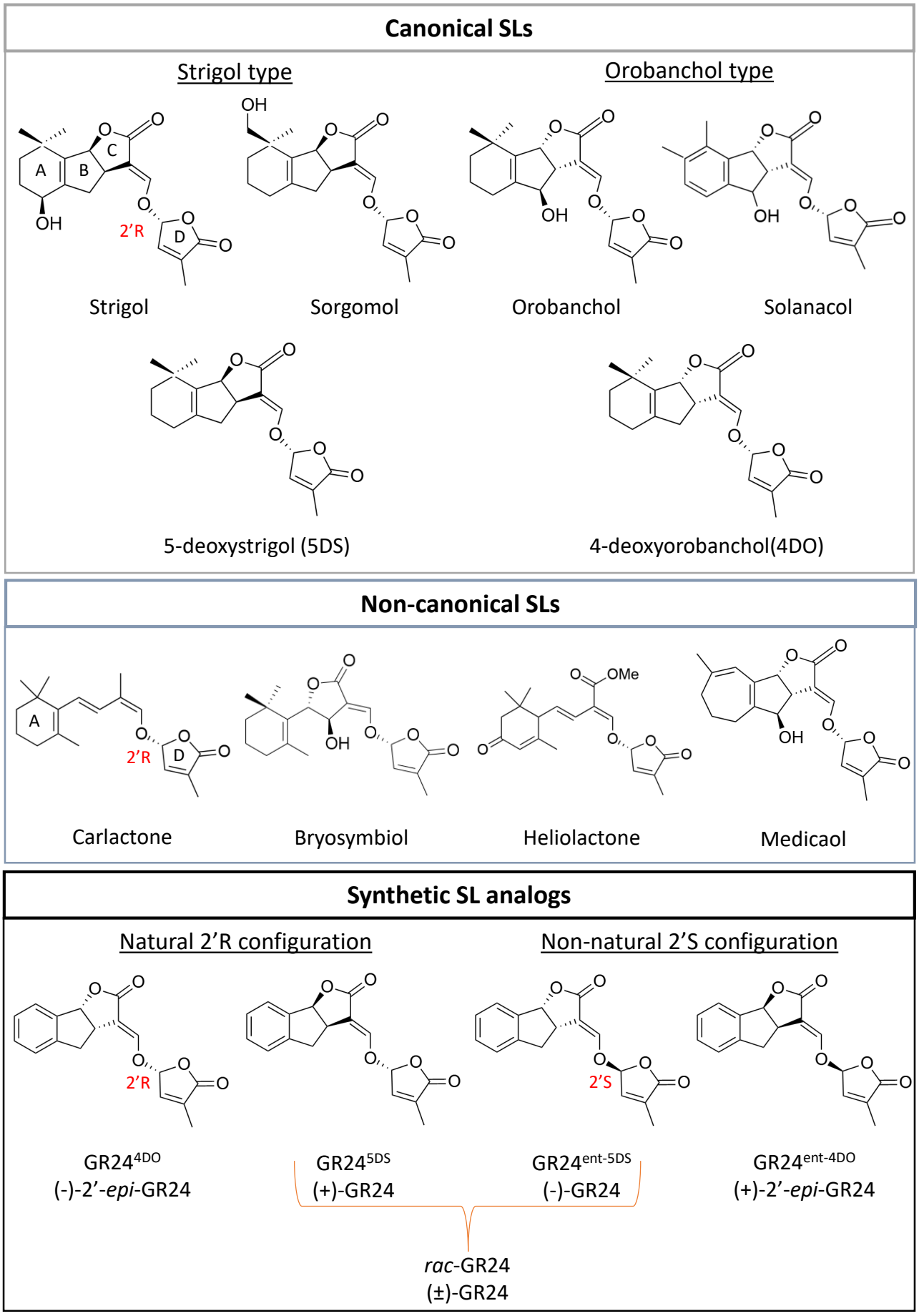

Figure 9. Chemical structure of canonical, non-canonical and synthetic analogs of strigolactones

All natural SLs identified to date harbor the conserved D-ring with a 2'R configuration. Non-canonical SLs lack an intact A-, B-, or C-ring. Four stereoisomers of the widely used synthetic SL analog GR24 exist. GR24 is mostly used as a racemic mixture named *rac*-GR24 or (±)-GR24.

was described as a mobile root-to-shoot signal, SLs were applied to the shoot vascular stream. Application of 10 nM of (±)-GR24 was sufficient to partially restore wild-type shoot branching in *ccd8* and *ccd7* mutants, but not in *rms4* mutants. Similar observations of (±)-GR24 effects were made in *Arabidopsis* using *max4* and *max2* mutants. Using rice as a model, Umehara et al. (2008) also observed a reduced level of SLs in *ccd7* and *ccd8* mutants. The germination-stimulant activity of their root exudates was severely reduced compared to wild-type root exudates. Moreover, *ccd8* roots were infected by fewer *Striga* plants. Exogenous application of SLs was able to inhibit tillering in these rice mutants but not in *d3* mutants affected in signaling. Accordingly, application of (±)-GR24 to *A. thaliana ccd7* and *ccd8* mutants but not to the signaling mutant *max2* rescued the shoot branching phenotype. Finally, SL production in *Arabidopsis* mutants was estimated indirectly through the ability of root exudates to stimulate *Striga* seed germination. This activity was reduced in *ccd7* and *ccd8* mutants, but not in *max2* mutants.

From these two articles and further analyses, SLs are now widely recognized as a new class of plant hormones. Since then, considerable progress in the understanding of SLs has been accomplished through the use of a combination of various models and methods.

II-2) Strigolactone structure and nomenclature

Structures of the first identified SLs, strigol and oranbanchol, were used as references to search for additional SLs. Later, other compounds displaying SL biological activities but differing in their structures were discovered. Strigolactones referred to as canonical SLs are composed of four carbon rings named A to D. The ABC tricyclic lactone is linked by an enol-ether bridge to an invariable methylbutenolide D-ring (Fig. 8). Two stereochemical centers exist in SLs. The first one is located at the junction of the B- and C-rings, and determines the classification of SLs between strigol and oranbanchol types. The second one is located at the junction of the D-ring and the enol-ether bridge, giving rise to the 2'S and 2'R configurations. All natural SLs produced in plants share the same 2'R configuration (Fig. 8-9) (Seto et al., 2014; Zhang et al., 2014). Non-canonical SLs also possess a D-ring, but are linked to diverse moieties that approximate the ABC-ring of canonical SLs (Fig. 9).

Natural SLs are produced in very low quantities in plants and their isolation is difficult. Therefore, several synthetic SL analogs have been developed over the years. The most

commonly used analog is called GR24. It is important to note that GR24 was selected on the basis of its activity on parasitic weeds. Its structure may not be optimal for activity on other plants and on AMF. Nonetheless, GR24 remains the most commonly used analog in SL studies. During GR24 synthesis, four stereoisomers are produced: two exhibit a natural 2'R configuration and are designated (-)-2'-*epi*-GR24 ($GR24^{4DO}$) and (+)-GR24 ($GR24^{5DS}$), while the other two have a non-natural 2'S configuration and are referred to as (+)-2'-*epi*-GR24 ($GR24^{ent\text{-}4DO}$) and (-)-GR24 ($GR24^{ent\text{-}5DS}$) (Fig. 9). In the literature, the widely used *rac*-GR24 is composed of an equimolar mix of (+)-GR24 and (-)-GR24. For more accuracy, in the following work, I will refer to *rac*-GR24 as (±)-GR24. The generic name GR24 will be used when the mix of stereoisomers used in the different studies is not known.

Chemical synthesis of GR24 and related compounds forms a by-product called contalactone, which has been shown to be active on parasitic weeds, AMF and plants albeit at higher concentrations than (±)-GR24 (de Saint Germain et al., 2019). The possible presence of such contaminants, together with the frequent use of mixes of stereoisomers, means that results obtained with synthetic products should be interpreted with caution. Such products proved however extremely useful for SL research. Many synthetic analogs have been produced to date, with variations on the core structure or addition of a fluorescent moiety. Several studies have taken this opportunity to perform structure-activity relationship (SAR) assays (which I will describe later in the introduction) and to test the different stereoisomers separately.

The name strigolactone was first given to compounds harboring a similar structure to strigol. Subsequently, compounds harboring the conserved D-ring but lacking the A-, B- or C-ring and exhibiting activities similar to those of SLs were also named SLs, but referred to as non-canonical. Broadly speaking, SLs described to date contain the D-ring and enol-ether bridge, and exhibit SL-like activity on at least one of the three target organisms (*i.e.* AMF, parasitic weeds and other plants). There is increasing evidence of a wide diversity of structures within non-canonical SLs, as will be described later in the introduction (Fig. 9). In addition, most SLs have been identified on the basis of their activity on parasitic weeds and AMF but not their hormonal activity in plants. New molecules exhibiting SL-like hormonal activities have probably not been identified yet, and their structure may differ from known SLs. As a result of this complexity, it is difficult to propose a definition of SLs that encompasses all situations and matches all purposes. It is likely that more precision will arise as further knowledge becomes available.

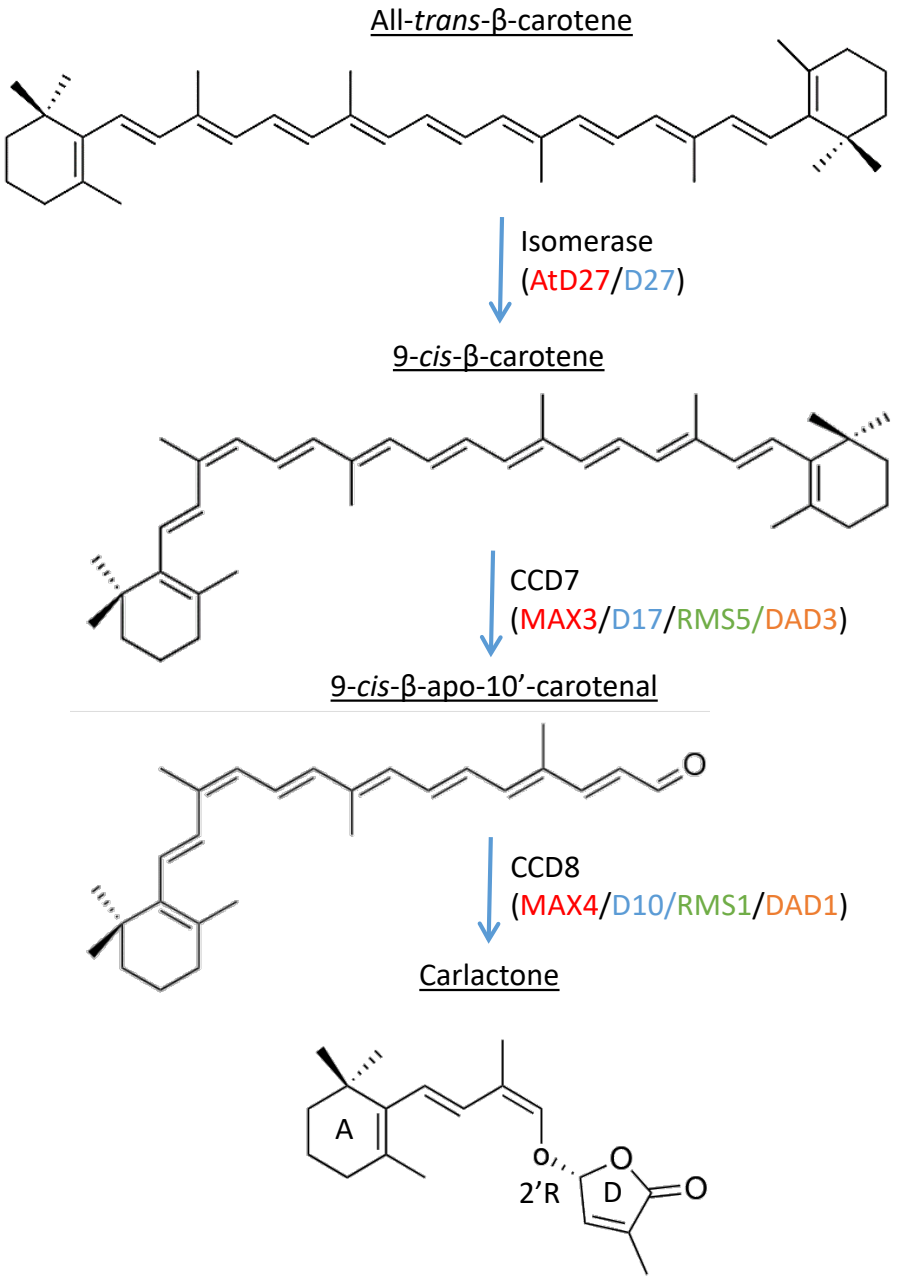

Figure 10. Core strigolactone biosynthetic pathway

Carlactone is synthesized from all-*trans*-β-carotene through sequential enzymatic reactions catalyzed by the isomerase D27 and two carotenoid cleavage dioxygenases: CCD7 and CCD8. Carlactone harbors the A- and D-rings of SLs and the 2'R configuration. It is considered to be the precursor of all natural SLs, canonical or not. Enzymes of *Arabidopsis*, rice, pea and *Petunia* are shown in red, blue, green and orange respectively.

II-3) Strigolactone biosynthesis

II-3-A) Strigolactone biosynthetic pathway

Analyses of shoot branching mutants led to the identification of *CCD7*, *CCD8*, *DWARF27 (D27)* and *MORE AXILLARY GROWTH1* (*MAX1)* genes encoding enzymes, which allowed rapid progress in the understanding of SL biosynthesis. To determine the biochemical function of AtCCD7 and AtCCD8, the proteins were expressed in a heterologous system consisting in carotenoid-accumulating strains of *E. coli.* AtCCD7 and AtCCD8 were shown to cleave β-carotene sequentially (Schwartz et al., 2004). Later, Alder et al. (2012) characterized the biochemical function of D27 and proposed a core SL biosynthetic pathway (Fig. 10). This starts from *trans*-β-carotene which is isomerized from a *trans* to a *cis* configuration by the isomerase D27. Then CCD7 cleaves *cis*-β-carotene to yield 9-cis-β-apo-10-carotenal, which is then converted into carlactone by CCD8 (Alder et al., 2012; Jia et al., 2018). Carlactone harbors the A- and D-rings of SLs and the 2'R configuration. It is considered as the precursor of all natural SLs, canonical or not.

Different molecules are produced by oxidation of carlactone (CL) through enzymes belonging to the cytochrome P450 family, named MAX1 in *Arabidopsis* (Booker et al., 2005; Stirnberg et al., 2002). AtMAX1 was reported to catalyze the oxidation of CL to produce carlactonoic acid (CLA) (Abe et al., 2014). The presence of canonical SLs such as orobanchol has been reported in *Arabidopsis* (Gholamhoseini et al., 2013; Kohlen et al., 2011). However, more recent mass spectrometry analyses failed to detect orobanchol or any known canonical SLs in *Arabidopsis* root exudates or root tissues (Yoneyama et al., 2018b, 2020a). It is currently assumed that *Arabidopsis* does not produce canonical SLs.

MAX1 is conserved in a number of plant species and has many homologs, for example the rice genome encodes five MAX1 homologs. Using heterologous systems like yeast or *Nicotiana benthamiana*, one homolog, Os900, was characterized to convert CL to 4-deoxyorobanchol (4DO). Another homolog, Os1400, was shown to convert 4DO to orobanchol (Zhang et al., 2014). Analysis of the enzymatic functions of MAX1 homologs across the plant kingdom led Yoneyama et al. (2020a) to classify MAX1 function into three types: A1-type, converting CL to CLA; A2-type, converting CL to 4DO via CLA; and A3-type, converting CL to CLA and 4DO to orobanchol (Yoneyama et al., 2018a). Screening cytochrome P450 genes, other P450 enzymes outside the MAX1 clade were shown to be involved in canonical SL biosynthesis. Wakabayashi

et al. (2019) identified P450 enzymes that convert CLA directly into orobanchol downstream of MAX1 (Wakabayashi et al., 2019), and CLA to 5DS (Wakabayashi et al., 2020). The same group demonstrated that another P450 enzyme from sorghum was able to convert 5DS into sorgomol (Wakabayashi et al., 2021).

In addition, feeding experiments demonstrated that an undescribed methyltransferase was able to convert CLA into methyl carlactonoate (MeCLA) *in planta* (Abe et al., 2014). Interestingly, application of MeCLA on *max1* mutants was able to rescue their shoot branching phenotype and MeCLA was demonstrated to bind the *Arabidopsis* SL receptor. This suggested that MeCLA could act as a non-canonical SL. Further analyses suggested that MeCLA was probably an intermediate to other non-canonical SLs.

An alternative approach to genetic analysis of SL-deficient mutants has allowed the discovery of a new enzyme involving MeCLA. The authors analyzed the expression pattern of known SL-biosynthesis genes and found an unknown gene sharing the same expression pattern across diverse conditions. This gene was named *LATERAL BRANCHING OXIDOREDUCTASE* (*LBO*). *LBO* was shown to encode an enzyme belonging to the 2OGD family. Recombinant LBO produces CLA and hydroxymethyl carlactonoate (1'–OH–MeCLA) from MeCLA (Brewer et al., 2016; Yoneyama et al., 2020a). In addition, lotuslactone was shown to be produced from MeCLA through the LOTUSLACTONE-DEFECTIVE (LLD) enzyme, a 2-oxoglutarate-dependent dioxygenase (2OGD), yet the catalytic function of LLD was not characterized (Mori et al., 2020). Finally, MeCLA can be converted into heliolactone (Wakabayashi et al., 2020). Thus, MeCLA does seem to be a common intermediate in the biosynthesis of non-canonical SLs.

To date, a wide diversity of SL structures has been described in the plant kingdom, and a given species usually produces a few different SLs. However, the evolutionary and biological relevance of this diversity remains unclear. One hypothesis is that this diversity could be linked to the multiple effects of SLs as rhizospheric signals and as endogenous plant hormones.

II-3-B) Evolution of strigolactone biosynthesis

The evolutionary origin of SL biosynthesis has long been debated in the literature. Delaux et al. (2012) reported the presence of sorgolactone in Charales, a sister group of the land plants. Nevertheless, these results were questioned with regards to the failure to detect SLs in other charophyte algae (Delaux et al., 2012). It has been suggested that the detection of sorgolactone in Charales could have been a false positive due to prior SL contamination of the

mass spectrometer (Walker et al., 2019). Similarly, the production of SLs was detected in the moss *Physcomitrium patens* (Proust et al., 2011) but this result was questioned in the literature since orthologs of *MAX1* in this species are missing (Walker et al., 2019). It was demonstrated that PpCCD8 could produce carlactone *in vitro* and that application of either (±)-GR24 or carlactone could restore the *Ppccd8* phenotype (Decker et al., 2017). Later, carlactone was detected in *P. patens* gametophores (Yoneyama et al., 2018a, 2018b). In addition, *P. patens* exudates but not *Ppccd8* exudates could trigger germination of parasitic seeds, suggesting the presence of SLs in *P. patens* exudates (Decker et al., 2017; Lopez-Obando et al., 2021). However, the nature of molecules derived from PpCCD8 other than carlactone is still unknown and other compounds with SL-like activity could be produced by *P. patens*.

Two recent studies have shed light on the origin of SLs. First, phylogenetic studies and genome sequences have revealed that the core genes of the SL-biosynthesis pathway *D27*, *CCD7* and *CCD8* were found in land plants but not in algae (Walker et al., 2019). Second, further analyses of SL contents in diverse bryophytes have allowed the identification of an ancestral SL, named bryosymbiol (BSB). This non-canonical SL (Fig. 9), was also detected in some vascular plants and the authors suggested that BSB was likely present in the most recent common ancestor of land plants (Kodama et al., 2021).

II-3-C) Localization of strigolactone biosynthesis

One of the main challenges regarding the characterization of SLs is their extremely low abundance in plants. The amount of SLs fluctuates depending on plant growth conditions such as nutrient availability (Yoneyama et al., 2007). Regardless, to give an idea, about 100 pg (g root FW)$^{-1}$ of 5DS were found in the roots of sorghum and rice, whereas in shoots, 1 to 10 pg (g shoot FW)$^{-1}$ were detected (Yoneyama et al., 2007; Umehara et al., 2010). Analysis of the expression of SL biosynthetic genes is unable to explain such differences. While some studies have reported a higher level of expression of SL biosynthetic genes in roots, others have found that their expression was similar between roots and shoots (reviewed in Kameoka & Kyozuka, 2018). Using grafting experiments of WT plant scions onto SL-deficient mutant rootstocks, it has been shown that SLs produced in the aerial part were sufficient to suppress shoot branching (Beveridge et al., 2000).

II-3-D) Regulation of strigolactone biosynthesis

II-3-D-a) Strigolactone biosynthesis is regulated by AM symbiosis

The expression of SL biosynthesis genes during AM symbiosis has been studied in several plant species. In response to Myc-LCO treatment, the expression of *D27* was up-regulated suggesting that SL biosynthesis was enhanced prior to contact between AMF and host plants (Hohnjec et al., 2015). The content of SLs in roots was increased in the early stages of the interaction, while at later stages when the fungus profusely colonized the plant the level of SLs decreased (Lanfranco et al., 2018). Nevertheless, the expression of SL-biosynthesis genes could not fully explain this variation. The expression of *CCD7*, *CCD8* and *MAX1* is spatially regulated within the root system in response to AMF (Fiorilli et al., 2015). Despite the heterogeneous results found in the literature, the expression of *CCD7* seems to be up-regulated during AM interaction, more specifically in cells containing arbuscules (Lanfranco, et al., 2018). It is important to note that *CCD7* is also involved in the production of other apocarotenoids involved in AM symbiosis, such as mycorradicin (Walter et al., 2007; López-Ráez et al., 2015). In some studies the expression of *CCD8,* which is more specific to SL synthesis, was not modified, while other studies have reported a positive regulation of *CCD8* expression during AM symbiosis. Nevertheless, the expression of SL-biosynthesis genes may not reflect the amount of SLs produced, as translational and post-translational levels of regulation could also be involved.

II-3-D-b) Strigolactone biosynthesis is regulated by plant hormones

It is well known that phytohormones interact with one another affecting their respective biosyntheses, signaling and transport. SL contents in root exudates and root tissues of rice plants were strongly reduced after application of cytokinins (Yoneyama et al., 2020b) and one gibberellin (Ito et al., 2017). In contrast, auxin application increased root contents of 5DS in sorghum plants (Yoneyama et al., 2015). Using genetic approaches and chemical inhibitors, ABA was suggested to up-regulate the production of SLs, even if ABA application did not result in an increase of SL content (López-Ráez et al., 2010).

In several plant species, higher expression of SL-biosynthesis genes such as *D27*, *CCD7*, *CCD8* and *MAX1* was observed in different SL biosynthesis and perception mutants (for review see Jia et al., 2019). This observation was consistent with the fact that exogenous application of (±)-GR24 decreased the expression of these genes (Mashiguchi et al., 2009). These results highlighted a negative feedback of SLs on their own biosynthesis.

II-3-D-c) Strigolactone biosynthesis is regulated by nutrients

Phosphate supply has long been known to decrease the susceptibility of crops to parasitic weeds, and low phosphate availability is a key factor in the establishment of AM symbiosis (Elias & Safir, 1987). In several plant species deprivation of inorganic phosphate increased the expression of SL biosynthetic genes such as *D27*, *CCD7*, *CCD8*, *MAX1* and *LBO*. This was consistent with an increase of SL content in root exudates (Andreo-Jimenez et al., 2015; Gamir et al., 2020; Umehara et al., 2010; Yoneyama et al., 2020b). In agreement, a high phosphate concentration led to down-regulation of SL biosynthesis genes and reduction of SL content in root exudates (Müller & Harrison, 2019). Moreover, using split-root experiments with root systems divided into two parts exposed to different concentrations of phosphate, a systemic downregulation of SL exudation by phosphate supply was reported (Balzergue et al., 2011). Possible regulatory mechanisms have been proposed. In *Medicago truncatula* two genes involved in the CSSP: *NSP1* and *NSP2*, were shown to upregulate the expression of *MtD27* and *MtMAX1* under phosphate starvation. In root extracts and root exudates of *nsp1* and *nsp1nsp2* double mutants an absence of didehydro-orobanchol and orobanchol was reported. In contrast, an accumulation of orobanchol was detected in root exudates of the *nsp2* mutant. The authors obtained similar results in rice (Liu et al., 2011). Later, Guillotin et al. (2017) showed that a repressor of auxin signaling in tomato, SlAA27, positively regulated the expression of *NSP1*, *D27* and *MAX1* under low phosphate conditions. Silencing the expression of *SlAA27* decreased the amount of SLs exuded into soil and the establishment of AM symbiosis. The authors proposed that SL biosynthesis was controlled by SlAA27 via the up-regulation of *SlNSP1* (Guillotin et al., 2017).

In addition to phosphate, nitrogen and sulfate deficiency were shown to increase SL levels through the up-regulation of *D27* in some plant species (Andreo-Jimenez et al., 2015; Yoneyama et al., 2012).

II-3-D-e) Additional regulators of strigolactone biosynthesis

Other factors have been shown to regulate SL content and SL biosynthesis, for review see Mashiguchi et al. (2020). Briefly, CLE peptides regulate SL content in *M. truncatula* root exudates (Müller et al., 2019). Nitric oxide negatively regulates SL biosynthesis depending on nutrient content (Oláh et al., 2020). Studies reported either a negative or a positive effect of zaxinone, a new apocarotenoid, on SL biosynthesis depending on plant species (Ablazov et al.,

2020; Wang et al., 2019). Last, abiotic stresses such as drought also regulate SL biosynthesis (Haider et al., 2018).

II-4) Transport of strigolactones

Roots and aerial parts from different genetic backgrounds (*i.e.* SL-biosynthesis and SL-perception mutants) were grafted in order to investigate the transport of SLs between plant organs (for review see Kameoka & Kyozuka, 2018). The first observation was that wild-type roots were able to rescue the hyperbranching phenotype of aerial parts mutated in the SL biosynthetic pathway. This result suggested the transport of SLs or their precursors from roots to shoots. Indeed, graft experiments combined with biochemical analysis allowed to demonstrate that SLs, CL, CLA, MeCLA, 1'-OH-MeCLA or derivatives (Brewer et al., 2016; Yoneyama et al., 2020a) are mobile signals from roots to shoots, but not 9-cis-β-carotene or 9-cis-β-apo-10'-carotenal (Waters et al., 2012). Nevertheless, CL, CLA, MeCLA and orobanchol were not detected in the xylem (Xie et al., 2015). Isotope-labeled orobanchol and 4-deoxyorobanchol applied to rice roots were not detected in the xylem but were found in the aerial part (Xie et al., 2015). Taken together, these results suggest that some SL forms or precursors and/or other unknown intermediates are transferred from the roots to the aerial part through cell-to-cell transport, but not likely through the xylem.

Using a reverse genetic approach, a transporter of SLs belonging to the ABC transporter family was described in *Petunia*. PLEIOTROPIC DRUG RESISTANCE 1 (PDR1) was first described as an SL exporter from roots to soil (Kretzschmar et al., 2012). Expression of *PDR1* in *Petunia* roots was localized in the root tips, the cortex and the hypodermis. In the latter cell layer, *PDR1* expression exhibited a cell-type specific localization corresponding to non-suberized hypodermal passage cells (HPCs) (Kretzschmar et al., 2012; Sasse et al., 2015). HPCs have been described in the hypodermis of some plant species and have been hypothesized to facilitate nutrient uptake. Moreover, in these species, mycorrhizal fungal penetration of the root cortex occurred exclusively through HPCs (Sharda & Koide, 2008). In response to phosphate starvation, the expression profile of *PhPDR1* was correlated with the amount of SLs exuded by roots. Smaller amounts of SLs were detected in the root exudates of *Phpdr1* mutants, while overexpression of *PDR1* increased the exudation of SLs (Kretzschmar et al., 2012). In addition, PhPDR1 has been proposed to be involved in SL root-to-shoot transport. First, *pdr1* mutants displayed a hyper-branching phenotype suggesting a role other than SL exudation. Then,

application of isotope-labeled GR24 ($^{[3H]}$GR24) to the root tips of *Phpdr1* mutants resulted in lower levels of $^{[3H]}$GR24 in shoots than in wild-type plants. PhPDR1 displayed a cell-type-specific asymmetric subcellular localization in different root tissues. It was localized at the apical membrane of hypodermal cells in root tips. Above the root tip, it was observed at the outer-lateral membrane of HPCs. Together, these results suggest that PhPDR1 intracellular localization mediates shoot-ward SL transport as well as SL exudation into the soil. Nevertheless, the presence of $^{[3H]}$GR24 was still detected in shoots of *Phpdr1* mutants, suggesting another mechanism independent of *PDR1* involved in SL long-distance transport (Sasse et al., 2015).

In another plant species, *Medicago truncatula,* differing by the absence of HPCs, three homologs of *PhPDR1* were identified. The expression of one of these genes, *MtABCG59,* was up-regulated in response to phosphate starvation and upon SL treatment. Expression of *MtABCG59* was observed in cortical cells and root tips using a promoter-GUS fusion. A mutant for this gene displayed a reduced level of colonization by AMF, and its root exudates exhibited a reduced ability to promote germination of parasitic weeds. Even if the content of SL in *Mtabcg59* root exudates was not directly investigated, the authors proposed that SLs were exuded into the soil through MtABCG59 to attract AMF (Banasiak et al., 2020). This does not exclude the existence of additional SL transporters.

II-5) Strigolactone and karrikin signaling

II-5-A) Strigolactone signaling

Genes involved in the SL signaling pathway were identified by analyzing shoot branching mutants of four plant species: *Arabidopsis*, rice, pea and *Petunia*. They will always be named in the following order: At/Os/Ps/Ph.

Strigolactone signaling begins with their perception by the receptor AtD14/OsD14/PsRMS3/PhDAD2 which belongs to the alpha/beta-hydrolase fold family (Arite et al., 2009; de Saint Germain et al., 2016; Hamiaux et al., 2012; Nakamura et al., 2013; Waters, Nelson, et al., 2012). Strigolactone receptors have the particularity to be receptor-enzyme proteins (Janssen & Snowden, 2012). Despite intensive research by several teams, their mechanisms of action are still debated and several models of SL perception have been proposed (Bürger & Chory, 2020a). The third part of this introduction will be entirely devoted

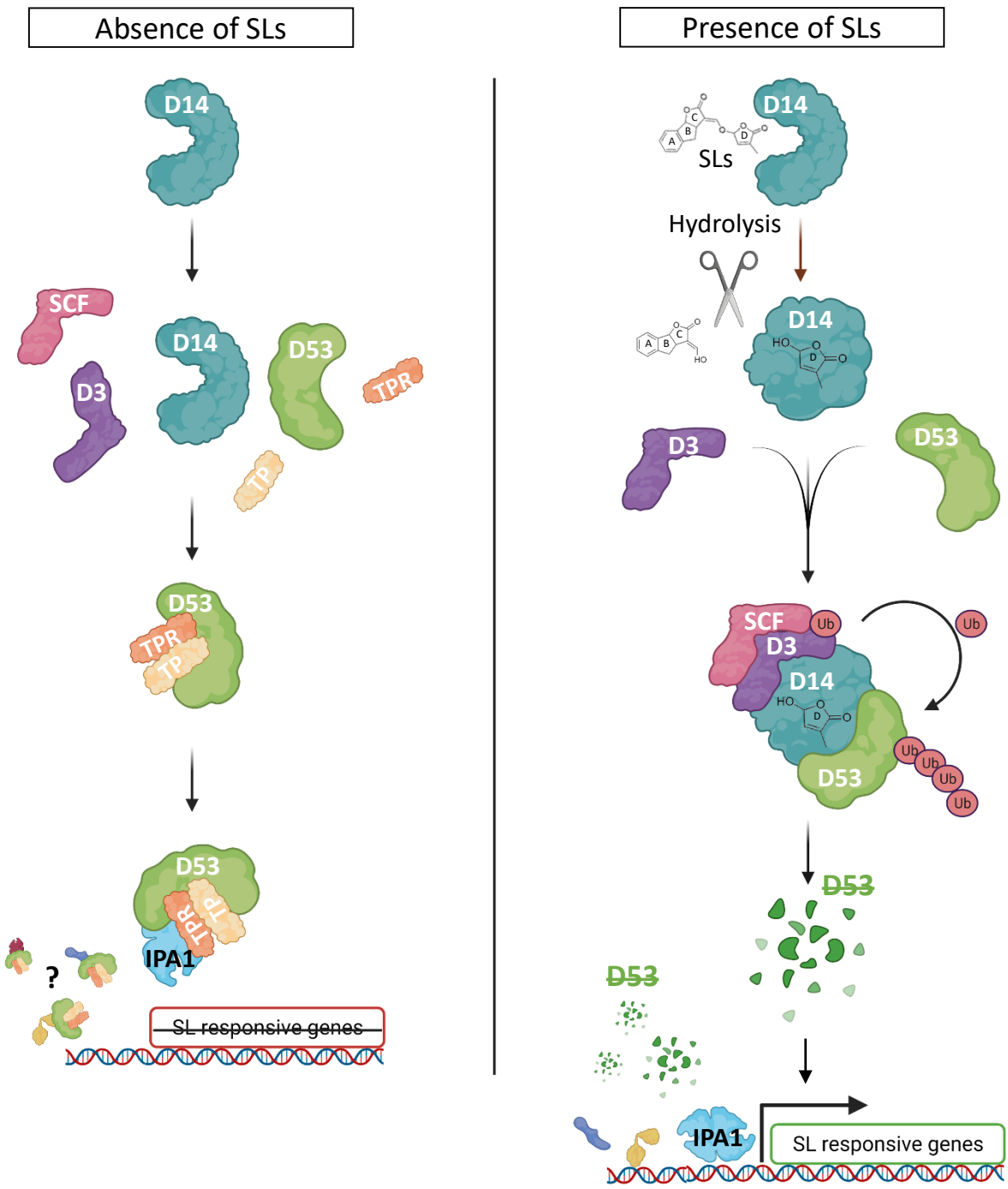

Figure 11. Strigolactone signaling pathway in rice

Left: In the absence of SLs, the SL receptor D14 does not interact with the transcriptional repressor D53, leaving it free to form a complex with corepressors TP/TPR. The complex can interact with transcription factors such as IPA1, inhibiting their transcriptional activity and repressing the expression of target genes.

Right: Upon binding to D14, SLs are cleaved and the D-ring covalently binds to D14. This process triggers a conformational change of D14 and facilitates its interaction with the F-box protein D3. D14 also interacts with the transcriptional repressor D53. The complex formed by D3-D14-D53 allows the degradation of D53 by the 26S proteasome. This releases the repression of IPA1, allowing the expression of SL-responsive genes. Created with BioRender.com.

to SL receptors. Thus, in the following paragraph, I will not go into details of SL perception.

Upon binding to their receptor, SLs undergo a cleavage between the ABC lactone and the butenolide D-ring (Hamiaux et al., 2012). The latter remains covalently attached to a conserved catalytic histidine residue (de Saint Germain et al., 2016; Yao et al. 2016). This leads to a conformational change of the receptor and the recruitment of an F-box protein, AtMAX2/OsD3/PsRMS4/PaMAX2A (Shabek et al., 2018; Stirnberg et al., 2007). MAX2 forms a part of the Skp–Cullin–F-box containing E3 ubiquitin ligase complex (Stirnberg et al., 2007; Zhao et al., 2014). The interaction between the SL receptor and SCF^{MAX2} leads to the ubiquitination of repressor proteins, named SUPPRESSOR OF MAX2 (SMAX1) / SUPPRESSOR OF MAX2-LIKE (SMXL), which causes their degradation by the 26S proteasome (Fig. 11) (Jiang et al., 2013; Soundappan et al., 2015; Wang et al., 2020c; Zhou et al., 2013). The *SMXL* family in *Arabidopsis* comprises eight members: *SMAX1* and *SMXL2/3/4/5/6/7/8* (Stanga et al., 2013), displaying distinct expression patterns and regulating different developmental processes. *Arabidopsis* SMXL6, SMXL7 and SMXL8 and their orthologs OsD53 (Jiang et al., 2013; Zhou et al., 2013) and PsSMXL7 (Kerr et al., 2021) were proposed to be transcriptional repressors regulating SL responses. In agreement, loss-of-function of these genes suppresses SL-related *max2* phenotypes (Soundappan et al., 2015; Wang et al., 2015). The degradation of the corresponding proteins through AtD14-SCF^{MAX2} leads to the relief of the transcriptional repression of their target genes. As a result, these target genes can be expressed and trigger SL-associated responses (Jiang et al., 2013; Soundappan et al., 2015; Wang et al., 2015). D53 directly interacts with transcription factors such as SQUAMOSA PROMOTER BINDING PROTEIN-LIKE (SPL) in wheat and IDEAL PLANT ARCHITECTURE 1 (IPA1) in rice, enabling transcriptional control of downstream genes (Liu et al., 2017; Song et al., 2017). Besides, SMXL6/7/8 interact with the family of corepressor proteins TOPLESS (TPL) and TOPLESS-RELATED (TPR). This interaction is thought to inhibit the expression of SL-responsive genes including *BRANCHED 1* (*BRC1*), *TCP DOMAIN PROTEIN 1* (*TCP1*) and *PRODUCTION OF ANTHOCYANIN PIGMENT* (*PAP*) (Jiang et al., 2013; Soundappan et al., 2015; Wang et al., 2015). Recently, a major breakthrough was achieved using RNA sequencing by Wang et al. (2020b). The authors identified more than 400 SL-responsive genes in *Arabidopsis* mainly regulated by BRC1, TCP1 and PAP1 after SMXL6/7/8 degradation. More importantly, they showed that SMXL6/7 could directly bind DNA to function as transcription factors regulating their own

transcription and that SMXL6 could bind to the promoter of *AtBRC1*, probably by forming a complex with other proteins.

Nevertheless, the transcriptional regulation of genes cannot fully explain all observed effects of SLs. For example, a fast relocalization of PIN proteins was shown to occur after SL application even in the presence of protein synthesis inhibitors (Shinohara et al., 2013), indicating that SL signaling can act through other mechanisms. Some protein members of the SMXL family have been shown to act independently of SLs. SMXL3/4/5 were shown to control phloem formation independently of SLs and of MAX2 (Wallner et al., 2017), while SMAX1 and SMXL2 were shown to act through MAX2 but independently of SLs (Soundappan et al., 2015; Stanga et al., 2013). Consistent with such observations, some phenotypes exhibited in *max2* mutants were not observed in SL-biosynthesis and SL-perception mutants, supporting the implication of MAX2 in another signaling pathway.

II-5-B) MAX2 at the interface between strigolactone and karrikin signaling pathways

Karrikins (KARs) are a set of small butenolide compounds produced upon combustion of plant material, but there are no endogenous karrikins in plants. In an ecological context, karrikins stimulate seed germination of some plant species following wildfires. Interestingly, even plants from environments with low fire frequencies such as *Arabidopsis* can respond to KAR. This has allowed to use genetic tools to study the KAR signaling pathway (Nelson et al., 2009). A first study used a genetic screen to identify two *KARRIKIN-INSENSITIVE* (*KAI*) allelic mutants named *kai1-1* and *kai1-2*, which were shown to correspond to two new *max2* alleles. This finding connected KARs to the SL signaling pathway (Nelson et al., 2011). A second study revealed that KARs and SLs have related signaling components in addition to MAX2 (Waters et al., 2012). *AtKAI2* was identified as a paralog of *AtD14*. While AtD14 mediated SL-specific responses, AtKAI2 mediated KAR responses (Waters et al., 2012) and both proteins were proposed to signal through AtMAX2. Shortly afterwards, the ortholog of *AtD14* in *Petunia PhDAD2*, and *AtKAI2*, were demonstrated to encode SL and KAR receptors respectively (Guo et al., 2013; Hamiaux et al., 2012). As KARs are not endogenous compounds in plants, they were proposed to mimic an endogenous signal that acts through KAI2 and MAX2 (Nelson et al., 2010; Nelson et al., 2011; Waters et al., 2011). This yet unknown signal is now referred to as the KAI2-ligand (KL) (Conn & Nelson, 2016).

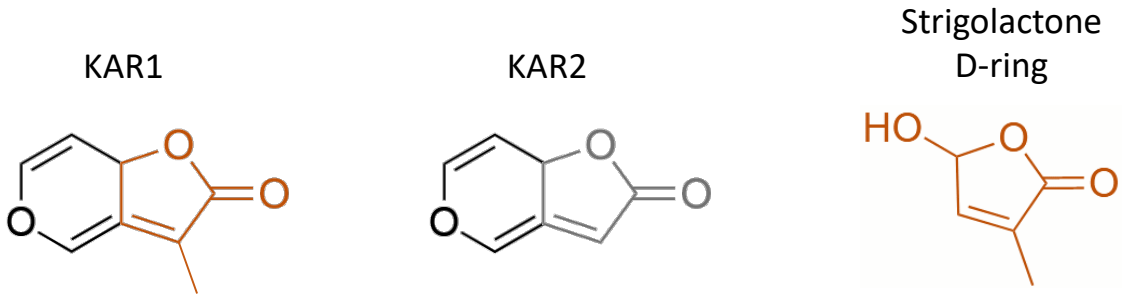

Figure 12. Structure of karrikin1, karrikin2 and the strigolactone D-ring

All SLs possess a methyl-butenolide moiety which is also found in KAR1. KAR2 possesses a unmethyl-butenolide moiety.

Two additional observations connect KARs to SLs. First, they share a structural similarity as they both possess a butenolide moiety (Fig. 12) (Flematti et al., 2004). Second, phylogenetic analyses revealed that SL signaling originates from the KAI2 signaling pathway (Bythell-Douglas et al., 2017; Walker et al., 2019; Waters et al., 2012). SL receptors seem to have evolved through gradual neo-functionalization of KAR receptors, and some proteins belonging to the SMXL family were supposed to be part of KAR signaling (Soundappan et al., 2015; Stanga et al., 2013, 2016).

The tight links between SL and KAR signaling pathways have created confusion at two levels. First, before these links were revealed some *max2* phenotypes were incorrectly attributed to defects in SL signaling. For instance, photomorphogenesis in *Arabidopsis* was thought to be promoted by SLs based on *max2* phenotypes, but was later shown to be rather associated with KL signaling (Waters et al., 2017). Second, the widely used SL analog *rac*-GR24 is a mixture of two stereoisomers, namely (+)-GR24 and (-)-GR24 (Scaffidi et al., 2014). While (+)-GR24 triggers typical SL responses mediated by SL receptors, (-)-GR24 triggers KAR-like responses through KAI2 (Scaffidi et al., 2014). The common use of *rac*-GR24 ((±)-GR24) has therefore added to the confusion by activating both pathways simultaneously. More recently, the use of pure stereoisomers and of mutants in receptors rather than *max2* has allowed to clarify many issues.

II-5-C) The karrikin signaling pathway

The proposed model for KAR signaling is similar to that of SL signaling (Fig. 13): the perception of KARs or KL by KAI2 triggers the recruitment of MAX2 (Toh et al., 2014), which leads to the polyubiquitination of SMAX1 and SMXL2 resulting in their proteolysis. Using co-immunoprecipitation assays in *Arabidopsis* protoplasts, Wang et al. (2020c) demonstrated that AtKAI2 and AtMAX2 interact in the presence of (-)-GR24, which mimics the KAI2 ligand. Moreover, KAI2 directly interacts with SMAX1 and SMXL2 independently of MAX2. Further, Khosla et al. (2020) presented evidence that AtSMAX1/SMXL2 degradation occurs through MAX2 and KAI2 after perception of appropriate ligands (*i.e.*. KARs, (±)-GR24).

The division between the developmental processes controlled by either KAI2 or D14 is not so clear-cut. While SMXL6/7/8 were considered to be specific of the SL pathway and SMAX1/SMXL2 to be specific of the KAR pathway, it was recently reported that application of (+)-GR24 can trigger degradation of SMXL2 by activating D14 (Wang et al., 2020c), and that

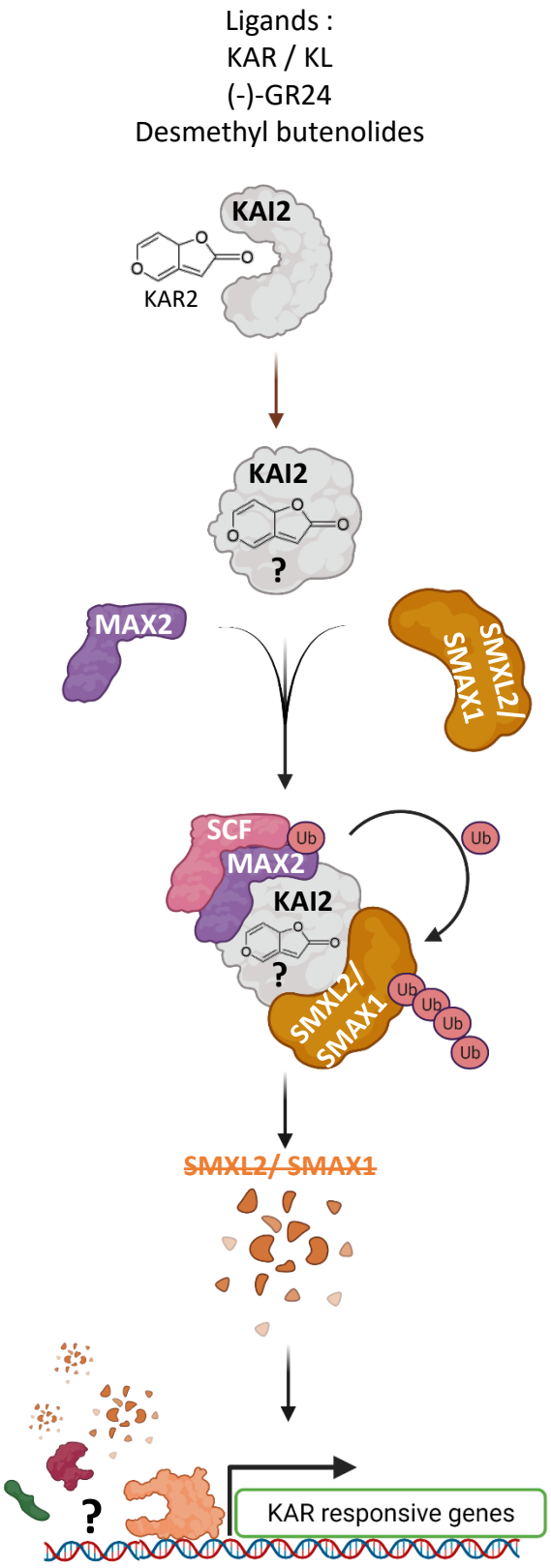

Figure 13. Proposed model for karrikin signaling

KAR, (-)-GR24, desmethyl-GR24 or the putative KAI2-ligand (KL) are recognized by KAI2, triggering the formation of the SCF^{MAX2}-KAI2-SMAX1/SMXL2 complex. This leads to the ubiquitination of SMAX1/SMXL2 and their degradation by the 26S proteasome. The degradation of SMAX1 and SMXL2 releases the transcriptional repression of transcription factors, allowing KAR/KL responses such as activation of germination. Created with BioRender.com.

rice mesocotyl elongation was regulated by both D14 and KAI2 through the degradation of OsSMAX1 (Zheng et al., 2020). These observations show for the first time that KAR and SL signaling pathways can act additively to regulate plant development and that a given SMXL protein might be degraded through both pathways. This makes deciphering the mechanism of action of SLs and KARs even more complex. In addition, a recent study has pointed out that plants responded to (±)-GR24 applications independently of MAX2 and KAI2 in *Lotus*, suggesting the existence of an additional signaling pathway (Carbonnel et al., 2021).

II-5-D) Strigolactone signaling in parasitic weeds

SL signaling downstream of the receptors is still not fully understood in parasitic weeds. *MAX2* and *SMAX1-like* genes were found in several parasitic species, and their functions were shown to be conserved as *Striga ShMAX2* could restore most defects of *Arabidopsis max2* mutants (Liu et al., 2014). Paralogs of *D14* were identified in several parasitic weed species, and referred to as *HTLs*/*KAI2* (HYPO-SENSITIVE TO LIGHT/KARRIKIN INSENSITIVE2 proteins). These proteins hydrolyse SLs and mediate SL-induced seed germination (Conn et al., 2015; Tsuchiya et al., 2015; Toh et al., 2015). An interaction between ShMAX2 and ShHTL7, the most active SL receptor in *S. hermonthica*, was demonstrated *in vitro* (Yao et al., 2017). The current model is that SLs bind KAI2/HTL proteins, which allows the recruitment of MAX2. This would lead to the proteasome-mediated degradation of the repressor SMAX1, and thus de-repress gene expression and allow seed germination (Bunsick et al., 2020).

II-6) Diverse roles of strigolactones

II-6-A) Strigolactones modulate the development of aerial plant organs

Many roles have been reported for SLs in the regulation of plant architecture and in developmental processes. This topic is covered by numerous recent reviews (Bhatt & Bhatt, 2020; De Cuyper et al., 2017; Moreno et al., 2021; Rameau et al., 2019). Here, I will only give a brief overview of these hormonal functions.

The first characterized hormonal role of SLs is their ability to inhibit shoot branching. Plants mutated in the SL biosynthetic pathway exhibit a hyper-branched phenotype that can be restored by applying exogenous SLs (Gomez-Roldan et al., 2008; Umehara et al., 2008). SLs do not regulate these processes alone, but other hormones such as auxin and cytokinins act either antagonistically or synergistically with SLs to regulate shoot architecture. Possible

mechanisms of shoot branching control via SL signaling have been proposed, but are still debated in the literature (for review see Barbier et al., 2019). Two major models which do not exclude one another have been proposed (Rameau et al., 2015). In the first model, SLs act at a systemic level by regulating the localization of auxin transporters. This modifies the auxin flow between the axillary buds and the main stem, increasing the level of competition between buds (Shinohara et al., 2013). Thus, rather than directly inhibiting the growth of axillary buds, SLs are supposed to focus growth into a single branch, resulting in an inhibition of shoot branching (van Rongen et al., 2019).

In the other model, SLs act locally in buds and downstream of auxin by modulating gene expression. SLs promote the expression of the *BRANCHED1* (*BRC1*) gene, a transcription factor known to be a growth suppressor (Brewer et al., 2015). More recently, sucrose signaling has also been connected to the bud outgrowth regulatory network involving auxin, CKs and SLs (Bertheloot et al., 2020; Wang et al., 2020a).

SLs play several other roles in plant aerial organs. Before their enumeration, it is important to note that different effects of SLs have been described using different plant models, and have not always been confirmed across a wide range of plant species. Thus, it is sometimes difficult to distinguish between SL functions conserved among land plants and functions that can be species-specific. SLs promote internode elongation via cell division in pea (de Saint Germain et al., 2013), inhibit hypocotyl growth (Scaffidi et al., 2014), affect leaf shape in *Arabidopsis* (Stirnberg et al., 2002) and *Medicago truncatula* (Lauressergues et al., 2015) and control leaf angle in rice (Shindo et al., 2020). Moreover SLs control vascular secondary growth in *Arabidopsis* (Agusti et al., 2011), induce leaf senescence in different plant species (Takahashi et al., 2021; Ueda & Kusaba, 2015; Yamada et al., 2014) and affect fruit development (Wu et al., 2019).

As mentioned earlier, some *max2* phenotypes were incorrectly attributed to defects in SL signaling but were later shown to depend on the karrikin pathway. The analysis of *kai2* mutants and the use of KARs and (-)-GR24 mimicking the KAI2-Ligand has allowed to identify the phenotypes associated to the KAR signaling pathway: seed germination (Nelson et al., 2012), seedling photomorphogenesis and leaf shape (Waters et al., 2012), leaf cuticle development (Li et al., 2017), root skewing and density of root hairs in *Arabidopsis* (Swarbreck et al., 2019; Villaécija-Aguilar et al., 2019).

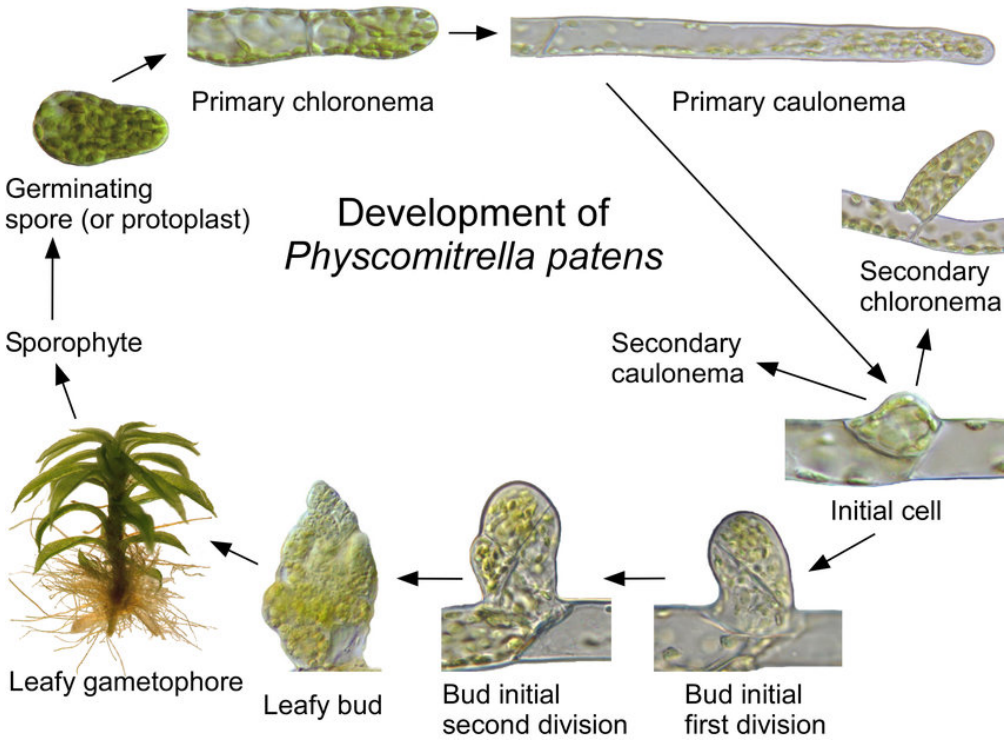

Figure 14. Development of *Physcomitrium patens*

A haploid spore or protoplast germinates to form primary chloronema which subsequently differentiate into more rapidly growing primary caulonema. Caulonemal cells divide to produce initials cells, which develop into lateral secondary choloronemata, secondary caulonemata or buds. Then, buds develop into leafy gametophores. Figure from Robert et al. (2012).

II-6-B) Strigolactones and plant root architecture

In addition to their developmental phenotypes in aerial parts, SL-deficient and SL-insensitive mutants exhibit an abnormal development of the root system. Nevertheless the effect of SLs on root development is not that clear. Depending on plant species, different studies reported opposite root phenotypes in SL-biosynthesis and SL-perception mutants. Furthermore, the growing conditions such as the availability of phosphate and nitrogen affect the root phenotype of SL mutants or the effects of SL application (Marzec & Melzer, 2018; Rameau et al., 2019).

II-6-C) Do strigolactones have a hormonal activity in bryophytes?

In addition to all these studies carried out in angiosperms, hormonal functions of SLs have also been investigated in bryophytes. In particular, they play essential roles in the development of the moss *Physcomitrium patens* (Guillory & Bonhomme, 2021; Hoffmann et al., 2014; Proust et al., 2011). The different developmental structures of *P. patens* are shown in Figure 14. Using SL-deficient mutants and exogenous application of (±)-GR24, two studies reported that SLs repress *P. patens* spore germination (Proust et al., 2011; Vesty et al., 2016) and increase rhizoid length (Delaux et al., 2012). *Ppccd7* and *Ppccd8* mutants displayed enhanced caulomena growth, which could be restored upon application of (±)-GR24. This resulted from a decreased cell division rate and possibly an inhibition of cell elongation (Decker et al., 2017; Hoffmann et al., 2014). Moreover, *Ppccd8* mutants display a strong increase of branches at the base of gametophores and this phenotype was supressed upon (±)-GR24 application (Coudert et al., 2015). In addition, It has been suggested that PpCCD8-derived compounds could act as quorum sensing molecules recruited to reflect plant density (Proust et al., 2011). Vesty et al. (2016) suggested that this quorum sensing mechanisms could prevent spore germination in order to reduce competition for resources. Last, SLs were demonstrated to enhance the resistance of *P. patens* against fungal pathogens (Decker et al., 2017).

In liverwort, the absence of BSB in *Marchantia paleacea* mutants had almost no effect on development or gene expression. In agreement, a small number of genes were differentially regulated upon BSB application (Kodama et al., 2021). With regards to the endogenous action of SLs in *P. patens*, it has been proposed that *P. patens* evolved a hormonal role for SLs independently from other bryophytes (Lopez-Obando et al., 2021; Kodama et al., 2021).

II-6-D) Roles of Strigolactones in biotic interactions

II-6-D-a) Effect of strigolactones on parasitic weeds

To investigate the mechanisms behind the SL-induced germination of parasitic weeds, Tsuchiya et al (2015) designed a fluorogenic SL analog, named Yoshimulactone Green (YLG). This compound has the particularity to generate a fluorescent product upon cleavage, allowing the detection of YLG cleavage *in planta*. First, the authors demonstrated that YLG could activate SL signaling through the SL receptor. Then, they observed the kinetics of YLG cleavage upon application on *S. hermonthica* seeds. Fluorescence was detected in the embryonic root tip within minutes after YLG applications, and then the signal diffused apically over several hours during what they called the "wake-up" phase. Finally, they observed the initiation of germination. This probe has allowed to observe for the first time the dynamics of SL perception in *Striga* seeds (Tsuchiya et al., 2015).

Several studies have investigated the connections between SL-dependent germination of parasitic weeds and ABA, GA and ET signaling. Transcriptomic analysis of *P. aegyptica* has revealed that 48h after (±)-GR24 application, the expression of ABA biosynthetic genes decreased while the expression of GA biosynthetic genes was upregulated (Bao et al., 2017). In agreement, exogenous application of (±)-GR24 decreased ABA contents and increased GA levels in *S. hermonthica*, *P. ramosa* and *P. aegyptiaca* (Lechat et al., 2012; Toh et al., 2012), suggesting that SL-dependent germination occurs via ABA and GA. Nevertheless, application of SL was able to induce germination of *S. hermonthica* seeds even in the presence of GA biosynthesis inhibitors, suggesting a mechanism of germination independent from GA (Bunsick et al., 2020). Ethylene has been known for a long time as a germination stimulant of *Striga* seeds and has been used in the field to trigger suicidal germination of witchweeds. Tsuchiya et al. (2015) showed that ethylene mediated SL-dependent germination by using an inhibitor of ethylene biosynthesis which was sufficient to block GR24-stimulated germination of *S. hermonthica.*

In addition to their effect on parasitic weed germination, SLs are important during the infection of the host plant. The infection process of *Phelipanche aegyptiaca* was affected after silencing of *PaCCD8* and *PaCCD7.* These observations support the possibility that parasitic weeds might also use SLs as endogenous signals (Das et al., 2015).

II-6-D-b) Nitrogen-fixing symbiosis

Given the importance of SLs as signaling molecules in the rhizosphere, their effects during the nitrogen-fixing symbiosis was studied. It is important to note that the effects of SLs during biotic interactions can result from the combination of the effects on the host plant, on the microorganisms and on the interaction between both organisms. To determine if SLs can be perceived by rhizobia, application of SLs on these organisms grown *in vitro* has been tested. GR24 application did not affect the growth nor the expression of *nod* genes of *Sinorhizobium meliloti* (Soto et al. 2010). Later, a study conducted by Tambalo et al. (2014) revealed that bacterial swarming was positively affected by legume seed exudates and crude extracts of *P. patens*. This effect was reduced when extracts of *Ppccd8* mutants were used. Subsequently, application of (-)-2'-*epi*-GR24 was found to increase swarming motility in *S. meliloti* in a dose-dependent manner (Peláez-Vico et al., 2016).

Regarding the role of SLs during the symbiotic phase of nitrogen-fixing symbiosis, contrasting results were reported (Lanfranco et al., 2018; López-Ráez et al., 2017; Rochange et al., 2019). SLs were first proposed to act as a positive regulators during nitrogen-fixing symbiosis (Foo & Davies, 2011; Soto et al., 2010). For instance, application of (±)-GR24 positively affects the nodule number for several plant species such as soybean, pea and *Medicago sativa*. Additionally, plants mutated for SL-biosynthesis genes produced lower number of nodules (López-Ráez et al., 2017). Nevertheless, other studies reported an increased nodule number of SL-insensitive pea mutants, and application of (±)-GR24 decreased the nodule number in concentration-dependent manner in *M. truncatula* (De Cuyper et al., 2015). It is thus difficult to conclude about the effects of SLs on nodulation.

II-6-D-c) Strigolactones modulate pathogenic interactions

The role of SLs in pathogenic interactions with either fungi or bacteria has not been thoroughly investigated (Lanfranco et al., 2018; López-Ráez et al., 2017; Rochange et al., 2019). Different studies reported contrasting results regarding the effects of SL application on the growth of different pathogenic fungi. However, the effects of SLs are observed at very high concentrations, in the order of 10 µM. An increase of hyphal branching has been reported by several studies (López-Ráez et al., 2017). Yet, the biological significance of this branching pattern has not been investigated. The induction of fungal branching in pathogenic fungi and in symbiotic fungi may reflect distinct physiological processes.

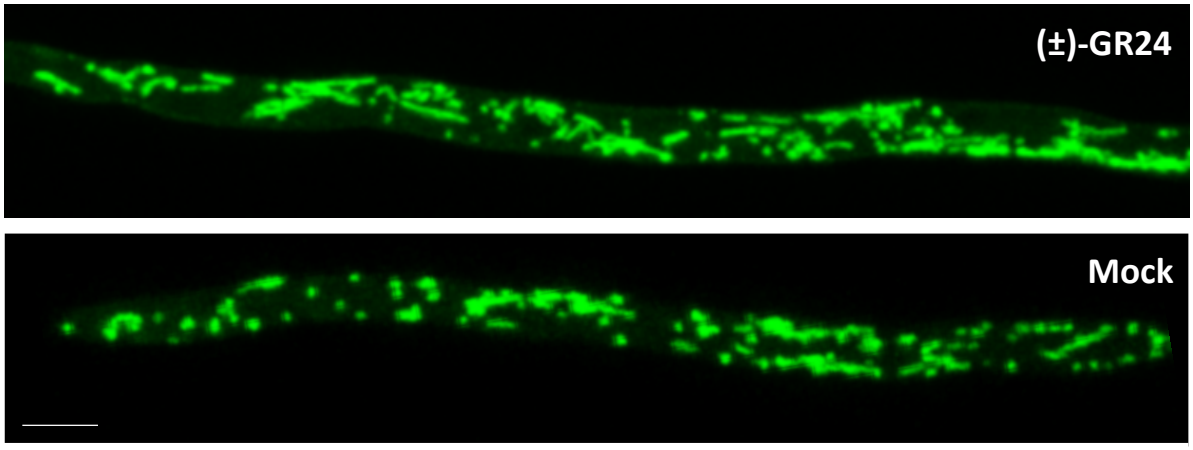

Figure 15. Effect of GR24 on mitochondrial shape and density in hyphae of *Rhizophagus irregularis*

Hyphae were stained with MitoTracker™ Green FM and treated with 100nM (±)-GR24 (top) or mock-treated (bottom) for 6 h. Scale bar = 5 µm. Credit: Auréile Le Ru. (Besserer et al., 2006).

Regarding the role of SLs during pathogenic interactions, a few studies reported a positive effect of SLs against pathogens such as the air-borne necrotrophic fungi *Botrytis cinerea* and *Sclerotinia sclerotiorum* (Decker et al., 2017; López-Ráez et al., 2017; Torres-Vera et al., 2014). In contrast, no differences in disease development caused by the soilborne fungus *Fusarium oxysporum* were observed between SL-deficient pea mutants and wild type plants (Foo et al., 2016).

II-6-D-d) Roles of strigolactones during AM symbiosis

Strigolactones stimulate hyphal branching of several species of the AMF at subnanomolar concentrations. Using Mitotracker, a fluorescent vital stain specific for mitochondria, Besserer et al. (2006) reported that the density, movement and shape of mitochondria in the AM fungus *Gigaspora rosea* were altered in response to SL applications. An increase of about 30% of mitochondrial density in SL-treated hyphae was reported. Moreover, in response to SL the mitochondria moved faster and in an oriented fashion, as compared to the control hyphae. Upon SL application, the mitochondria adopted a thread-like structure oriented parallel to the hyphal axis, while in the absence of SL they were spherical and randomly distributed in the cytoplasm. This was also observed in *Glomus intraradices* (later renamed *Rhizophagus irregularis*) (Fig. 15). An increased germination rate in the presence of SLs was also reported in *R. irregularis* (Besserer et al., 2008). From these observations the authors proposed that SLs induce a metabolic switch reflected by a mitochondrial reorganization, allowing the germinating spore to fully use its energy potential to initiate AM symbiosis (Besserer et al., 2006). To further investigate this hypothesis the associated molecular responses were examined. Application of (±)-GR24 was shown to elicit a fast synthesis and utilization of NADH by fungal mitochondria, which was correlated with an increase of ATP production. In agreement, application of pharmacological inhibitors of ATP synthesis inhibited hyphal ramifications upon SL application, and suppression of mitochondrial biogenesis abolished branching (Besserer et al., 2009). The fast activation of oxidative metabolism upon GR24 treatment suggested that the regulation of this initial boost was mostly post-transcriptional. Indeed, the expression of genes involved in mitochondrial metabolism and hyphal growth was not induced during the initial phase, but was only observed several days later. This late up-regulation of gene expression was correlated with an increase of nuclear division 5 days after treatment with (±)-GR24 or root exudates (Besserer et al., 2008; Buée et al., 2000).

The level of AM fungal colonization in plants deficient in SLs is severely decreased in several plant species (Gomez-Roldan et al., 2008; Vogel et al., 2010). Addition of (±)-GR24 restores the colonization rate of these plants (Gomez-Roldan et al., 2008). Further investigation showed that in SL-deficient plants the level of fungal colonization is affected through a diminution of the number of infection units resulting from a decrease in the number of hyphopodia (Kobae et al., 2018). Nevertheless, no alterations of the symbiotic structures such as truncated arbuscules were observed in these SL-deficient plants. This shows that SLs are not required for hyphal penetration into the roots or for arbuscule formation, but rather for efficient hyphopodium formation (Kobae et al., 2018). Similar observations were made for plants mutated in the SL transporter which mediates SL exudation into the soil. In these mutants, the amount of SLs synthesized by the plants is similar to wild-type plants but the quantity of SLs exuded into the soil is severely decreased (Kretzschmar et al., 2012). This suggests that during AM symbiosis the endogenous role of SLs is not important, but rather that SLs act as rhizospheric signals triggering physiological modifications in the fungal partner. In agreement, plants mutated for the SL receptor do not show a decrease of the level of colonization but rather show a slight increase of fungal colonization. This could be explained by a higher amount of SL biosynthesized by the plants, and therefore an increased quantity of SLs exuded into the rhizosphere (Yoshida et al., 2012).

Bryosymbiol (BSB) is present in several *Marchantia* species which are able to interact with AMF, but not found in those that do not establish AM symbiosis. *Marchantia* mutants affected in BSB synthesis were not colonized by AM fungi. In particular, the pre-symbiotic phase was altered as very few infection points were observed. Treatment of BSB-deficient plants with (±)-GR24 restored a similar colonization level to the control lines. Moreover, application of BSB triggered hyphal branching of an AM fungus grown *in vitro*. These observations showed that in bryophytes, BSB plays a similar role in AM symbiosis as other SLs found in angiosperms.

A reduction in root colonization and arbuscule formation has been observed in rice and pea plants mutated in signaling components downstream of SL receptors, like *d3*/*rms4* (*max2*) (Yoshida et al., 2012; Foo et al., 2013). Yet, these phenotypes did not seem to be associated with the SL signaling pathway, because AM symbiosis was not negatively impacted in plants mutated for the SL receptor. In 2015, Gutjahr et al. demonstrated that the symbiotic interaction was completely abolished in rice *Oskai2* mutants. A complete absence of hyphopodia and intraradical colonization was observed. In addition, induction of marker gene

expression after application of fungal germinated spore exudates was defective in the *Oskai2* line. In addition, *Oskai2* mutants were normally susceptible to colonization by the root pathogen *Magnaporthe oryzae* and by the root endophyte *Piriformospora indica.* This suggested that OsKAI2 may be specifically involved in AM symbiosis and not in interactions with other microorganisms (Gutjahr et al., 2015).

In 2020, Choi et al. investigated the molecular components recruited in response to AMF downstream of the KAI2 receptor. They characterized OsSMAX1, the ortholog of the *Arabidopsis* SMAX1, as a negative regulator of AM symbiosis. *Ossmax1* mutants exhibited an increased number of hyphopodia, intraradical hyphae and arbuscules compared to the wild-type line. This indicated that SMAX1 negatively regulates the AM symbiosis. In addition, mutation of *SMAX1* fully suppressed the phenotypes of *kai2* and *d3* mutants, demonstrating that OsSMAX1 operates downstream of OsKAI2 and OsD3. Transcriptional responses in the *smax1* background revealed that SMAX1 negatively regulates several members of the common symbiotic signaling pathway. Interestingly, SMAX1 also negatively controls the expression of SL biosynthesis genes, highlighting a new crosstalk between the SL and KAR pathways. The authors concluded that activation of the KAI2 signaling pathway results in the removal of SMAX1 (which is further supported by the detection of SMAX1 protein in *kai2* and *d3* mutants but not in wild-type plants) to de-repress critical symbiosis programs (Choi et al., 2020). Interestingly, AM symbiosis was not affected in *kai2* or *max2* mutants of the bryophyte *M. paleacea*, suggesting that the function of KAI2 during AM symbiosis evolved in vascular plant lineages (Kodama et al., 2021).

The SL and KAR receptors, D14 and KAI2 respectively, belong to two different clades of the same protein family. A third clade of the same protein family exists. Recently, a study investigated whether tomato SlDLK2 which belongs to the third clade, was a new regulatory component in the AM symbiosis (Ho-Plágaro et al., 2021). First, *SlDLK2* expression was AM-dependent and associated with cells containing arbuscules. Silencing of *SlDLK2* and *MtDLK2* resulted in increased root colonization and arbuscule abundance. Furthermore, DLK2 interacted with DELLA proteins. DELLAs are known to regulate arbuscule formation/degradation in AM roots. The authors concluded that DLK2 is a negative regulator of arbuscule development and acts as a new component of a protein complex regulating the life cycle of arbuscules (Ho-Plágaro et al., 2021).

II-7) Structure-activity relationship studies

Structure-activity relationship (SAR) studies aim to establish a link between the structural characteristics of a family of compounds and their respective bioactivities. SAR studies on SLs have first been carried out with the aim of managing parasitic weed infections. Several approaches for parasitic weed management have been proposed over the years. One method referred to as the "suicide germination" strategy consists in inducing the germination of parasitic weeds in the absence of host crops, in order to reduce the parasitic seed pool in infected fields. Therefore, SAR studies have aimed to identify synthetic SL analogs that are able to induce parasitic weed germination and that could be produced simply and on a large scale. Subsequently, SARs studies were also performed on plants to take advantage of the ability of SLs to control plant aerial architecture. Because SLs are active on diverse organisms, it was important to search for compounds that are active on some but not on others. In addition, SAR studies were used in fundamental research to unravel the core structure of SLs required for activity on the three kinds of target organisms, as well as the structural characteristics required for specific action on plants, parasitic weeds and AMF. Each study used a different set of SL analogs and measured effects associated with the target organism such as shoot branching, germination or hyphal branching respectively. From these assays, conclusions have been drawn about the minimal structure required for bioactivity on each organism, and this structure is referred to as the SL bioactiphore.

Two types of data can be obtained in SAR studies. The first one is obtained by quantitatively measuring the activity of the different analogs at a given concentration: the potency of each analog is assessed. The second one is obtained by determining qualitatively whether an analog is active at various concentration: the minimum effective concentration (MEC) of each compound is determined. This allows to rank the different analogs according to the minimum concentration required for bioactivity. Both types of data were acquired for SAR studies conducted on plants and parasitic weeds, but generally only the MEC was determined for AMF.

II-7-A) Structure-activity relationship studies on plants

The structural requirements of SLs for hormonal activity were determined by measuring the inhibition of shoot branching/tillering in pea, *Arabidopsis* and rice mutants affected in SL biosynthesis (Fig. 16). Both the MEC and the potency of the compounds were estimated.

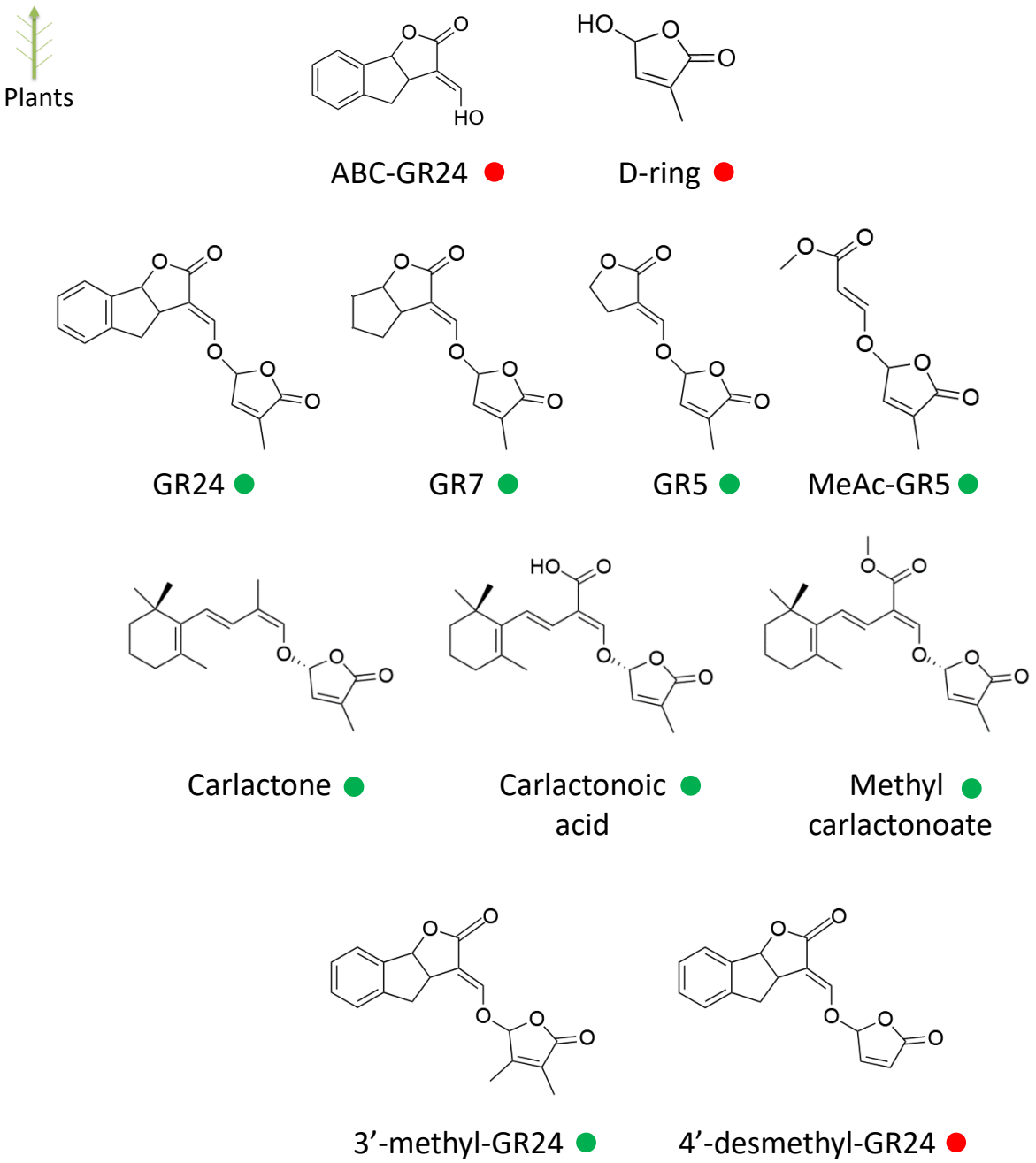

Figure 16. Summary of SAR studies for strigolactone activity on non-parasitic plants

Natural or synthetic SL analogs were tested for their ability to inhibit shoot branching/tillering in pea, *Arabidopsis* and rice mutants affected in SL biosynthesis. Green dots show bioactivity while red dots indicate inactivity of the SL analog (Abe et al., 2014; Boyer et al., 2012; Boyer et al., 2014; de Saint Germain et al., 2021; Nakamura et al., 2013; Umehara et al. 2015).

For example by measuring the number of outgrowing tillers per rice plant at several concentrations, Umehara et al. (2015) were able to compare the MEC required for bioactivity as well as the potency of the different analogs.

The synthetic SL analog GR24 is a canonical strigol-type analog with a modified aromatic A-ring, and is used as a reference in SL research. GR7 and GR5 harbor a simpler structure lacking the A- or AB-rings of GR24, respectively (Fig. 16). Because SLs were shown to be cleaved upon perception by their receptor, the ABC scaffold of GR24 and the D-ring alone were tested. Both were inactive in pea even at very high concentrations (100 µM) (Fig. 16) (de Saint Germain et al., 2021). Nevertheless, at a very high concentration (50 µM) the D-ring alone was bioactive in rice (Nakamura et al., 2013). All four stereoisomers of GR24, GR7 and the two stereoisomers of GR5 are active in rice (Umehara et al., 2015). In pea, the MEC and the potency of GR5 were similar compared to GR24 (Boyer et al., 2012). This indicates that the AB part of the GR24 backbone can be removed in both plant species without losing bioactivity (Boyer et al., 2012; Umehara et al., 2015).

GR5 analogs whose C-ring is not closed, for instance MeAc-GR5 (Fig. 16) were nearly as active as GR5 indicating that the C-ring does not have to be intact to exhibit activity in rice (Umehara et al., 2015). Carlactone, a precursor of SLs in which the B- and C-rings are modified into a carbon chain, is active in rice (Alder et al., 2014) and in *Arabidopsis* (Abe et al., 2014) but with a lower potency compared to GR24. Nevertheless, the carlactone derivatives carlactonoid acid (CLA) and methyl carlactonoate (MeCLA) (Fig. 16) are equally active compared to GR24 in *Arabidopsis* (Abe et al., 2014). This suggests that the non-canonical CLA and MeCLA can function as active hormones for shoot branching inhibition.

The enol-ether bridge connecting the C- and D-rings is a common feature in all natural SLs. In pea and rice, modifications of the enol-ether bridge strongly suppress bioactivity. As the D-ring is also invariable in all SLs identified to date, its importance for bioactivity has been investigated. The methylbutenolide D-ring connected with an enol-ether unit is essential for bioactivity in pea (Boyer et al., 2012) and the replacement of the D-ring lactone group by lactams leads to much weaker activity in *Arabidopsis* (Sanchez et al., 2018). Besides, suppression of the methyl group at position C4’ of the D-ring of GR24 suppresses its activity in pea (Boyer et al., 2012) while addition of a methyl group at the C3’ position (3’-methyl-GR24) enhances GR24 bioactivity in pea (Boyer et al., 2014). Furthermore, reduction of the D-

ring double bond severely reduces bioactivity (Boyer et al., 2012; Umehara et al., 2015). Interestingly, a recent study pointed out that root exudates of cowpea and sorghum plants can reduce the double bond between C3' and C4'. It was postulated that this reduction could represent a new mechanism of SL inactivation (Yamauchi et al., 2018).

Finally, SAR studies pointed out the importance of SL stereochemistry (Flematti et al., 2016). In *Arabidopsis* and in rice, analogs with the natural 2'R configuration are more active compared to those with a 2'S configurations (Scaffidi et al., 2014; Umehara et al., 2015), but this was not observed in pea where 2'S and 2'R SL analogs showed similar activities (F. D. Boyer et al., 2012).

To sum up the results of all these studies, it seems difficult to conclude on a single bioactiphore that would be required for shoot branching inhibition, but it appears that the structure of SL precursors (CLA, MeCLA) is a good start.

II-7-B) Structure-activity relationship study on parasitic weeds

To identify the structural features of SLs necessary to induce parasitic weed germination, various natural SLs and SL analogs have been tested. Both the MEC and the potency of the compounds were determined. The MEC was estimated based on the minimum concentration required to trigger germination of parasitic weeds. The potency of each analog was calculated based on the maximum rate of germination induced by each analog at a given concentration. The potency and the MEC are combined in the EC50 which corresponds to the half maximal effective concentration.

By gathering the different studies conducted on parasitic weeds, it appears that *Striga*, *Orobanche* and *Phelipanche spp.* do not respond in a similar way to SLs. Most broomrapes were more responsive to orobanchol-type SLs, whereas most witchweeds were more responsive to strigol-type SLs (Bouwmeester et al., 2021). For instance the MEC of sorgomol is up to 1000 times higher on *O. minor* compared to *S. hermonthica* (Xie et al., 2008). Among the different orobanchol-type or strigol-type SLs, several compounds exhibited different activities depending on the parasitic weed species. For instance, *O. Cumana* was shown to preferentially germinate upon strigol application compared to fabacyl acetate. In contrast, *O. hedera* was more reactive to fabacyl acetate (Fernández-Aparicio et al., 2011). Furthermore, different sensitivities to SLs were observed within species. For instance, variants of *S. hermonthica* collected from different host plants (maize, sorghum and millet) responded

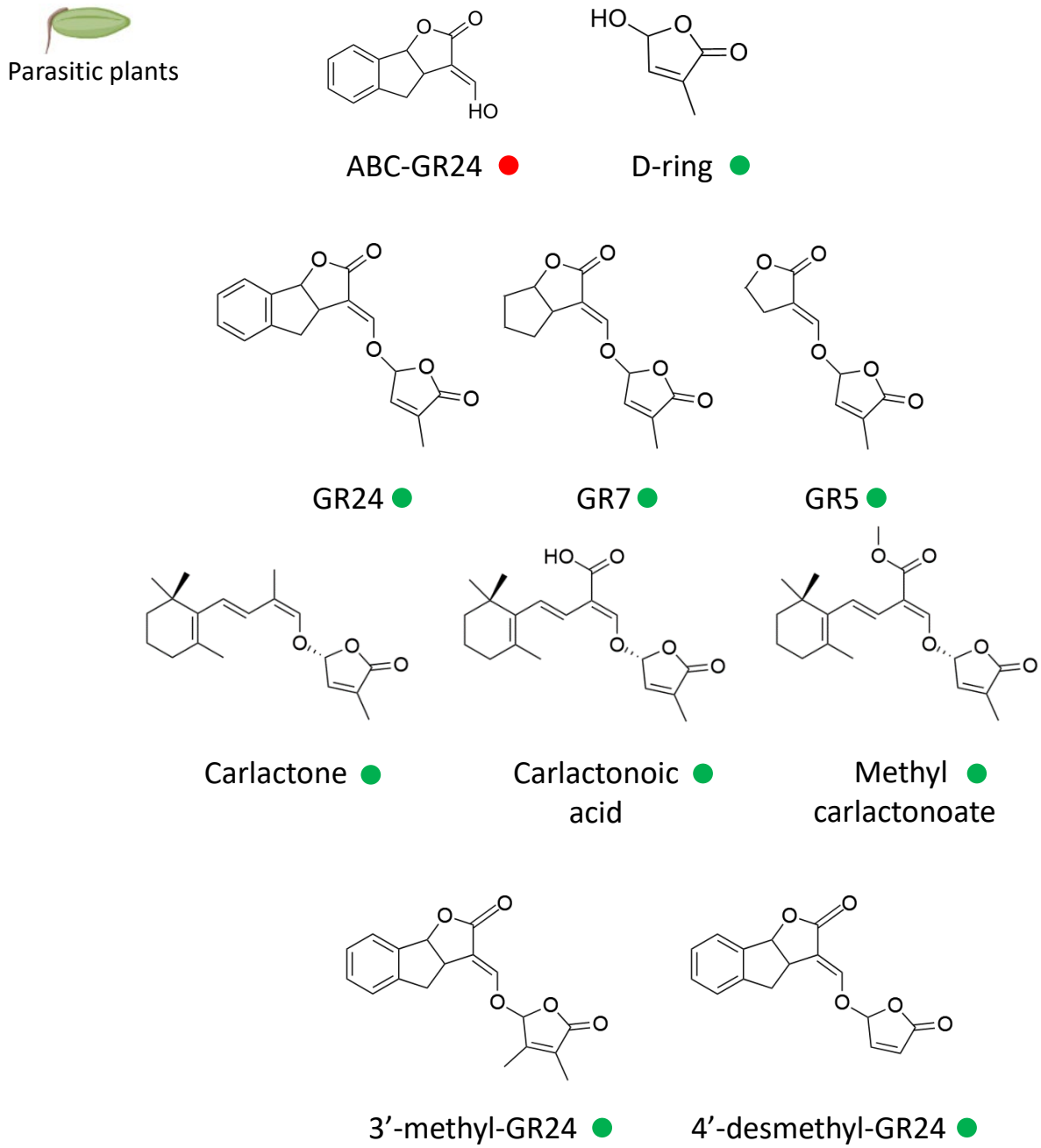

Figure 17. Summary of SAR studies for strigolactone activity on parasitic weeds

Natural or synthetic SL analogs were tested for their ability to trigger seed germination in several species of parasitic weeds. Green dots show bioactivity while red dots indicate inactivity of the SL analog (Boyer et al., 2014; de Saint Germain et al., 2021; Mangnus & Zwanenburg, 1992; Zwanenburg et al., 2009).

differentially both to plant exudates and to GR24 (Bouwmeester et al., 2021). Interestingly a *Sorghum* genotype producing orobanchol instead of 5-deoxystrigol was more resistant against *Striga* (Mohemed et al., 2016, 2018). Therefore, the differential sensitivity of parasitic plants to different SLs may contribute to their host specificity. Nevertheless, from the studies summarized below a general conclusion about the SL bioactiphore required to induce parasitic weed germination has been drawn (Fig. 17).

GR24 induces germination of several parasitic weed species. Nevertheless, its potency is lower than that of natural SLs such as strigol (Zwanenburg et al., 2009). The ABC scaffold of GR24 was inactive. In contrast, the D-ring alone was able to induce germination of *P. ramosa* and *S. hermonthica* at high concentrations (de Saint Germain et al., 2021). However, because D-OH is about 10,000 times less potent than (±)-GR24 at activating *Striga hermonthica* germination, this may not represent a biologically relevant response.

Using GR7 and GR5, the A- and B-rings were shown to be dispensable for bioactivity on *S. hermonthica* and *O. crenata* (Fig. 17) (Mangnus & Zwanenburg, 1992; Zwanenburg et al., 2009). However, the EC50 of GR7 and GR5 were 100-fold higher than that of GR24 in *S. hermonthica* and 10-fold higher in *O. crenata.*

The SL precursor carlactone exhibits a similar germination-inducing activity compared to GR24 on *O. minor*. CLA was less active, but MeCLA was highly active compared to GR24 (Fig. 17) (Abe et al., 2014). The activity of analogs with a modified D-ring has been tested. Addition of a methyl group at the C3' position of the D-ring or suppression of the methyl at the C4' position (Fig. 17) decreased GR24 bioactivity on *P. ramosa* and *S. hermonthica* (de Saint Germain et al., 2021; Mangnus et al., 1992). However, 3'-methyl-GR24 remains as active as GR24 on *O. minor* (Boyer et al., 2014).

Stereochemistry also modulates germination-inducing activity. The GR24 stereoisomers with a 2'R configuration displayed the highest activity, whereas those with a 2'S configuration, and in particular (-)-GR24, were poorly active on *S. hermontica* and *P. ramosa* (de Saint Germain et al., 2021; Mangnus et al., 1992; Thuring et al., 1997).

From these SAR studies the major bioactiphore required to induce parasitic weed germination at low concentrations was proposed to be the D-ring linked to an enol-ether bridge conjugated to a carbonyl group (Takahashi & Asami, 2018).

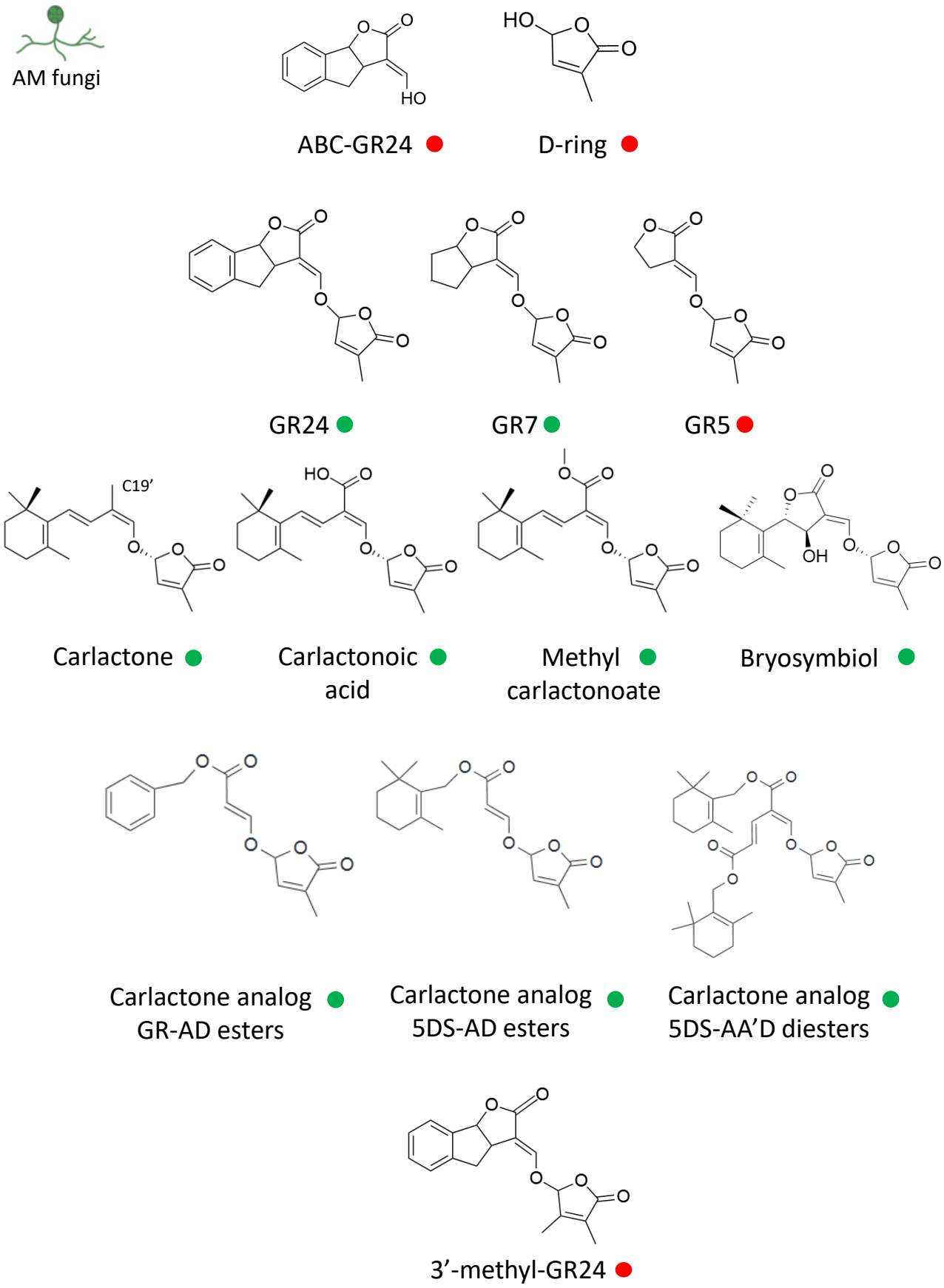

Figure 18. Summary of SAR studies for strigolactone activity on AM fungi

Natural or synthetic SL analogs were tested for their ability to trigger hyphal branching of AM fungi. Green dots show bioactivity while red dots indicate inactivity of the SL analog (Akiyama et al., 2010; Borghi et al., 2021; Kodama et al., 2021; Mori et al., 2016).

II-7-C) Structure-activity relationship studies on AM fungi

The structural requirements for SL activity on AMF were mainly determined by observing hyphal branching activity in germinating spores of the AM fungus *Gigaspora margarita*. To determine their MEC, SL analogs were loaded onto a paper disk placed in front of the tips of secondary hyphae, and were considered active if new hyphal branches developed in the vicinity of the paper disk. The observations were qualitative and the number of new hyphal branches was not counted (Akiyama et al., 2010; Kodama et al., 2021; Mori et al., 2016; Tokunaga et al., 2015; Xie et al., 2019).

Gi. margarita responded differentially to natural SLs. For instance, the MEC of (+)-orobanchol was a 100-fold lower compared to that of (+)-strigol (Akiyama et al., 2010). Similarly, the MEC of medicaol was lower than that of heliolactone (Tokunaga et al., 2015). Even if the MEC of canonical SLs was generally lower, some non-canonical SLs exhibited a low MEC, for instance this was the case of medicaol and carlactonoic acid (Mori et al., 2016; Tokunaga et al., 2015).

Stereochemistry also modulates hyphal branching activity (Akiyama et al., 2010). The 2'S and 2'R configurations do not affect the activity of 4DO stereoisomers (*i.e.* (+)-2'-*epi*-GR24 *vs* (-)-2'-*epi*-GR24), whereas 2'S configuration considerably decreases bioactivity of 5DS stereoisomers (*i.e.* (+)-GR24 *vs* (-)-GR24). This shows that the activities of the different stereoisomers rely on the combination of the B-C and the C-D stereochemistries.

To investigate the SL bioactiphore required for branching activity, analogs of the GR series were used. The ABC scaffold of GR24 was inactive, and so was the D-ring alone (Fig. 18). The enol-ether bridge between the C- and D-rings could be replaced by alkoxy or imino ethers without suppressing activity, even if the MEC was much higher (Akiyama et al., 2010). GR7 was active at high concentration (Akiyama et al., 2010; Besserer et al., 2006). Suppression of the A- and B-rings (GR5) of GR24 suppressed branching activity (Fig. 18). In addition, the importance of the D-ring was assessed in a recent study. Addition of a methyl group at the C3' position of the D-ring suppressed GR24 bioactivity (Borghi et al., 2021; Boyer et al., 2014).

In order to investigate the importance of the B- and C-rings, the activity of carlactone and carlactone derivatives was assessed. The MEC of carlactone was very high whereas that of its derivatives, carlactonoic acid and methyl-carlactonoate (Fig. 18), was low (Mori et al., 2016). Thus, substitutions on C19' modulates the MEC required for branching activity. For further investigations, Mori et al. (2016) designed a set of MeCLA derivatives. The core structure of

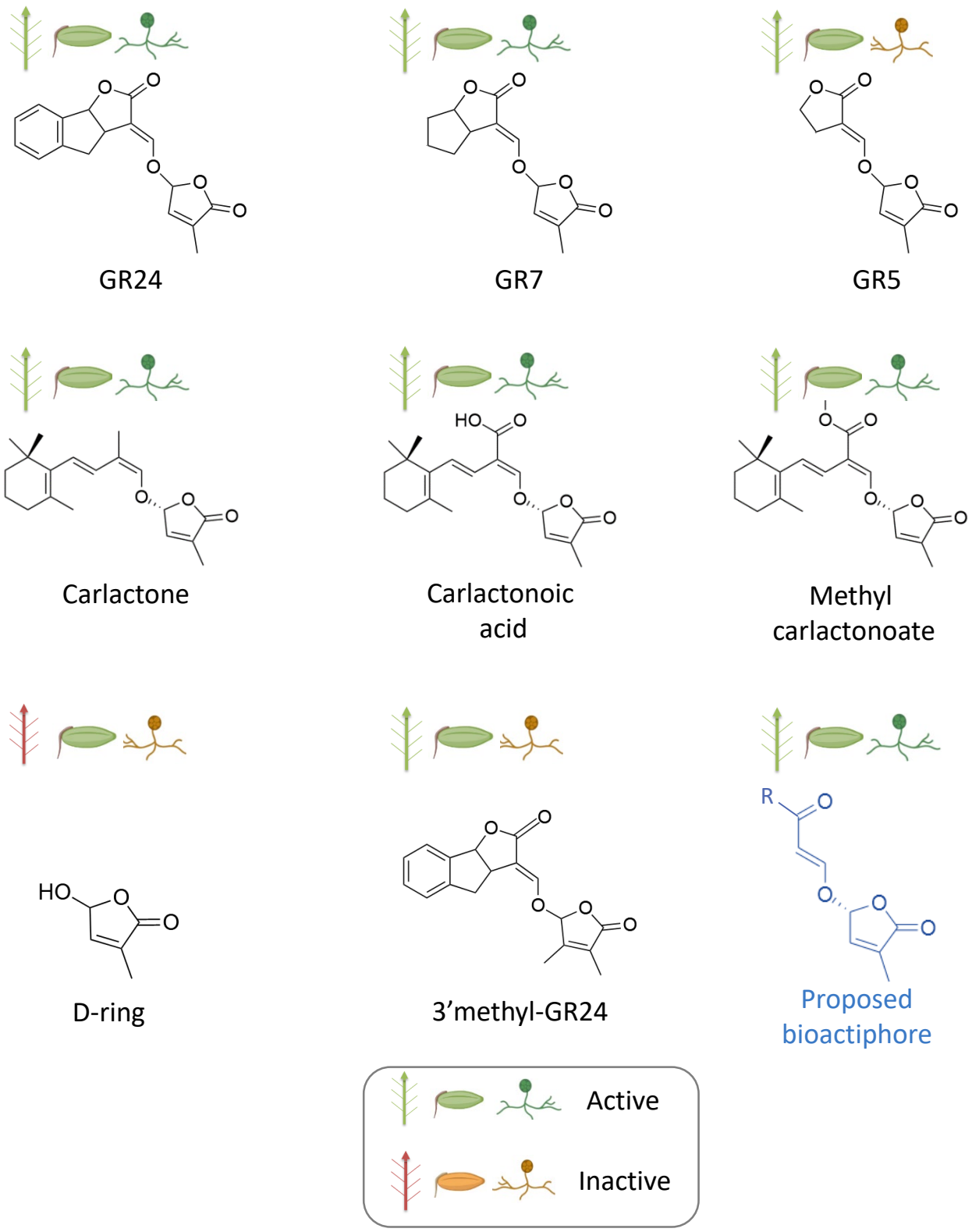

Figure 19. Overview of results of SAR studies on non-parasitic plants, parasitic weeds and AM fungi

The activity of natural and synthetic SL analogs was tested on plants, parasitic weeds and AM fungi. The green color indicates bioactivity, while red indicates inactivity of the SL analog on the given organisms. Comparison of the activity of the different SL analogs led to the proposal of a shared bioactiphore between the three organisms.

these analogs is composed of the D-ring connected to an enol-ether moiety that is conjugated with a carbonyl group. They differ in what connects the carbonyl group to the A ring. Two families of analogs were synthesized, the first carrying the A-ring of GR24 while the second carried the A-ring of 5-deoxystrigol. All these analogs were active and some of them exhibited a low MEC. In addition, the MEC of the recently discovered non-canonical SL bryosymbiol, which harbors an unclosed B-ring, was very low (Fig. 18) (Kodama et al., 2021) and other non-canonical SLs harboring modified A-, B- or C-rings were active such as medicaol, a non-canonical SL harboring an extra carbon on the A-ring (Tokunaga et al., 2015; Xie et al., 2019). Together, these studies suggest that the B- and C-rings are dispensable and that variations on the A-ring can be tolerated (Mori et al., 2016).

In addition to the MEC, different patterns of hyphal branching induced by SL applications have been reported by several studies. The formation of low-order branches composed of long tertiary hyphae was observed after application of 5DS, orobanchol, deoxyorobanchol, while short tertiary hyphae were observed after treatment with GR24, GR7, and medicaol (Akiyama et al., 2010; Tokunaga et al., 2015). Tokunaga et al. (2015) suggested that the structure of the A-ring determines the hyphal branching pattern. Nevertheless, the more recently characterized non-canonical lotuslactone which possesses a similar A-ring as medicaol triggered a long tertiary hyphal branching pattern, invalidating this hypothesis (Xie et al., 2019). Consistent with this observation, carlactone derivatives differing only in C-19 hydroxylation triggered different branching patterns (Mori et al., 2016).

In conclusion, individual SAR studies reveal the importance of some SL structural features for bioactivity on a range of target organisms. They represent an important first step to understand the biological relevance of the structural diversity of SLs produced by plants. Collectively, these studies carried out on plants, parasitic weeds and AMF have led to suggest a shared bioactiphore composed of the D-ring connected to an enol-ether bridge conjugated with a carbonyl group (Fig. 19). The closest chemical structures found in natural SLs are those of carlactonoic acid and methyl carlactonoate. Both are highly active and are considered to be precursors of natural canonical and non-canonical SLs.

II-7-D) Limitations of SAR studies

The first limitation of SAR studies is that the activity of each SL analog is generally evaluated on a single effect for each organism. On the plant hormonal side, bioactivity is measured as

the ability to complement the hyper-branched shoot phenotype of SL-deficient plants. Several observations show that depending on the effect measured, the activity of some compounds may vary. For instance, solanacyl acetate was reported as equally active compared to GR24 in shoot branching assays but was less able to induce SL-associated gene expression (Boyer at al., 2012). Therefore, the bioactiphore for a biological activity such as shoot branching inhibition might differ from that necessary for another activity, for instance fruit development.

In addition, a given visible effect does not necessarily always reflect the same underlying cellular processes. For instance, SAR studies performed on AMF measured the ability of SL analogs to induce hyphal branching as described for natural SLs. Nevertheless, hyphal branching can also be triggered by stresses, hence this response is not specific to SL-like activity. Besides, it is also conceivable that an SL analog activates the fungus to favor the symbiosis independently of hyphal branching. It would thus be interesting to complement hyphal branching tests with assays that evaluate more directly the fungal ability to initiate a symbiotic interaction.

The second limitation is that each SAR study is conducted on one or two species. Thus, one should avoid to draw general conclusions. This is particularly important in situations where differential responses to SL analogs across species are biologically relevant, like in the case of parasitic weeds where they likely contribute to host specificity.

The third limitation concerns the comparison of SAR studies which can involve different experimental designs. Umehara et al. (2015) have shown that SL activity could vary depending of the method of application. For example, when applied hydroponically GR5 was found to be more active than GR24, while when directly applied to axillary buds, the activity of GR5 was weaker. The authors suggested that the uptake of GR5 by the plant was not so efficient when applied on the buds. These observations raise interesting questions about the importance of the physicochemical properties of SL analogs. Properties such as volume, molecular polarity and stability might affect their uptake and transport. For example, Umehara et al. (2015) showed that 5-deoxystrigol was much less stable than GR5. Thus, the lack of effect observed in an experiment could reflect the inactivity of the compound, but also its instability or inability to penetrate into target cells.

III) Strigolactone perception

III-1) First identification of plant strigolactone receptors

Characterization of SLs as plant hormones was achieved by analyzing plant mutants exhibiting a hyper-branched phenotype (Gomez-Roldan et al., 2008; Umehara et al., 2008). Several genes responsible for this phenotype were characterized as genes encoding proteins associated with SL biosynthesis. Other genes were associated with the signaling pathway. The mechanism behind SL perception was first described in 2012 with the identification of the SL plant receptor in *Petunia*, DAD2 (Hamiaux et al., 2012). Two studies in particular had paved the way to the identification of the plant SL receptor.

The first study (Simons et al., 2007), published before the identification of SLs as a plant hormone, was focused on the characterization of dwarf and hyper-branched mutants in *Petunia*. Using graft experiments with different combinations of mutants, two genes named *DAD1* and *DAD3* were shown to be affected in the production of a mobile signal in the plant (later identified as SLs). A third gene, named *DAD2*, was described to act in the perception or in the transduction of the branch-inhibiting signal produced by DAD1 and DAD3 (Simons et al., 2007). Preliminary results indicated that DAD2 was not an ortholog of MAX2, which had been previously identified in *Arabidopsis* and in pea. Thus, they suggested that both genes were signaling components for the branch-inhibiting-signal (Simons et al., 2007). Later the same group characterized DAD2 as the SL receptor of *Petunia*, as will be detailed below.

The second study (Arite et al., 2009) focused on a previously uncharacterized high-tillering dwarf mutant in rice, named *d14-1* (Ishikawa et al., 2005). In order to determine whether the gene associated with the phenotype of *d14-1* played a role in the SL pathway, they produced double mutants of *d14-1* and *d10*, an SL-deficient mutant. The double mutants exhibited the same phenotype as the single mutants. However, while the phenotype of *d10* could be complemented by exogenous treatment with GR24, the phenotype of *d14* and the double mutants could not. Therefore, the *D14* gene played a role in SL signaling rather than in SL biosynthesis. This was supported by an increased amount of SLs in root exudates of *d14-1* mutants compared to root exudates of wild-type plants. The *OsD14* gene was identified by map-based cloning as encoding a protein of the alpha/beta-hydrolase fold family.

III-1-A) The alpha/beta-hydrolase fold family

Alpha/beta-hydrolases (ABHs) are a large family of proteins found in bacteria, animals, plants and fungi (for review see Holmquist, 2005; Mindrebo et al., 2016). ABHs exhibit a wide range of enzymatic functions that primarily consist of the hydrolysis of ester, peptide and carbon-carbon bonds from a wide variety of substrates. Several subfamilies comprise the large family of ABHs such as peroxidases, esterases or lipases. Their hydrolytic activity relies on a catalytic triad composed of a serine, a histidine and an aspartate or a glutamate residue. The catalytic process starts with the nucleophilic attack of the substrate by the catalytic serine, followed by the nucleophilic attack of a water molecule by the catalytic histidine. This first step occurs rapidly and cleaves the substrate. A part of it is quickly released while the other part can remains covalently bound to the enzyme. The second reaction step is slower and consists in the release of the covalently bound part of the substrate. Then the enzyme returns to its initial conformation and can repeat a reaction cycle. A common structure of ABHs is composed of parallel β-sheets surrounded by α-helices. The number of β-strands and α-helical segments varies, but the intermediate loops carrying the catalytic Ser, His, and Asp/Asn residues are the most conserved features defining the ABH family. Nevertheless, structural variations can occur which often reflect the appearance of new biological functions. It is important to mention that ABHs share a highly conserved three-dimensional core architecture but their protein sequences are highly variable. For example, some ABHs have less than 10% sequence similarity but share very similar three-dimensional structures.

In plants, some ABHs have been recruited in hormonal pathways (Mindrebo et al., 2016). For example, salicylic acid binding protein (SABP2) is an esterase that regulates the level of free salicylic acid in plants. Surprisingly, a similar enzyme is present in bacteria of the genus *Paenibacillus,* named PnbE (Wilkinson et al., 2020). PnbE shares only 25% sequence homology with SABP2. Nevertheless, comparison of the two proteins showed that their core structure and the position of catalytic residues were similar. *In vitro* characterization of PnbE demonstrated that the enzyme could bind salicylic acid and exhibited a methyl salicylate esterase activity similar to that of SABP2 (Wilkinson et al., 2020). Although the origin of PnbE has not been studied, it is interesting to note that some microorganisms that interact with plants have acquired the ability to metabolize plant hormones by recruiting enzymes belonging to the ABH family.

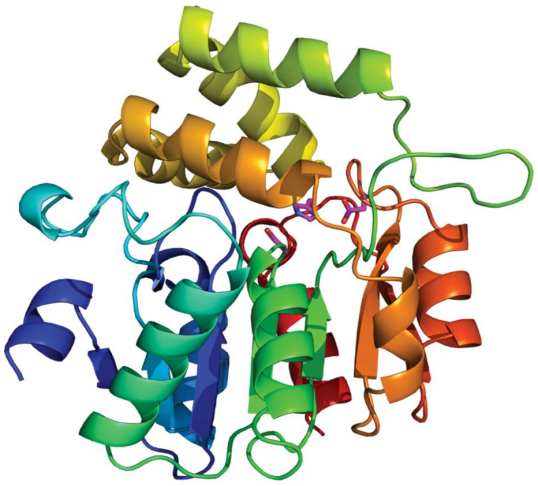

Figure 20. 3D representation of the structure of the plant strigolactone receptor PhDAD2

The catalytic residues are shown in pink while the ribbon structure is colored in rainbow mode from N terminus (blue) to C terminus (red). Figure from Hamiaux et al. (2012).

More surprisingly in a family of enzymes, the gibberellin receptor GID1 has been characterized as an ABH in the lipase subfamily (Ueguchi-Tanaka et al., 2005). GID1 has lost its enzymatic function due to the loss of the catalytic histidine residue, and is able to bind GA (Davière & Achard, 2013; Ueguchi-Tanaka et al., 2005). This triggers a conformational change in GID1 allowing the GID1-GA complex to recruit an SCF-E3-ubiquitin-ligase-complex through the F-BOX protein SLY1. Then, the complex interacts with DELLA proteins, ubiquitinating them and causing their degradation by the 26S proteasome. The destruction of DELLA proteins allows the release of transcriptional repression, thereby inducing the expression of GA-responsive genes.

III-1-B) Identification of DA2, a plant strigolactone receptor

In 2012, Hamiaux et al. identified *DAD2* as an ortholog of rice *D14.* Plants mutated for *dad2* were insensitive to (±)-GR24, confirming that DAD2 was involved in the perception of SLs (Simons et al., 2007). The ability of recombinant DAD2 to bind SLs was first investigated using differential scanning fluorimetry (DSF) assay. In these tests, the melting temperature (Tm) of a target protein in presence or absence of a putative substrate is measured. The interaction between a protein and a compound is reflected by a shift in the melting temperature of the protein in the presence of the compound. This assay has since become a standard reference method to study the interaction between SLs and their receptors. In the presence of (±)-GR24, the Tm of DAD2 was significantly decreased. The authors were the first to establish that DAD2 could bind SLs, and proposed that the destabilization of DAD2 in presence of (±)-GR24 was due to conformational changes, possibly through movement of the lid. The crystal structure of DAD2 was solved revealing that its three-dimensional structure is composed of a 7-stranded β-sheet "core" domain flanked by seven α-helices and a lid composed of four α-helices and connected to the core by a short β-hairpin (Fig. 20). A large hydrophobic cavity lined by seven phenylalanine residues was described between the core and the lid domain and the size of the cavity, named binding pocket, was sufficient to accommodate SL molecules. By comparing the structure of DAD2 with that of GID1, the canonical ABH catalytic triad was identified as the set of S96, H246 and D217 residues. Unexpectedly, the structure of DAD2 and the presence of these three amino acids prompted the authors to suspect that DAD2 may have retained catalytic activity. Using thin layer chromatography and LC-MS analysis, they showed that DAD2 catalyzed the hydrolysis of (±)-GR24 to yield the ABC tricyclic lactone of GR24. To investigate the possibility that DAD2 produced bioactive compounds from SLs, they tested the

effect of the hydrolysis products on bud growth *in planta*, and found that these products were inactive. Interestingly, the Tm shift in DSF assays was no longer observed with two catalytic triad mutants: DAD2^{S96A} and DAD2^{H246A}, both of which exhibited a strongly decreased hydrolase activity. This suggested that the conformational change of DAD2 might be induced by SL degradation. In addition, DAD2^{S96A} was no longer able to complement the phenotype of *dad2* mutants, suggesting that the hydrolase activity of DAD2 was required to trigger the SL signaling pathway *in planta*. Finally, DAD2 interacted with MAX2 in an SL-dependent manner (Hamiaux et al., 2012). Taken together, the results presented in this study highlighted a very particular mechanism of SL perception, in which the DAD2 receptor has retained an enzymatic activity that appears to be essential to activate the SL signaling pathway.

A year later, three different groups reported the crystal structure of rice and *Arabidopsis* D14 (Kagiyama et al., 2013; Nakamura et al., 2013; Zhao et al., 2013). Nakamura et al. (2013) obtained the crystal structure of AtD14 in the presence or absence of GR7. They revealed that the D-ring was trapped inside the binding pocket of D14. Surprisingly, they did not observe large structural changes between the SL-free and the D-OH-bound D14 crystal structures. Mutation of the catalytic histidine residue abolished the capacity of D14 to interact with SLR1, a component of the SCF complex and decreased the hydrolase activity of the protein. The authors suggested that the hydrolysis of SLs led to the formation of the D-OH-bound-D14 complex, allowing its interaction with signaling proteins and the transduction of the SL signal (Nakamura et al., 2013). In parallel, Zhao et al. (2013) obtained the crystal structure of both OsD14 and AtD14 covalently bound to a GR24-degradation intermediate. They reported that a nucleophilic attack of the catalytic serine on GR24 leads to the hydrolysis of GR24 and the release of the ABC moiety, while the intermediate D-ring product remains bound to the catalytic serine (Zhao et al., 2013). At the same time, two studies identified the SL repressor D53 which interacts with D14 in an SL-dependent manner. In the presence of SL, the D53 protein is degraded by the 26S proteasome via MAX2 (Jiang et al., 2013; Zhou et al., 2013). Mutation at any site of the catalytic triad of D14 weakens the interaction between D53 and D14 and results in less degradation of D53 (Jiang et al., 2013).

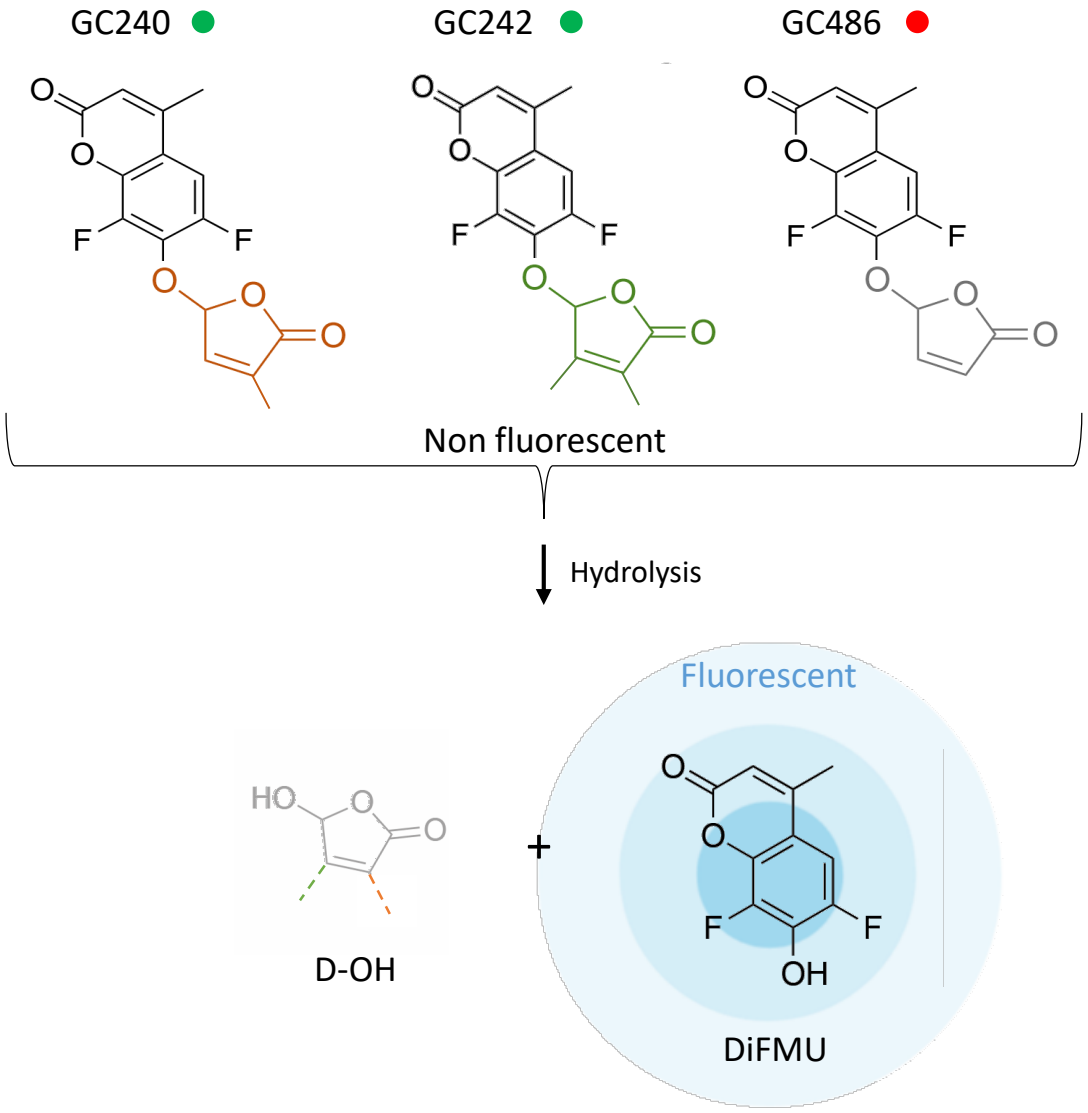

Figure 21. Chemical structures and principle of the GC series of profluorescent probes

This series of probes combine a fluorophore (DiFMU) with a D-ring of SLs. Upon hydrolysis, the fluorophore is released and becomes fluorescent, allowing to monitor the hydrolytic activity of different recombinant proteins (de Saint Germain et al., 2016).

The methyl-butenolide moiety of GC240 (orange) is identical to the conserved D-ring of SLs. GC242 harbors an extra methyl at the C3' position of the D-ring (green), while GC486 lacks the methyl at the C4' position (grey). *In planta*, GC240 and GC242 are active on shoot branching in pea (green dots) while GC486 is inactive (red dot).

III-2) Different models of plant strigolactone perception

III-2-A) The hydrolysis-dependent model of strigolactone perception

In 2016, two studies made major advances in deciphering the mechanism of SL perception. de Saint Germain et al. (2016) identified the ortholog of *AtD14* in pea, named *RMS3*. Using DSF assays they observed that RMS3 was destabilized in the presence of (±)-GR24 and that RMS3 hydrolyzed (±)-GR24. In addition, mutation of the catalytic serine or histidine residue abolished the ability of the receptor to be destabilized by SLs and to hydrolyze them. To investigate the kinetics of RMS3 enzymatic activity, the authors designed profluorescent SL analogs, referred to as the GC series (Fig. 21). GC240 is composed of a 6,8-difluoro-7-hydroxy-4-methylcoumarin26 (DiFMU) linked to the D-ring. Upon hydrolysis the fluorophore (DiFMU) is released, allowing to quantify the receptor hydrolytic activity through the increase of fluorescence. They observed a biphasic time course of fluorescence increase, consisting of a burst phase followed by a plateau phase that was reached within 5 min of incubation. Thus, they hypothesized that the turnover to release the D-ring was extremely slow, suggesting a strong interaction between the D-ring and RMS3. Using mass spectrometry, they detected a mass shift corresponding to the D-ring covalently bound to RMS3 and more specifically to the catalytic histidine (de Saint Germain et al., 2016). The same authors designed two GC analogs exhibiting either an extra methyl at the C3' position of the D-ring (named GC242) or the suppression of the methyl group at the C4' of the D-ring (named GC486) (Fig. 21). Interestingly, they demonstrated that GC486 which did not have biological activity on pea was cleaved by RMS3 significantly more rapidly compared to GC240 and GC242 which were active on pea. This faster hydrolysis was correlated with the absence of covalent binding between RMS3 and GC486 probe. Thus, the methyl group at the C4' of the D-ring, conserved in all natural SLs, is essential for the formation of the covalent complex between the catalytic histidine and the D-ring to trigger SL signal transduction (de Saint Germain et al., 2016).

In parallel, Yao et al. (2016) suggested a similar mechanism of SL perception based on crystal structures. The authors obtained the crystal structure of the SL-induced SL-AtD14-D3-ASK1 complex. They observed that upon binding to SLs AtD14 undergoes an open-to-closed state transition, allowing the interaction with MAX2 to trigger signaling. This transition is mediated by the covalent binding of a D-ring-derived intermediate to the receptor (referred to as Covalently-Linked Intermediate Molecule: CLIM). The authors suggested that CLIM represents

a novel active hormone related to SLs, that is generated by AtD14-mediated SL hydrolysis and sealed inside AtD14 through covalent binding with the catalytic histidine and probably also with the catalytic serine (Yao et al., 2016).

The model emerging from these two studies has since been challenged and other models independent of SL hydrolysis have been proposed.

III-2-B) The hydrolysis-independent model

Three major observations challenged the SL hydrolysis-dependent model. The first observation is that several non-hydrolysable SL agonists are still active on plants (McCourt et al., 2017). The second argument presented by Seto et al. (2019) is that the kinetics of SL cleavage does not fit the kinetics of SL signal transduction: the rate of hydrolysis of (±)-GR24 by the SL receptor is too slow compared to the activation of the SL signaling pathway. The last observation came from the re-examination of the crystallographic structure of several SL receptors by Carlsson et al. (2018). The authors claimed that the molecule observed by Yao et al. (2015) and referred to as CLIM is not related to SLs, but most likely involves a buffer or crystallization compound such as an iodide ion. Yet, further analysis of the crystallography data by Burger et al. (2020) suggested that the D-ring was indeed attached to the catalytic histidine as proposed by Zao et al. (2015) and de Saint Germain et al. (2016).

From these observations, two studies proposed an SL hydrolysis-independent-model. First, Shabek et al. (2018) obtained crystals for rice OsD3 (MAX2) and the D3-D14-D53 complex. D3 has a C-terminal helix that can switch between two conformational states. The first state can bind the closed conformation of CLIM-bound-D14, while the second state allows the interaction with SL-bound-D14. The hydrolase function of D14 is strongly reduced upon interaction with D3, but the addition of D53 can reactivate the hydrolytic function of the SL receptor. Therefore, the authors proposed that D3 could bind hormone-bound-D14 and prevent SL hydrolysis by D14. The hormone-bound-D14-D3 complex is then able to interact with D53 which is polyubiquitinated and degraded. D53 degradation leads to the re-activation of D14, allowing it to hydrolyze SLs. Then, upon SL cleavage the SL receptor can in turn be polyubiquitinated by the SCF^{-D3} complex and degraded by the proteasome. In this model, the hydrolysis of SL is not required for signal transduction but occurs afterwards, to regulate homeostasis of the substrate (Shabek et al., 2018).

The second study (Seto et al., 2019) established a link between the ability of SL analogs to be active in plants and their ability to induce a melting temperature shift of AtD14 in DSF assays. This correlation is in line with the hypothesis that SLs induce conformational changes of SL receptors to allow the recruitment of partner proteins. However, this correlation is no longer found when it comes to link the biological activity of SL analogs to their capacity to be cleaved by SL plant receptors. Indeed, the SL analogs debranones are bioactive on plants and can induce a conformational change of AtD14, but are only poorly hydrolyzed by AtD14. From this observation, the authors raised the question of whether receptor-mediated SL hydrolysis is required for signal transduction, challenging the SL hydrolysis-dependent model.

To further investigate their hypothesis, Seto et al. (2019) performed a time-course DSF experiment coupled with quantitative detection of SL analogs and their hydrolysis products. They reported that the conformational change induced by several SLs occurs before SL hydrolysis. Moreover, they observed that both hydrolysis products, the ABC moiety and D-ring, are released at almost the same rate as GR24 is consumed. This observation did not support the model in which the D-ring is covalently trapped in the SL receptor. If this model was correct, the D-ring should be released later compared to the ABC moiety. The authors suggested that uncleaved SL, not the hydrolysis intermediate (CLIM), induces the conformational change of AtD14 to allow signal transduction, even if they also observed the presence of the D-ring covalently bound to AtD14. They suggested that the D-ring did bind to AtD14 but was released rapidly without being trapped tightly in the binding pocket. Next, they evaluated the correlation between the hydrolytic activities of recombinant AtD14 mutated for one of the three catalytic residues (AtD14^{S97A}, AtD14^{D218A}, and AtD14^{H247A}) and the capacity of the corresponding genes to restore responses to SLs in *Atd14* mutants. The hydrolase activity of the three recombinant proteins *in vitro* was drastically reduced (Seto et al., 2019) and *Atd14* mutants expressing *AtD14^{S97A}* or *AtD14^{H247A}* were deficient for SL responses. Yet, the most striking result of this study was that expression of *AtD14^{D218A}* fully restored responses to SLs in *Atd14* mutants. Thus, despite lacking hydrolase activity, AtD14^{D218A} was still able to trigger SL signaling *in planta*. The activity of AtD14^{D218A} was confirmed by the capacity of this protein to interact with SMXL7 in an SL-dependent manner in yeast two-hybrid assays, and with MAX2 in yeast three hybrid. Moreover, plants expressing AtD14^{D218A} were more sensitive to GR24 treatment, which may be explained by the accumulation of GR24 due to the lack of hydrolytic degradation of GR24 by AtD14^{D218A}. Thus,

they proposed that the hydrolytic degradation of SLs by D14 would only serve to deactivate bioactive SL to prevent an excessive SL response. In addition, another *Arabidopsis* mutant, AtD14^{R183H}, could not complement the phenotype of *Atd14* mutants which was confirmed by the incapacity of AtD14^{R183H} proteins to interact with SMXL7 protein. Yet AtD14^{R183H} protein could still exhibited similar hydrolase activity compared to AtD14 (Seto et al., 2019).

In *Arabidopsis*, AtD14 has been shown to undergo 26S proteasome-dependent degradation (Chevalier et al., 2014). Hu et al. (2017) showed that SL perception and receptor degradation could be uncoupled. Further, receptor degradation depended on D3 and D53. More importantly, D14 proteins mutated in the catalytic triad were much less degraded, suggesting that the hydrolase activity of D14 could be important for the SL-induced degradation of the receptor. These data seem consistent with the model proposed by Shabeck et al. (2018) and Seto et al. (2019) where hydrolysis of SLs would not be required for signal transduction, but for the degradation of the receptor and the SL molecule.

III-3) Evolution of plant strigolactone perception

Plant SL receptors are thought to have originated from an expansion of the streptophyte *KAI2-like* family, forming two ancient lineages named *eu-KAI2* and *DDK* (D14/DLK2/KAI2) (Bythell-Douglas et al., 2017). In contrast to D14 which is only found in seed plants (Delaux et al., 2012), the DLK and KAI2 proteins are present in all land plants. The KAI2 proteins cannot perceive natural SLs. However, KAI2 proteins can bind to SLs harboring the non-natural 2'S configuration between the C- and D-rings. It has been proposed that D14 evolved the capacity to perceive natural 2'R SLs in flowering plants through neo-functionalization of KAI2-like proteins (Bythell-Douglas et al., 2017). In the bryophyte *M. paleacea*, *Mpkai2* and *Mpmax2* mutants exhibited developmental phenotypes such as reduced growth of the thallus, which could not be restored upon (+)-GR24 application. Biochemical analysis showed that MpKAI2 was not able to bind SLs harboring a 2'R configuration but rather could bind to 2'S stereoisomers, similarly to the KAI2 receptor in angiosperms. This suggested that MpKAI2 does not mediate the perception of SLs but rather has a similar function to that of the angiosperm KAI2 proteins (Kodama et al., 2021). Because *M. paleacea* SL-deficient mutants did not show any developmental phenotypes, the authors hypothesized that SL does not function as an endogenous hormone in bryophytes, as these lack of a receptor capable of perceiving SLs. To test their hypothesis, the authors expressed an angiosperm SL receptor,

AtD14, in *Mpkai2* mutants. In these transgenic lines, treatment with GR24 stereoisomers harboring the 2'R configuration was able to rescue the developmental phenotype. This showed that *M. paleacea* was not able to respond to SLs due to the lack of a cognate SL receptor.

A recent study examined the taxonomic distribution of the *KAI2* gene family outside the plant kingdom using BLAST searches. Significant homologs were found in bacteria and streptophytes and annotated as RsbQ proteins. Phylogenetic analyses suggested that the plant *KAI2* gene family was acquired from bacteria by horizontal gene transfer, probably before the emergence of streptophyte algae (Wang et al., 2021b).

III-4) Strigolactone perception in mosses

In the genome of the moss *Physcomitrium patens*, 13 *KAI2-LIKE* (*PpKAI2L*) genes were identified. These genes were classified into 4 clades named *PpKAI2L-(A-E)*, (*FK*), (*HIL*) and (*JGM*) respectively. Phylogenetic analyses grouped the three clades (FK), (HIL) and (JGM) into the super-clade DDK, while the clade (A-E) belongs to the eu-KAI2 clade (Lopez-Obando et al., 2021). Burger et al. (2019) showed that *in vitro*, the proteins PpKAI2L-C, -D and -E bind (-)-5-deoxystrigol (exhibiting a 2'S configuration) whereas PpKAI2L-H, -K and -L bind karrikin 1 (Bürger et al., 2019). Yet, proteins able to perceive (+)-SL were not identified in this study.

Lopez-Obando et al. (2021) used a combination of *P. patens* mutants, pharmacological treatments, *in vitro* binding assays, and cross-species complementation to dissect the roles of the proteins involved in SL and KL perception in *P. patens*. Recombinant proteins belonging to the clade (A-E) were destabilized by (-)-GR24 (2'S configuration) and were able to hydrolise it. Both developmental phenotypes and transcriptional response upon application of (+)-SL were unaffected in the clade (A-E) *Ppkai2l* mutant, suggesting that clade (A-E) PpKAI2L proteins are not receptors for SLs. Analysis of *Ppkai2l-f, -k* did not reveal a clear phenotype of these mutants nor any difference in the capacity to respond to different GR24 stereoisomers (Lopez-Obando et al., 2021). Therefore, the clade (FK) was not supposed to comprise SL receptor(s) and the biological role of these proteins remains to be discovered. Unfortunately, the authors were unable to produce recombinant proteins in the clade (JGM). Nevertheless, in the dark the caulonema number in the triple mutants no longer decreased in presence of (+)-GR24, suggesting that PpKAI2L (JGM) might act as SL receptors.

To conclude, it can be proposed that SL perception arose in *P. patens* through neo-functionalization of some *KAI2-like* paralogs, resulting in convergent evolution with regards to D14-mediated SL perception in angiosperms. Nevertheless, differences exist between the moss and angiosperm pathways since *P. patens* seems to respond to SLs independently of PpMAX2, and none of the *PpKAI2L* genes could significantly rescue the branching phenotype of the *Arabidopsis d14 kai2* double mutant (Lopez-Obando et al., 2021).

III-5) Strigolactone perception in parasitic weeds

Parasitic weeds use a very sensitive mechanism to detect SLs, at concentrations as low as picomolar, as an indication of the proximity of a host plant. By searching homologs of SL and KAR plant receptors in the genome of parasitic weeds, two major studies have shed light on the evolutionary process that gave rise to the SL dependency of germination in these species. Gene sequence analysis revealed a large expansion of *KAI2/ HYPOSENSITIVE TO LIGHT* (*HTL*) copy number in parasitic weed species (Conn et al., 2015; Toh et al., 2015), while a single homologous copy of *D14* was found in different species of parasitic and non-parasitic plants belonging to the *Lamiidae* clade. The number of *KAI2/HTL* copies depends on the parasitic weed species: for example, *S. hermonthica* has 13 *KAI2* paralogs, while *S. asiatica* has 21 (Conn et al., 2015; Yoshida et al., 2019). These paralogs have been classified into three clades, the ancestral conserved clade (*KAI2c*), the intermediate clade (*KAI2i*) and the rapidly-evolving-divergent clade (*KAI2d*). Proteins from each clade exhibit different capacities to bind KARs and SLs. The conserved clade does not bind to either KARs or SLs. The intermediate clade binds to KARs but not to SLs, while KAI2d binds to SLs but not to KARs (Nelson, 2021). In agreement, the latter proteins harbor binding pockets which resemble that of AtD14 (Conn et al., 2015; Toh et al., 2015; Xu et al., 2016).

In order to investigate whether KAI2d proteins are SL receptors or simply SL-binding proteins, several approaches have been used. Briefly, *in vitro* characterization showed that KAI2d proteins were able to hydrolyze SLs (Xu et al., 2018). In addition, calorimetry assay, differential scanning fluorimetry (DSF) and nano-DSF showed that KAI2d proteins have a high affinity for several SLs (de Saint Germain et al., 2021; Wang et al., 2021c). Last, in cross-species complementation experiments, *KAI2d* genes from *S. hermonthica* and *P. ramosa* were able to restore responses to SLs in *Atd14* mutants (de Saint Germain et al., 2021; Nelson, 2021; Toh et al., 2015). Together, these results demonstrated that KAI2d proteins are SL receptors.

One of the proteins of *Striga hermonthica*, ShHTL7, has received a lot of interest due to its high sensitivity to SLs. The mechanisms of SL perception and signal transduction of ShHTL are similar to those of SL receptors in non-parasitic plants. Upon hydrolysis of SLs, a covalent binding to the D-ring occurs. The complex ShHTL7-CLIM is formed and allows the recruitment of ShMAX2 (Yao et al., 2017). Using molecular dynamics simulations, Burger et al. (2020) suggested that SLs could sometimes enter into the plant receptor binding pocket but in the wrong orientation, which prevents their hydrolysis. The binding pockets of SL receptors in parasitic weeds would be flexible enough to allow the reorientation of the SL molecule and its subsequent hydrolysis (Bürger & Chory, 2020b). Chen et al. (2021) showed that ShHTL7 was more efficient than AtD14 at positioning (+)-GR24 in the right orientation to be hydrolyzed. In conclusion, it appears that the hypersensitivity of ShHTL7 is the result of its enhanced ability to bind and hydrolyze SLs, and its flexibility to switch from an inactive to an active state (for review, see Nelson, 2021).

Parasitic weed germination can also be triggered by other compounds that have no common structural features with SLs, such as ITCs (isothiocyanates). Interestingly, ITCs are perceived by the same receptors as SLs (de Saint Germain et al., 2021). This shows the high flexibility of these receptors to perceive a wide range of molecules.

III-6) Strigolactone perception in AM fungi

Mycorrhizal fungi respond to a wide variety of SLs at very low concentrations, however the mechanisms of SL perception remain unknown. To date, there is no hint available in the literature as to the nature of fungal SL receptors. No strong homologs of plant SL receptors have been identified so far in AM fungal genomes using sequence alignments (BLAST). To overcome the lack of mutants in AMF, Fiorilli et al. (2022) searched for fungal SL receptors in the plant pathogenic fungus *Cryphonectria parasitica*, for which mutants can be generated. They identified a structural homologue of D14, which could covalently bind and cleave (+)-GR24 *in vitro* (Fiorilli et al., 2022). The weakness of the *C. parasita* model is that this fungus only responds to SLs at high concentrations (in the range of 10 to 100 µM). Furthermore, the observed response is a reduction of fungal colony diameter. The sensitivity and developmental responses triggered by SLs are quite different inAM fungi, suggesting that the associated perception and signaling mechanisms are also different. In my PhD project, we took a more directapproach to gain insight into the nature of SL receptors in AM fung

Thesis outline

The Mycormones project aims to study the importance of phytohormones in the biology of mycorrhizal fungi. My contribution concerns more specifically the perception and responses to SLs in these fungi.

The first chapter aims to enrich the SAR studies regarding SLs and AMF. The use of SL analogs bearing variations on the D-ring has improved the understanding of SL perception in plants. However, activities on AMF of these analogs have not yet been tested. We thus decided to use such analogs in a SAR study based on two different bioassays.

The second chapter focuses on the characterization of SL perception mechanisms in AMF. Prior the beginning of my thesis, preliminary data obtained by the team suggested that AM fungal SL receptor shared structural and functional features with plant SL receptors. Following this hypothesis, eight putative SL receptors were identified in the genome of the AM fungus *Rhizophagus irregularis*. One of the major goals of my thesis was to characterize these proteins. Their capacities to bind and to cleave SL analogs were evaluated *in vitro*. To investigate their biological function, the results of the SAR study (chapter 1) were compared with the ability of these SL analogs to bind and/or to be cleaved by the candidate proteins, and the activity of inhibitors known to target SL plant receptors was assessed.

The third chapter aims to investigate whether phytohormones could be transferred between plants connected by a common mycorrhizal network (CMN). Experimental setups were designed and implemented to address the transport of hormones between *Medicago* or tomato plants connected by a CMN. I will briefly report the results of this part of my PhD project.

Finally, I will propose a general discussion of my results as well as perspectives for future developments of this work.

Chapter 1
Structure-activity relationships of strigolactones on *R. irregularis*

Background

Prior to the beginning of my thesis, the group was investigating the structure-activity relationships (SAR) of SLs on AMF. At my arrival, I continued this project. We combined two different approaches. First, we pursued the investigation of SL activity in symbiotic conditions by using an experimental setup based on SL-deficient mutants. Second, we developed a bioassay (referred to as branching bioassay) to investigate the effects of SL analogs on the growth and hyphal morphology of *R. irregularis* grown *in vitro* in the absence of a host plant.

This chapter is composed of three parts. The first part describes and discusses the two experimental setups used in our SAR studies. The second part reports the effects of SL analogs carrying modifications on the D-ring. It begins with a published article, followed by additional results. The last part briefly mentions my involvement in the characterization of a new SL identified in hemp, named cannalactone, and its synthetic analog SdL19.

Experimental procedures

I) Strigolactone activity in a context of symbiotic interaction

To investigate the bioactivity of SL analogs in a context of interaction with a host plant, the team developed a dedicated bioassay. This bioassay investigates the capacity of SL analogs to restore root colonization in plant mutants affected in SL biosynthesis. *M. truncatula ccd8* mutants (Lauressergues et al., 2015) were inoculated with spores of *R. irregularis*, and the number of infection units was assessed at an early stage of the symbiotic interaction. Infection units were defined as areas of the root cortex that host fungal structures (arbuscules, vesicles or intraradical hyphae), and derive from a single epidermal penetration event (Kobae, 2019). Detailed methods are described in Taulera et al. (2020). It is important to note that the capacity of SL analogs to restore root colonization in the mutants can result from their activity on the AM fungus, on the host plant or on the interaction itself.

In the second year of my thesis, we observed in these assays the colonization of *Mtccd8* roots by an unidentified fungus. In addition to its potential effects on the symbiosis, its presence prevented an accurate assessment of root colonization. After many attempts to perform this bioassay in different growth rooms and conditions, we could not eliminate this unwanted fungus. Consequently, some experiments could not be repeated, and some compounds could not be tested at all.

II) Hyphal branching bioassay

II-1) Remarks about experimental designs used in the literature

Assays described in the literature to measure the bioactivity of SLs on AMF usually document hyphal branching of germinated spores of *Gigaspora margarita* treated with SLs, following the protocol of Akiyama et al. (2005) (Akiyama et al., 2010; Kodama et al., 2021; Mori et al., 2016; Tokunaga et al., 2015; Xie et al., 2019), with the exception of a few studies on *R. irregularis* (Besserer et al., 2006; Cohen et al., 2013). Although the protocol of Akiyama et al. (2005) was helpful to test a large number of compounds at various concentrations, it suffers from several limitations.

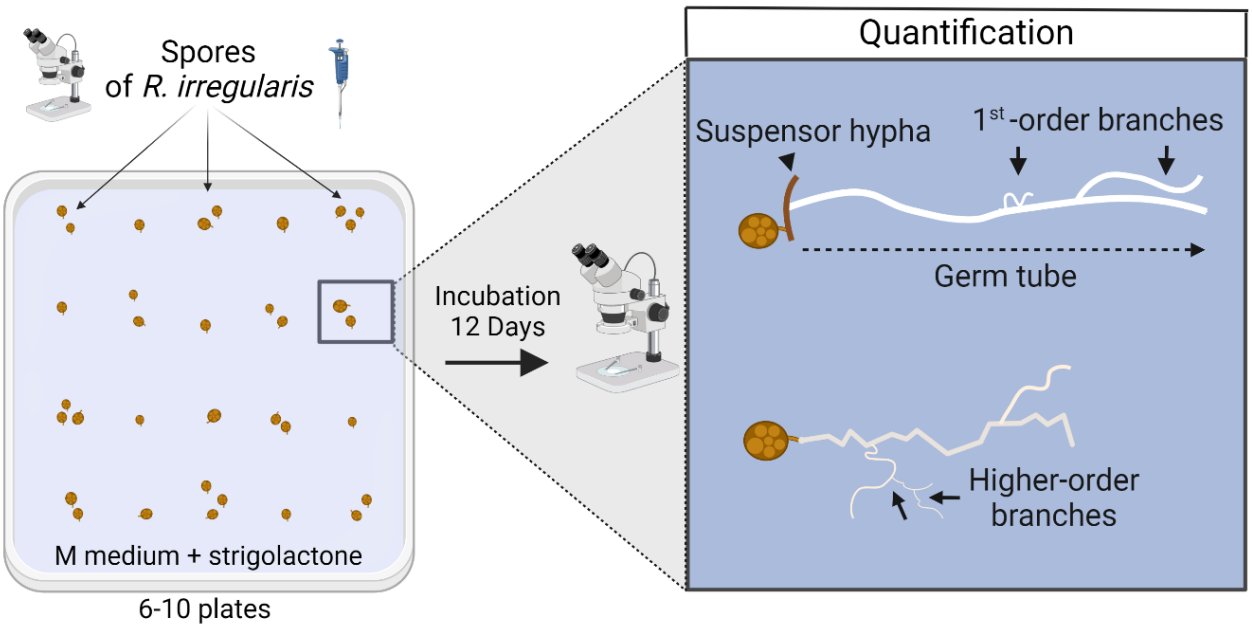

Figure 22. Experimental setup to study the activity of SL analogs on the hyphal development of *R. irregularis in vitro*

SL analogs were diluted into the medium. One to three spores of *R. irregularis* were deposited per droplet, and each Petri dish contained 20 deposits. After 12 days of incubation, the length of germ tube and number of 1st- and higher-order branches were determined using a dissecting microscope.

First, the SL analogs are loaded onto a paper disk placed in front of hyphal tips. Therefore, the exact concentration of SL analogs to which the fungus is exposed is not known.

A second limitation relates to the evaluation of branching activity. SL analogs are considered active if new ramifications are observed in the vicinity of the paper disk, and the minimum effective concentration (MEC) is derived from these observations. The number of new hyphal branches is not counted, hence this test does not quantitatively estimate the level of activity.

A third limitation is the number of spores analyzed. Only three to five spores are analyzed per treatment. The protocol does not specify how many treated spores should display enhanced branching for an SL analog to be considered bioactive. This is an important question as the authors report that hyphal branching is occasionally observed in negative control treatments.

Finally, the MECs of different SL analogs determined in separate studies are often compared with one another (for example, the activity of a compound tested in Xie et al., 2019 can be compared with the activity of another compound reported in Akiyama et al., 2005).

This can be questioned since experimental conditions may vary slightly, and more importantly the behavior of the biological material fluctuates over time. In our group we have experienced some versatility in the response of *Gigaspora rosea* to SLs. This fungus does not display a clear-cut branching/no branching response, but variable numbers of new hyphal branches. Similarly, we observed variations in the behavior of *R. irregularis,* even in the mock treatment. This makes it necessary to include negative and positive controls in each experiment, and to avoid comparisons of compounds tested in separate experiments.

II-2) Development of a new bioassay

Rhizophagus irregularis as a model

For many years *Rhizophagus irregularis* has been used as a model species to study AMF. Considerable knowledge, including genomic and transcriptomic data, has been accumulated during this time. In addition, we have a partnership with the company Agronutrition which can supply us with large amounts of *R. irregularis* spores obtained in axenic conditions and free of plant contaminants. For these reasons, *R. irregularis* was chosen as model species for my PhD, although its hyphal branching responses to SLs are not as easily visible as in *Gigaspora spp*. Another reason to use *R. irregularis* is that it allows to extend the data available in the literature to a different species of AMF, and thus to evaluate the diversity of SL responses across distant AMF species.

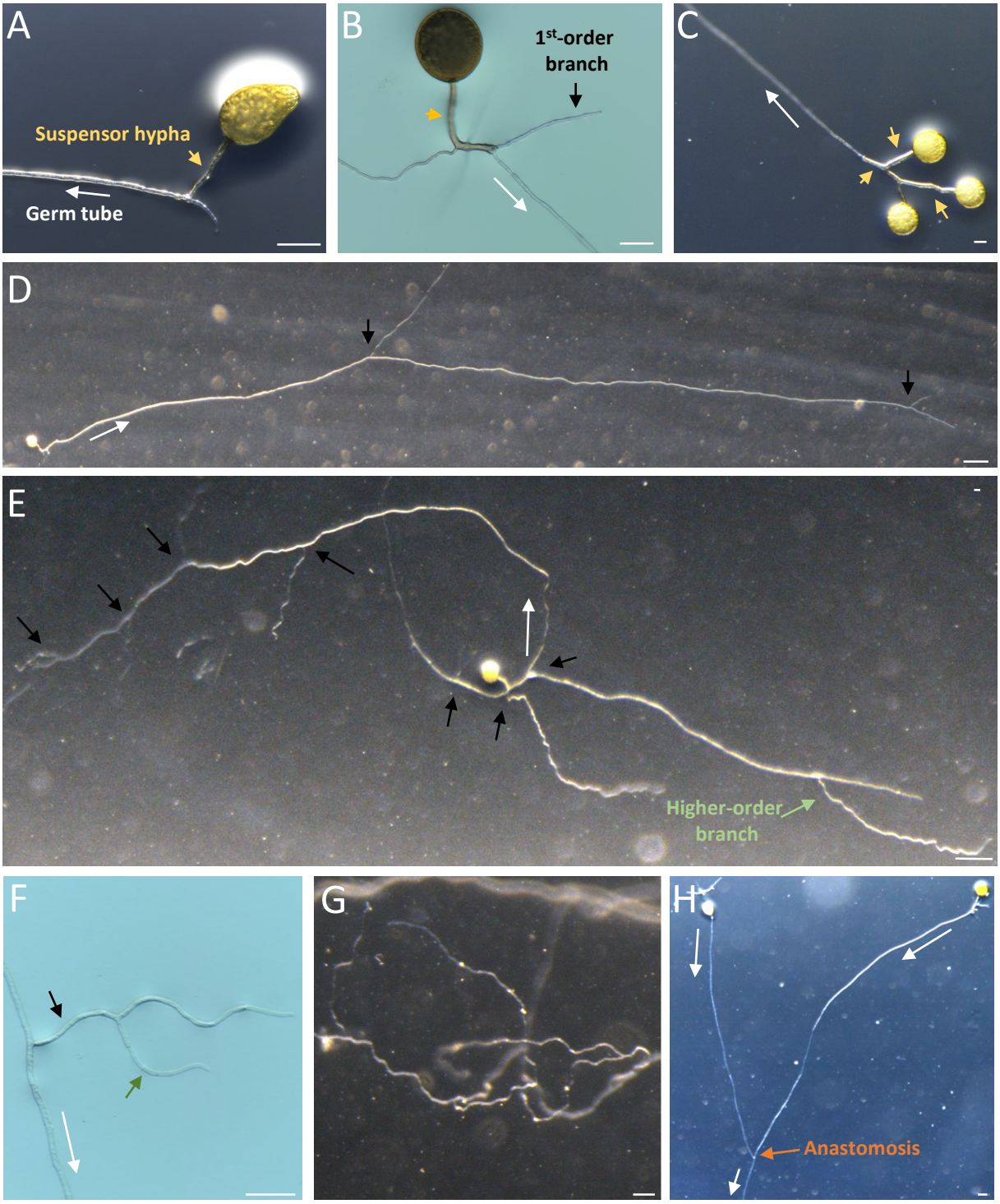

Figure 23. Hyphal development of *Rhizophagus irregularis* grown *in vitro*

Germinating spores of *R. irregularis were* observed under a dissecting microscope.

(A) A germ tube (white arrow) emerges from a suspensor hypha (yellow arrow).

(B) The germ tube is identified as the longest hypha.

(C) Several spores attached to the same suspensor hypha.

(D) From the germ tube, 1st-order branches emerge (black arrows)

(E) Several hyphae growing angularly in all directions emerge. An important number of 1st-order branches is observed as well as some higher-order branches (green arrow).

(F) Zoom on 1st-order and higher-order branches (black and green arrows, respectively).

(G) Zoom on coiled, curly hyphae.

(H) Two germ tubes form an anastomosis (orange arrow).

Scale bars = 50 µm for A,B,C,F and G and 250 µm for D,E and H.

Methods

Spores purchased from AgroNutrition (strain DAOM197198) are packaged in a long-term storage buffer. In order to eliminate this buffer and allow germination, the spore suspension was diluted in sterile water for two days, then washed with a large volume of sterile water on a 40 µm sieve before use.

Tested compounds were directly diluted into the medium after autoclaving to expose the fungus to known concentrations of SL analogs. All compounds were tested at a concentration of 100 nM. Droplets of 10 µL of spore suspension were laid down on the surface of the medium, to get an average of three to five spores per droplet. After 12 days of incubation, the length of the germ tube and the number of branches were recorded for each germinated spore (Fig. 22). Each treatment was applied to 200 to 400 spores distributed in 6 to 10 plates. For statistical analyses, each plate was treated as a replication unit, represented by its mean values.

I defined several rules to ensure a consistent counting of hyphal branches. For most spores, a single germ tube emerged out of the suspensor hypha (Fig. 23A). The branches emerging from this germ tube were counted as 1st-order branches (Fig. 23D, E, F), and those emerging from 1st-order branches were recorded as higher-order branches (Fig. 23E, F). There were however a few exceptions to this standard behavior:

- Two or even three hyphae could emerge from the same suspensor hypha (Fig. 23B). In this case, the germ tube was defined as the longest of these hyphae.
- In the case of anastomosis (Fig. 23H), all branches were counted and the mean number of branches was assigned to both spores.
- Occasional contact of hyphae with the Petri dish induced the emergence of 1st-order branches. As this was unrelated to SL responses, these branches were not counted.
- Finally, two situations were excluded from analysis: when two or more spores shared the same suspensor hypha (Fig. 23C), and when spores exhibited ultra-ramified septated hyphae close to the spore.

On average, in addition to the controls, four compounds were tested per experiment. The data presented in figures correspond to a representative experiment. The statement “the experiment was performed twice” refers to two experiments testing the same compounds. In some cases, two compounds were tested together in one experiment and then a second time

in separate experiments. This situation is reported as “the compound was tested twice”, to indicate that the comparison between this compound and the positive and negative controls has been validated, but that the comparison between the different compounds has not been repeated.

Two modifications were made to the protocol described in Taulera et al. 2020 for the experiments that followed:

- Some batches of spores contained a significant amount of residual dead hyphae that could interfere with fungal development or its observation. To remove these dead hyphae, the spore suspension was diluted in sterile water in a Petri dish and left to sediment for 3 minutes. The spores sank to the bottom of the Petri dish, while residual hyphae remained close to the surface and could be removed by pipetting.
- I noticed a cooperative effect between spores, which could be assimilated to quorum sensing. When more than five spores were laid down together, a significant increase in spore germination and hyphal branching was observed. To avoid any impact on the results, deposits containing more than five spores were excluded from analysis in the experiments described in the published article. In subsequent experiments I used a dissecting microscope to lay down a maximum of three spores per droplet (Fig. 22).

R. irregularis spore germination

Dedicated experiments were carried out to monitor spore germination over time in the presence of SL analogs. These experiments were performed in 96-well plates, in liquid M medium (Bécard & Fortin, 1988) supplemented with one of the tested compounds at 100 nM or the solvent alone (mock). A single spore was added into each well. The plates were sealed using micropore tape and incubated at 30 °C under 2% CO_2. The germination rate was recorded after 5, 7, 9 and 12 days. For each treatment 5 to 8 rows of 12 spores were analyzed. For statistical analysis, each row was treated as a replication unit (represented by its germination rate).

Statistical analyses

Datasets were analysed using one-way ANOVA followed by Fisher’s least significant difference (LSD) test when they met normality or homoscedasticity criteria. Otherwise, non-parametric tests were used: Kruskal-Wallis test was followed by pairwise comparisons with Mann and Whitney’s test. Data were analysed using Statgraphics Centurion software (SigmaPlus).

Results

I) Initiation of arbuscular mycorrhizal symbiosis involves a novel pathway independent from hyphal branching (published article)

SAR studies on plants have highlighted the utmost importance for SL hormonal activity of the methylbutenolide D-ring, an invariable component of all known natural SLs. Consequently, we focused on the importance of the D-ring for bioactivity on AM fungi. The following work was published in the journal *Mycorrhiza* in May 2020. Briefly, we evaluated the bioactivity of two analogs of GR24 with modifications on the D-ring. (±)-H2-2'-*epi*-GR24 harbors a reduced C3'-C4' bond, and (±)-4'-desmethyl-2'-*epi*-GR24 lacks the conserved methyl group at the C4' position. Both compounds were able to restore root colonization in *Mtccd8* mutants. Surprisingly, exposition of *R. irregularis* spores grown *in vitro* to (±)-4'-desmethyl-2'-*epi*-GR24 resulted in an inhibition of hyphal branching. This highlighted that initiation of arbuscular mycorrhizal symbiosis can occur independently of hyphal branching, and challenges the hypothesis that pre-symbiotic fungal branching is required for the fungus to colonize host roots.

Initiation of arbuscular mycorrhizal symbiosis involves a novel pathway independent from hyphal branching

AUTHORS

Quentin Taulera [1], Dominique Lauressergues [1], Katie Martin [1], Maïna Cadoret [1], Vincent Servajean [2], François-Didier Boyer [2] and Soizic Rochange [1*]

AFFILIATIONS

1 Laboratoire de Recherche en Sciences Végétales, Université de Toulouse, CNRS, UPS, 24 chemin de Borde Rouge, Auzeville, 31320, Castanet-Tolosan, France

2 Université Paris-Saclay, CNRS, Institut de Chimie des Substances Naturelles, UPR 2301, 91198, Gif-sur-Yvette, France

* Corresponding author (e-mail: rochange@lrsv.ups-tlse.fr)

ORCID: François-Didier Boyer 0000-0001-9855-7234; Soizic Rochange 0000-0002-3889-7859

ACKNOWLEDGMENTS

This study was partly funded by the Agence Nationale de la Recherche (ANR-18-CE20-0001-01). It was also supported by the TULIP LabEx (ANR-10-LABX-41) and the Stream COST Action FA1206. The Institut de Chimie des Substances Naturelles benefits from the support of the Labex CHARM3AT program (ANR-11-LABX-39). We thank Mégane Gaston and Nicolas Cadilhac for technical assistance with some experiments.

Abstract

The arbuscular mycorrhizal symbiosis is a very common association between plant roots and soil fungi, which greatly contributes to plant nutrition. Root-exuded compounds known as strigolactones act as symbiotic signals stimulating the fungus prior to root colonization. Strigolactones also play an endogenous role *in planta* as phytohormones and contribute to the regulation of various developmental traits. Structure-activity relationship studies have revealed both similarities and differences between the structural features required for bioactivity in plants and arbuscular mycorrhizal fungi. In the latter case, bioassays usually measured a stimulation of hyphal branching on isolated fungi of the *Gigaspora* genus, grown *in vitro*. Here, we extended these investigations with a bioassay that evaluates the bioactivity of strigolactone analogs in a symbiotic situation, and the use of the model mycorrhizal fungus *Rhizophagus irregularis*. Some general structural requirements for bioactivity reported previously for *Gigaspora* were confirmed. We also tested additional strigolactone analogs bearing modifications on the conserved methylbutenolide ring, a key element of strigolactone perception by plants. A strigolactone analog with an unmethylated butenolide ring could enhance the ability of *R. irregularis* to colonize host roots. Surprisingly, when applied to the isolated fungus *in vitro*, this compound stimulated germ tube elongation but inhibited hyphal branching. Therefore, this compound was able to act on the fungal and/or plant partner to facilitate initiation of the arbuscular mycorrhizal symbiosis, independently from hyphal branching and possibly from the strigolactone pathway.

KEYWORDS

Arbuscular mycorrhiza; strigolactone; symbiosis; *Rhizophagus*; signaling

ABBREVIATIONS

SL: strigolactone; AM: Arbuscular Mycorrhiza; WT: wild-type; KL: KAI2 ligand

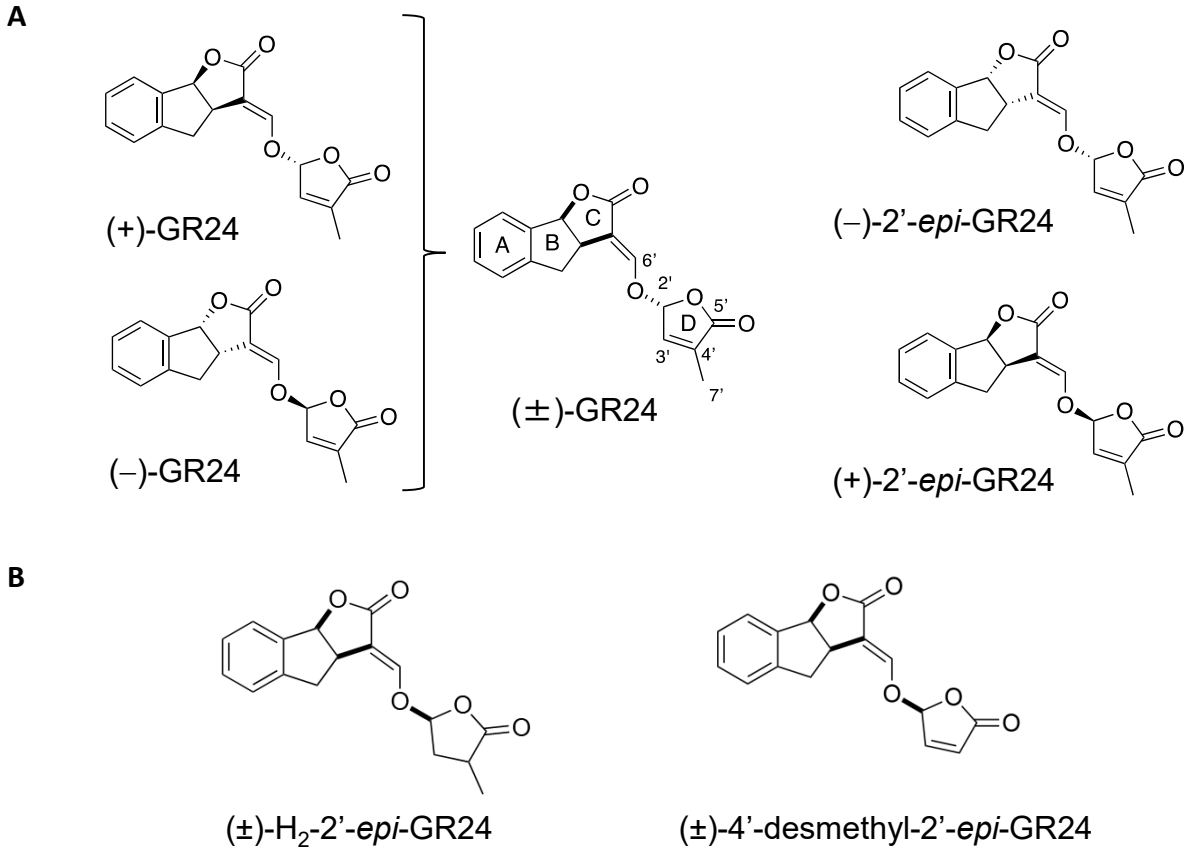

Taulera et al., 2020 - Figure 1. Strigolactone analogs used in this study

(A) Structure and stereochemistry of the SL analog GR24. The synthetic SL analog (±)-GR24 (middle) comprises the four characteristic carbon rings, named A to D, of canonical SLs. Different stereochemical configurations of the C and D rings give rise to four possible stereoisomers (left and right).

(B) Analogs with modifications on the D ring: reduction of the C3'-C4' double bond (left), or absence of the methyl group at C4' (right)

Introduction

Strigolactones (SLs) are carotenoid-derived compounds produced by plants and exuded by roots into the rhizosphere. They were first characterized as germination stimulants for seeds of the parasitic weeds *Striga* and *Orobanche* (Cook et al., 1966). It was later discovered that SLs also stimulate arbuscular mycorrhizal (AM) fungi (Akiyama et al., 2005; Besserer et al., 2006), which develop a root endosymbiosis with most land plants and play important roles in natural and agricultural ecosystems (Smith & Read 2008; Chen et al., 2018). More recently still, SLs were identified as a novel class of phytohormones, contributing to the control of shoot branching (Gomez-Roldan et al., 2008; Umehara et al., 2008) and a number of other developmental traits in shoots and roots (Lopez-Obando et al., 2015; Matthys et al., 2016). The bioactivity of SLs on such diverse organisms raises interesting questions about the evolution of their perception.

Since the identification of SLs as phytohormones, genetics has allowed rapid progress in the understanding of their biosynthesis, perception, and hormonal effects (Seto and Yamaguchi 2014; Al-Babili and Bouwmeester 2015; Bürger and Chory 2020). The core biosynthetic pathway from β-carotene to SLs involves, after *cis/trans* isomerization by DWARF27, two Carotenoid Cleavage Dioxygenase (CCD) enzymes. CCD7 carries out a first cleavage step yielding 9-*cis*-β-apo-10′-carotenal, which is processed by CCD8 into the common SL precursor carlactone (Alder et al., 2012; Bruno et al., 2017). From that step the pathway diverges among plant species to afford a diversity of SL forms (Jia et al., 2018).

Over 30 different natural SLs have been described to date (Yoneyama et al., 2018; Xie et al., 2019; Mori et al., 2020), and numerous chemically synthesized analogs are available (Takahashi & Asami 2018). Canonical SLs comprise four carbon rings named A to D. This general structure is mimicked in GR24 (Fig. 1a), a synthetic compound used as a universal analog in SL studies (Johnson et al., 1981; Zwanenburg & Pospisil 2013). In known natural SLs, the ABC tricyclic lactone is linked by an enol ether bridge to an invariable methylbutenolide D ring. While the C ring can adopt a β- or an α-orientation, all natural SLs have the same *R*-configuration at the C-2' position, which corresponds to the configuration of their common precursor carlactone (Flematti et al., 2016). Non-canonical SLs comprise an enol-ether-D-ring moiety but lack the A, B or C rings, and include carlactone as their simplest form (Yoneyama et al., 2018).

Structure-Activity Relationship studies have been carried out to link SL structural features with their bioactivity on different organisms. Each study used a different set of SL analogs and measured particular biological responses on a given species. Still, some general conclusions can be drawn from these data. Hormonal activities in pea, rice and *Arabidopsis* have generally been measured on SL-deficient *ccd8* mutants (*rms1*, *d10* and *max4,* respectively). In all three plant species, bioactivity largely depends on the methylbutenolide D ring associated with an enol ether unit. At the other end of this enol ether bridge, the C ring can be replaced by an acyclic moiety without substantial loss of activity (Boyer et al., 2012; Boyer et al., 2014; Umehara et al., 2015). *The importance of stereochemistry* varies among plant species (Flematti et al., 2016). As for variations on the D ring, the conserved methyl group at C4' is absolutely required to suppress outgrowth of pea buds (Boyer et al., 2012). The importance of the D ring has been further supported by recent studies on plant SL receptors (de Saint-Germain et al., 2016; Yao et al., 2016). These receptors, called D14 in rice and *Arabidopsis*, DAD2 in *Petunia* and RMS3 in pea, belong to the alpha/beta-hydrolase fold family of proteins (Arite et al., 2009; Hamiaux et al., 2012; Nakamura et al., 2013; Zhao et al., 2013). In a proposed mode of action of these receptors, a nucleophilic attack on the D ring results in the cleavage of SLs and the release of the ABC moiety. The D ring forms a transient covalent linkage with the receptor and is later released as hydroxymethylbutenolide (de Saint Germain et al., 2016; Yao et al., 2016; Seto et al., 2019). The use of profluorescent SL analogs has revealed that the conserved methyl at position C4' on the D ring strongly influences this hydrolytic process (de Saint Germain et al., 2016; Yao et al., 2018). SL receptors of root parasitic weeds seem to share their general properties, including hydrolytic activity, with SL receptors from other plants (Yao et al., 2017; Xu et al., 2018).

Ancient paralogs of SL receptors are involved in the perception of chemically related signals called karrikins (Bythell-Douglas et al., 2013). Karrikins are produced upon combustion of plant material and possess like SLs a butenolide moiety. In an ecological context, karrikins stimulate seed germination of some plant species and thereby facilitate vegetation recovery following wildfires. They turned out to be of broader interest when it was discovered that *Arabidopsis* mutants in the karrikin receptor KAI2 exhibit germination and seedling development phenotypes, suggesting that a yet unidentified signal (termed karrikin-like or KAI2 ligand, KL) exists in plants to regulate these developmental steps (Conn and Nelson 2016). Interestingly, in addition to the perception of karrikins and KL, KAI2 is involved in the response to a subset of SL stereoisomers (namely those with a *2'S* configuration, Scaffidi et al.,

2014). A final and very intriguing observation is that rice mutants in the karrikin receptor KAI2 are unable to develop AM symbiosis (Gutjahr et al., 2015). At this stage it remains unclear whether the cause of this phenotype is the absence of the protein itself, or a defect in the perception of a fungus- or plant-derived signal.

The discovery of a role for SLs in AM symbiotic signaling stemmed from the observation that AM fungi grown *in vitro* exhibit profuse hyphal branching in the vicinity of host roots. This morphological response can be reproduced to some extent in isolated fungi grown *in vitro* and treated with root exudates mixed into the medium or applied locally near hyphal tips (Nagahashi et al., 1996; Nagahashi & Douds 1999; Buée et al., 2003). SLs were later identified as essential components of the so-called "branching factor" responsible for this effect (Akiyama et al., 2005; Besserer et al., 2006). Other fungal responses to SLs have been reported, such as increased spore germination (Besserer et al., 2006; Kountche et al., 2018) or the production of chito-oligosaccacharides (Genre et al., 2013). Nevertheless, hyphal branching remains the classical bioassay to measure SL activity on AM fungi. It is mainly carried out on species of the genus *Gigaspora*, although hyphal branching induction by GR24 has also been documented in the model AM fungus *Rhizophagus irregularis* (Cohen et al., 2013). Structure-activity relationship studies on *Gigaspora margarita* have highlighted that linked ABC and D moieties were necessary for bioactivity, although the enol ether bridge between the C and D rings could be replaced by alkoxy or imino ethers (Akiyama et al., 2010a). Truncation of the A ring markedly reduced hyphal branching activity (Akiyama et al., 2010a). In contrast, the B and C rings appear partially dispensable, as attested by the activity of some carlactone derivatives (Mori et al., 2016) and other non-canonical strigolactones (Xie et al., 2019). Although canonical SLs are generally more active, some non-canonical SL forms can reach high levels of activity on AM fungi. For example, carlactonoic acid, which is exuded by a wide range of plant species, has been proposed to be a common inducer of hyphal branching (Yoneyama et al., 2018). It is also noteworthy that active SL analogs can trigger different hyphal branching patterns, stimulating the formation of short or long hyphae of different orders (Akiyama et al., 2010; Mori et al., 2016; Xie et al., 2019).

In addition to this morphological response of AM fungi to SLs *in vitro*, the importance of SLs in AM symbiosis was first shown through the analysis of SL-deficient pea mutants. AM fungi displayed a reduced ability to colonize these mutants, reaching a level of root colonization of only one third of the level observed in WT plants (Gomez-Roldan et al., 2008). Therefore, in

addition to their visible effects on fungal development *in vitro*, SLs are important for the symbiotic interaction to take place.

In this article, we focus on SL bioactivity on the AM fungus *R. irregularis*. We report the development of a novel bioassay to measure the activity of SL analogs in symbiotic conditions. We also extend previous structure-activity relationship studies by testing two new SL analogs bearing modifications on the D ring.

Materials and Methods

Biological material

The study was carried out on *Medicago truncatula* Gaertn. transposon insertional mutants of the R108 genotype: *ccd8-1*, *ccd7-1* and *d14-1* (Lauressergues et al., 2015). Backcrossed homozygous *ccd8-1* and *ccd7-1* mutants were compared to their wild-type siblings. Homozygous *d14-1* mutants were compared to wild-type R108. Seeds were sterilized and allowed to germinate for 24 h as described in Lauressergues et al., (2015).

Rhizophagus irregularis spores (strain DAOM197198) were purchased from Agronutrition (France). They were rinsed twice with sterile water before use.

Chemicals

(±)-GR24 was purchased from Chiralix (The Netherlands), and corresponding enantiopure stereoisomers were purchased from StrigoLab (Italy). The two other SL analogs (Fig. 1b) were synthesized as described in Boyer et al. (2012). All SL analogs were dissolved in acetone and stored at 20 °C. Freshly prepared 1000X stock solutions in acetone were added to the nutrient solution. An identical volume of acetone was added to nutrient solution for the mock treatments.

Plant growth and AM inoculation

Seedlings were transferred to 50 mL Falcon tubes pierced at the bottom (three holes in the conical part of the tubes) and containing sterilized substrate (OilDri UK) inoculated with 150 spores of *R. irregularis* per plant: 75 spores mixed with the substrate and 75 spores added halfway up the Falcon tube. Each tube was inserted through the lid, pierced to the diameter of the Falcon tube, of a 150 mL pot containing 85 mL of nutrient solution. This volume was sufficient for the duration of the experiments (three weeks). At the start of experiments, the nutrient solution level in pots reached roughly the lower 20 mL mark of the Falcon tubes, then it decreased gradually due to evaporation and plant growth. Throughout the experiments, the substrate acted as a coarse wick to keep all the tube content wet but aerated. At the time of harvest, the holes at the bottom of the tubes were still under the nutrient solution surface. The nutrient solution was a modified half-strength low-phosphate and low-nitrogen Long Ashton solution (Hewitt, 1966), containing 7.5 µM Na_2HPO_4, 750 µM KNO_3, 400 µM $Ca(NO_3)_2$, 200 mg/L MES buffer, pH 6.5. Treatments were applied by adding the tested compounds to the nutrient solution at the beginning of the experiment. The concentration of the tested compounds was 100 nM unless otherwise stated. Plants were kept in a growth chamber under a 16 h photoperiod (light intensity: 300 $\mu mol \cdot m^{-2} \cdot s^{-1}$). The temperature was set to 22 °C day and 20°C night, with 70% humidity.

Staining and observation of mycorrhizal structures

Roots were harvested three weeks post-inoculation and carefully separated from the substrate. They were cleared in 10% KOH (w/v) for three days at room temperature and stained with Schaeffer black ink (Vierheilig et al., 1998) for 8 min at 95 °C. Whole root systems were examined under a Leica RZ75 stereomicroscope, and the total number of AM infection units was counted for each plant. Infection units were defined as areas of the root cortex that host fungal structures (arbuscules, but also vesicles and intraradical hyphae), and derive from a single epidermal penetration event (Kobae 2019).

Analysis of AM fungal development *in vitro*

Experiments were carried out in plates containing M medium (Bécard and Fortin 1988) without sucrose and solidified with 0.4% (w/v) phytagel. SL analogs (100 nM), or the solvent alone for mock treatments, were added to the medium after autoclaving. Spores of *R. irregularis* were suspended in sterile water and 10 µL droplets containing 1 to 5 spores were placed on the medium. Plates were incubated horizontally at 30 °C under 2% CO_2 for 12 days. Germ tubes could easily be identified as the longest hypha coming out of each spore. Their length, from spore to tip and excluding any branches, was measured using ImageJ software after scanning the plates. The number of hyphal branches of the 1st order (growing from the germ tube) and 2nd order (growing from 1st-order branches) was determined using a dissecting microscope for each germinated spore. The average length of germ tubes, and average number of branches of each order were calculated for all the germinated spores on a plate (typically 30 to 40 spores). For statistical analysis, each plate was treated as a replication unit (represented by the plate mean) and 11 plates were analysed for each treatment.

Statistical analyses

Data were analysed using Statgraphics Centurion software (SigmaPlus). Non-parametric tests were used because normality or homoscedasticity criteria were not met. Datasets were analysed using the Kruskal-Wallis test, followed by pairwise comparisons with Dunn's test.

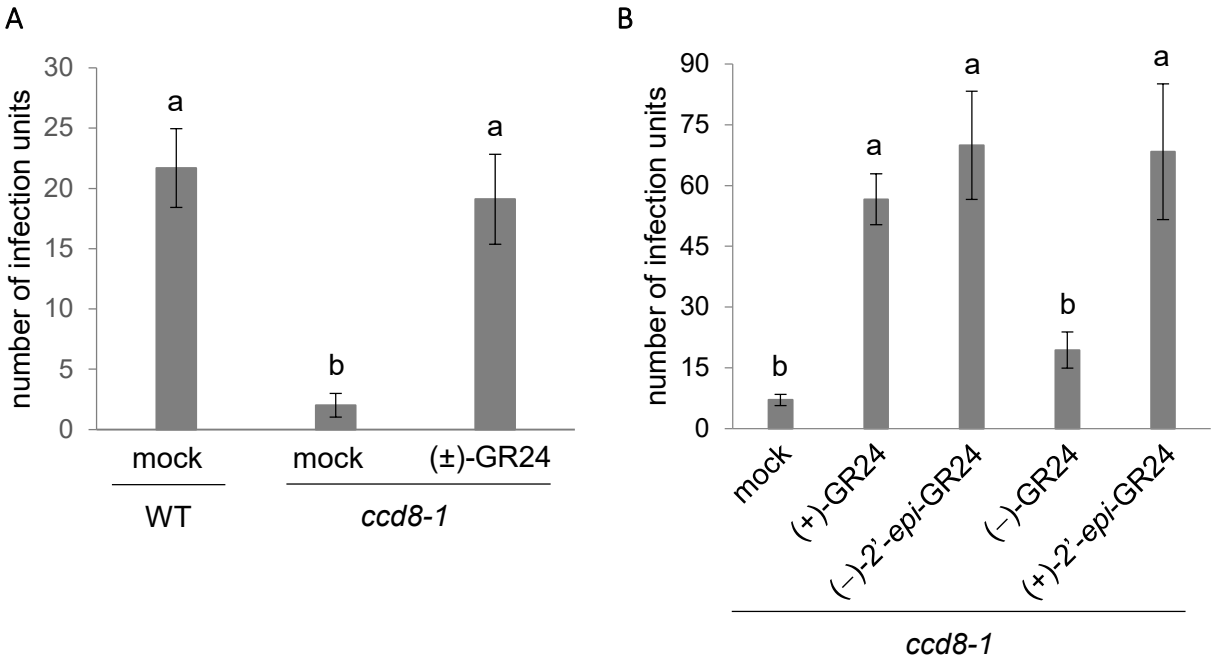

Taulera et al., 2020 - Figure 2. Mycorrhizal phenotype of *Mtccd8-1* mutants and its rescue by (±)-GR24

Plants were inoculated with *R. irregularis* and watered with a nutrient solution supplemented with the solvent alone (mock), or 100 nM SL analogs. Root colonization was assessed three weeks post-inoculation.

(A) Wild-type plants or *Mtccd8-1* mutants treated or not with (±)-GR24.

(B) M*tccd8-1* mutants treated with enantiopure stereoisomers of GR24.

Bars represent the mean number of infection units per plant, ± s.e.m. n = 9-10 plants per condition. Means topped by the same letter do not differ significantly according to Dunn's test (P > 0.05).

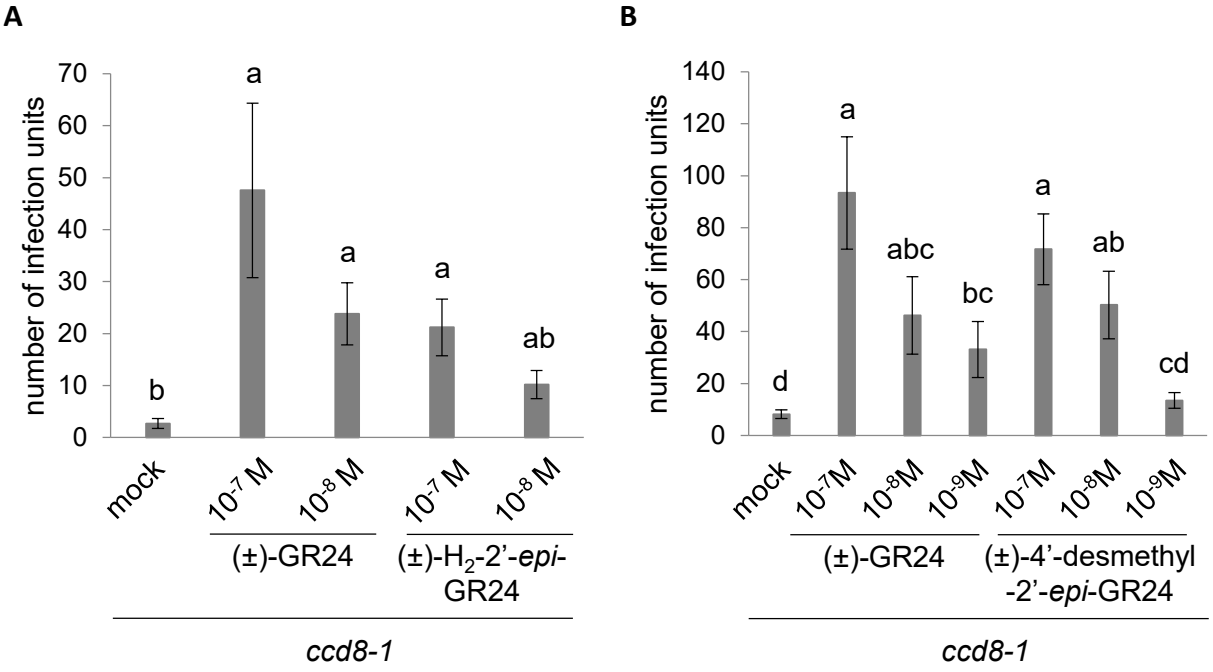

Taulera et al., 2020 - Figure 3. Effect of SL analogs modified on the D-ring on symbiosis initiation

Mtccd8-1 mutants were inoculated with *R. irregularis* and watered with a nutrient solution supplemented with SL analogs: (A) (±)-H_2-2'-*epi*-GR24; (B) (±)-4'-desmethyl-2'-*epi*-GR24. (±)-GR24 was used as positive control. Root colonization was assessed three weeks post-inoculation. Bars represent the mean number of infection units per plant ± s.e.m. n = 9-10 plants per condition. Means topped by the same letter do not differ significantly according to Dunn's test (P > 0.05).

Results

A novel bioassay to measure the effect of SLs on symbiosis initiation

We aimed to assess the bioactivity of SL analogs in a context of interaction with a host plant. To avoid any interference with endogenous SLs, we used as hosts *M. truncatula* mutants affected in the SL biosynthetic pathway. We have previously described *ccd7-1* and *ccd8-1* mutants of this species, which are affected in genes encoding two key enzymes in SL biosynthesis (D. Lauressergues et al., 2015). On average, *Mtccd8-1* mutants inoculated with spores of *R. irregularis* exhibited after three weeks of co-culture only 2 root colonization events per plant, *vs* 21.7 in wild-type plants. Exogenous treatment with the SL analog (±)-GR24 supplied in the nutrient solution restored normal levels of root colonization (Fig. 2a). A similar defect in root colonization was observed with *Mtccd7-1* mutants (Supp. Fig. 1a). In contrast, mutants carrying a mutation in the SL receptor D14 were normally colonized (Supp. Fig. 1b).

Bioactivity of SL analogs on symbiosis initiation: a structure-activity relationship study

The ability of (±)-GR24 to favour symbiosis initiation, *i.e.* to enhance root colonization of *Mtccd8-1* mutants by *R. irregularis* (Fig.2a), allowed us to use this experimental set-up as a bioassay to test the activity of other SL analogs. The first tested compounds were the ABC and D moieties of GR24, which can be generated by the hydrolase activity of plant SL receptors (Hamiaux et al., 2012). We observed that the tricyclic ABC lactone or the hydroxymethylbutenolide D-ring supplied individually, or as an equimolar mix, were unable to restore *R. irregularis* ability to colonize roots of *Mtccd8-1* mutants (Supp. Fig. 2).

We next tested the importance of SL stereochemistry. Synthetic SL analogs exist in four stereochemical configurations (Fig. 1a). We compared the biological activities of the four enantiopure stereoisomers of GR24. Three of them were highly active in symbiotic conditions, while (-)-GR24 was not significantly active as compared with the mock treatment (Fig. 2b).

We then evaluated two compounds bearing modifications on the conserved D ring part of SLs. A GR24 analog with a reduced C3'-C4' bond, (±)-H_2-2'-*epi*-GR24 (Fig. 1b; compound **35** in Boyer et al., 2012), was able to restore symbiosis initiation in *Mtccd8-1* mutants inoculated with *R. irregularis* (Fig. 3a). Like (±)-GR24, (±)-H_2-2'-*epi*-GR24 exhibited significant activity at the standard concentration of 100 nM (Dunn's test *vs* mock treatment, P=0.017). However, its activity was not statistically significant at 10 nM (P=0.052).

Finally, we evaluated an analog lacking the conserved methyl group at C4': (±)-4'-desmethyl-2'-*epi*-GR24 (Fig. 1b). This compound efficiently promoted the symbiosis between *R.*

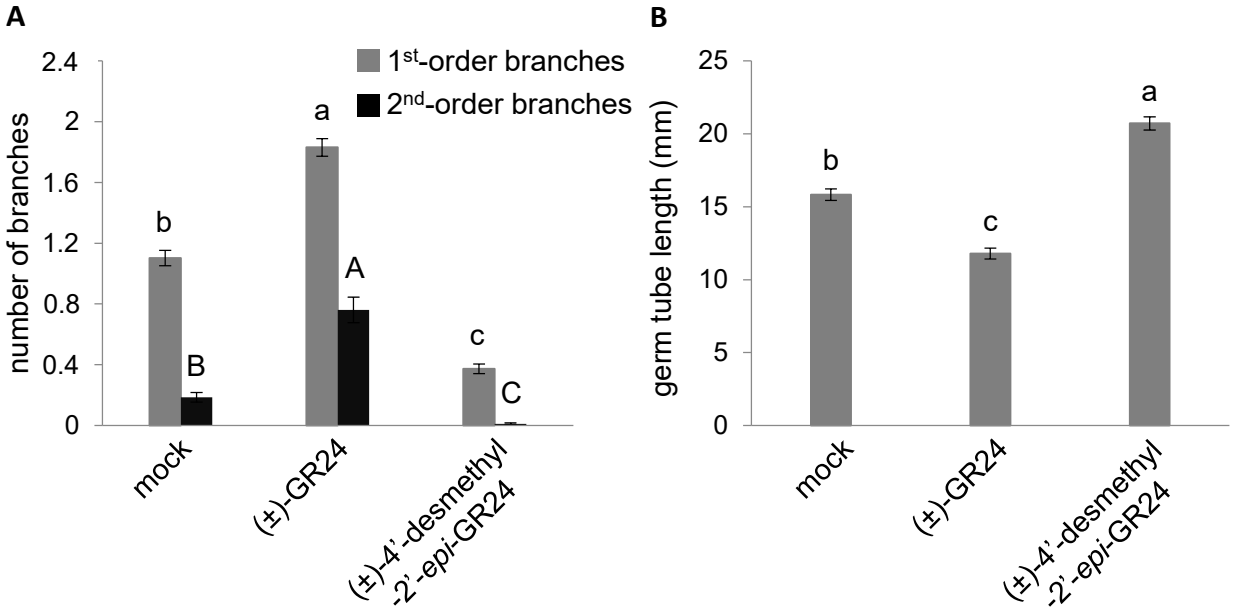

Taulera et al., 2020 - Figure 4. Effect of (±)-4'-desmethyl-2'-*epi*-GR24 on *R. irregularis* development *in vitro*

R. irregularis was grown from spores for 12 days on medium containing 100 nM (±)-GR24 or (±)-4'-desmethyl-2'-*epi*-GR24, or the solvent alone (mock), then developmental parameters were measured.

(A) Number of branches of first order (grey bars) and second order (black bars).

(B) Length of the germ tube.

Bars represent the mean ± s.e.m, n = 11 plates per condition. Means topped with the same letter do not differ significantly according to Dunn's test ($P > 0.05$).

irregularis and *M. truncatula* (Fig. 3b). To compare the bioactivity of (±)-4'-desmethyl-2'-*epi*-GR24 to that of (±)-GR24, we used a dilution series of the two compounds. (±)-4'-desmethyl-2'-*epi*-GR24 was significantly active at concentrations down to 10 nM (Dunn's test, P=0.003). Contrary to (±)-GR24, however, it failed to exhibit significant activity at 1 nM (Fig. 3b).

Activity of (±)-4'-desmethyl-2'-*epi*-GR24 on fungal development *in vitro*

To investigate the effects of (±)-4'-desmethyl-2'-*epi*-GR24 on *R. irregularis* in terms of presymbiotic growth and hyphal morphology, we recorded fungal development from spores laid on solid medium and exposed to (±)-GR24, (±)-4'-desmethyl-2'-*epi*-GR24 or a mock treatment. The SL analogs were diluted into the medium rather than applied locally, which ensures uniform treatment of all spores and allows knowing precisely the SL concentration to which the fungus is exposed. After 12 days of incubation the germ tube was measured, and the number of 1st-order and 2nd-order hyphal branches was determined (Fig. 4). Treatment with (±)-GR24 increased the number of 1st- and 2nd-order branches (Fig. 4a). Germ tubes were shorter in *R. irregularis* treated with (±)-GR24 than in control fungi (Fig. 4b). In contrast, (±)-4'-desmethyl-2'-*epi*-GR24 stimulated the elongation of the germ tube (Fig. 4b), while the number of 1st-order and 2nd-order branches was lower than in the control treatment (Fig. 4a). On average across three repeats of the experiment shown in Fig. 4, (±)-4'-desmethyl-2'-*epi*-GR24 increased germ tube length by 23 %. It triggered 2.1-fold and 6.5 fold reductions of the number of 1st-order and 2nd-order branches, respectively. Together, results presented in Fig. 4a and Fig. 3b indicate that this compound markedly inhibits hyphal branching, while it can efficiently restore fungal colonization of *Mtccd8* mutant roots.

Supplementary data

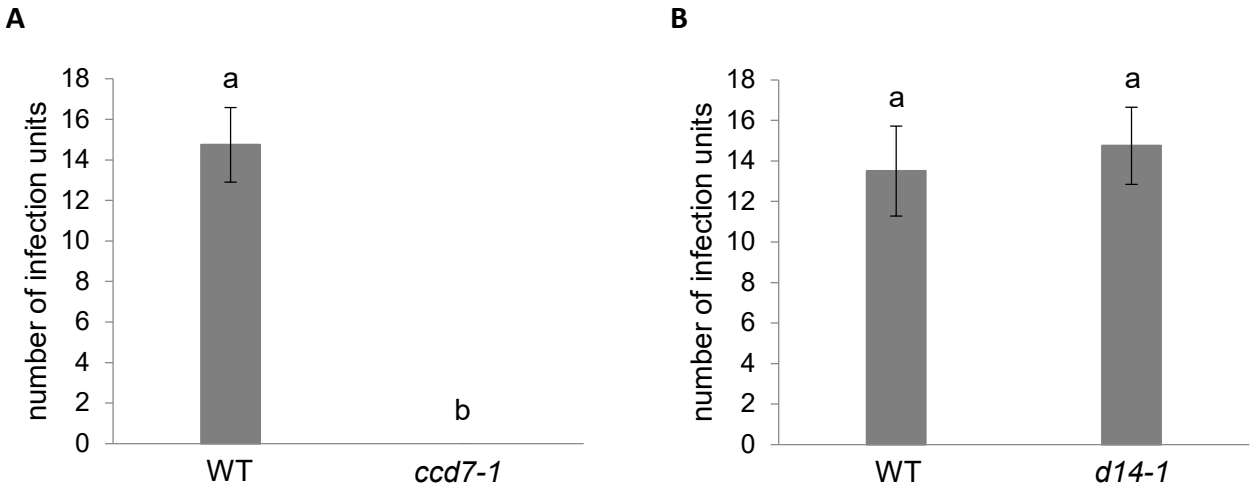

Taulera et al., 2020 - Supplementary Figure. 1 Mycorrhizal phenotype of *Medicago truncatula ccd7-1* and *d14-1* mutants

Wild-type and mutant plants were grown in small containers and inoculated with pre-germinated spores of *R. irregularis* as described in Balzergue et al. (2013). Bars indicate the mean number of infection units per plant, ± s.e.m. n = 7-8 plants per genotype. Means topped with the same letter do not differ significantly according to Dunn's test ($P > 0.05$).

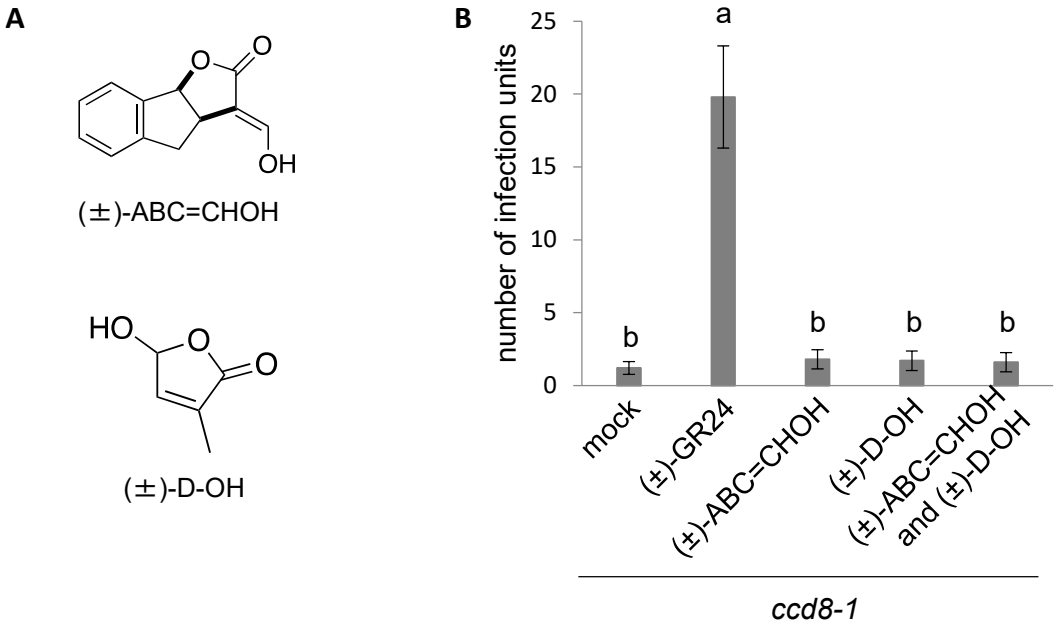

Taulera et al., 2020 - Supplementary Figure. 2 Effects of ABC and D moieties on symbiosis initiation

(A) Structure of the ABC and D moieties of GR24.

(B) M*tccd8-1* mutants were inoculated with *R. irregularis* and watered with a nutrient solution supplemented with 100 nM (±)-ABC=CHOH, (±)-D-OH, or a mixture of both (100 nM each). (±)-GR24 was used as positive control. Root colonization was assessed three weeks post-inoculation. Bars represent the mean number of infection units per plant ± s.e.m. n = 10 plants per condition. Means topped with the same letter do not differ significantly according to Dunn's test ($P > 0.05$).

Discussion

In the present work, we aimed to extend previous structure-activity relationship studies for SL activity on AM fungi. These studies have essentially been based on *in vitro* hyphal branching assays. Although such tests are extremely sensitive to SLs and informative from the point of view of fungal development, the relevance of hyphal branching to the symbiosis has not yet been firmly established. It is therefore of interest to supplement these observations with an assessment of SL bioactivity in a context of interaction with a host plant. An obvious obstacle to this in wild-type plants is the presence of endogenous SLs that could mask the activity of added compounds. We thus took advantage of *M. truncatula* mutants affected in the SL biosynthesis pathway. Consistent with the fact that the CCD7 and CCD8 enzymes act consecutively in this pathway (Alder et al., 2012), *Mtccd7-1* and *Mtccd8-1* mutants display similar defects in mycorrhizal root colonization. *Mtccd8* mutants were preferred for the rest of the study because CCD8 is to the best of our knowledge specifically involved in SL biosynthesis, while CCD7 activity can also lead to the formation of C_{14} and C_{13} apocarotenoids which could be involved in the progression of AM intraradical colonization (Vogel et al., 2009; Lopez-Raez et al., 2015; Walter et al., 2007; Stauder et al., 2018). Unlike mutants in the SL biosynthesis pathway, mutants affected in the SL receptor D14 were not hampered in their ability to host mycorrhizal interactions (Supp. Fig. 1). This observation is consistent with the analysis of corresponding mutants in rice (Yoshida et al., 2012) and indicates that hormonal effects of SLs *in planta* are not required for the symbiosis to take place. Therefore, defective mycorrhizal colonization of *Mtccd8-1* and *Mtccd7-1* mutants can be attributed to insufficient stimulation of the fungal partner.

The reduced mycorrhizal capacity we observed in *M. truncatula ccd8-1* mutants is more severe than that reported in corresponding mutants of other species like pea (Foo, et al., 2013; Gomez-Roldan et al., 2008), rice (Kobae et al., 2018; Yoshida et al., 2012) or *Petunia* (Kretzschmar et al., 2012). One hypothesis to explain this discrepancy could be the presence of biochemically undetectable residual SLs in some of those other mutants, or alternatively the production in these species of other compounds able to stimulate AM fungi. In any case, the very strong defect in mycorrhizal colonization observed with *Mtccd8-1* mutants, together with the complete restoration of root colonization upon treatment with exogenous SLs (Fig. 2a), allowed the development of a reliable bioassay to assess the bioactivity of SL analogs in symbiotic conditions. Importantly, since the read-out is the number of root colonization sites, bioactivity

encompasses the stimulation of any biological process allowing the fungus to progress from spore germination to successful root colonization.

A structure-activity relationship study was undertaken using this bioassay. All tested compounds were variations of the widely used SL analog GR24. In the first part of this study, we evaluated compounds that have already been tested for hyphal branching activity on *G. margarita* (Akiyama et al., 2010a). The ABC and D moieties, supplied individually or as an equimolar mix, were inactive (Supp. Fig. 2). Thus, SL cleavage products released upon SL perception by the host plant (and possibly by the fungus) do not by themselves stimulate the interaction between *R. irregularis* and *M. truncatula*. Among stereoisomers of GR24, (+)-GR24, (+)-2'-*epi*-GR24 and (-)-2'-*epi*-GR24 exhibited similar levels of bioactivity, while (-)-GR24 was inactive (Fig. 2b). These observations show consistency between hyphal branching tests (Akiyama et al., 2010a; Artuso et al., 2015) and our root colonization-based bioassay. They also indicate that the corresponding structural requirements are shared between *R. irregularis* and *G. margarita*. Preferences for SL stereochemical configurations vary across plant species (Boyer et al., 2012; Scaffidi et al., 2014; Umehara et al., 2015, Flematti et al., 2016). We did not observe such discrepancies among the two distant AM fungus species that have been considered so far, although available data are insufficient to conclude that stereochemical requirements are broadly conserved among AM fungi.

In the second part of the structure-activity relationship study, we included compounds bearing modifications on the methylbutenolide D ring. This invariable component of all known natural SLs is of utmost importance for SL perception by plants, but analogs with variations on this part of the molecule have not yet been tested on AM fungi. We first investigated the importance of the C3'-C4' double bond of the D ring. Analysis of (±)-H_2-2'-*epi*-GR24 revealed that reduction of the double bond resulted in a moderate decrease of bioactivity on *R. irregularis* (Fig. 3a). This effect was comparable to that observed on pea bud elongation (Boyer et al., 2012), while the loss of activity on rice tillering and on *Striga* and *Orobanche* seed germination was more pronounced (Umehara et al., 2015; Yamauchi et al., 2018). It was recently shown that the C3'-C4' double bond could be reduced to a single bond in the presence of root exudates (Yamauchi et al., 2018). Because this yielded compounds with limited activity on shoot branching and parasitic seed germination (Boyer et al., 2012; Umehara et al., 2015; Yamauchi et al., 2018), it was postulated that this modification could represent a biochemical pathway to inactivate SLs. Given that the biological reduction of this double bond is less effective on natural SL forms (Yamauchi et al., 2018), and that the resulting compounds retain some activity

on *R. irregularis*, this reduction process seems unlikely to interfere significantly with AM symbiotic signaling.

We then focused on the conserved methyl group at C4' of the butenolide D ring. Based on the current understanding of the SL biosynthetic pathway, this methyl group comes from the SL precursor 9-cis-β-carotene (Bruno et al., 2017). Studying the effects of (±)-4'-desmethyl-2'-*epi*-GR24, which lacks this methyl group, led to the most striking observations in our study. Indeed, this compound retains high activity to promote the initiation of symbiosis, as well as on the isolated fungus. These results contrast with observations made on pea: removal of the methyl group at C4' resulted in a complete loss of ability to suppress shoot branching *in planta* (Boyer et al., 2012), and altered the binding and hydrolytic properties of SL analogs with the pea SL receptor RMS3 (de Saint-Germain et al., 2016).

Our observations of *R. irregularis* development *in vitro* raised interesting questions about the relevance of pre-symbiotic fungal development to the initiation of symbiosis. As expected, (±)-GR24 stimulated 1st- and 2nd-order branching (Fig. 4). This confirmed previous observations (Cohen et al., 2013) and showed that the experimental conditions were adequate to detect positive effects of SL analogs on hyphal branching. Interestingly, germ tubes were shorter in *R. irregularis* treated with (±)-GR24 than in control fungi, a response that to our knowledge has not been reported previously. In contrast, (±)-4'-desmethyl-2'-*epi*-GR24 stimulated elongation of the germ tube and inhibited the formation of new hyphal branches, which to our knowledge is a novel combination of effects. This complete contrast with the effects of (±)-GR24 may reflect a trade-off between hyphal branching and extension growth. Still, although some SL analogs stimulate the formation of long branches of low order rather than the formation of many short high-order branches (Akiyama et al., 2010a; Mori et al., 2016; Xie et al., 2019), an inhibition of branching is quite unusual. Such effects have been reported in root-exuded compounds from non-host species and were accompanied by a similar inhibition of hyphal growth (Akiyama et al., 2010b). In our case, the branching inhibition cannot be attributed to toxicity because treatment with the same compound stimulated germ tube elongation and enhanced fungal ability to colonize roots. Positive effects on hyphal elongation are common: root exudates and a number of compounds therein, like flavonoids, polyamines or jasmonate, trigger this response in *Rhizophagus* or *Gigaspora* species (Elias & Safir 1987; Scervino et al., 2005; Cheng et al., 2012; Nagata et al., 2016). Over the years, such effects have however not attracted as much attention as hyphal branching, which is considered a hallmark of fungal stimulation by its host. It is commonly assumed that hyphal branching itself is important to

increase the chances for the fungus to encounter a host root, although this idea has not been supported by experimental evidence. Alternatively, hyphal branching could be a mere side-effect of important physiological or metabolic changes induced by SLs. Our observations challenge both hypotheses, as they indicate that hyphal branching and root colonization capacity can be uncoupled. Another implication is that important bioactive compounds may have escaped identification due to the focus on hyphal branching in previous studies.

That (±)-4'-desmethyl-2'-*epi*-GR24 was active on isolated *R. irregularis* (Fig. 4) indicates the existence of a fungal signaling pathway for this compound. Furthermore, the effects are the opposite of those observed upon treatment with (±)-GR24. This rules out the possibility that the fungal SL receptor is simply permissive to the absence of the methyl group at C4'. Rather, it points towards a perception system that allows discriminating between C4'-methylated and unmethylated forms of GR24, activating two different pathways to trigger different biological responses. This situation brings to mind an interesting parallel with the activation of homologous, yet distinct pathways by SLs and karrikins in plants. The main active karrikin form in *Arabidopsis*, KAR2, is likely structurally similar to endogenous plant compounds such as the elusive KL. Its unmethylated butenolide moiety is identical to the D-ring of (±)-4'-desmethyl-2'-*epi*-GR24, and the absence of a methyl group at C4' is important to activate the KL rather than SL pathway in *Arabidopsis* (Yao et al., 2018). Like plants, AM fungi could possess two pathways to deal with methylated and unmethylated butenolides. If the ability of (±)-4'-desmethyl-2'-*epi*-GR24 to restore the symbiosis in *Mtccd8* mutants is to be explained by effects on the fungus alone, this hypothesis implies that activation of the "unmethylated butenolide" pathway somehow makes the SL pathway dispensable.

An alternative and non-exclusive possibility is that in addition to stimulating the fungus, (±)-4'-desmethyl-2'-*epi*-GR24 acts on the plant host to facilitate fungal entry into roots. This hypothesis is consistent with the importance of the receptor protein KAI2 for AM symbiosis in rice (Gutjahr et al., 2015). Its ortholog in *Arabidopsis* seems strongly involved in the perception of C4'-unmethylated butenolides such as KAR2 (Villaécija-Aguilar et al., 2019). Therefore, it can be envisaged that a KAI2 protein in *M. truncatula* responds to unmethylated butenolides in a way that favours root colonization by AM fungi. Such unmethylated butenolides would comprise (±)-4'-desmethyl-2'-*epi*-GR24 as well as potential plant- or fungus-derived signals. At this stage, we do not have data to either support or rule out this possibility.

Interestingly, untreated *Mtccd8-1*/*R. irregularis* co-cultures failed to establish a successful interaction, but the exogenous supply of either (±)-GR24 or (±)-4'-desmethyl-2'-*epi*-GR24 was

sufficient to restore the symbiosis. This suggests that, in addition to the expected absence of SLs, natural equivalents of (±)-4'-desmethyl-2'-*epi*-GR24 or their receptors are absent or inactive in these co-cultures. Further investigations will be needed to understand how the two fungal pathways, and possibly a plant pathway responding to (±)-4'-desmethyl-2'-*epi*-GR24, interplay to allow the initiation of symbiosis.

In conclusion, our structure-activity relationship analysis on the broad requirements for SL structure and stereochemical configuration was congruent with previous hyphal branching assays. A focus on D-ring modifications, however, revealed that hyphal branching is not always a good proxy to estimate symbiosis-relevant bioactivity. This study also highlighted the importance of the methyl group on the D-ring, and the ability of methylated and unmethylated variants to trigger differential developmental responses in the fungus. Once again, as in many key studies on SL perception by plants, synthetic analogs were instrumental to unravel new biological events. Ultimately, deciphering the perception of SLs and other butenolides by AM fungi should shed light on how these compounds evolved to become both important regulators of plant development and interkingdom mediators.

References

Al-Babili S, Bouwmeester HJ (2015) Strigolactones, a novel carotenoid-derived plant hormone. Annu Rev Plant Biol 66:161–186. https://doi.org/10.1146/annurev-arplant-043014-114759

Akiyama K, Matsuzaki K, Hayashi H (2005) Plant sesquiterpenes induce hyphal branching in arbuscular mycorrhizal fungi. Nature 435:824–827. https://doi.org/10.1038/nature03608

Akiyama K, Ogasawara S, Ito S, Hayashi H (2010a) Structural requirements of strigolactones for hyphal branching in AM fungi. Plant Cell Physiol 51:1104–1117. https://doi.org/10.1093/pcp/pcq058

Akiyama K, Tanigawa, Kashihara T, Hayashi H (2010b) Lupin pyranoisoflavones inhibiting hyphal development in arbuscular mycorrhizal fungi. Phytochemistry 71:1865–1871. https://doi.org/10.1016/j.phytochemistry.2010.08.010

Alder A, Jamil M, Marzorati M, Bruno M, Vermathen M, Bigler P, Ghisla S, Bouwmeester H, Beyer P, Al-Babili S (2012) The Path from □-Carotene to Carlactone, a Strigolactone-Like Plant Hormone. Science 335:1348–1351. https://doi.org/10.1126/science.1218094

Arite T, Umehara M, Ishikawa S, Hanada A, Maekawa M, Yamaguchi S, Kyozuka J (2009) D14, a Strigolactone-Insensitive Mutant of Rice, Shows an Accelerated Outgrowth of Tillers. Plant Cell Physiol 50:1416–1424. https://doi.org/10.1093/pcp/pcp091

Artuso E, Ghibaudi E, Lace B, Marabello D, Vinciguerra D, Lombardi C, Koltai H, Kapulnik Y, Novero M, Occhiato E G, Scarpi D, Parisotto S, Deagostino A, Venturello P, Mayzlish-Gati E, Bier A, Prandi C (2015) Stereochemical Assignment of Strigolactone Analogues Confirms Their Selective Biological Activity. J Nat Prod 78:2624–2633. https://doi.org/10.1021/acs.jnatprod.5b00557

Balzergue C, Chabaud M, Barker DG, Bécard G, Rochange SF (2013) High phosphate reduces host ability to develop arbuscular mycorrhizal symbiosis without affecting root calcium spiking responses to the fungus. Front Plant Sci 4:426. https://doi.org/10.3389/fpls.2013.00426

Bécard G, Fortin JA (1988) Early events of vesicular-arbuscular mycorrhiza formation on Ri T-DNA transformed roots. New Phytol 108:211-218. https://doi.org/10.1111/j.1469-8137.1988.tb03698.x

Besserer A, Puech-Pagès V, Kiefer P, Gomez-Roldan V, Jauneau A, Roy S, Portais J-C, Roux C, Bécard G, Séjalon-Delmas N (2006) Strigolactones stimulate arbuscular mycorrhizal fungi by activating mitochondria. PLoS Biol 4:e226. https://doi.org/10.1371/journal.pbio.0040226

Boyer FD, de Saint Germain A, Pillot JP, Pouvreau JB, Chen VX, Ramos S, Stévenin A, Simier P, Delavault P, Beau JM, Rameau C (2012) Structure-Activity Relationship Studies of Strigolactone-Related Molecules for Branching Inhibition in Garden Pea: Molecule Design for Shoot Branching. Plant Phys 159:1524–1544. https://doi.org/10.1104/pp.112.195826

Boyer FD, de Saint Germain A, Pouvreau JB, Clavé G, Pillot JP, Roux A, Rasmussen A, Depuydt S, Lauressergues D, Frei Dit Frey N, Heugebaert TS, Stevens CV, Geelen D, Goormachtig S, Rameau C (2014) New Strigolactone Analogs as Plant Hormones with Low Activities in the Rhizosphere. Mol Plant 7:675–690. https://doi.org/10.1093/mp/sst163

Bruno M, Vermathen M, Alder A, Wüst F, Schaub P, van der Steen R, Beyer P, Ghisla S, Al-Babili S (2017) Insights into the formation of carlactone from in-depth analysis of the CCD8-catalyzed reactions. FEBS Lett 591:792–800. https://doi.org/10.1002/1873-3468.12593

Buée M, Rossignol M, Jauneau A, Ranjeva R, Bécard G (2000) The pre-symbiotic growth of arbuscular mycorrhizal fungi is induced by a branching factor partially purified from plant root exudates. Mol Plant Microbe Interact 13:693-698. https://doi: 10.1094/MPMI.2000.13.6.693

Bürger M, Chory J (2020) The Many Models of Strigolactone Signaling. Trends Plant Sci 25:395–405. https://doi.org/10.1016/j.tplants.2019.12.009

Chen M, Arato M, Borghi L, Nouri E, Reinhardt D (2018) Beneficial Services of Arbuscular Mycorrhizal Fungi – From Ecology to Application. Front Plant Sci 9:1270. https://doi.org/10.3389/fpls.2018.01270

Cheng Y, Ma W, Li X, Miao W, Zheng L, Cheng B (2012) Polyamines stimulate hyphal branching and infection in the early stage of *Glomus etunicatum* colonization. World J Microbiol Biotechnol 28:1615–1621. https://doi.org/10.1007/s11274-011-0967-0

Cohen M, Prandi C, Occhiato EG, Tabasso S, Wininger S, Resnick N, Steinberger Y, Koltai H, Kapulnik Y (2013) Structure–Function Relations of Strigolactone Analogs: Activity as Plant Hormones and Plant Interactions. Mol Plant 6:141–152. https://doi.org/10.1093/mp/sss134

Conn CE, Bythell-Douglas R, Neumann D, Yoshida S, Whittington B, Westwood JH, Shirasu K, Bond CS, Dyer KA, Nelson DC (2015) Convergent evolution of strigolactone perception enabled host detection in parasitic plants. Science 349:540–543. https://doi.org/10.1126/science.aab1140

Conn CE, Nelson DC (2016) Evidence that KARRIKIN-INSENSITIVE2 (KAI2) Receptors may Perceive an Unknown Signal that is not Karrikin or Strigolactone. Front Plant Sci 6:1219. https://doi.org/10.3389/fpls.2015.01219

Cook CE, Whichard LP, Turner B, Wall ME (1966) Germination of witchweed (*Striga lutea* Lour.): isolation and properties of a potent stimulant. Science 154:1189–1190. https://doi.org/10.1126/science.154.3753.1189

de Saint Germain A, Clavé G, Badet-Denisot MA, Pillot JP, Cornu D, Le Caer JP, Burger M, Pelissier F, Retailleau P, Turnbull C, Bonhomme S, Chory J, Rameau C, Boyer FD (2016) An histidine covalent receptor and butenolide complex mediates strigolactone perception. Nat Chem Biol 12:787–794. https://doi.org/10.1038/nchembio.2147

Elias KS, Safir GR (1987) Hyphal Elongation of *Glomus fasciculatus* in Response to Root Exudates. Appl Environ Microbiol 53:1928-1933.

Flematti GR, Ghisalberti EL, Dixon KW, Trengove RD (2009) Identification of Alkyl Substituted 2H-Furo[2,3-c]pyran-2-ones as Germination Stimulants Present in Smoke. J Agric Food Chem 57:9475–9480. https://doi.org/10.1021/jf9028128

Flematti GR, Scaffidi A, Waters MT, Smith SM (2016) Stereospecificity in strigolactone biosynthesis and perception. Planta 243:1361–1373. https://doi.org/10.1007/s00425-016-2523-5

Foo E, Ross JJ, Jones WT, Reid JB (2013) Plant hormones in arbuscular mycorrhizal symbioses: An emerging role for gibberellins. Ann Bot 111:769–779. https://doi.org/10.1093/aob/mct041

Genre A, Chabaud M, Balzergue C, Puech-Pagès V, Novero M, Rey T, Fournier J, Rochange S, Bécard G, Bonfante P, Barker DG (2013) Short-chain chitin oligomers from arbuscular mycorrhizal fungi trigger nuclear Ca^{2+} spiking in *Medicago truncatula* roots and their production is enhanced by strigolactone. New Phytol 198:190–202. https://doi.org/10.1111/nph.12146

Gomez-Roldan V, Fermas S, Brewer PB, Puech-Pagès V, Dun EA, Pillot JP, Letisse F, Matusova R, Danoun S, Portais JC, Bouwmeester H, Bécard G, Beveridge CA, Rameau C, Rochange SF (2008) Strigolactone inhibition of shoot branching. Nature 455:189–194. https://doi.org/10.1038/nature07271

Hamiaux C, Drummond RSM, Janssen BJ, Ledger SE, Cooney JM, Newcomb RD, Snowden KC (2012) DAD2 Is an α/β Hydrolase Likely to Be Involved in the Perception of the Plant Branching Hormone, Strigolactone. Current Biol 22:2032–2036. https://doi.org/10.1016/j.cub.2012.08.007

Hewitt E (1966) Sand and water culture methods used in the study of plant nutrition, 2nd edn. Commonwealth Agricultural Bureau, London

Jamil M, Kountche BA, Haider I, Wang JY, Aldossary F, Zarban RA, Jia KP, Yonli D, Shahul Hameed UF, Takahashi I, Ota T, Arold ST, Asami T, Al-Babili S (2019) Methylation at the C-3' in D-Ring of Strigolactone Analogs Reduces Biological Activity in Root Parasitic Plants and Rice. Front Plant Sci 2:10:353. https://doi.org/10.3389/fpls.2019.00353

Jia KP, Baz L, Al-Babili S (2018) From carotenoids to strigolactones. J Exp Bot 69:2189-2204. https://doi: 10.1093/jxb/erx476

Johnson A, Gowada G, Hassanali A, Knox J, Monaco S, Razavi Z, Roseberry G (1981) The preparation of synthetic analogues of strigol. J Chem Soc Perkin Trans 1:1734–1743. https://doi.org/10.1039/P19810001734

Kobae Y (2019) The Infection Unit: An Overlooked Conceptual Unit for Arbuscular Mycorrhizal Function. In: Ohyama T (ed) Root Biology - Growth, Physiology, and Functions. http://doi.org/10.5772/intechopen.86996

Kobae Y, Kameoka H, Sugimura Y, Saito K, Ohtomo R, Fujiwara T, Kyozuka J (2018) Strigolactone Biosynthesis Genes of Rice are Required for the Punctual Entry of Arbuscular Mycorrhizal Fungi into the Roots. Plant Cell Physiol 59:544–553. https://doi.org/10.1093/pcp/pcy001

Kountche BA, Novero M, Jamil M, Asami T, Bonfante P, Al-Babili S (2018) Effect of the strigolactone analogs methyl phenlactonoates on spore germination and root colonization of arbuscular mycorrhizal fungi. Heliyon 4:e00936. https://doi.org/10.1016/j.heliyon.2018.e00936

Kretzschmar T, Kohlen W, Sasse J, Borghi L, Schlegel M, Bachelier JB, Reinhardt D, Bours R, Bouwmeester HJ, Martinoia E (2012) A *Petunia* ABC protein controls strigolactone-dependent symbiotic signaling and branching. Nature 483:341–344. https://doi.org/10.1038/nature10873

Lauressergues D, André O, Peng J, Wen J, Chen R, Ratet P, Tadege M, Mysore KS, Rochange SF (2015) Strigolactones contribute to shoot elongation and to the formation of leaf margin serrations in *Medicago truncatula* R108. J Exp Bot 66:1237–1244. https://doi.org/10.1093/jxb/eru471

Lopez-Obando M, Ligerot Y, Bonhomme S, Boyer F-D, Rameau C (2015) Strigolactone biosynthesis and signaling in plant development. Development 142:3615–3619. https://doi.org/10.1242/dev.120006

López-Ráez JA, Fernández I, García JM, Berrio E, Bonfante P, Walter MH, Pozo MJ (2015) Differential spatio-temporal expression of carotenoid cleavage dioxygenases regulates apocarotenoid fluxes during AM symbiosis. Plant Sci 230:59-69. https://doi.org/10.1016/j.plantsci.2014.10.010

Matthys C, Walton A, Struk S, Stes E, Boyer F-D, Gevaert K, Goormachtig S (2016) The Whats, the Wheres and the Hows of strigolactone action in the roots. Planta 243:1327–1337. https://doi.org/10.1007/s00425-016-2483-9

Mori N, Nishiuma K, Sugiyama T, Hayashi H, Akiyama K (2016) Carlactone-type strigolactones and their synthetic analogues as inducers of hyphal branching in arbuscular mycorrhizal fungi. Phytochemistry 130:90–98. https://doi.org/10.1016/j.phytochem.2016.05.012

Mori N, Sado A, Xie X, Yoneyama K, Asami K, Seto Y, Nomura T, Yamaguchi S, Yoneyama K, Akiyama K (2020) Chemical identification of 18-hydroxycarlactonoic acid as an *LjMAX1* product and *in planta* conversion of its methyl ester to canonical and non-canonical strigolactones in *Lotus japonicus*. Phytochemistry 174, 112349. https://doi.org/10.1016/j.phytochem.2020.112349

Nagahashi G, Douds DD (1999) Rapid and sensitive bioassay to study signals between root exudates and arbuscular mycorrhizal fungi. Biotechnol Tech 13:893–897. https://doi.org/10.1023/A:1008938527757

Nagahashi G, Douds DD, Abney GD (1996) Phosphorus amendment inhibits hyphal branching of the VAM fungus *Gigaspora margarita* directly and indirectly through its effect on root exudation. Mycorrhiza 6:403–408. https://doi.org/10.1007/s005720050139

Nagata M, Yamamoto N, Miyamoto T, Shimomura A, Arimaa S, Hirsch AM, Suzuki A (2016) Enhanced hyphal growth of arbuscular mycorrhizae by root exudates derived from high R/FR treated *Lotus japonicus*. Plant Signal Behav 11:e1187356. https://doi.org/10.1080/15592324.2016.1187356

Nakamura H, Xue YL, Miyakawa T, Hou F, Qin HM, Fukui K, Shi X, Ito E, Ito S, Park SH, Miyauchi Y, Asano A, Totsuka N, Ueda T, Tanokura M, Asami T (2013) Molecular mechanism of strigolactone perception by DWARF14. Nat Commun 4:2613. https://doi.org/10.1038/ncomms3613

Scaffidi A, Waters MT, Sun YK, Skelton BW, Dixon KW, Ghisalberti EL, Flematti GR, Smith SM (2014) Strigolactone Hormones and Their Stereoisomers Signal through Two Related Receptor Proteins to Induce Different Physiological Responses in *Arabidopsis*. Plant Physiol 165:1221-1232. https://doi.org/10.1104/pp.114.240036

Scervino JM, Ponce MA, Erra-Bassells R, Vierheilig H, Ocampo JA, Godeas A (2005) Flavonoids exhibit fungal species and genus specific effects on the presymbiotic growth of *Gigaspora* and *Glomus*. Mycol Res 109:789–794. https://doi.org/ 10.1017/s0953756205002881

Seto Y, Yamaguchi S (2014) Strigolactone biosynthesis and perception. Curr Opin Plant Biol 21:1–6. https://doi.org/10.1016/j.pbi.2014.06.001

Seto Y, Yasui R, Kameoka H, Tamiru M, Cao M, Terauchi R, Sakurada A, Hirano R, Kisugi T, Hanada A, Umehara M, Seo E, Akiyama K, Burke J, Takeda-Kamiya N, Li W, Hirano Y, Hakoshima T, Mashiguchi K, Noel JP, Kyozuka J, Yamaguchi S (2019) Strigolactone perception and deactivation by a hydrolase receptor DWARF14. Nat Commun 10:191. https://doi.org/10.1038/s41467-018-08124-7

Smith S, Read D (2008) Mycorrhizal symbiosis, 3rd edn. Academic Press, London

Stauder R, Welsch R, Camagna M, Kohlen W, Balcke GU, Tissier A, Walter MH (2018) Strigolactone Levels in Dicot Roots Are Determined by an Ancestral Symbiosis-Regulated Clade of the PHYTOENE SYNTHASE Gene Family. Front Plant Sci 9:255. https://doi.org/10.3389/fpls.2018.00255

Sun YK, Yao J, Scaffidi A, Melville KT, Davies SF, Bond CS, Smith SM, Flematti GR, Waters MT (2020) Divergent receptor proteins confer responses to different karrikins in two ephemeral weeds. Nat Commun 11:1264. https://doi.org/10.1038/s41467-020-14991-w

Takahashi I, Asami T (2018) Target-based selectivity of strigolactone agonists and antagonists in plants and their potential use in agriculture. J Exp Bot 69:2241-2254. https://doi.org/10.1093/jxb/ery126

Tsuchiya Y, Yoshimura M, Sato Y, Kuwata K, Toh S, Holbrook-Smith D, Zhang H, McCourt P, Itami K, Kinoshita T, Hagihara S (2015) Probing strigolactone receptors in *Striga hermonthica* with fluorescence. Science 349:864-868. https://doi.org/ 10.1126/science.aab3831

Umehara M, Cao M, Akiyama K, Akatsu T, Seto Y, Hanada A, Li W, Takeda-Kamiya N, Morimoto Y, Yamaguchi S (2015) Structural Requirements of Strigolactones for Shoot Branching Inhibition in Rice and *Arabidopsis*. Plant Cell Physiol 56:1059–1072. https://doi.org/10.1093/pcp/pcv028

Umehara M, Hanada A, Yoshida S, Akiyama K, Arite T, Takeda-Kamiya N, Magome H, Kamiya Y, Shirasu K, Yoneyama K, Kyozuka J, Yamaguchi S (2008) Inhibition of shoot branching by new terpenoid plant hormones. Nature 455:195–200. https://doi.org/10.1038/nature07272

Vierheilig H, Coughlan A, Wyss U, Piche Y (1998) Ink and vinegar, a simple staining technique for arbuscular-mycorrhizal fungi. Appl Environ Microbiol 64:5004–5007.

Villaécija-Aguilar JA, Hamon-Josse M, Carbonnel S, Kretschmar A, Schmidt C, Dawid C, Bennett T, Gutjahr C (2019) SMAX1/SMXL2 regulate root and root hair development downstream of KAI2-mediated signaling in *Arabidopsis*. PLoS Genet 15:e1008327. https://doi.org/10.1371/journal.pgen.1008327

Vogel JT, Walter MH, Giavalisco P, Lytovchenko A, Kohlen W, Charnikhova T, Simkin AJ, Goulet C, Strack D, Bouwmeester HJ, Fernie AR, Klee HJ (2009) SlCCD7 controls strigolactone biosynthesis, shoot branching and mycorrhiza-induced apocarotenoid formation in tomato. Plant J 61: 300–311. https://doi.org/10.1111/j.1365-313X.2009.04056.x

Walter MH, Floss DS, Hans J, Fester T, Strack D (2007) Apocarotenoid biosynthesis in arbuscular mycorrhizal roots: contributions from methylerythritol phosphate pathway isogenes and tools for its manipulation. Phytochemistry 68:130-138. https://doi.org/10.1016/j.phytochem.2006.09.032

Xie X, Mori N, Yoneyama K, Nomura T, Uchida K, Yoneyama K, Akiyama K (2019) Lotuslactone, a non-canonical strigolactone from *Lotus japonicus*. Phytochemistry 157:200–205. https://doi.org/10.1016/j.phytochem.2018.10.034

Xu Y, Miyakawa T, Nosaki S, Nakamura A, Lyu Y, Nakamura H, Ohto U, Ishida H, Shimizu T, Asami T, Tanokura M (2018) Structural analysis of HTL and D14 proteins reveals the basis for ligand selectivity in *Striga*. Nat Commun 9:3947. https://doi.org/10.1038/s41467-018-06452-2

Yamauchi M, Ueno K, Furumoto T, Wakabayashi T, Mizutani M, Takikawa H, Sugimoto Y (2018) Stereospecific reduction of the butenolide in strigolactones in plants. Bioorg Med Chem 26:4225–4233. https://doi.org/10.1016/j.bmc.2018.07.016

Yao J, Mashiguchi K, Scaffidi A, Akatsu T, Melville KT, Morita R, Morimoto Y, Smith SM, Seto Y, Flematti GR, Yamaguchi S, Waters MT (2018) An allelic series at the KARRIKIN INSENSITIVE 2 locus of *Arabidopsis thaliana* decouples ligand hydrolysis and receptor degradation from downstream signaling. Plant J 96:75–89. https://doi.org/10.1111/tpj.14017

Yao R, Ming Z, Yan L, Li S, Wang F, Ma S, Yu C, Yang M, Chen L, Chen L, Li Y, Yan C, Miao D, Sun Z, Yan J, Sun Y, Wang L, Chu J, Fan S, He W, Deng H, Nan F, Li J, Rao Z, Lou Z, Xie D (2016) DWARF14 is a non-canonical hormone receptor for strigolactone. Nature 536:469–473. https://doi.org/10.1038/nature19073

Yao R, Wang F, Ming Z, Du X, Chen L, Wang Y, Zhang W, Deng H, Xie D (2017) ShHTL7 is a non-canonical receptor for strigolactones in root parasitic weeds. Cell Res 27:838–841. https://doi.org/10.1038/cr.2017.3

Yoneyama K, Xie X, Yoneyama K, Kisugi T, Nomura T, Nakatani Y, Akiyama K, McErlean CSP (2018) Which are the major players, canonical or non-canonical strigolactones? J Exp Bot 69:2231-2239. https://doi.org/10.1093/jxb/ery090

Yoshida S, Kameoka H, Tempo M, Akiyama K, Umehara M, Yamaguchi S, Hayashi H, Kyozuka J, Shirasu K (2012) The D3 F-box protein is a key component in host strigolactone responses essential for arbuscular mycorrhizal symbiosis. New Phytol 196:1208–1216. https://doi.org/10.1111/j.1469-8137.2012.04339.x

Zhao LH, Zhou XE, Wu ZS, Yi W, Xu Y, Li S, Xu TH, Liu Y, Chen RZ, Kovach A, Kang Y, Hou L, He Y, Xie C, Song W, Zhong D, Xu Y, Wang Y, Li J, Zhang C, Melcher K, Xu HE (2013) Crystal structures of two phytohormone signal-transducing α/β hydrolases: karrikin-signaling KAI2 and strigolactone-signaling DWARF14. Cell Res 23: 436–439. https://doi.org/10.1038/cr.2013.19

Zwanenburg B, Ćavar Zeljković S, Pospíšil T (2016) Synthesis of strigolactones, a strategic account. Pest Manag Sci 72:15–29. https://doi.org/10.1002/ps.4105

Zwanenburg B, Pospísil T (2013) Structure and activity of strigolactones: new plant hormones with a rich future. Mol Plant 6:38–62. https://doi.org/10.1093/mp/sss14

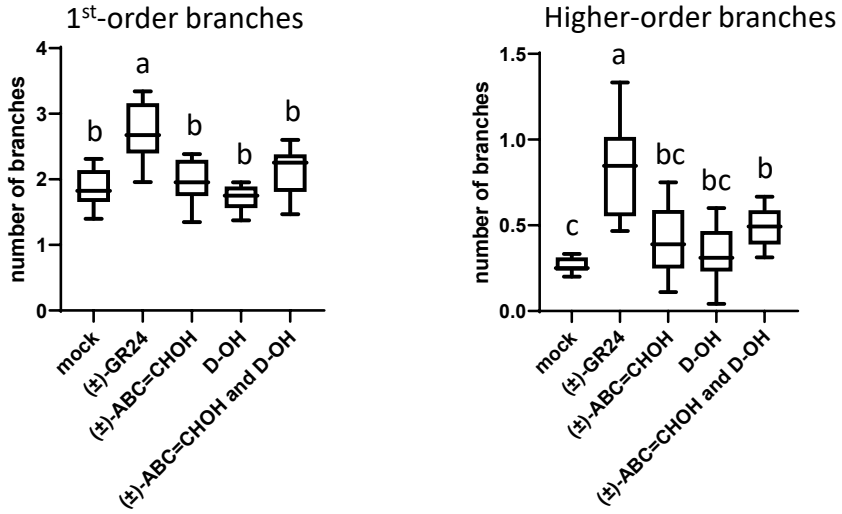

Figure 24. Effect of ABC and D moieties on *R. irregularis* development *in vitro*

R. irregularis germinating spores were exposed to 100 nM of (±)-ABC=CHOH, D-OH, a mix of both (100 nM each) or the solvent alone (mock). The boxes represent the median and 25th and 75th percentiles, whereas whiskers represent the maximum and minimum values. n = 7-8 plates per condition. The experiment was performed once. Conditions topped with the same letter do not differ significantly according to Mann and Whitney's test (P > 0.05).

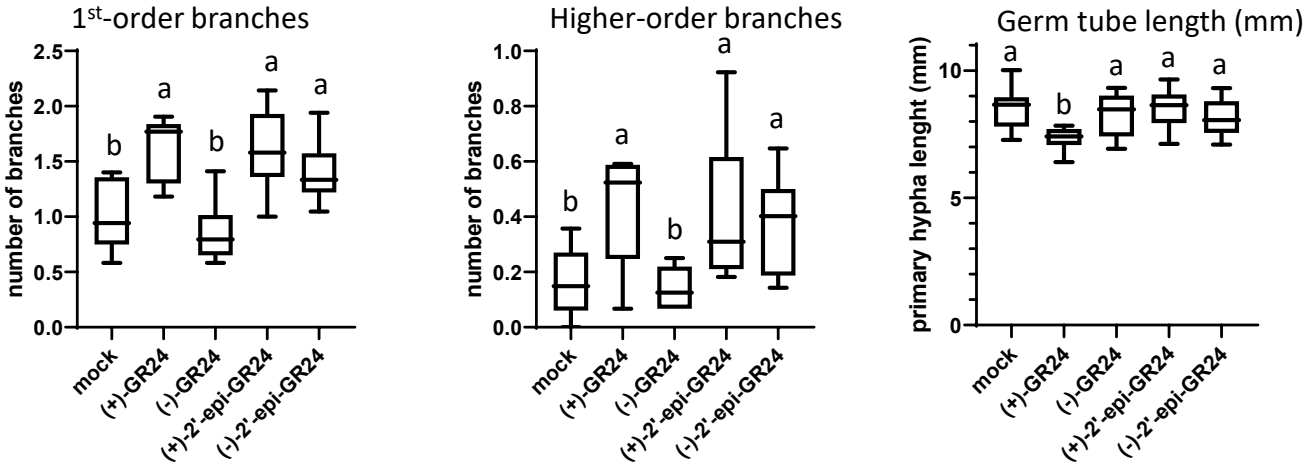

Figure 25. Effect of GR24 stereoisomers on *R. irregularis* development *in vitro*

Activity of GR24 stereoisomers on hyphal branching of *R. irregularis* grown *in vitro* n = 10 plates per condition. The experiment was performed twice. Conditions topped with the same letter do not differ significantly according to Mann and Whitney's test (P > 0.05). Data: Lukas Brichet.

II) Additional SAR studies on *R. irregularis*

Results reported in Taulera et al. 2020 were complemented by hyphal branching tests with the following compounds: ABC lactone and the hydroxymethylbutenolide D-ring, stereoisomers of GR24 and 4'-desmethyl-GR24, two karrikins, and 3'-methyl-GR24. Spore germination assays were also carried out.

II-2) ABC lactone and D-ring moieties

ABC lactone or the hydroxymethylbutenolide D-ring supplied individually were unable to induce hyphal branching (Fig. 24). Treatment with an equimolar mix of these two compounds did not affect the formation of 1st-order branches, and led to a modest but significant increase of higher-order branches (Fig. 24).

II-3) GR24 stereoisomers

The activities of the four enantiopure stereoisomers of GR24 were tested. In line with their activity in *Mtccd8* bioassays (Taulera et al., 2020), (-)-GR24 did not show significant activity on hyphal branching, while the other three stereoisomers increased the number of 1st- and higher-order branches. A reduction of germ tube length was only observed in the (+)-GR24 treatment (Fig. 25).

II-4) 4'-desmethyl-GR24 stereoisomers

We aimed to evaluate the effect of 4'-desmethyl-GR24 stereochemistry on *R. irregularis* development. Racemic mixes of two stereoisomers were available (Fig. 26A). Both (±)-4'-desmethyl-2'-*epi*-GR24 and (±)-4'-desmethyl-GR24 treatments decreased the number of 1st- and higher-order branches (Fig. 26B). However, in contrast to (±)-4'-desmethyl-2'-*epi*-GR24, (±)-4'-desmethyl-GR24 did not increase germ tube length.

II-5) Karrikins

The activity of both 4'-desmethyl-GR24 stereoisomer mixes on *R. irregularis* indicates the existence of a fungal signaling pathway for these compounds. Their opposite effects to those of (±)-GR24 suggest a perception system that allows the fungus to discriminate between methylated and unmethylated butenolides. This pattern is reminiscent of the situation

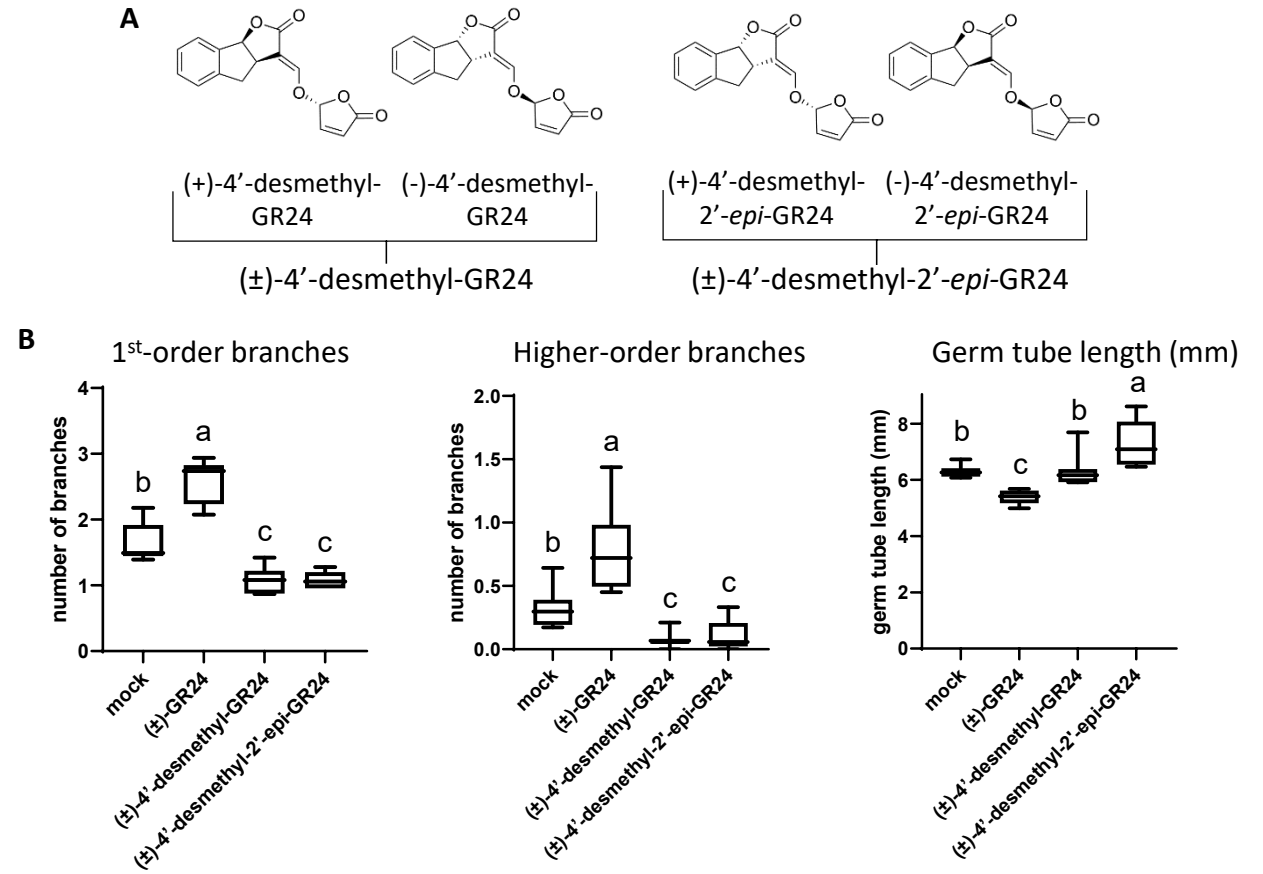

Figure 26. Effect of (±)-4'-desmethyl-GR24 and (±)-4'-desmethyl-2'-*epi*-GR24 on *R. irregularis* development *in vitro*

(A) Structure of the four stereoisomers of 4'-desmethyl-GR24.

(B) Activity of desmethyl-GR24 on *R. irregularis* development.

n = 5-8 plates per condition. The compounds were tested twice. Conditions topped with the same letter do not differ significantly according to Mann and Whitney's test ($P > 0.05$).

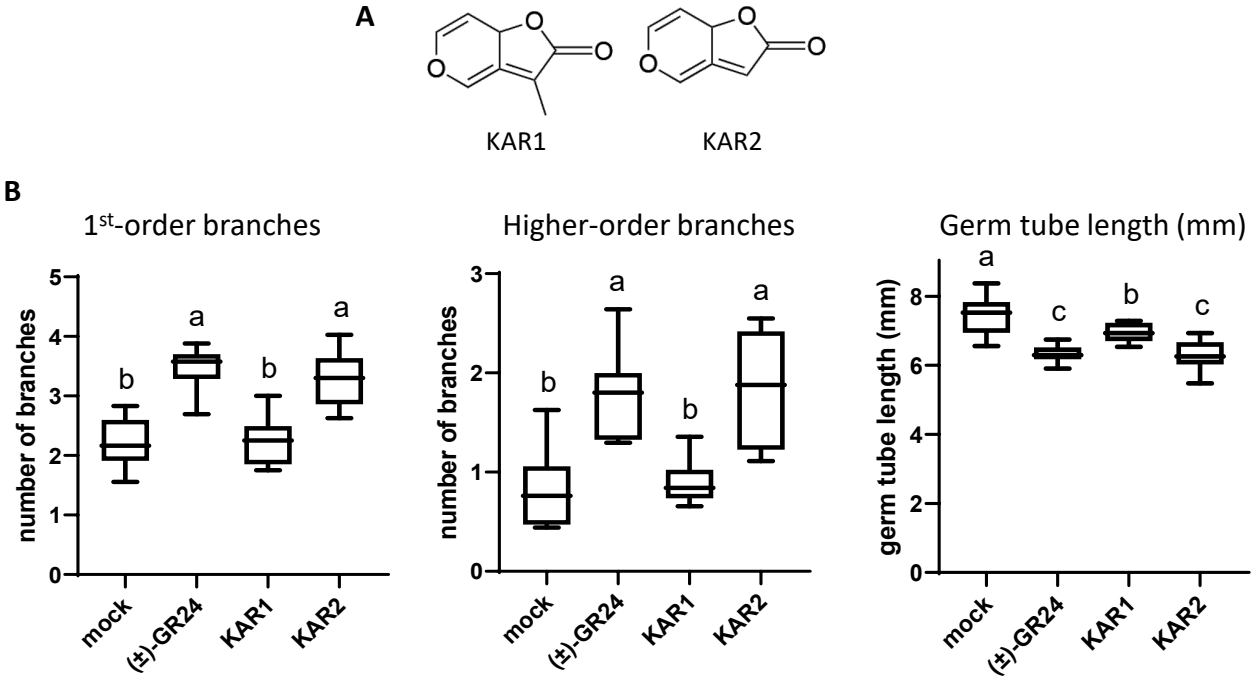

Figure 27. Effects of karrikins on *R. irregularis* development *in vitro*

(A) Structure of KARs.

(B) Activity of KARs on *R. irregularis* development.

n = 8-10 plates per condition. Each compound was tested three times. Conditions topped with the same letter do not differ significantly according to Mann and Whitney's test ($P > 0.05$).

observed in plants, where SLs and KARs activate parallel signaling pathways though either D14 or KAI2 proteins.

Unmethylated butenolides like (±)-4'-desmethyl-GR24 or KAR2 preferentially activate KAR-related responses, whereas methylbutenolides such as (±)-GR24 or KAR1 preferentially induce SL-related responses (Villaécija-Aguilar et al., 2019; Yao et al., 2021).

The ability of *R. irregularis* spores to respond to KAR1 and KAR2 was evaluated. Exposition to KAR1 did not trigger *R. irregularis* branching responses, but the length of the germ tube was slightly reduced (Fig. 27). Unexpectedly, an increase of the number of 1st- and higher-order branches and a reduction of germ tube length were observed in response to KAR2, similarly to (±)-GR24 treatment (Fig. 27).

We next tested whether the application of KAR1 or KAR2 was able to restore the symbiotic deficiency of *Mtccd8* mutants. Preliminary observations suggested that both KARs were inactive (data not shown).

II-6) 3'-methyl-GR24

To further extend structure-activity relationship studies on SL analogs bearing modifications on the D-ring, we tested GR24 analogs with an additional methyl at the C3' position. Two stereoisomer mixes were tested. (±)-3'-methyl-2'-*epi*-GR24 increased the number of 1st- and higher-order branches and decreased germ tube length, while (±)-3'-methyl-GR24 had no effect (Fig. 28). In line with these observations, (±)-3'-methyl-2'-*epi*-GR24 could restore the ability of *R. irregularis* to colonize roots of *Mtccd8* mutants, while (±)-3'-methyl-GR24 could not (Fig. 29).

II-7) Effect of SL analogs on hyphal morphology

We observed that the architecture and the aspect of hyphae were quite different in spores treated with the different analogs. Spores in the mock condition showed mostly white hyphae growing regularly on the medium. Spores exposed to SL analogs that induce increased hyphal branching (i.e. the three active stereoisomers of GR24, (±)-3'-methyl-2'-*epi*-GR24 and KAR2) showed thinner and transparent hyphae compared to the mock condition. Instead of showing a straight and regular development, the hyphae were curled and grew more angularly (Fig. 2E-G). In contrast, hyphae exposed to (±)-4'-desmethyl-2'-*epi*-GR24 were whiter, longer and straighter compared to the mock condition.

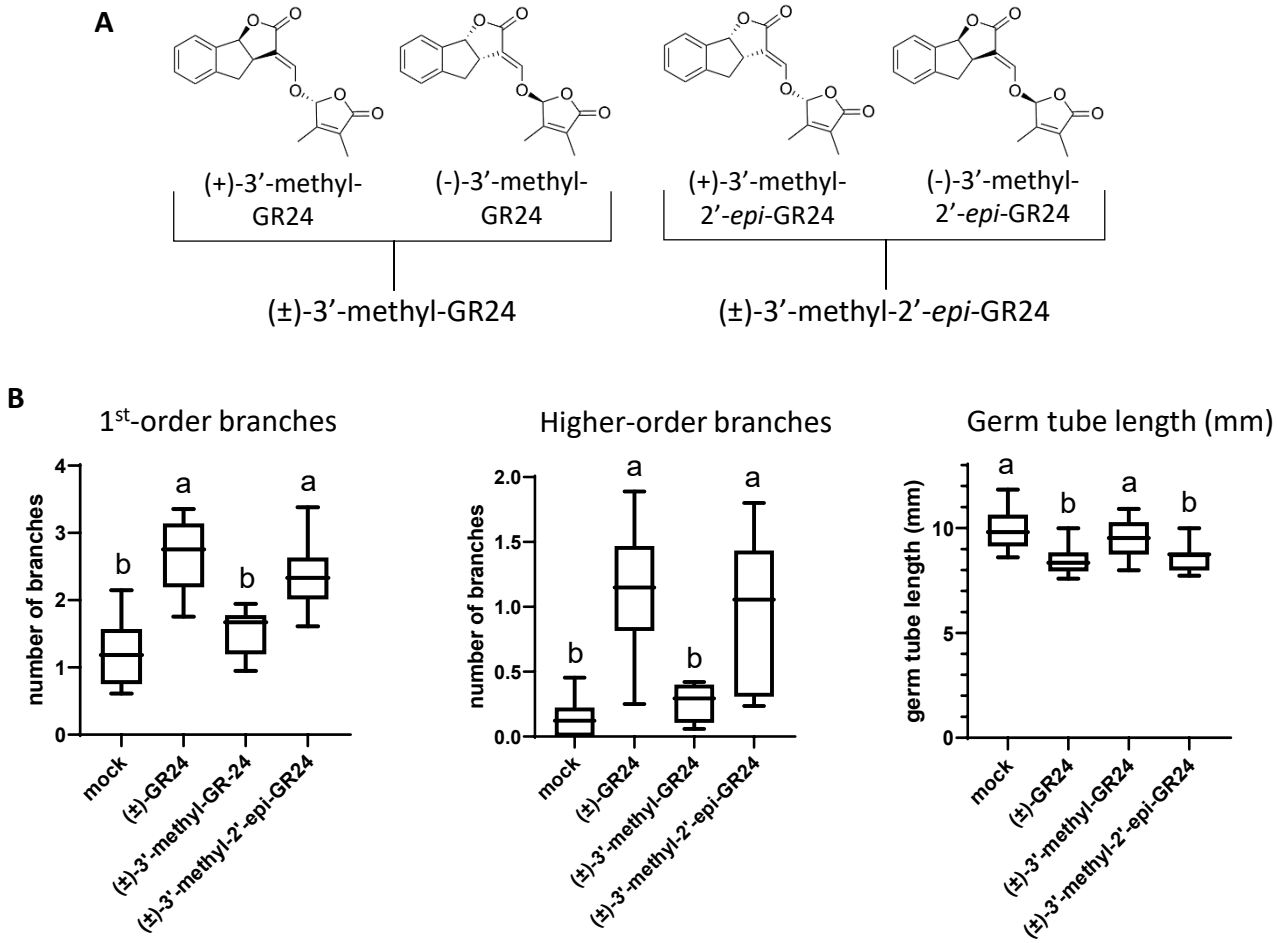

Figure 28. Effect of (±)-3'-methyl-GR24 and (±)-3'-methyl-2'-*epi*-GR24 on *R. irregularis* development *in vitro*

(A) Structure of the four stereoisomers of 3'-methyl-GR24.

(B) Activity of 3'-methyl-GR24 on *R. irregularis* development.

n = 8-10 plates per condition. Each compound was tested three times. Conditions topped with the same letter do not differ significantly according to Mann and Whitney's test (P > 0.05).

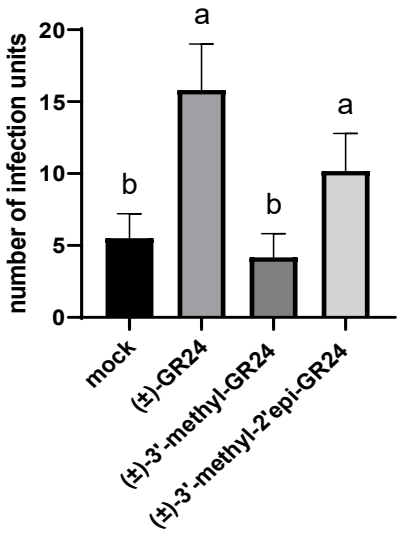

Figure 29. Activity of (±)-3'-methyl-GR24 and (±)-3'-methyl-2'-*epi*-GR24 on symbiosis initiation

Mtccd8-1 mutants were inoculated with *R. irregularis* and watered with a nutrient solution supplemented with 100 nM (±)-GR24, (±)-3'-methyl-GR24, (±)-3'-methyl-2'-*epi* GR24, or the solvent alone (mock). Root colonization was assessed 3 weeks post inoculation. Bars represent the mean number of infection units per plant ± s.e.m. n = 10-12 plants per condition. Each compound was tested three times. A representative experiment is shown. Means topped by the same letter do not differ significantly according to Mann and Whitney's test (P > 0.05).

II-8) Effect of SL analogs on *R. irregularis* spore germination

Aside from hyphal growth and branching, spore germination is another parameter of presymbiotic development that can be observed in response to SLs. I thus carried out time-course experiments on *R. irregularis* spore germination (Fig. 30).

Treatment with ABC lactone, the hydroxymethylbutenolide D-ring or an equimolar mix did not affect spore germination (data not shown). (±)-GR24 treatment increased the germination rate significantly at the late time point (12 days). Likewise, the germination rate of spores exposed to (±)-3'-methyl-2'-*epi*-GR24 and (±)-3'-methyl-GR24 was significantly increased after 12 days. In contrast, (±)-4'-desmethyl-2'-*epi*-GR24 and (±)-4'-desmethyl-GR24 decreased the germination rate.

In addition, all four individual stereoisomers of GR24 increased the germination rate significantly after 5 days (Fig. 31). In this particular experiment, the germination rate was already high after 5 days and very few new germinating spores were observed after 7 days.

III) Effect of a newly discovered strigolactone on *R. irregularis*

During my thesis, I was involved in a side project to characterize a non-canonical SL newly identified by our colleagues Jean-Bernard Pouvreau and Philippe Delavault at the University of Nantes, and François-Didier Boyer at the ICSN of Gif-sur-Yvette. This work will be the focus of two articles which are currently being written. I will briefly summarize my involvement in this project.

Phelipanche ramosa is a parasitic weed that attacks among others rapeseed and hemp plants. Two genotypes of *P. ramosa* show different host specificities. While the first genotype, *P. ramosa* 1 attacks rapeseed, the second genotype *P. ramosa* 2a preferentially attacks hemp. Our colleagues were interested in identifying the molecular actors responsible for this host selectivity. They identified a seed germination stimulant of *P. ramosa* 2a in hemp root exudates, named cannalactone or HGS (hemp germination stimulant). Characterization of its structure revealed that cannalactone was a non-canonical SL. *In vitro* germination assays confirmed that seed germination of *P. ramosa* 2a but not *P. ramosa* 1 was induced by cannalactone. The minimal structure required for host selectivity was further investigated using synthetic cannalactone analogs. My contribution to this project was to test the activity

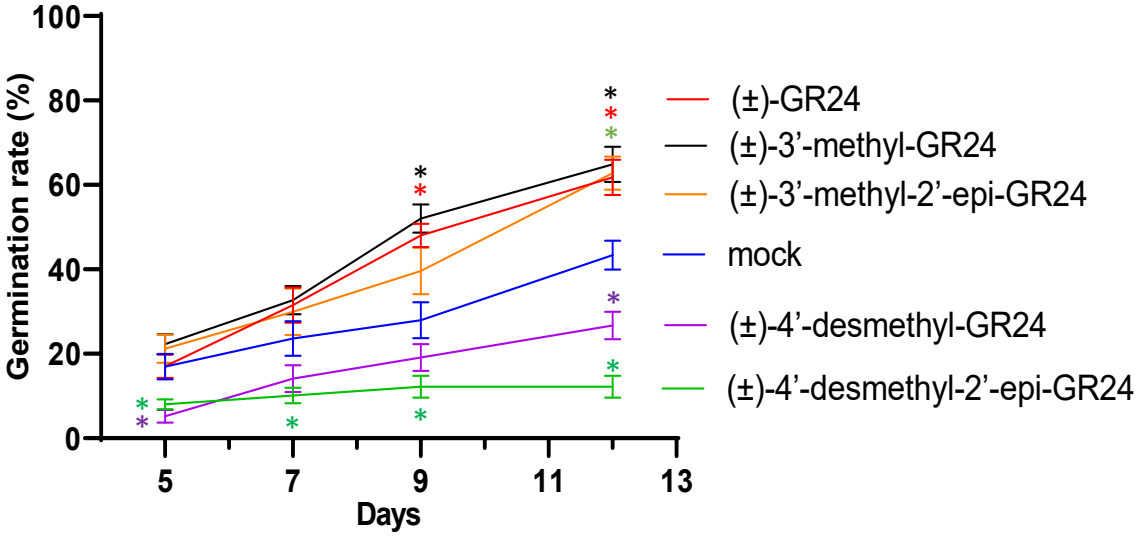

Figure 30. Time-course analysis of spore germination of *R. irregularis* in response to SL analogs harboring modifications of the D-ring

R. irregularis spores were grown in liquid medium supplemented with 100 nM of SL analog. The mean germination rate ± s.e.m is shown. n=8 rows of 10 to 12 spores. The experiment was performed twice. Conditions topped by a star differ significantly from the mock treatment according to one-way ANOVA followed by Fisher's LSD test ($P < 0.05$).

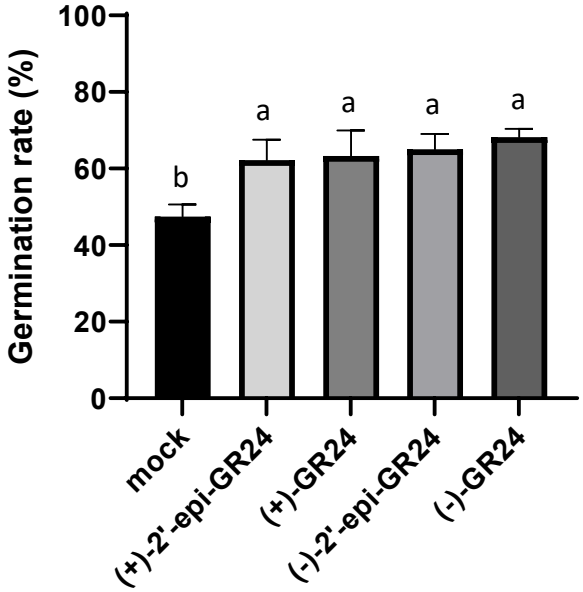

Figure 31. Effect of GR24 stereoisomers on *R. irregularis* spore germination

The germination rate was counted at 5 days. The mean germination rate ± s.e.m is shown. n=5 rows of 10 to 12 spores. The experiment was performed once. Means topped by the same letter do not differ significantly according to one-way ANOVA followed by Fisher's LSD test ($P > 0.05$).

on AMF of cannalactone and (±)-SdL19, the most active synthetic cannalactone analog on *P. ramosa* 2a germination. Both molecules were able to restore symbiosis initation in *Mtccd8* mutants, in a similar manner to GR24 (Fig. 32A). Next, I investigated the activity of (±)-SdL19 on the development of *R. irregularis in vitro*. The presence of (±)-SdL19 increased the number of 1st- and higher-order branches compared to the mock treatment (Fig. 32B).

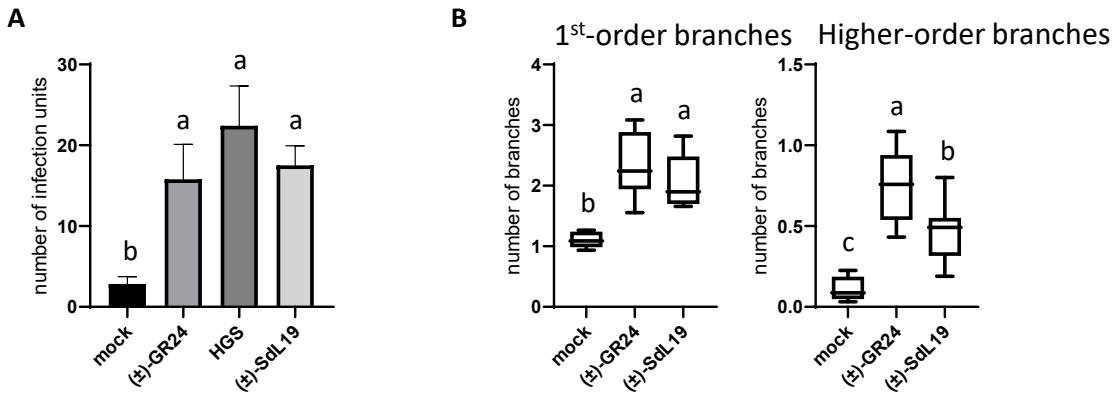

Figure 32. Activity of HGS and (±)-SdL19 on the symbiotic ability and the development of the AM fungus *R. irregularis*

(A) Activity of HGS and (±)-SdL19 on symbiosis initiation of *Mtccd8* roots. Bars represent the mean number of infection units per plant ± s.e.m. n = 10-12 plants per condition.

(B) Activity of (±)-SdL19 on hyphal branching of *R. irregularis* grown *in vitro*. n = 7-8 plates per condition.

The experiments were performed three times. Conditions topped with the same letter do not differ significantly according to Mann and Whitney's test ($P > 0.05$).

Discussion

Initiation of AM symbiosis can occur independently of hyphal branching

In the present work, we aimed to extend previous structure-activity relationship studies for SL activity on AM fungi. To this end, we developed two different bioassays. The first one was designed to study the bioactivity of SL analogs in a context of interaction with a host plant. The second one was designed to study hyphal development of *R. irregularis* grown *in vitro*. Using these two bioassays, we investigated the importance of the SL D-ring. One of the most unexpected observations of our study was that an SL analog lacking the methyl at the C4' position of the D-ring, (±)-4'-desmethyl-2'-*epi*-GR24, could restore the symbiotic defect in *Mtccd8* mutants while inhibiting hyphal branching of *R. irregularis*. These observations challenge the widespread idea that hyphal branching reflects the ability of AM fungi to initiate root colonization. Hyphal branching has been proposed to increase the chances for the fungus to encounter a host root (Buée et al., 2020; Mosse & Hepper, 1975), but this idea has not been supported by experimental evidence. This visible effect of SLs may only be distantly related to their truly important impacts. In addition, hyphal branching is also observed in branched absorbing structures specialized in nutrient absorption (Bago et al., 1998). The fact that hyphal branching occurs in such different physiological contexts is another indication that it is not directly related to the ability of the fungus to infect a host plant.

There is little information in the literature regarding the biological significance of hyphal morphological traits (transparency, straightness *etc*). However, the germ tube elongation and inhibition of hyphal branching triggered by (±)-4'-desmethyl-2'-*epi*-GR24 could be associated with the hyphal morphology described for runner hyphae (long, white, straight hyphae without branches, Bécard & Fortin, 1988). These were first considered as exploratory hyphae, but have later been reported to be able to infect host roots (Bécard & Fortin, 1988; Frieze & Allen, 1991). Development of such hyphae could be the means by which (±)-4'-desmethyl-2'-*epi*-GR24 stimulates symbiosis initiation in SL-deficient mutants.

Does (±)-4'-desmethyl-2'-*epi*-GR24 create a permissive state in the plant root?

An alternative, non-exclusive hypothesis to explain the ability of (±)-4'-desmethyl-2'-*epi*-GR24 to restore root colonization in SL-deficient plants is that this compound creates a permissive state in the root, enabling fungal entry. This hypothesis is consistent with the facts that AM symbiosis is completely abolished in *kai2* mutants (Gutjahr et al., 2015, Meng et al., 2021) and

	Spore Germination	1st-order branches	Germ tube growth	Symbiotic bioassays
Mock				
(±)-GR24				
(+)-GR24				
(-)-GR24				
(+)-2'-*epi*-GR24				
(-)-2'-*epi*-GR24				
(±)-4’-desmethyl-2’-GR24				
(±)-4’-desmethyl-2’-*epi*-GR24				
(±)-3‘-methyl-GR24				
(±)-3'-methyl-2’-*epi*-GR24				
KAR2				
KAR1				

Figure 33. Overview of the activity of the different SL analogs

The activity is similar (blue), higher (green) or lower (red) compared to the mock condition. In grey, activities that have not been tested.

that (±)-4'-desmethyl-2'*epi*-GR24 activates preferentially the KAR-related pathway through KAI2 (Villaécija-Aguilar et al. 2019; Yao et al., 2021). Therefore, (±)-4'-desmethyl-2'*epi*-GR24 could activate the KAR pathway in plants in a way that favors root colonization. However, the fact that KAR2 (perceived in plants by KAI2 similarly to (±)-4'-desmethyl-2'-*epi*-GR24) is not able to restore root colonization in *Mtccd8* mutants suggests that activation of the KAR pathway is no sufficient to enable root colonization. Based on these observations, it appears that the ability of (±)-4'-desmethyl-2'-*epi*-GR24 to restore symbiosis in *Mtccd8* mutants could reflect its effects on both the fungus and the plant.

Do effects of SL analogs on spore germination have an impact on symbiosis initiation?

In previous experiments (data not shown) we observed that the number of infection units depended on the number of spores in the inoculum, and therefore indirectly on the number of germinated spores. Thus, restoration of symbiosis in *Mtccd8* mutants may simply result from an increased number of germinated spores triggered by (±)-GR24. We cannot formally rule out this hypothesis. Nevertheless, (-)-GR24 increased spore germination but failed to restore symbiosis in *Mtccd8* mutants, showing that a stimulation of spore germination is not sufficient. Moreover, (±)-4'-desmethyl-2'-*epi*-GR24 inhibited spore germination but was able to restore symbiosis in *Mtccd8* mutants. Collectively, these results suggest that effects of SL analogs on spore germination have a minor impact, if any, on symbiosis initiation in our bioassays.

Importance of stereochemistry for bioactivity on *R. irregularis*

Preferences for SL stereochemical configurations have been described in the various SAR studies performed on plants, parasitic weeds and AMF. Here we reported that among the four stereoisomers of GR24 only (-)-GR24 was inactive, indicating similar stereochemical preferences in *R. irregularis* and *Gi. margarita* (Akiyama et al., 2010).

Perception of karrikins by *R. irregularis*

KAR1 did not show any hyphal branching activity on *R. irregularis*, consistent with assays performed on *Gi. margarita* (Akiyama et al., 2010).

Because (±)-4'-desmethyl-2'-*epi*-GR24 and KAR2 share the unmethylated butenolide moiety, and both compounds can be perceived by the same receptor in plants and activate the KAR-related pathway, we investigated whether the fungus could respond to KAR2 similarly to (±)-4'-desmethyl-2'-*epi*-GR24. We observed an opposite effect to that expected. In contrast to (±)-4'-desmethyl-2'-*epi*-GR24, KAR2 triggered hyphal branching similarly to (±)-GR24. This

suggests that the mechanisms of (±)-4'-desmethyl-2'-*epi*-GR24 and KAR2 perception differ between plants and AM fungi.

Spore germination, hyphal branching and germ tube elongation are regulated through different pathways

The tested compounds exhibited differential abilities to affect (positively or negatively) the examined aspects of fungal development *in vitro*: hyphal branching, germ tube elongation and spore germination (Fig. 33). This strongly suggests that these developmental responses can be triggered by at least partly separate signaling pathways involving distinct receptors. In a natural soil environment, AM fungi are exposed to a range of (methyl)butenolide compounds released by different plant species and possibly other microbes, and their development is likely regulated through a complex interplay of such molecular signals. In addition to its activity on *R. irregularis* reported here, 3'-methyl-GR24 was shown to be active as a shoot branching inhibitor in pea and to induce parasitic weed germination (Boyer et al., 2014; de Saint Germain et al., 2021).

Perspectives

Recent articles have reported major advances in the culture of AM fungi *in vitro*, as novel methods allowing the completion of a full developmental cycle from spores to spores have been established (Kameoka et al., 2019; Sugiura et al., 2020; Tanaka et al., 2022). These methods rely on the supply of lipids in the form of palmitoleate or myristate, as well as organic nitrogen. Tanaka et al. (2022) have reported the production of large numbers of infectious secondary spores of *Rhizophagus clarus*, and a positive effect of added GR24 on sporulation. In addition to this new response to SLs, the culture system allows the continuous observation of the different stages of fungal development *in vitro*: germ tubes, runner hyphae, branched structures, secondary spores. It also allows to grossly monitor lipid consumption: myristate is insoluble and makes the culture medium opaque, and clear zones appear as it is taken up and used by the fungus. It would be of great interest to test additional SL analogs in this system, such as (±)-4'-desmethyl-2'-*epi*-GR24, to further document their effects on fungal development and physiology.

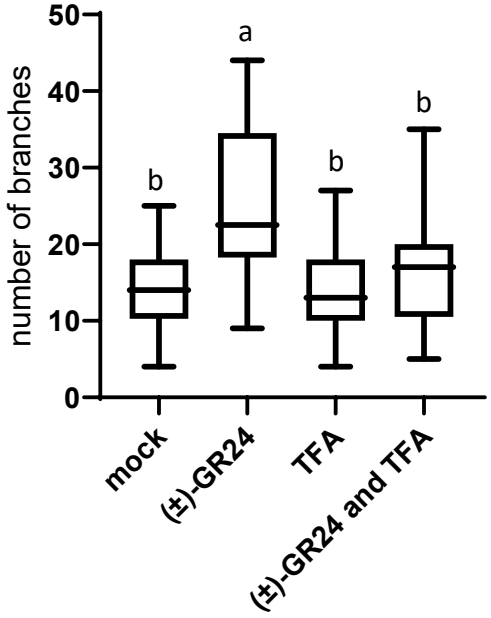

Figure 34. Activity of TFA on *Gi. rosea* developmental responses to (±)-GR24

Gi. rosea was grown from spores on solid M medium. Six days after, small wells were made with the tip of a Pasteur pipette at a distance of 5mm of the tip of each germ tube; 5 µl of 100 nM (±)-GR24, TFA, an equimolar mix of (±)-GR24 and TFA or the solvent alone was applied. Newly formed apices were counted 36h after molecule application. Conditions topped with the same letter do not differ significantly by Mann and Whitney's test ($P > 0.05$).

Chapter 2
Towards identification of strigolactone receptor(s) in *R. irregularis*

Background

This second chapter focuses on the identification and characterization of putative SL receptors in AMF. Prior the beginning of my thesis, indirect evidence obtained by the team suggested structural similarities between plant and fungal SL receptors. In particular, AMF spores were able to cleave SLs into their ABC and D moieties, and an inhibitor of the *Petunia* SL receptor DAD2 was also able to inhibit the effect of SLs on hyphal branching in the AM fungus *Gigaspora rosea* (Fig. 34). Our working hypothesis was thus that like plant SL receptors, fungal receptors of SLs could also belong to the α/β-fold hydrolase family. The project developed in the following sequence of events:

- A collaboration was established with the group of Kim Snowden at Plant & Food Research, Auckland, New Zealand (notably involving Bart Janssen and Cyril Hamiaux). This group was the first to report the identification and characterization of a plant SL receptor (*Petunia* DAD2, Hamiaux et al. 2012). Using 3D modeling, they identified several AM fungal proteins that shared strong structural similarities with PhDAD2.
- I joined the group and focused on one of these proteins, BJ318. I obtained a corresponding recombinant protein and carried out preliminary experiments to investigate its capacities to bind and cleave SLs.
- Our long-standing collaboration with colleagues at INRAE Versailles and ICSN Gif-sur-Yvette extended to work on additional proteins with Alexandre de Saint Germain and François-Didier Boyer. They also have a great expertise in the production and characterization of plant SL receptors (de Saint Germain et al., 2021; de Saint Germain et al., 2016; Fiorilli et

al., 2022; Lopez-Obando et al., 2021). I visited the Versailles lab twice during my PhD to carry out experimental work with Alexandre and François-Didier. In parallel, I carried out bioassays on *R. irregularis* as well as additional biochemistry experiments in our lab.

Early work on BJ318 carried out in Toulouse will be described first. The rationale used for the identification of candidate proteins, a phylogenetic analysis of the corresponding sequences and the bulk of experimental results will be presented in the form of an independent article, to be submitted soon. Finally, I will report additional results related to the characterization of candidate protein

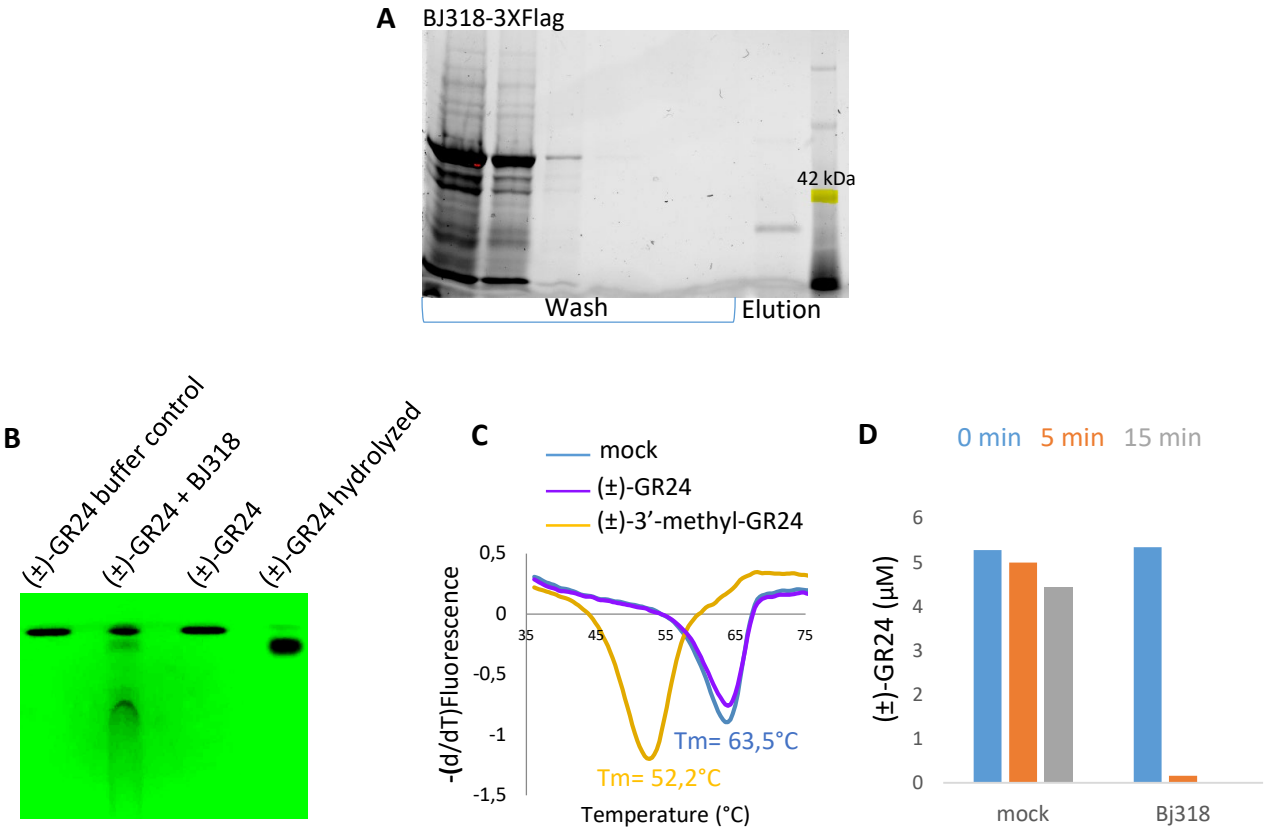

Figure 35. Preliminary results obtained with BJ318

(A) Expression and purification of BJ318-3xFLAG proteins produced in *N. benthaniama.*

(B) Thin layer chromatography of (±)-GR24 incubated with either BJ318 or the solvent alone. Chemically hydrolyzed GR24 was used as a positive control.

(C) DSF assays with 2,5 µM BJ318 incubated with 200 µM of (±)-3'methyl-GR24, (±)-GR24 or in absence of ligand.

(D) Mass spectrometry analysis of BJ318 cleavage toward (±)-GR24. 5 µM (±)-GR24 was incubated with BJ318 (1 µM) or the solvent alone (mock).

Results

I) Early work on candidate protein BJ318

I-1) Production of recombinant BJ318

Prior the beginning of my thesis, Bart Janssen had started to produce recombinant proteins for some of the candidates in *Escherichia coli*. One of these candidates, named BJ318, was obtained in relatively large quantities. In our laboratory some colleagues also tried to produce BJ318 in *E. coli*, but with little success. Therefore, at the beginning of my thesis, my first goal was to obtain sufficient quantities of pure BJ318 protein to be able to characterize it *in vitro*. To this end, I continued the production trials using two heterologous protein expression systems: E. coli and *Nicotiana benthamiana.*

Despite several attempts and an optimization of the experimental procedure, we were not able to sufficiently purify BJ318 produced in *E. coli*. Production in *N. benthamiana* allowed to obtain pure protein, but the quantity produced was too low to perform a complete series of *in vitro* experiments (Fig. 35). Nevertheless, in order to gain insight into the enzymatic activity of BJ318 and to make a decision on whether to pursue work on this protein, we used the small amount of pure BJ318 produced in *N. benthamiana* to study its ability to cleave SLs.

I-2) Preliminary characterization of BJ318

We performed a thin layer chromatography (TLC) experiment to observe the hydrolysis of SLs, as described by Hamiaux et al. (2012). We observed the cleavage of (±)-GR24 upon incubation with BJ318 (Fig. 35B). This encouraged us to pursue the characterization of this protein, and to this end we had BJ318 protein produced by the company Genscript.

I-3) Binding assays

In order to investigate the ability of BJ318 to bind SLs, we carried out thermal shift assays (DSF = Differential Scanning Fluorimetry, described in the Introduction) as well as thermophoresis experiments. Thermophoresis was performed in collaboration with Jean-Jacques Bono and Virginie Gasciolli (LIPME, Toulouse). This method is based on the differential mobilities of a protein *vs* a protein-ligand complex in a temperature gradient. In addition to giving indications

of protein-ligand binding, it allows to estimate a binding affinity by using titration series of the ligand. If there is an interaction, the thermophoresis profile changes for each concentration of the ligand due to a change in the ratio between unbound and bound proteins. After several attempts and an optimization of buffer composition, of the BJ318/GR24 ratio and of incubation time, we were able to observe small differences of thermophoresis signals in the presence of (±)-GR24. These observations seemed promising but the differences were too small and too fluctuant to conclude (data not shown).

Using DSF, we were able to observe a shift in the Tm of the protein in the presence of the non-natural SL (±)-3'-methyl-GR24, but not with (±)-GR24 (Fig. 35C). Together, these data suggested that BJ318 could bind SL analogs, but in the case of (±)-GR24 a robust demonstration of binding was difficult to obtain.

I-4) Cleavage assays

In parallel, we investigated the ability of BJ318 to cleave (±)-GR24 using LC-MS analysis. The concentrations of intact (±)-GR24 as well as of the ABC moiety produced upon cleavage were monitored over time as the protein was incubated with its potential substrate. This experiment showed a very fast cleavage: 1µM BJ318 could hydrolyse 5 µM of (±)-GR24 within 5 minutes (Fig. 35D). This observation could explain why we were not able to obtain clear results in thermophoresis and DSF assays: most SLs were probably cleaved at the time of measurements because of the time needed to prepare samples and to start the analysis.

Later, we ordered three additional protein candidates from Genscript. Regrettably, only BJ309 seemed to be folded correctly. BJ309 did not exhibit a typical DSF profile, preventing us from testing its ability to bind SLs. Nevertheless, using mass spectrometry, we showed that BJ309 was able to cleave (±)-GR24 (data not shown). At this point, we had two fungal proteins that were able to cleave SLs. In view of those results, during the last year of my thesis, we decided to pursue the characterization of these two proteins and other candidates. Most of this work is presented in the form of an article as follows.

II) Identification of alpha/beta-hydrolase fold proteins from *Rhizophagus irregularis* displaying enzymatic activity towards methylated and unmethylated strigolactone analogs

Abstract

Arbuscular mycorrhizal (AM) symbiosis is a widespread mutualistic association between plant roots and soil fungi of the Glomeromycotina subphylum. The initiation of AM symbiosis involves diffusible molecules secreted by both partners. Strigolactones (SLs) are carotenoid-derived compounds produced by plants and exuded into the soil. They are required at the early stages of symbiosis and trigger in AM fungi cellular, metabolic and developmental responses such as the stimulation of hyphal branching. In addition to their bioactivity on AM fungi, SLs induce seed germination of parasitic weeds and act in plants as phytohormones. The mechanisms of SL perception remain unknown in AM fungi but are well documented in plants: they involve receptors belonging to the alpha/beta-hydrolase fold family of proteins. Here, we report that two chemical inhibitors known to target plant SL receptors also suppress responses of the AM fungus *Rhizophagus irregularis* to SLs. This suggests that AM fungal SL receptors share structural similarities with those of plants. By using tridimensional modeling, we identified eight fungal alpha/beta-hydrolase fold proteins sharing structural similarities with a plant SL receptor. *In vitro* characterization revealed that two of them were able to cleave synthetic SL analogs. Moreover, both inhibitors of plant SL receptors decreased this enzymatic activity. Taken together, these observations lend support to the hypothesis that AM fungi perceive SLs through alpha-beta hydrolase fold proteins.

Key words

Arbuscular mycorrhiza**,** *Rhizophagus irregularis*, Strigolactone

Abbreviations

SL: Strigolactone; AM: Arbuscular mycorrhiza; KAR: Karrikin

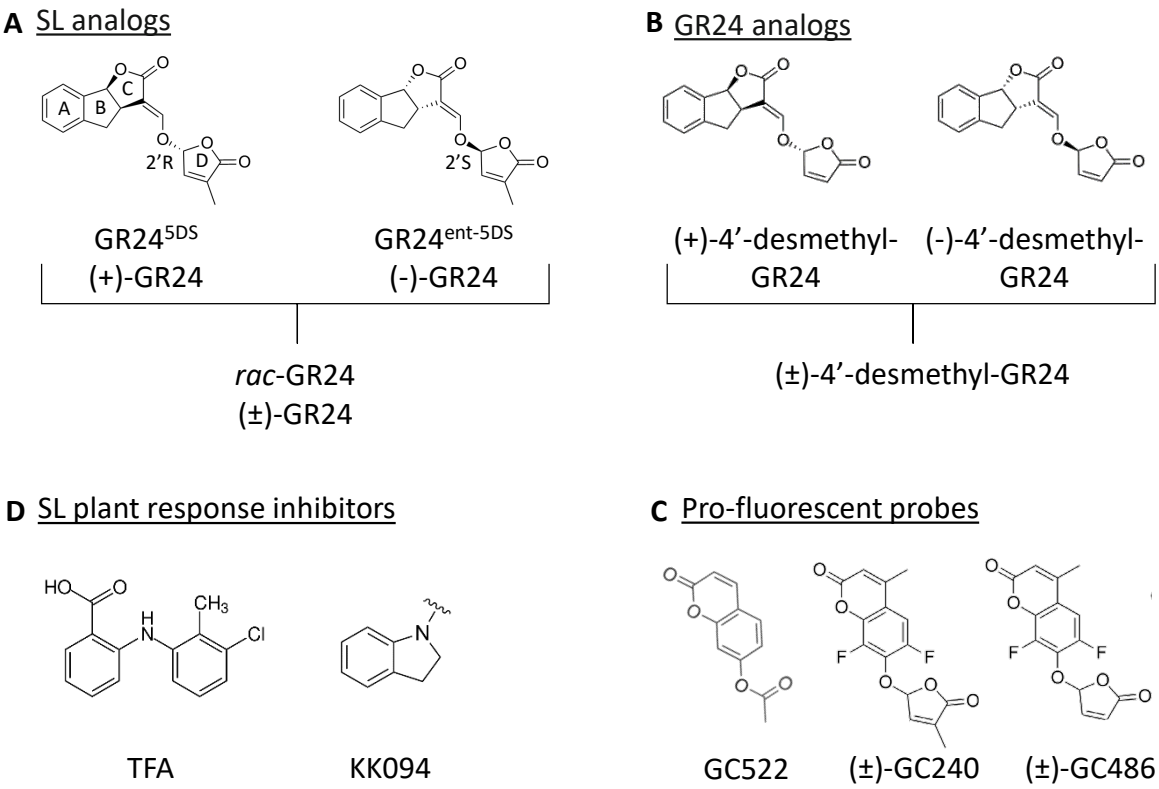

Taulera et al. (*in prep*) - Figure 1. Compounds used in this study

Structure of:

(A) The SL analog (±)-GR24.

(B) (±)-4'-desmethyl-GR24 exhibiting an unmethylated D-ring.

(C) SL plant response inhibitors: tolfenamic acid (TFA) (Hamiaux et al., 2018) and KK094 (Nakamura et al., 2019)

(D) Pro-fluorescent molecular probes: the generic esterase pro-fluorescent probe GC522, SL pro-fluorescent mimics (±)-GC240 and (±)-GC486. The methyl-butenolide moiety of (±)-GC240 is similar to the D-ring of (±)-GR24, whereas (±)-GC486 harbours an unmethylated D-ring (de Saint Germain et al., 2016).

Introduction

Arbuscular mycorrhizal (AM) symbiosis is an ancient root endosymbiosis associating the vast majority of land plant species with AM fungi from the Glomeromycotina subphylum. This interaction represents the most common situation of plants in all kinds of terrestrial ecosystems and agrosystems, where it greatly contributes to carbon cycling as well as plant nutrition and health. During symbiosis, the fungus provides water and nutrients such as nitrogen and phosphate to the plant (Smith & Read, 2008), while the plant supplies carbon in the form of lipids and carbohydrates to the fungus (Luginbuehl et al., 2017). The establishment of the AM symbiosis relies on mutual recognition between the host plant and the fungus. This is mediated by diffusible molecules secreted by both partners. One of the key signals produced and exuded by plants to stimulate AM fungi are strigolactones (SLs).

SLs are carotenoid-derived compounds, composed of an invariable methylbutenolide D-ring linked by an enol-ether bridge to a variable ABC tricyclic lactone (Fig. 1; Xie et al., 2019). They were first characterized as germination stimulants for seeds of parasitic weeds (Cook et al., 1966). Later, SLs were demonstrated to stimulate several species of AM fungi at subnanomolar concentrations, triggering a number of cellular, metabolic and developmental responses such as the stimulation of hyphal branching (Akiyama et al., 2005; Besserer et al., 2006, 2008). More recently still, SLs were defined as a new class of phytohormones contributing to the regulation of shoot branching (Gomez-Roldan et al., 2008; Umehara et al., 2008) and to the control of other developmental processes in angiosperms (Rameau et al., 2019).

The level of AM fungal colonization in SL-deficient mutants of several angiosperm species is severely decreased, and addition of SL analogs restores root colonization in these plants (Gomez-Roldan et al., 2008; Taulera et al., 2020; Yoshida et al., 2012). In contrast, plants mutated in their SL receptor are normally colonized by AM fungi (Taulera et al., 2020; Yoshida et al., 2012). These observations, together with a fine characterization of the role of SLs in the extension of root colonization (Kobae et al., 2018), indicate that SLs mostly function in the AM symbiosis as fungal stimulants rather than endogenous plant hormones. To try to identify the ancestral function of SLs, Kodama et al. (2021) analysed mutants of *Marchantia paleacea* (a bryophyte*),* deficient in the production of the newly identified SL bryosymbiol. These mutants could not be colonized by AM fungi. However, in contrast to their angiosperm counterparts, they did not display any developmental phenotypic differences to the wild-type. The authors proposed that SLs originally functioned as signals in the AM symbiosis, and that their hormonal

roles evolved later (Kodama et al., 2021.). Although the ability to stimulate AM fungi is by far the most ancient of SL known functions, the mechanisms of SL perception in these fungi remain unknown. In contrast, SL perception and signaling are well documented in plants. Plant SL receptors PhDAD2/OsD14/PsRMS3/AtD14 (de Saint Germain et al., 2016; Hamiaux et al., 2012; Nakamura et al., 2013; Yao et al., 2016) have been identified as alpha/beta-hydrolase fold proteins (ABHs) (Hamiaux et al., 2012). ABHs comprise a large family of proteins found in all kingdoms (Mindrebo et al., 2016). They exhibit a wide range of enzymatic functions including the hydrolysis of ester, peptide and carbon-carbon bonds in a variety of substrates. Despite low sequence homology, ABHs share a highly conserved three-dimensional core architecture. Their hydrolytic activity relies on a catalytic triad composed of a serine, a histidine and an aspartate or glutamate residue. Uncommonly for receptors, SL receptors identified to date have retained their enzymatic activity through the conservation of the catalytic triad, suggesting that hydrolysis could be important for signaling. In addition to substrate hydrolysis, these receptors can covalently bind to the D-ring of SLs and undergo conformational changes, as reflected by protein melting temperature shifts observed through differential scanning fluorimetry (DSF) (de Saint Germain et al., 2016; Hamiaux et al., 2012).

The sequence of events by which SL receptors are activated to trigger the associated signaling pathway is currently under debate. Two main models have been proposed, contrasting in their requirements for ligand hydrolysis and conformational change of the receptor. The first model suggests that upon binding to their receptor, SLs undergo a cleavage between the ABC lactone and the methylbutenolide D-ring (Hamiaux et al., 2012). The latter remains covalently attached to the conserved catalytic histidine residue of the receptor (de Saint Germain et al., 2016; Yao et al., 2016), resulting in a conformational change of the receptor and the creation of a complex with an F-box protein (OsD3/AtMAX2) which targets proteins for degradation (Jiang et al., 2013; Zhou et al., 2013). In contrast, the second model proposes a cleavage-independent SL perception model (Seto et al., 2019; Shabek et al., 2018) in which binding to an uncleaved SL molecule triggers the conformational change of the receptor. This leads to activation of the signaling pathway and subsequent hydrolysis of SLs by the receptor, presumably to contribute to the turnover of active SLs.

From an evolutionary perspective, it has been proposed that D14 SL receptors evolved the capacity to perceive SLs through neo-functionalization of KAI2 proteins, which mediate responses to karrikins, and other currently unknown ligands (Bythell-Douglas et al., 2017). Karrikins are a set of small butenolide compounds produced upon combustion of plant material

(Flematti et al., 2004). They are thought to be structurally related to a yet unidentified endogenous plant signal (termed KAI2 ligand). KAI2 proteins cannot perceive natural SLs but respond to SLs harboring the non-natural 2'S configuration between the C- and D-rings, such as the synthetic SL analog (-)-GR24 (Fig. 1) (Scaffidi et al., 2014). Gene sequence analysis revealed a large expansion of *KAI2/ HYPOSENSITIVE TO LIGHT* (*HTL*) genes in parasitic weed species (Conn et al., 2015; Toh et al., 2015). For example, *Phelipanche aegyptiaca* and *Striga hermonthica* possess 5 and 11 *KAI2-LIKE* genes, respectively (Conn et al., 2015). Each protein exhibits different capacities to bind and to hydrolyze GR24 stereoisomers with 2'S or 2'R configuration. Cross-species complementation experiments revealed that several *KAI2-LIKE* genes from *S. hermonthica* and *P. ramosa* were able to restore responses to SLs in *Atd14* mutants (de Saint Germain et al., 2021; Nelson, 2021; Toh et al., 2015). This highlights that SL perception in parasitic and non-parasitic plants arose from convergent evolution of *KAI2-LIKE* genes (Conn et al., 2015). In addition, SLs trigger developmental responses in the moss *Physcomitrium patens* (Guillory & Bonhomme, 2021) but not likely in other bryophytes, suggesting that *P. patens* evolved the capacity to perceive SLs independently from seed plants (Walker et al., 2019). Phylogenetic analysis revealed the existence of 13 *KAI2-LIKE* genes in *P. patens* (Delaux et al., 2012; Lopez-Obando et al., 2016) and some of the associated proteins could bind and cleave SLs *in vitro*. Further genetic analysis identified two *KAI2-LIKE* genes involved in *P. patens* developmental responses to SLs in the dark (Lopez-Obando et al., 2021). It has thus been proposed that SL perception in *P. patens* also arose through evolutionary convergence after expansion and diversification of *KAI2-LIKE* genes. From these observations we hypothesize that the unknown SL receptor(s) in AM fungi may have evolved in a similar fashion.

Forward genetics have been instrumental to uncover the mechanisms of SL perception and signaling in plants. Unfortunately, as coenocytic organisms with hundreds to thousands of nuclei per cell, AM fungi are not amenable to such genetic approaches. Recently, to investigate SL perception in fungi, Fiorilli et al. (2022) used the plant pathogenic fungus *Cryphonectria parasitica* for which mutants can be generated. They identified in this species a structural homologue of D14, which could covalently bind and cleave (+)-GR24 *in vitro. Cpd14* knock-out mutants exhibited a reduced response to (+)-GR24. However, there are important differences in SL responses between AM fungi and *C. parasitica.* The latter shows a moderate response to 100 µM (+)-GR24, and a weak and transient response to 10 µM (+)-GR24. Furthermore, the measured response is a reduction of fungal colony diameter (Belmondo et al.,

2017; Fiorilli et al., 2022). The sensitivity and developmental responses exhibited by AM fungi are quite different (formation of new hyphal branches and enhanced respiratory metabolism are observed in response to SL concentrations in the nanomolar range or below: Akiyama et al., 2005; Besserer et al., 2006, 2008). This suggests that AM fungi have evolved receptors and signaling pathways that could be absent in other fungi.

In the present work, we aimed to investigate the mechanisms of SL perception in the model arbuscular mycorrhizal fungus *Rhizophagus irregularis*. We used pharmacological tools to investigate the possibility that SL perception in AM fungi also involves ABHs. Further, we identified eight ABH proteins in *R. irregularis* that share structural similarities with plant SL receptors. Their abilities to bind and cleave SL analogs *in vitro* were examined.

Materials and methods

Chemicals

(±)-GR24 used in biological assays was purchased from Chiralix (The Netherlands). For biochemical assays, (±)-GR24, (+)-GR24, (±)-4'-desmethyl-GR24, GC522, (±)-GC240 and (±)-GC486 were synthesized as described in de Saint Germain et al. (2016). Tolfenamic acid (Hamiaux et al., 2018) was purchased from Merck and KK094 (Nakamura et al., 2019) was kindly provided by T. Asami. All compounds were dissolved in DMSO or acetone and stored at −20 °C. Freshly prepared 1000X stock solutions in DMSO or acetone were used for each assay.

Biological material

Rhizophagus irregularis spores (strain DAOM197198) were purchased from Agronutrition (France). They were washed three times and left at 4°C in sterile water for 48h, then rinsed using a 40 µM nylon mesh with 800 mL sterile water and resuspended in a small volume of sterile water before use.

Analysis of AM fungal development *in vitro*

Experiments were carried out in 10 cm square plates containing 25 mL of M medium (Bécard and Fortin 1988) without sucrose and solidified with 0.4% (w/v) phytagel. Tested compounds were added to the medium after autoclaving at a final concentration of 100 nM. An equivalent concentration of DMSO or acetone (0.1% v:v) was used for mock treatments.

Using a dissecting microscope, 20 droplets of spore suspension, each containing one to three spores of *R. irregularis*, were placed on each plate. The plates were sealed using micropore film and incubated horizontally at 30 °C under 2% CO_2 for 12 days. Germ tubes were identified as the longest hypha coming out of each spore. Their length, from spore to tip and excluding any

branches, was measured using ImageJ software after scanning the plates. The number of hyphal branches of the 1st-order (growing from the germ tube) and higher-order (growing from 1st-order branches) was determined for each germinated spore.

The experiments were performed at least twice, and data presented in figures correspond to a representative experiment. For statistical analysis, each plate was treated as a replication unit (represented by the mean germ tube length and mean number of branches), and 6 to 11 plates were analyzed. Data were analyzed using Statgraphics Centurion software (SigmaPlus). Non-parametric tests were used because normality or homoscedasticity criteria were not met. Datasets were analyzed using the Kruskal-Wallis test, followed by pairwise comparisons with Mann and Whitney's test.

Phylogenetic analysis

Each candidate protein sequence identified in *R. irregularis* was used as a query for a tBLASTn+ v2.1.11 analysis (Camacho et al., 2009) using the fungal genomes available at the Joint Genome Institute's MycoCosm website. Ascomycetes and Basidiomycetes are overrepresented in this database compared to other phyla, therefore only one species for each order of these two phyla was randomly chosen. Two species in the subphylum Glomeromycota, *Diversispora versicolor* and *Geosiphon pyriformis* (Archaeosporales) were added to represent the basal evolutionary lineages of AMFs (Krüger et al., 2021). Sequences were aligned using MAFFT v7.453 (Katoh & Standley, 2013) and positions with more than 80% of gaps removed with trimAl v1.4 (Capella-Gutierrez et al., 2009). Alignments served as a matrix for tree reconstructions by the maximum likelihood method with IQ-TREE2 v2.1.2 program (Minh et al., 2020). The best-fitting evolutionary model was estimated prior to reconstruction with ModelFinder (Kalyaanamoorthy et al., 2017) and branch supports estimated with 10,000 replicates of both SH-aLRT (Guindon et al., 2010) and UltraFast Bootstraps (Hoang et al., 2018). Trees were visualized and annotated in the iTOL v5 platform (Letunic & Bork, 2021). Signal peptides were predicted using SignalP v5 (Almagro Armenteros et al., 2019) with default parameters.

3D modeling

Secondary and tertiary structures of *R. irregularis* ABHs were predicted with the iTasser website. Then the CASTp server was used to estimate pocket sizes for the best 3D model produced by iTasser. Predicted binding pockets were examined using Pymol for their shape, and for the presence of catalytic serine and histidine residues, as well as phenylalanine residues lining the pocket.

Recombinant protein expression and purification

BJ309 and BJ318 fused to a 6-His tag were produced in *E. coli* by GenScript Biotech (The Netherlands). The N-terminal sequences encoding predicted signal peptides of BJ309, BJ311 and BJ313 were removed, and coding sequences were optimized for expression in *E. coli* prior to cloning. Expression of BJ311, BJ313, BJ316, BJ317, BJ318^{H208A} and BJ318^{S122A} proteins was performed as described in de Saint Germain et al. (2016) with the following modifications. Coding sequences were fused to a cleavable N-terminal MBP tag. Following IPTG induction, *E. coli* was grown at 28°C to optimize protein expression. Protein purification was performed using amylose resin for BJ318^{H208A} and BJ318^{S122A} and the MBP tag was cleaved. BJ311, BJ313, BJ316, BJ317 were purified by gel filtration and retained the MBP-tag. The identity of the purified proteins was verified using mass spectrometry.

Enzymatic assays with profluorescent probes

Enzymatic assays were performed as previously described (de Saint Germain et al., 2016, 2021), using a TriStar LB 941 Multimode Microplate Reader (Berthold Technologies). Parameters were optimized as follows: protein concentration was set to 1 µM, except for BJ318 (200 nM). For the GC522 assay (A. de Saint Germain, personal communication) the release of fluorescent coumarin was recorded with an excitation filter of 355 ± 14 nm and an emission filter of 460 ± 25 nm. Each experiment included at least two technical replicates per condition.

The enzymatic constants of BJ309 (400 nM) and BJ318 (80 nM) were estimated using a profluorescent probe concentration range of 3.125 µM to 400 µM. For competition and inhibition assays, the initial velocity was determined in the presence of 0, 1, 10 or 50 µM of (+)-GR24, TFA or KK094. Before each assay, the competitor/inhibitor was diluted into the GC522 solution, and measurements were performed as previously described (de Saint Germain et al., 2016). At least two technical replicates were performed for each condition. Data were analyzed using GraphPad Prism 8.0.2 software using non-linear regression.

Enzymatic cleavage of SL analogs

Cleavage of GR24 analogs was monitored using UPLC-MS as described previously (de Saint Germain et al., 2021) with the following modifications. Ten µM was incubated with or without 2.5 µM protein for 2 hours at 25ºC. (±)-1-indanol (10 mM) was used as an internal standard. The experiment included three technical replicates.

The hydrolysis of (±)-GR24 by BJ318 was also analyzed in a shorter time frame as follows. Ten µM (±)-GR24 was incubated with 5 µM of BJ318, and samples were taken after one or three minutes of incubation at 25°C. Chromatographic separation was performed on a UHPLC system (Ultimate 3000 RSLc, Thermo Scientific) equipped with a phase column (ACQUITY

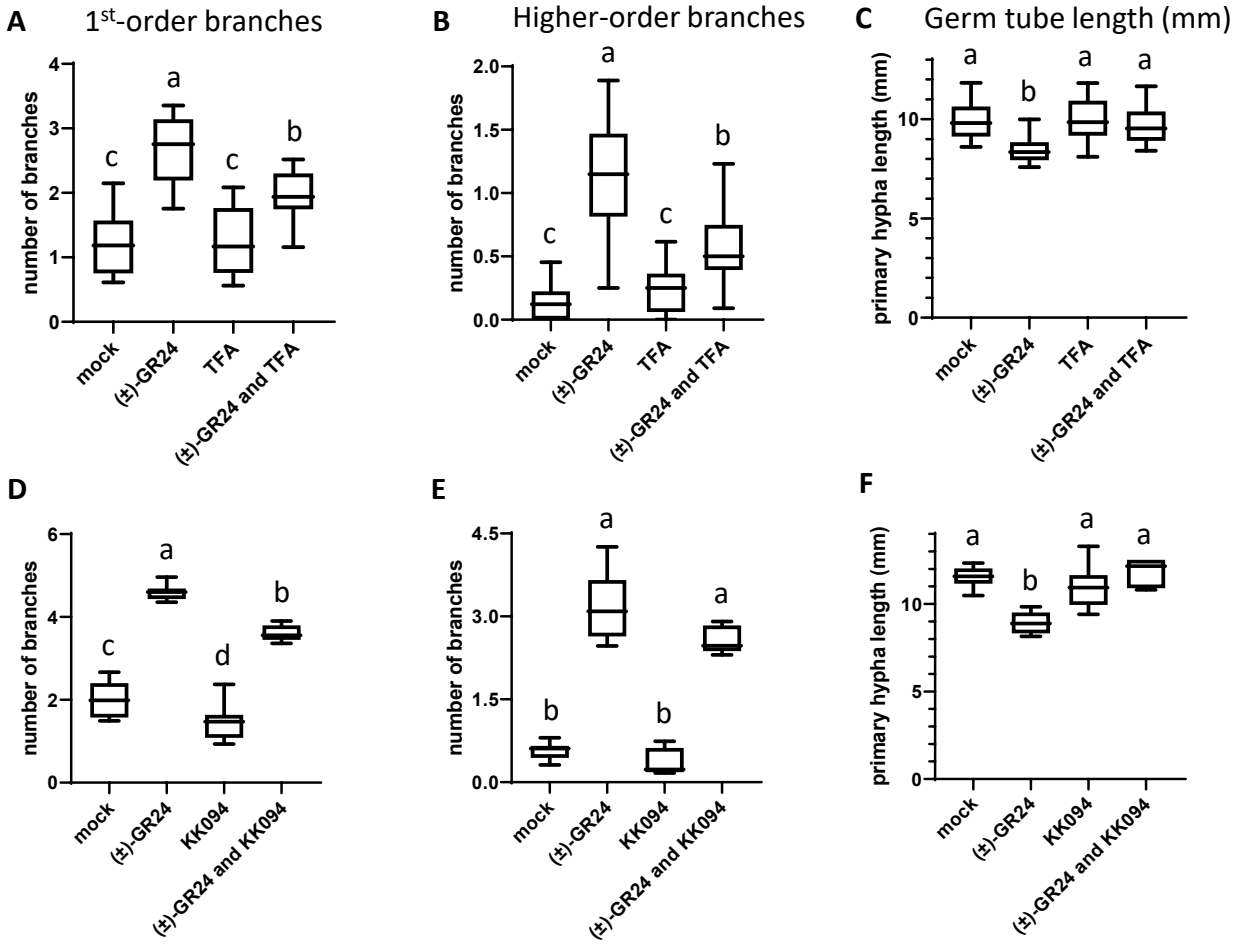

Taulera et al. (*in prep*) - Figure 2. Activity of TFA and KK094 on *R. irregularis* developmental responses to (±)-GR24

R. Irregularis developmental responses to (±)-GR24 in presence of TFA and KK094. The boxes represent the median and 25th and 75th percentiles, whereas whiskers represent the maximum and minimum values. n = 9-12 plates per condition. The experiments were performed at least twice. Conditions topped with the same letter do not differ significantly according to Mann and Whitney's test ($P > 0.05$).

UPLC HSS T3, 2.1 x 100 mm, 1.8µm, Waters) heated at 35°C. Five-µL samples were injected. Separation was performed at a constant flow rate of 0.3 $mL.min^{-1}$, in a gradient of solvent A (water + 0.05% formic acid) and B (acetonitrile + 0.05% formic acid): 1 min 5% B; 8 min 5% to 96% B; 1 min 96% B, and re-equilibration to the initial conditions in 3 min.

A Q-Exactive Plus mass spectrometer (ThermoFisher) was used with an electro-spray ionization source H-ESI II (ThermoFisher) operated in the positive ion mode. Full-scan analysis was performed within a mass range of *m*/*z* 50–600. Sheath gas was set to 48 psi, sweep gas to 2 psi and auxiliary gas to 11 psi. Capillary (256°C) voltage was set to 3.5 kV on Electrospray Ionization (ESI) source (413°C). Data were acquired in MS-centroid mode at a resolution of 35.000 and analyzed using Tracefinder 3.2 hardware.

NanoDSF

NanoDSF assays were performed as described previously (de Saint Germain et al., 2021). Ligands were tested at a concentration of 500 µM. One technical replicate was performed for BJ311, BJ313, BJ316 and BJ317 and two replicates were performed for BJ318, $BJ318^{H208A}$ and $BJ318^{S122A}$.

Analysis of protein-ligand covalent binding

Detection of covalently bound ligands was performed using direct electrospray ionization (ESI)-MS under denaturing conditions, as previously described (de Saint Germain et al., 2021).

Results

Are alpha/beta-hydrolase fold proteins involved in *R. irregularis* responses to SLs?

BLAST searches using plant SL receptors as query sequences did not yield significant homologs in the genomes of AM fungi. We thus took a different approach to try and detect meaningful similarities between fungal ABHs and plant SL receptors. We reasoned that if some fungal ABHs contribute to SL perception, they should bind similar ligands and share structural features with plant SL receptors. If such is the case, their activity may be reduced by inhibitors known to target plant SL receptors and to inhibit plant SL responses.

Two inhibitors were tested: tolfenamic acid, an *N*-phenylanthranilic acid derivative (Fig. 1), identified using chemical genetics against the *Petunia* SL receptor PhDAD2 (Hamiaux et al., 2018); and KK094, a triazole urea compound, synthesized to prevent SL-dependent OsD14-D53 interaction in yeast two-hybrid assays and which covalently binds OsD14 (Nakamura et al., 2019). Both inhibitors were able to supress SL responses *in planta* (Hamiaux et al., 2018; Nakamura et al., 2019). We used *in vitro* bioassays to compare the effects on *R. irregularis* presymbiotic development of (±)-GR24 alone *vs* an equimolar mix of (±)-GR24 and one of the

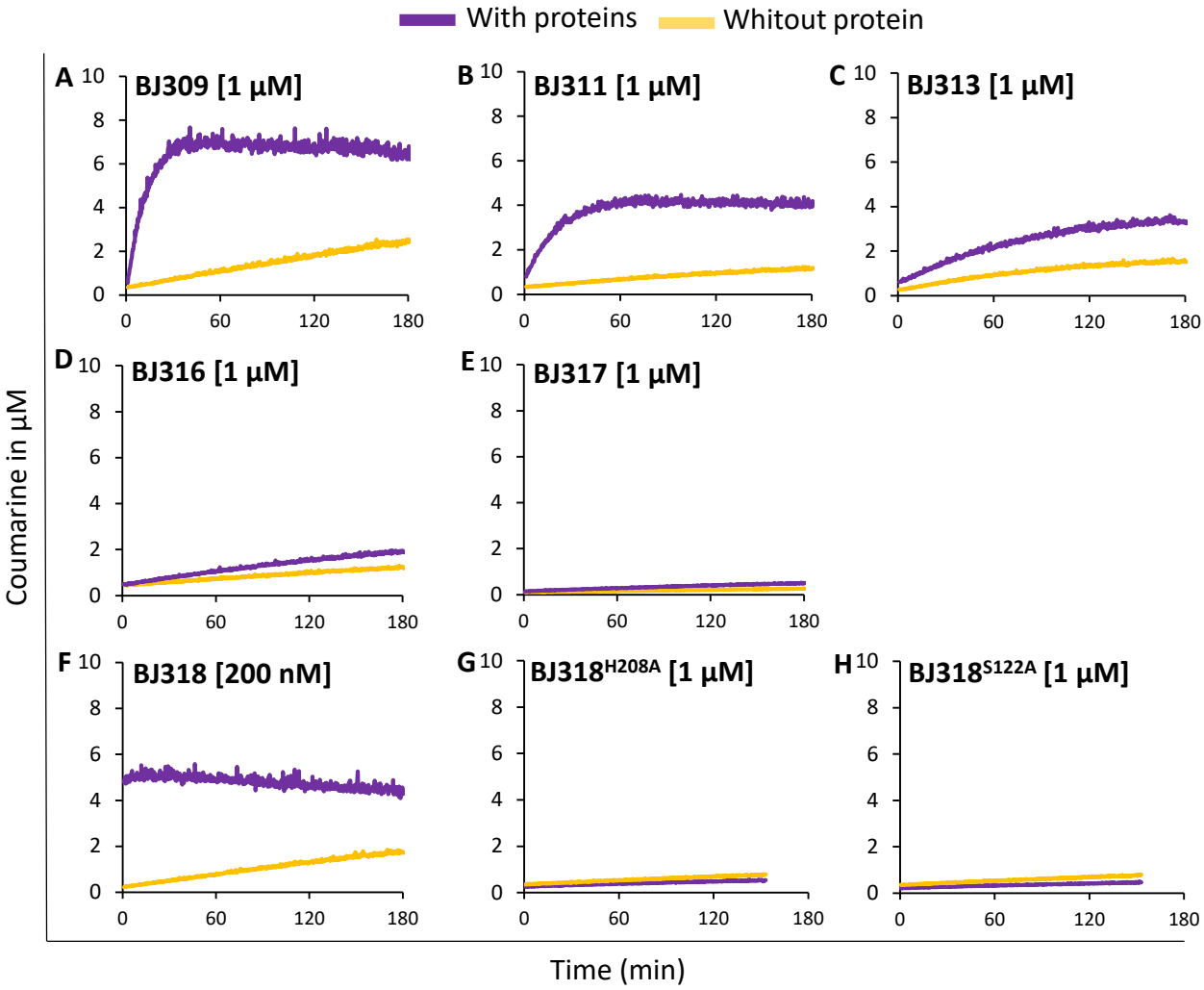

Taulera et al. (*in prep*) - Figure 3. Enzymatic kinetics for the fungal candidate proteins incubated with GC522

Progress curves during hydrolysis of the fluorescent probe GC522 at 10 µM incubated with candidate proteins (purple) or without protein (yellow). The traces represent one of two replicates.

inhibitors. When exposed to an equimolar mix of TFA and (±)-GR24, *R. irregularis* germinating spores exhibited a reduced number of 1st-order and higher-order branches compared to spores exposed to (±)-GR24 alone (Fig. 2A-B). Moreover, the decreased germ tube elongation triggered by (±)-GR24 was suppressed in the presence of TFA (Fig. 2C). Treatment with TFA alone at the same concentration had no effect on either branching or germ tube growth (Fig. 2A-C). The second inhibitor, KK094, did not exhibit clear effects on hyphal branching. The number of branches was slightly lower in the (±)-GR24/KK094 mix as compared with (±)-GR24 alone, but KK094 alone had similar effects when compared to the mock treatment (Fig. 2D, E). In contrast, KK094 could clearly inhibit the effects of (±)-GR24 on germ tube elongation, but had no effect if its own on this developmental parameter (Fig. 2F). Together, these findings indicate that chemicals targeting plant SL receptors can also interfere with *R. irregularis* responses to SLs.

Identification of *R. irregularis* ABH proteins sharing structural similarities with PhDAD2

To try to reveal structural similarities between fungal ABHs and plant SL receptors, we used 3D modelling. The predicted structures of some *R. irregularis* ABHs were compared with the structure of the *Petunia* receptor PhDAD2 determined by crystallography (Hamiaux et al., 2012). A set of fungal ABHs were scored from 0 to 10 based on their overall structure, the presence of the catalytic triad residues, and the characteristics of their binding pocket, such as its size, shape and presence of hydrophobic residues. The highest scores identified eight candidate genes in *R. irregularis* genome encoding proteins with potential good structural similarity with PhDAD2. These proteins are referred to as BJ309, BJ311, BJ312, BJ313, BJ315, BJ316, BJ317 and BJ318.

Despite a predicted shared 3D structure with PhDAD2, the candidate proteins share little amino acid sequence identity (12 to 20%) with the plant SL receptor (Supplementary Fig. 1A). The serine and the histidine of the catalytic triad are present in all the candidate proteins, except for BJ316 in which the serine residue is replaced by an alanine (Supplementary Fig. 1B). The position of the catalytic Asp residue was not determined in the candidate proteins. Intriguingly, an N-terminal signal peptide was predicted using SignalP v5 (Armenteros et al., 2019) for four proteins: BJ309, BJ311, BJ313 and BJ315.

Phylogenetic analysis

We examined the evolutionary context of the identified proteins in the fungal kingdom. To this end, each candidate protein sequence was used as a query for a tBLASTn+ analysis using the fungal genomes available at the Joint Genome Institute's MycoCosm website. After identifying

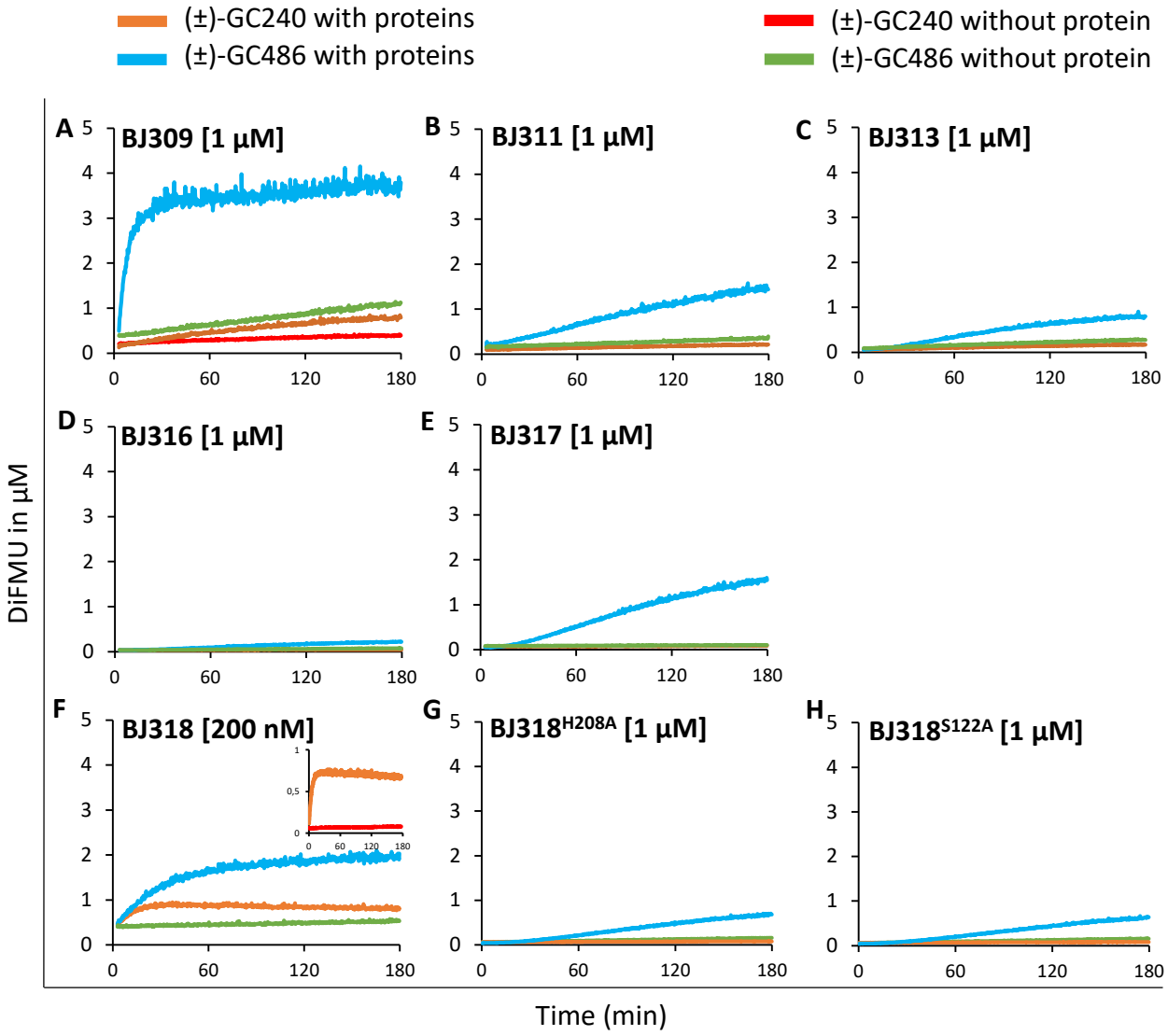

Taulera et al. (*in prep*) - Figure 4. Enzymatic kinetics for the fungal candidate proteins incubated with pro-fluorescent SL mimics

Progress curves during hydrolysis of the fluorescent probes at 10 µM incubated with candidate proteins or without protein. The traces represent one of two replicates.

homologs of each candidate protein, a phylogenetic analysis was performed to uncover its evolution among the fungal kingdom. Based on the phylogeny of the candidate proteins, we observed that BJ309, BJ311, BJ313, and BJ315 share a common ancestor and underwent several rounds of duplication in the Glomeromycota subphylum (Supplementary Fig. 2). Extensive phylogenomic analysis of the presence of the signal peptide revealed that this signal peptide is more present in the subphylum Glomeromycota than in the other phyla, where only a few proteins possess it (Supplementary Fig. 2). Rare duplicated protein sequences were observed for BJ312 in the fungal kingdom. However, the protein was highly divergent in the subphylum Glomeromycota (data not shown). Homologs of BJ316 were found in most fungal phyla but were likely absent in *Geosiphon pyriformis*. Moreover, BJ316 underwent an independent duplication event in the Glomeromycota subphylum and its paralog corresponds to BJ317 (Supplementary Fig. 3). Last, homologs of BJ318 were found in all fungal phyla without specificity in the Glomeromycota subphylum (data not shown).

In vitro characterization of six candidate proteins

To investigate the biochemical properties of the candidate proteins, we attempted to produce corresponding recombinant proteins in *E. coli.* BJ311, BJ313, BJ316 and BJ317 could be produced in a soluble form and were successfully purified. Another two proteins, BJ309 and BJ318, were produced in *E. coli* by a company. We failed to obtain BJ312 and BJ315.

All six candidate proteins display an esterase activity

We first evaluated the esterase activity of the recombinant fungal proteins using a pro-fluorescent probe named GC522 (A. de Saint Germain, personal communication). This probe is composed of a coumarine moiety linked to an acetate moiety (Fig. 1). Like para-nitrophenylacetate, this compound can act as a generic substrate for ABHs. Upon hydrolysis the fluorophore (coumarine) is released, allowing us to evaluate the esterase activity over time as fluorescence increases. All six proteins showed hydrolytic activity towards GC522 (Fig. 3A-F), although BJ316 and BJ317 showed very low activities (Fig. 3D, E). A group composed of BJ309, BJ311 and BJ313 exhibited a higher activity (Fig. 3A, B, C). Among the six proteins BJ318 showed by far the highest esterase activity, as all the substrate was cleaved within the first seconds of incubation with the protein (Fig. 3F).

All six candidate proteins are able to cleave pro-fluorescent SL mimics

To further investigate the enzymatic activities of these proteins, we used additional pro-fluorescent molecular probes in the GC series (de Saint Germain et al., 2016). These compounds possess a methylbutenolide moiety similar to the D-ring of SLs, but the ABC moiety is replaced by a coumarine derivative (6,8-difluoro-7-hydroxy-4-methylcoumarin, DiFMU) (Fig. 1C).

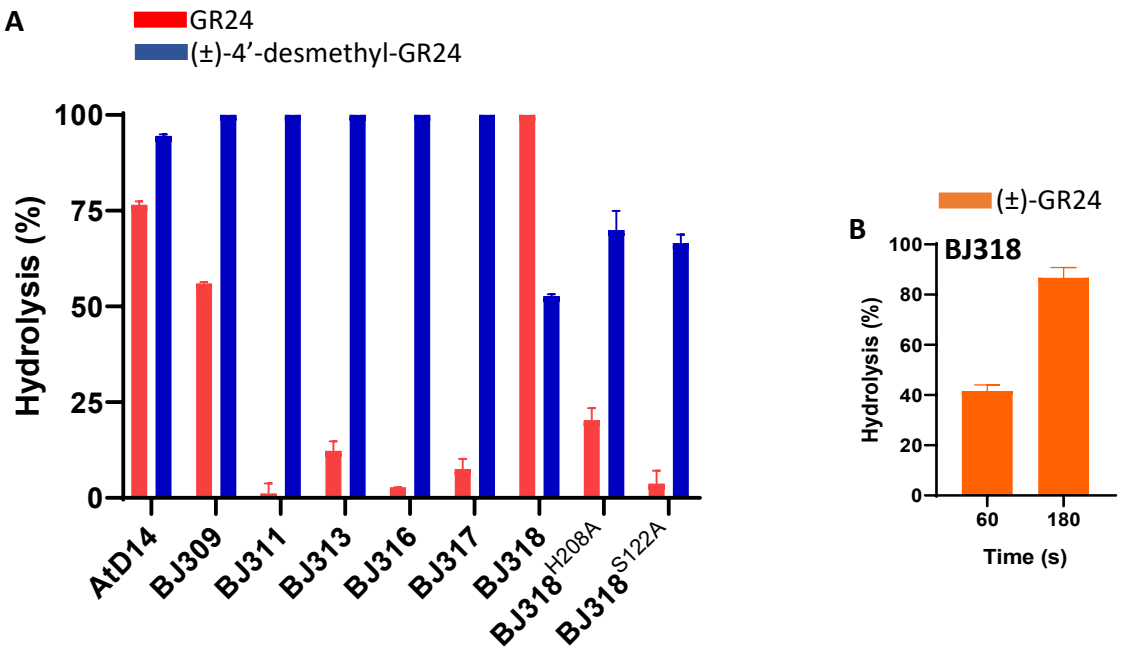

Taulera et al. (*in prep*) - Figure 5. Enzymatic activity of fungal candidate proteins toward SL analogs

(A) 2.5 µM proteins were incubated with 10 µM of GR24 or (±)-4'-desmethyl-GR24 for 2 hours.

(B) 5 µM BJ318 was incubated with 10 µM of (±)-GR24.

Hydrolysis was quantified by UPLC-UV by analyzing the remaining amount of SL analogs. Bars represent the mean ± s.e.m of hydrolysis rate of (A) three and (B) two replicates.

Although they are structurally quite different from natural SLs, they mimic SL analog activity in plants (de Saint Germain et al., 2016) and have the important advantage of releasing the fluorescent moiety (DiFMU) upon cleavage. This allows us to follow their cleavage in real time during incubation with ABHs.

Because *R. irregularis* can perceive the unmethylated butenolide (±)-4'desmethyl-2'*epi*-GR24 which triggers hyphal branching inhibition and germ tube elongation (Taulera et al., 2020), we also investigated the capacities of the candidate proteins to bind and to cleave unmethylated butenolides. Two different GC probes were used. The methylbutenolide moiety of (±)-GC240 is similar to the D-ring of (±)-GR24. In contrast, (±)-GC486 lacks the methyl at C4' position like (±)-4'desmethyl-GR24 (Fig. 1C). Both probes display similar biological activities on *R. irregularis* as their GR24 counterparts (Supplementary Fig. 4): (±)-GC240 induces the formation of hyphal branches similarly to (±)-GR24, while (±)-GC486 decreases the number of branches like (±)-4'-desmethyl-2'*epi*-GR24 (Taulera et al., 2020). These results indicate that both probes can be perceived by fungal cells despite the absence of a canonical ABC moiety.

No hydrolytic activity was observed for BJ311, BJ313, BJ316 or BJ317 towards (±)-GC240 (Fig. 4B-E). A progressive increase of fluorescence was observed for BJ311, BJ313 and BJ317 proteins incubated with (±)-GC486, showing slow hydrolysis of this unmethylated butenolide substrate. A very low residual activity was observed for BJ316 (Fig. 4B-E). BJ309 and BJ318 cleaved (±)-GC486 much more efficiently than the other candidates (Fig. 4). They displayed a short burst phase quickly followed by a plateau. In addition, low but significant hydrolytic activity was observed for both proteins towards (±)-GC240 (Fig. 4), although this activity was much lower than with (±)-GC486 and GC522. While BJ318 displayed a short burst phase, BJ309 showed progressive hydrolysis toward (±)-GC240 (Fig. 4A, F).

The enzymatic constants of BJ309 and BJ318 toward GC probes were estimated: k_{cat} as the catalytic constant of the pre-steady-state phase (initial phase), and $K_{1/2}$ as the probe concentration with half-maximal velocity (V_{max}). (Supplementary Fig. 5). BJ318 exhibited a sixty-fold higher k_{cat} than BJ309 towards GC522 (3.582 min^{-1} vs 0.0591 min^{-1}). The two proteins exhibited similar activities towards (±)-GC486 (0.0498 min^{-1} vs 0.0321 min^{-1}). $K_{1/2}$ values of both proteins for GC522 and (±)-GC486 were in the range of 100 µM (Supplementary Fig. 5). The enzymatic parameters could not be calculated for both proteins towards (±)-GC240 because saturating substrate concentrations could not be reached.

Competitor :
[0 µM] [1 µM] [10 µM] [50 µM]

A

BJ309 [400 nM] + GC522 [12,5 µM]

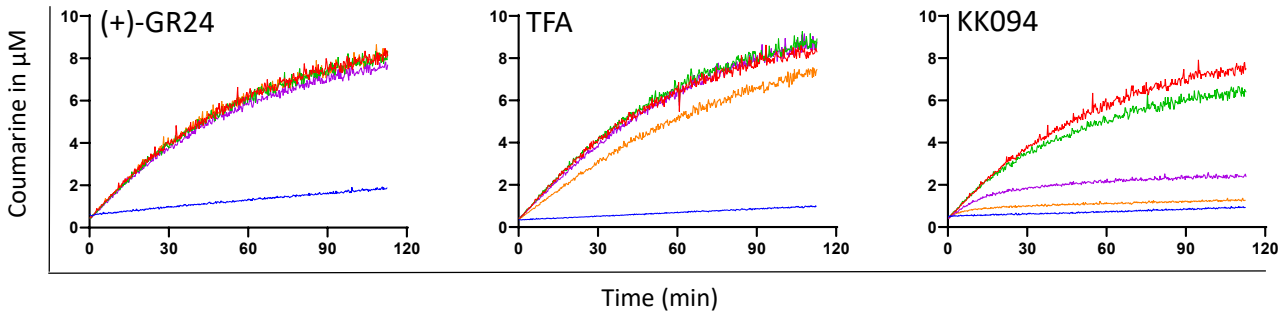

B

Competitor	[µM]	0	1	10	50
(+)-GR24	V_{max} (µM.min^{-1})	0.032	0.034	0.033	0.034
	$K_{1/2}$ (µM)	161	161	144	167
TFA	V_{max} (µM.min^{-1})	0.030	0.027	0.027	0.030
	$K_{1/2}$ (µM)	157	138	160	242
KK094	V_{max} (µM.min^{-1})	0.031	0.031	0.032	0.032
	$K_{1/2}$ (µM)	161	189	268	406

C

BJ318 [80 nM] + GC522 [12,5 µM]

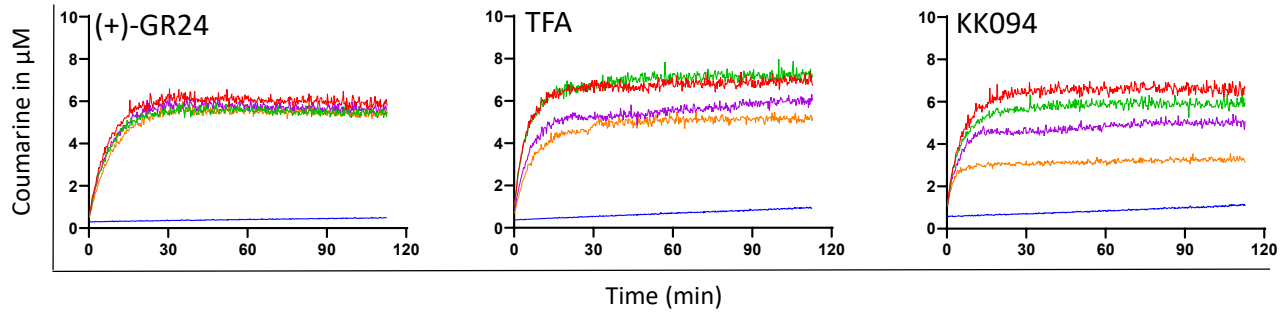

D

Competitor	[µM]	0	1	10	50
(+)-GR24	V_{max} (µM.min^{-1})	0.227	0.236	0.220	0.257
	$K_{1/2}$ (µM)	230	253	264	326
TFA	V_{max} (µM.min^{-1})	0.172	0.171	0.125	0.126
	$K_{1/2}$ (µM)	102	91	72	147
KK094	V_{max} (µM.min^{-1})	0.180	0.165	0.171	0.170
	$K_{1/2}$ (µM)	140	128	141	169

Taulera et al. (*in prep*) - Figure 6. Competition assays of GC522 hydrolysis by TFA or KK094

(A, C) Progress curves of hydrolysis of the fluorescent probe GC522 (12.5 µM) by BJ309 or BJ318 in the presence of different concentrations of (+)-GR24, TFA or KK094. A control condition without protein is shown in blue. These plots represent one of the two replicates.

(B,D) Estimated enzymatic parameters.

All six candidate proteins are able to cleave SLs analogs

We next characterized the hydrolytic activities of the fungal proteins towards SL analogs using mass spectrometry (MS) analysis. Compared with the previous experiments, this method allows the use of substrates with a typical SL structure, including an ABC moiety similar to those of natural SLs. Its main drawback is that hydrolysis cannot be followed in real time. The proteins were incubated either with a mix of (±)-GR24 and (±)-2'*epi*-GR24 (hereafter GR24) or with (±)-4'-desmethyl-GR24, with a four-fold excess of substrate (2.5 µM protein and 10 µM substrate). The percentage of hydrolyzed substrate was determined after two hours of incubation (Fig. 5A). AtD14 was used as a control for comparison of the hydrolytic activities of the candidate proteins with those of plant SL receptors.

BJ311 and BJ316 were unable to cleave GR24. BJ313 and BJ317 displayed a low activity towards this substrate, and BJ309 and BJ318 exhibited the highest activities: they cleaved 55% and 100% of GR24 respectively in two hours (Fig. 5A). To further document the speed of hydrolysis by BJ318, we carried out a similar experiment in a shorter time frame. This revealed a very strong hydrolytic activity of BJ318 towards (±)-GR24, with 40% of (±)-GR24 cleaved in the first minute of incubation, and 85% cleaved within 3 min (Fig. 5B).

All six fungal candidate proteins were able to hydrolyze 100% of (±)-4'-desmethyl-GR24, except BJ318 which left 50% of (±)-4'-desmethyl-GR24 intact after two hours (Fig. 5A).

TFA and KK094 interfere with BJ309 and BJ318 hydrolytic activities

Our next goal was to investigate whether inhibitors of fungal responses to SLs (TFA and KK094, described above) had an impact on the biochemical properties of candidate proteins. We took advantage of the capacity of BJ309 and BJ318 to cleave GC522 to carry out enzymatic competition assays with these inhibitors. (+)-GR24 was also used as a competitor for comparative purposes. The initial velocity of the reaction was determined using a constant concentration of protein incubated with different concentrations of GC522 to estimate V_{max} and $K_{1/2}$ values. This was repeated under different concentrations of competitor or inhibitors (Fig. 6). Protein concentrations were adjusted to respect the initial velocity conditions (Brooks et al., 2012).

An increase of the apparent $K_{1/2}$ and a constant V_{max} value with increasing competitor concentration is indicative of a competitive inhibition. In the absence of inhibitors, hydrolysis of GC522 by BJ318 resulted in a plateau representative of a maximum of substrate cleaved. In contrast, BJ309 displayed a linear activity without reaching a plateau. Diminution of the plateau

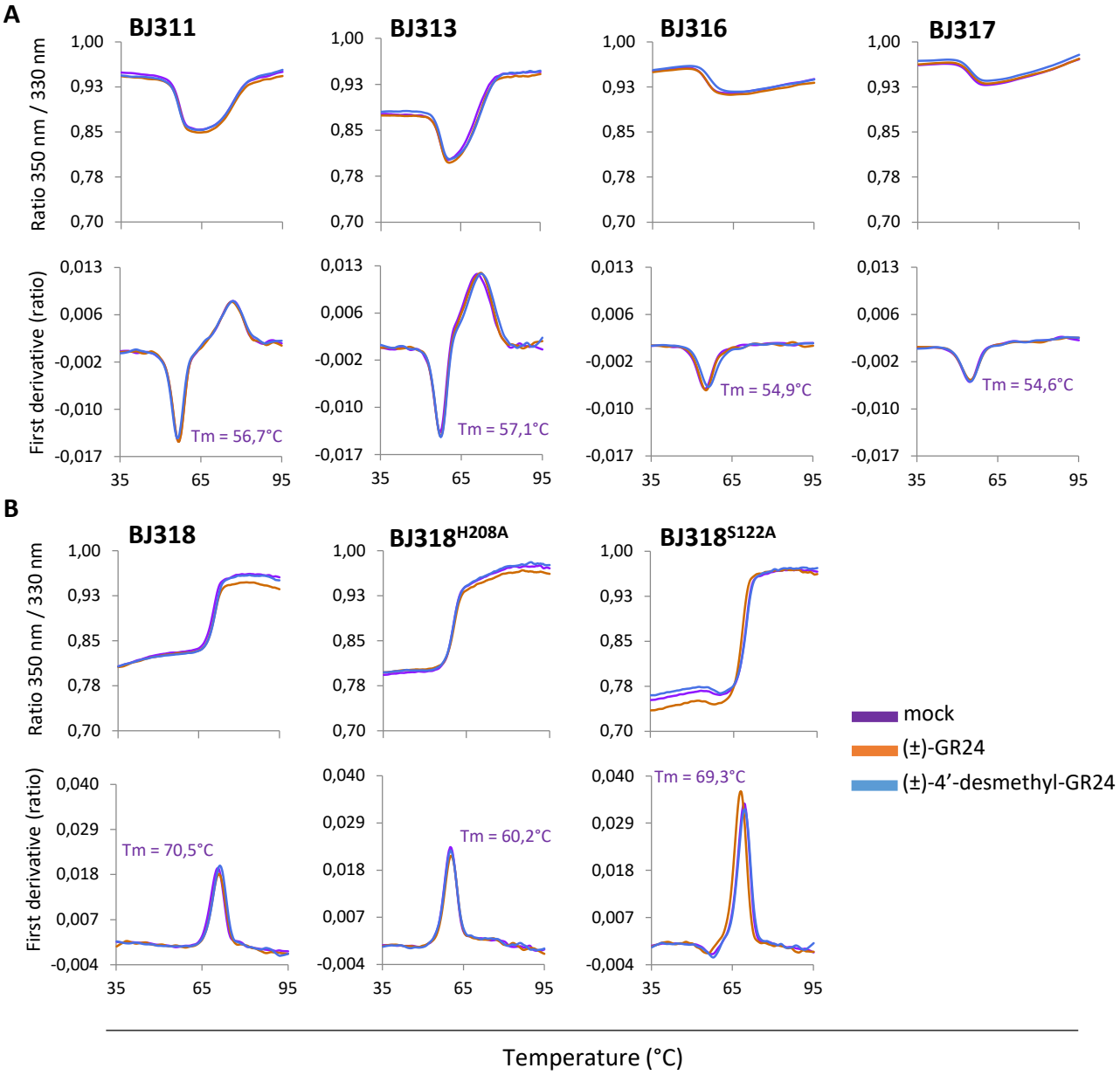

Taulera et al. (*in prep*) - Figure 7. Nano differential scanning fluorimetry (nanoDSF) analysis of the fungal candidate proteins in the presence of SL analogs

Thermostability of (A) BJ309, BJ311, BJ316 and BJ317 and (B) BJ318, BJ318^{H208A} and BJ318^{S122A} proteins in the absence of a ligand or in the presence of (±)-GR24 or (±)-4'-desmethyl-GR24. For each protein, changes in fluorescence (ratio F_{350nm}/F_{330nm}) and the first derivative for the F_{350nm}/F_{330nm} curve are plotted against the temperature. The apparent melting temperature (T_m) for each sample was determined. The experiment was performed once.

or apparition of one in the presence of inhibitors indicates the reduction of enzymatic activity and a possible deactivation of the protein.

The apparent $K_{1/2}$ and V_{max} values of BJ309 did not change with increasing (+)-GR24 concentration (Fig. 6B). When a four-fold increase in TFA-to-substrate ratio is incubated with BJ309, a small shift of the enzymatic activity was observed (Fig. 6A) reflected by an increase of the $K_{1/2}$ value (Fig. 6B). A stronger increase of the $K_{1/2}$ value was observed in the presence of an increased concentration of KK094 (Fig. 6B). More relevant, addition of KK094 results in the apparition of a plateau. The enzymatic activity of BJ309 toward GC522 in the presence of a four-fold excess of KK094 is almost supressed as compared to the control condition (without protein) (Fig. 6A). This is indicative of the deactivation of BJ309 by KK094.

An increased concentration of (+)-GR24 increased the $K_{1/2}$ values of BJ318 (Fig. 6D) but did not change the plateau (Fig. 6C). This is indicative of a competitive inhibition. A decrease in V_{max} in the presence of an increased concentration of TFA was observed, while the effect on $K_{1/2}$ values was not clear. No clear effect of an increased concentration of KK094 on the enzymatic parameters of BJ318 was observed (Fig. 6D). However, the plateau was severely decreased (Fig. 6C). This is indicative of the possible deactivation of BJ318 by both inhibitors.

Thermal shift assays did not reveal conformational changes of the candidate proteins

In addition to their hydrolytic properties, we investigated the ability of the recombinant proteins to bind SLs using thermal shift assays (nano differential scanning fluorimetry, or nanoDSF). In these tests, the melting temperature (Tm) of a target protein in the presence or absence of a putative ligand is measured by recording changes in tryptophan fluorescence (tryptophan emission at 330 nm and 350 nm) as the temperature increases. In the presence of a ligand a shift in the melting temperature of the protein indicates a protein-ligand interaction (Hamiaux et al., 2021). No interaction between BJ311, BJ313, BJ316, BJ317 or BJ318 with either (±)-GR24 or (±)-4'desmethyl-GR24 was recorded (Fig. 7). BJ309 did not exhibit a typical nanoDSF profile, hence this method could not be used to test its ability to bind SLs.

Mutations of the catalytic serine or histidine reduce the enzymatic activity of BJ318 towards (±)-GR24

To investigate the mechanisms of BJ318 enzymatic activity, we produced two BJ318 versions mutated for either the catalytic serine or histidine. The consequences of H208A and S122A substitutions on the catalytic properties of BJ318 were examined. $BJ318^{H208A}$ and $BJ318^{S122A}$ were unable to hydrolyze the GC probes, except (±)-GC486 for which a low residual activity was observed (Fig. 3, 4). Both substitutions drastically reduced GR24 hydrolysis as shown by

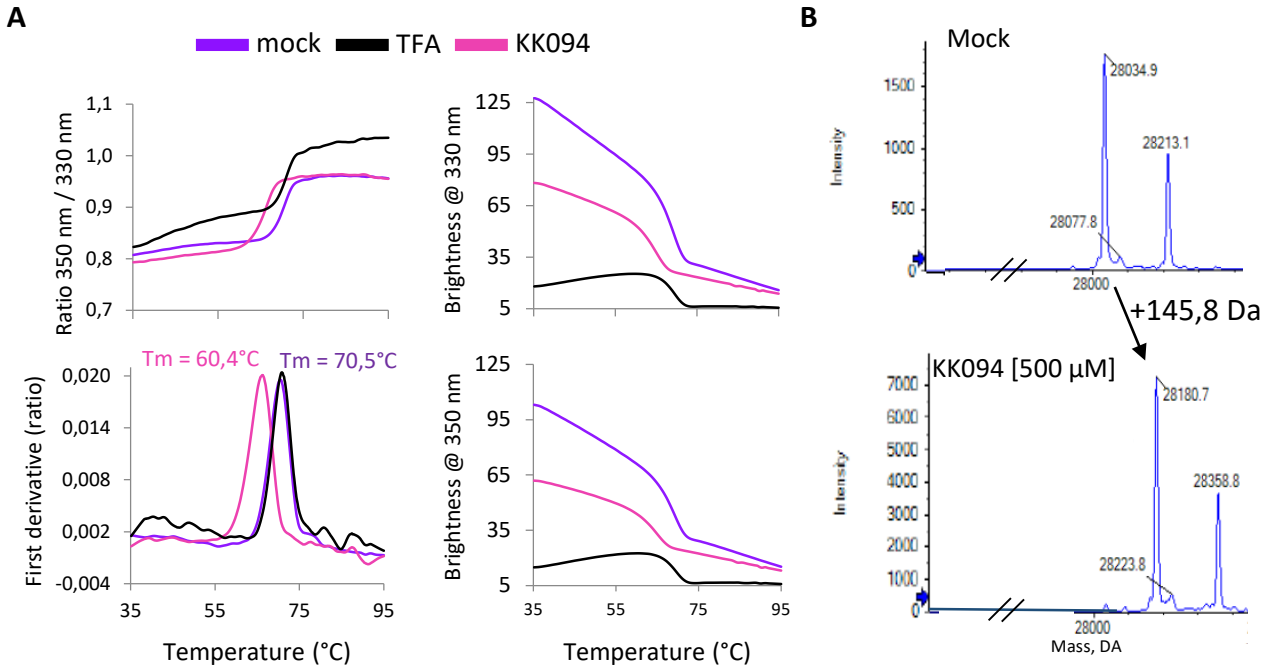

Taulera et al. (*in prep*) – Figure 8. Binding analysis of BJ318 to TFA and KK094

(A) NanoDSF profile of BJ318 incubated with TFA, KK094 or in the absence of ligand (mock).

(B) Mass spectrometry characterization of a covalent BJ318-KK094 complex. Deconvoluted electrospray mass spectra of the BJ318 protein in the absence (top panel) or presence (bottom panel) of KK094. A mass increment of +145.8 DA (corresponding to the KK094 mass) was observed.

mass spectrometry: less than 20% of GR24 was cleaved in two hours, *vs* 80% in 3 min for the WT protein. Surprisingly, both mutated proteins were slightly more efficient at cleaving (±)-4'-desmethyl-GR24 (70% after two hours, compared to 50% for the wild-type BJ318 protein) (Fig 5A). We next investigated their ability to bind SLs. Neither BJ318^{H208A} nor BJ318^{S122A} exhibited binding to SL using the nanoDSF assay (Fig. 7B). In addition, there was a significant difference in melting temperature between BJ318 and BJ318^{H208A} (-10°C) in the absence of any ligand (Fig. 7). This shows that the structure of BJ318^{H208A} is much less stable compared to the wild-type protein.

KK094 covalently binds BJ318

Tolfenamic acid and KK094 were shown to inhibit the enzymatic activity of plant SL receptors and to induce stabilization of these proteins (Hamiaux et al., 2018; Nakamura et al., 2019). We thus examined the impact of these two inhibitors on BJ318 stability using nanoDSF assays. The presence of TFA did not induce a shift of the melting temperature of BJ318 (Fig. 8A). However, an important decrease of the initial fluorescence was observed, pointing towards an interaction between BJ318 and TFA. KK094 markedly destabilized the protein, as shown by a decrease of 10°C of the melting temperature (Fig. 8A).

Finally, a possible covalent linkage of BJ318 to either (±)-GR24, TFA or KK094 was investigated by recording mass spectrometry spectra under denaturing conditions. These analyses did not reveal a mass shift when BJ318 was incubated with either (±)-GR24 or TFA (Supplementary Fig. 3, 4). In contrast, in the presence of KK094 a mass shift of 145.8 *m/z* (corresponding to the mass of the covalently bound KK094, Nakamura et al., 2019) occurred, showing that BJ318 could covalently bind KK094 (Fig. 8B).

Discussion

Our working hypothesis was that SL receptors in AMF may have evolved in a similar fashion to those in parasitic weeds or mosses, *i.e.* through expansion and neofunctionalization of ABHs. Two inhibitors known to target plant SL receptors could also inhibit *R. irregularis* responses to SLs. This suggests that AMF perceive SLs through ABH proteins which could share structural features with plant SL receptors. We used 3D modelling to identify eight ABH proteins of *R. irregularis* showing structural similarities with the plant SL receptor DAD2.

(±)-4'-desmethyl-*epi*-GR24 triggered opposite developmental responses in *R. irregularis* compared to (±)-GR24 (Taulera et al., 2020), suggesting the existence of fungal receptors mediating responses to unmethylated butenolides. *In vitro* characterization revealed that (±)-4'-

desmethyl-GR24 was hydrolysed by all candidate proteins without inducing conformational changes. The lack of conformational changes coupled with a strong enzymatic activity towards desmethylated compounds was previously described for SL receptors such as AtD14 (Yao et al., 2018, 2021) or PsRMS3 (de Saint Germain et al., 2016). *In planta*, these proteins are not involved in responses to desmethylated butenolides. In contrast AtKAI2, which mediates responses to (±)-4'-desmethyl-GR24 in *A. thaliana,* exhibited a slower hydrolytic activity and was destabilized by (±)-4'-desmethyl-GR24 (Yao et al., 2021). In view of these results, the data presented here do not support a role as desmethylated butenolide receptors for the fungal candidate proteins.

Among the candidates, BJ311 and BJ316 were not able to cleave GR24. BJ313 and BJ317 cleaved it with very low efficiency, while BJ309 and BJ318 exhibited a significant hydrolytic activity towards GR24 (Fig. 5). The enzymatic activity of BJ309 towards (±)-GR24 was similar to that of AtD14 (Fig. 5). Unfortunately, we could not investigate conformational changes in BJ309 nor its covalent binding to SLs. Nevertheless, in competition assays (+)-GR24 did not drastically inhibit BJ309 enzymatic activity towards GC522, suggesting that (+)-GR24 could not covalently bind to the protein. Phylogenetic analysis revealed that BJ309, BJ311 and BJ313 arose following a gene expansion from a common ancestor in the Glomeromycota subphylum (Supplementary Fig. 2). The presence of a signal peptide in these proteins raises questions about their potential role as SL receptors. Although their secretion outside of fungal cells needs to be confirmed, their putative secretion rather suggests a biological function distinct from SL perception.

The enzymatic activity of BJ318 towards (±)-GR24 was much higher than that reported for plant SL receptors (Fig. 5B) (de Saint Germain et al., 2021; de Saint Germain et al., 2016; Seto et al., 2019). This enzymatic activity could be favored by the apparent lack of covalent linkage to (±)-GR24 (Supplementary Fig. 6). The existence of ABH proteins with high capacities to hydrolyse SLs was recently reported in plants: the carboxyl esterase AtCXE15 cleaved SLs much more efficiently compared to AtD14 (Xu et al., 2021). AtCXE15 was not associated with SL signaling since no interaction with SL signaling components such as AtD14, AtMAX2 or AtSMXL was detected. Rather, the authors proposed that the strong hydrolytic activity of AtCXE15 possibly regulates the homeostasis of active SLs in plants (Xu et al., 2021). In view of these results, we suggest that BJ318 could act similarly, as an enzyme regulating SL content in AM fungi. The fact that BJ318 homologs were found throughout the fungal kingdom (Supplementary Fig. 3) supports the idea that BJ318 may not be an SL receptor in AMF and

suggests that its enzymatic activity toward SLs could be conserved among fungi. In line with this idea, other filamentous fungi were able to cleave SLs (including GR24) (Boari et al., 2016) showing that the ability to degrade SLs is more widespread than expected and may involve ABH proteins.

The importance of the catalytic serine or histidine of BJ318 to hydrolyse SL analogs was investigated. The capacity of BJ318^{S122A} and BJ318^{H208A} to hydrolyse GR24 was drastically decreased but not suppressed (Fig. 5), as previously described for DAD2^{S96A} and the *Phelipanche ramosa* KAI2d3^{S98A} protein (de Saint Germain et al., 2021; Lee et al., 2020). Surprisingly, we observed an increase of the hydrolytic activity of BJ318^{S122A} and BJ318^{H208A} towards (±)-4'-desmethyl-GR24 as compared to wild-type BJ318. In contrast, the enzymatic activity of AtKAI2^{S95A} and PrKAI2d3^{S98A} towards unmethylated butenolides was significantly decreased (de Saint Germain et al., 2021; Yao et al., 2021). This highlights that the mechanism of (±)-4'desmethyl-GR24 hydrolysis by BJ318 differs from that of these two plant KAI2-LIKE proteins. Interestingly, mutation of the catalytic serine of PrKAI2d3 changed its preferences for the different GR24 stereoisomers (de Saint Germain et al., 2021). This shows that the catalytic serine can determine substrate preferences and is dispensable for the hydrolysis of some substrates.

AM fungi are not amenable to forward genetics, similarly to parasitic weeds. The biological function of putative SL receptors in parasitic weeds was assigned by expressing the candidate proteins in *Arabidopsis d14* or *kai2* mutants (Conn et al., 2015; Toh et al., 2015). In the case of AM fungi, we believe that such trans-complementation experiments are unlikely to work because of the poor homology between the candidate proteins and plant SL receptors (Supplementary Fig. 1). In particular, fungal proteins are unlikely to interact with the required plant proteins to activate the SL signaling pathway. In line with this concern, SL-related responses in the moss *P. patens* are independent of PpMAX2 (Lopez-Obando et al., 2018), and the putative SL receptors failed to complement *Atd14* mutants (Lopez-Obando et al., 2021). An alternative possibility to demonstrate biological functions for the fungal candidate proteins is the Host-induced Gene Silencing (HIGS) technique. This consists of introducing an RNAi construct targeting a fungal gene of interest into a host plant via genetic transformation. During the symbiotic interaction, intermediate molecules of the RNA interference process can be transferred to the fungal cells, resulting in the silencing of the gene of interest (Helber et al., 2011). However, although we have identified several SL-cleaving proteins, other unidentified proteins may be involved in SL perception by the fungus. Therefore, HIGS may not be efficient

as a reverse genetic tool because of functional redundancy. As an alternative approach to investigate the biological function of the candidate proteins in *R. irregularis*, we aimed to correlate the bioactivity of inhibitors with their ability to inhibit the enzymatic activity of the candidate proteins. In the presence of TFA and KK094, *R. irregularis* responses to (±)-GR24 were suppressed (Fig. 2). In parallel, TFA and KK094 were able to inhibit the enzymatic activity of at least two candidates: BJ309 and BJ318 (Fig. 6). That plant SL response inhibitors are able to suppress both the effect of SLs on *R. irregularis* and the enzymatic activity of two fungal ABHs, led us to propose that ABH proteins are part of the signaling pathways regulating *R. irregularis* responses to SLs, although we cannot exclude the possibility that additional proteins targeted by TFA and KK094 are involved. Phylogenetic analysis revealed an expansion in Glomeromycota of some of the candidate genes. The encoded proteins exhibited different hydrolytic activities toward GR24 (Fig. 5). Taken together, these observations lend support to the hypothesis that like parasitic weeds and mosses, AM fungi evolved the capacity to perceive SLs through expansion and neo-functionalization of ABH proteins. In conclusion, through this study, we have gathered indirect evidence regarding the nature of SL receptors in AMF, which reduces the scope of investigation needed for more precise identification of the SL receptor(s) in these fungi.

Supplementary data

A

Amino acid sequence identity (%)

	PhDAD2								
BJ309	15.8	BJ309							
BJ311	12.1	55.2	BJ311						
BJ312	20.6	19.5	17.4	BJ312					
BJ313	17.4	27.9	27.2	15.3	BJ313				
BJ315	11.7	45.1	48.8	15.2	30.0	BJ315			
BJ316	14.2	15.8	17.9	16.7	18.2	16.8	BJ316		
BJ317	14.3	15.8	18.7	14.7	23.1	20.3	38.5	BJ317	
BJ318	16.0	19.5	18.2	17.9	14.7	20.0	13.5	14.5	BJ318

B

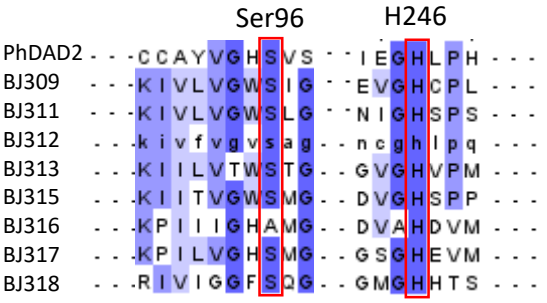

Taulera et al. (*in prep*) - Supplementary Figure 1. Amino acid sequence identities of PhDAD2 and the fungal candidate proteins

(A) Multiple sequence alignments were performed with Clustal Omega program. Sequence identities > 30% are shown in green.

(B) The red boxes indicate the catalytic residues. The catalytic serine and histidine are shown in the candidate protein sequences. Dark blue shows identity in the majority of the proteins; light blue indicates similarities among several of the proteins. The amino acid positions refer to PhDAD2 sequence.

Taulera et al. (in prep) - Supplementary Figure 2. Phylogenetic analysis of signal peptide presence in BJ309, BJ311, BJ313 and BJ315 homologs in the fungal kingdom

The presence of signal peptides (blue square) was predicted using SignalP v5. A phylogenetic tree was generated by the maximum likelihood method. The best-fitting evolutionary model was estimated and branch supports estimated with 10,000 bootstrap replicates.

Taulera et al. (*in prep*) - Supplementary Figure 3. Phylogenetic analysis of BJ316 and BJ317 homologs in the fungal kingdom

A phylogenetic tree was generated by the maximum likelihood method. The best-fitting evolutionary model was estimated and branch supports estimated with 10,000 bootstrap replicates.

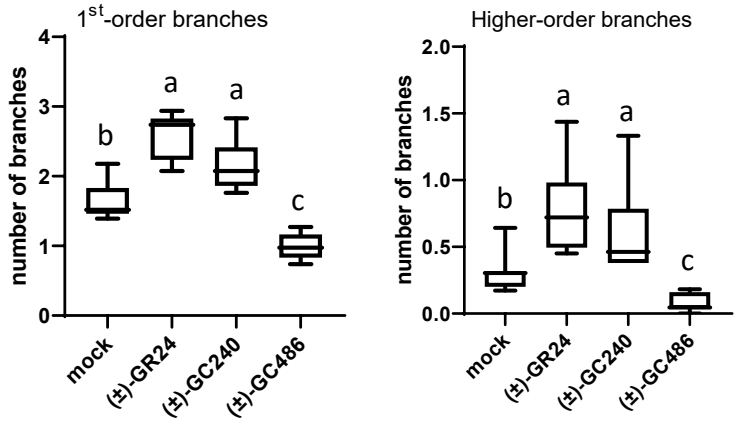

Taulera et al. (*in prep*) - Supplementary Figure 4. Effect of (±)-GC240 and (±)-GC486 on *R. irregularis* development

R. irregularis developmental responses to the profluorescent probes (±)-GC240 and (±)-GC486. n = 7-9 plates per condition. Each compound was tested three times. Conditions topped with the same letter do not differ significantly according to Mann and Whitney's test ($P > 0.05$).

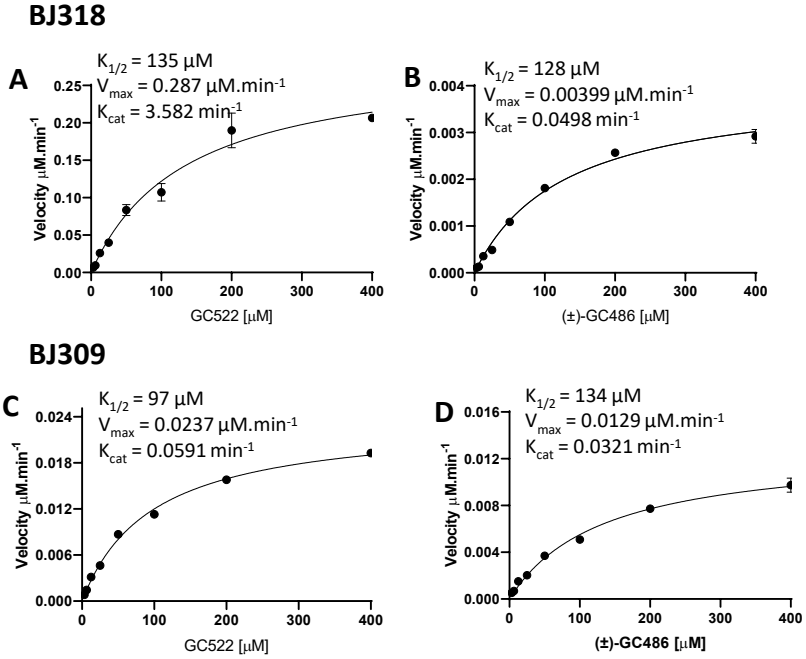

Taulera et al. (*in prep*) - Supplementary Figure 5. Hyperbolic plot of BJ318 and BJ309 towards profluorescent GC probes

Hyperbolic plot of BJ318 or BJ309 pre-steady-state kinetics reaction velocity with (±)-GC522 or (±)-GC486. Error bars represent the s.e.m. of three replicates. The initial velocity was determined and the enzymatic constants were estimated using GraphPad prism software.

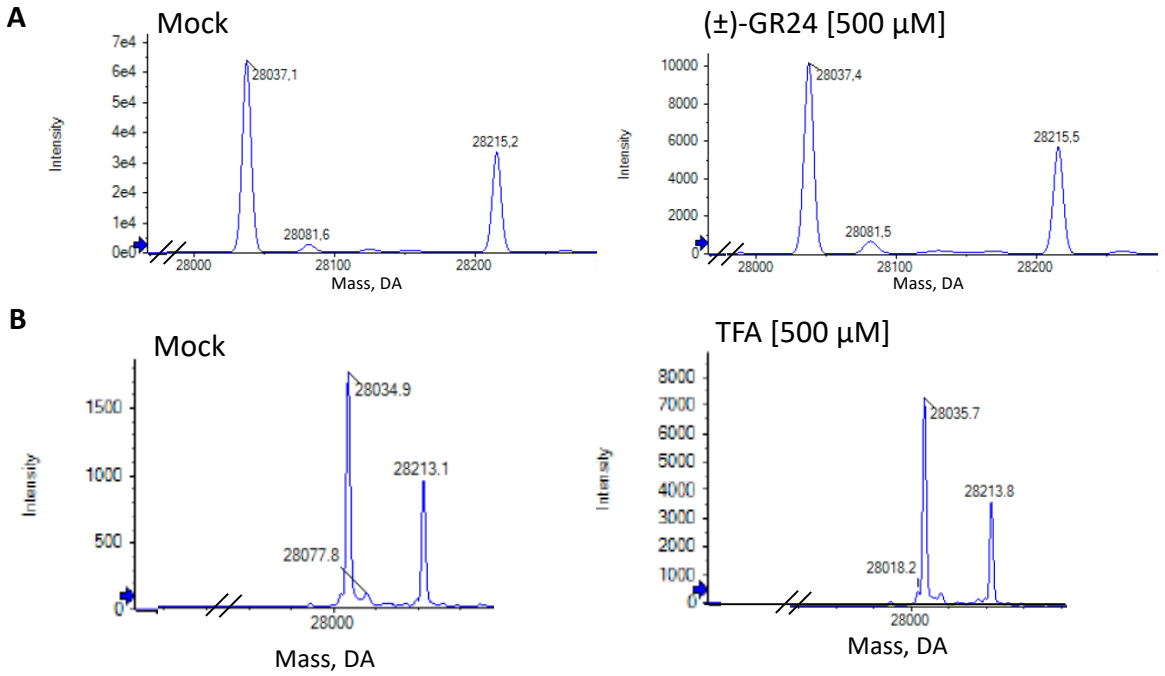

Taulera et al. (*in prep*) - Supplementary Figure 6. Analysis of covalent linkage of BJ318 to (±)-GR24 and TFA by mass spectrometry under denaturing conditions

Deconvoluted electrospray mass spectra of the BJ18 protein before (left column) and after (right column) adding (A) (±)-GR24 or (B) TFA. No mass increment was observed.

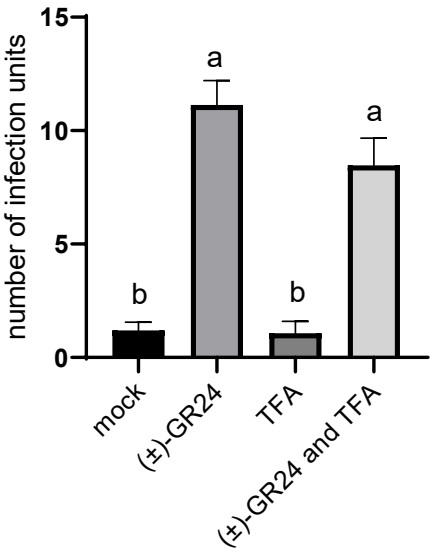

Figure 36. Effect of tolfenamic acid on symbiosis initiation in the presence of GR24

Mtccd8-1 mutants were inoculated with *R. irregularis* and watered with a nutrient solution supplemented with 100 nM (±)-GR24, tolfenamic acid (TFA), an equimolar mix of (±)-GR24 and TFA (100 nM each), or the solvent alone (mock). Bars represent the mean number of infection units per plant ± s.e.m. n = 15 plants per condition. The experiment was performed once. Means topped by the same letter do not differ significantly according to Mann and Whitney's test (P > 0.05).

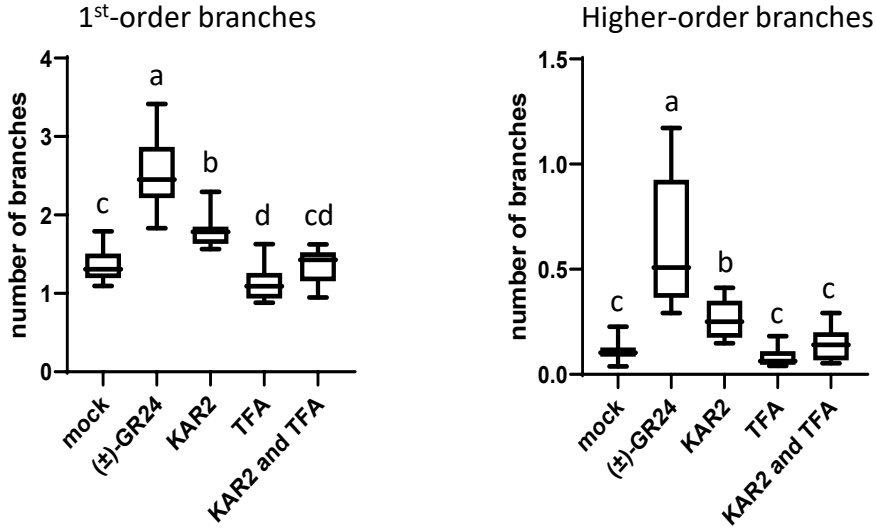

Figure 37. Effect of tolfenamic acid on *R. irregularis* hyphal branching responses to KAR2

Activity of TFA on hyphal branching of *R. irregularis* treated with KAR2. n = 7-10 plates per condition. The experiment was performed twice. Conditions topped with the same letter do not differ significantly according to Mann and Whitney's test (P > 0.05).

III) Additional experiments

Additional results were obtained regarding the effect of TFA: in a symbiotic context in the presence of (±)-GR24, and on *R. irregularis* developmental responses to KAR2. The effects of TFA and KK094 on *R. irregularis* spore germination in response to SL analogs were recorded. Additional data regarding the biochemical properties of the candidate proteins towards (±)-3'-methyl-GR24 are also presented. Finally, the expression profiles of the genes encoding the candidate proteins are briefly discussed.

III-1) Tolfenamic acid effects in a symbiotic context

We characterized the effect of TFA on the ability of *R. irregularis* to initiate symbiosis with *Mtccd8* mutants in the presence of (±)-GR24. The experiment was performed in poor conditions (presence of an additional endophytic fungus) and could not be repeated. In this experiment, TFA did not reduce the capacity of *R. irregularis* to colonize *Mtccd8* roots in the presence of (±)-GR24 (Fig. 36).

III-2) Tolfenamic acid decreases hyphal branching triggered by KAR2

The similar effects of (±)-GR24 and KAR2 on hyphal branching suggested the existence of a common pathway shared by both compounds. We thus investigated whether TFA could suppress hyphal branching responses triggered by KAR2, as it inhibits hyphal branching triggered by (±)-GR24. TFA alone slightly decreased the number of 1st-order branches compared to the mock treatment but the number of higher-order branches was similar (Fig. 37). The induction of 1st- and higher-order branches by KAR2 was suppressed in the presence of TFA (Fig. 37).

III-3) Effects of tolfenamic acid on spore germination in the presence of SL analogs

We aimed to evaluate the activity of TFA on spore germination responses to (±)-GR24. TFA alone, like (±)-GR24, significantly increased the spore germination rate compared to the mock treatment (Fig. 38A). Accordingly, the mix of TFA and (±)-GR24 also stimulated spore germination. It is thus impossible to conclude on any inhibitory action of TFA on this response of *R. irregularis* to (±)-GR24. We further assessed the capacity of TFA to affect spore

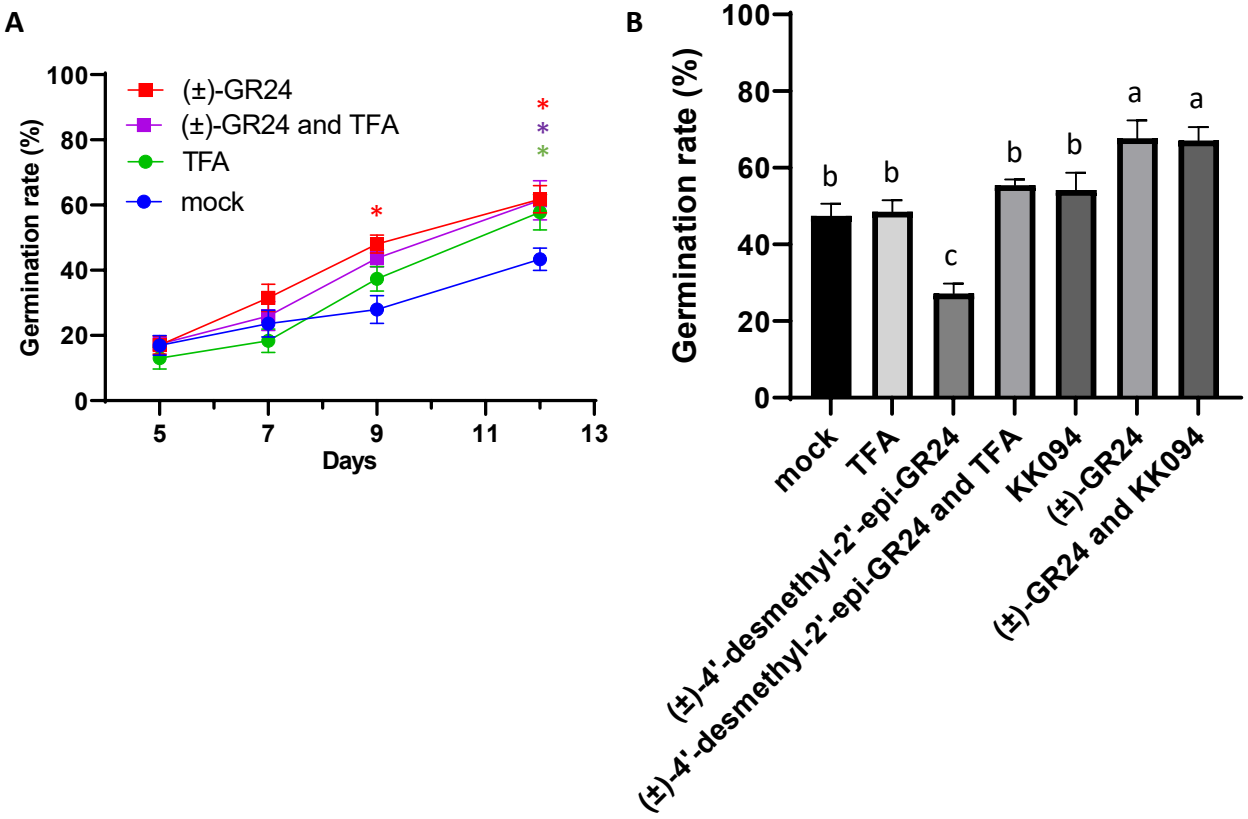

Figure 38. Effect of tolfenamic acid and KK094 on *R. irregularis* spore germination

(A) Activity of TFA on spore germination of *R. irregularis* treated with (±)-GR24. The mean germination rate ± s.e.m is shown. n=8 rows of 10 to 12 spores. The experiment was performed twice.

(B) Activity of TFA or KK094 on spore germination of *R. irregularis* treated with (±)-4'desmethyl-2'-*epi*-GR24 or (±)-GR24. The germination rate was determined after 5 days. The mean germination rate ± s.e.m is shown. n=5 rows of 10 to 12 spores. The experiment was performed once.

Means topped by the same letter do not differ significantly according to one-way ANOVA followed by Fisher's LSD test (P > 0.05).

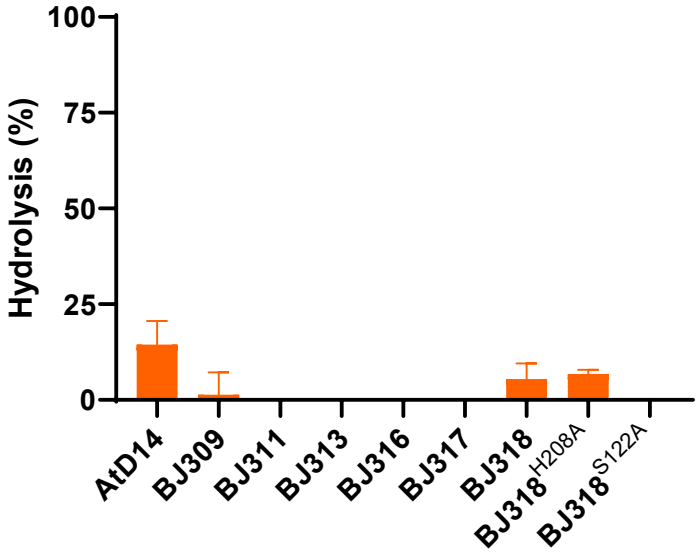

Figure 39. Enzymatic activity of fungal candidate proteins towards (±)-3'-methyl-GR24

Proteins (2.5 µM) were incubated with 10 µM (±)-3'-methyl-GR24 for 2 hours at 25°C. Bars represent the means ± s.e.m of three replicates. The experiment was performed once.

germination inhibited by (±)-4'-desmethyl-2'-*epi*-GR24. Because in the presence of (±)-4'-desmethyl-2'-*epi*-GR24 spore germination was already inhibited at 5 days, and that only rare germination events occurred at later time points, we recorded the germination rate at 5 days (Fig. 38B). The germination rate was similar between the mock treatment and TFA. Upon application of an equimolar mix of TFA and (±)-4'-desmethyl-2'-*epi*-GR24, the inhibition of spore germination induced by (±)-4'-desmethyl-2'-*epi*-GR24 was suppressed (Fig. 38B).

III-4) Effect of KK094 on spore germination in the presence of (±)-GR24

The presence of KK094 did not suppress the increase of spore germination triggered by (±)-GR24 at 5 days, while the germination of spores exposed to KK094 alone was comparable to that observed in mock conditions (Fig. 39B).

III-5) BJ318 is destabilized by (±)-3'-methyl-GR24

In chapter 1, we showed that (±)-3'-methyl-GR24 stimulated *R. irregularis* spore germination (Fig. 30). We investigated whether the biological activity of (±)-3'-methyl-GR24 could be correlated with its interaction with the receptor candidates.

We first characterized the hydrolytic activities of the fungal candidate proteins towards (±)-3'-methyl-GR24 using mass spectrometry. Only BJ309 and BJ318 were able to hydrolyze this substrate, and their activity was very low (Fig. 39). The enzymatic activity of BJ318^{H208A} towards (±)-3'-methyl-GR24 was not impaired, while that of BJ318^{S122A} was suppressed (Fig. 39). A marked shift of BJ318 melting temperature was observed in the presence of (±)-3'-methyl-GR24 in DSF assays, indicative of a destabilization of the protein (Fig. 35). We confirmed using nanoDSF the destabilization of BJ318 by (±)-3'-methyl-GR24 (Fig. 40). This destabilization was no longer observed for the mutated proteins BJ318^{H208A} and BJ318^{S122A} (Fig. 40).

To further investigate the biochemical properties of BJ309 and BJ318 proteins towards (±)-3'-methyl-GR24, we performed competition assays measuring the hydrolytic activity of BJ309 and BJ318 towards GC522 in the presence of (±)-3'-methyl-GR24. The enzymatic activity of both enzymes was reduced (decreased height of the plateau) in the presence of (±)-3'-methyl-GR24 (Fig. 41). This indicated a possible deactivation of the protein, possibly through covalent linkage to the protein as observed for PsRMS3 (de Saint Germain et al., 2016). Unexpectedly,

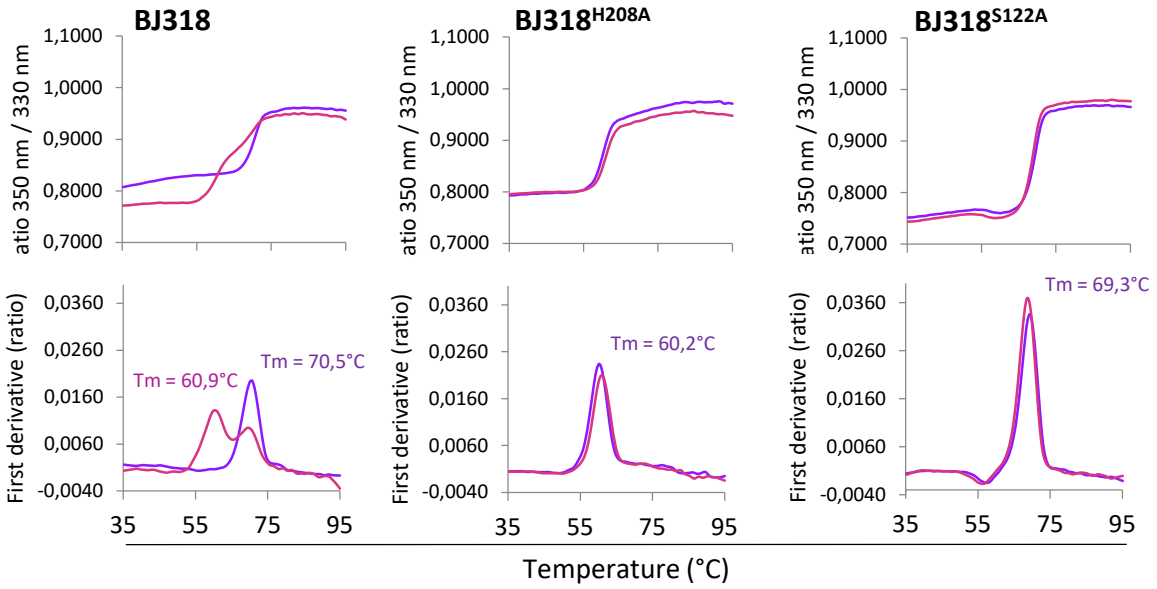

Figure 40. Nano Differential Scanning Fluorimetry (nanoDSF) analysis of wild-type and mutant BJ318 in the presence of (±)-3'-methyl-GR24

Thermostability of BJ318, BJ318^{H208A} and BJ318^{S122A} proteins (10 µM) in the absence of a ligand (blue) or in the presence of 200 µM (±)-3'-methyl-GR24 (pink). The apparent melting temperatures (T_m) for each sample was determined using the first derivative of the fluorescence ratio. The experiment was performed twice.

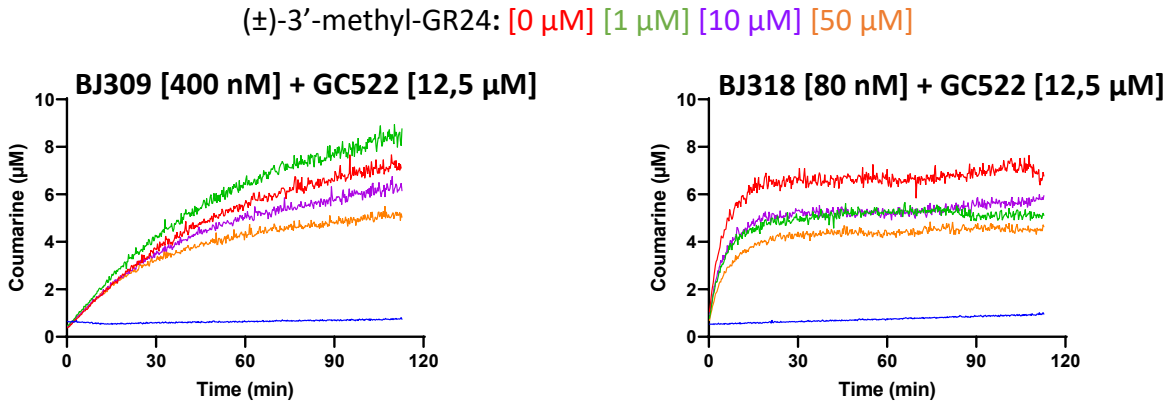

Figure 41. Competition assays for GC522 hydrolysis by BJ309 and BJ318 in the presence of (±)-3'-methyl-GR24

Progress curves of BJ309 or BJ318 hydrolysis of GC522 in competition with (±)-3'-methyl-GR24. A control condition without protein is shown in blue. These plots represent one of the two replicates.

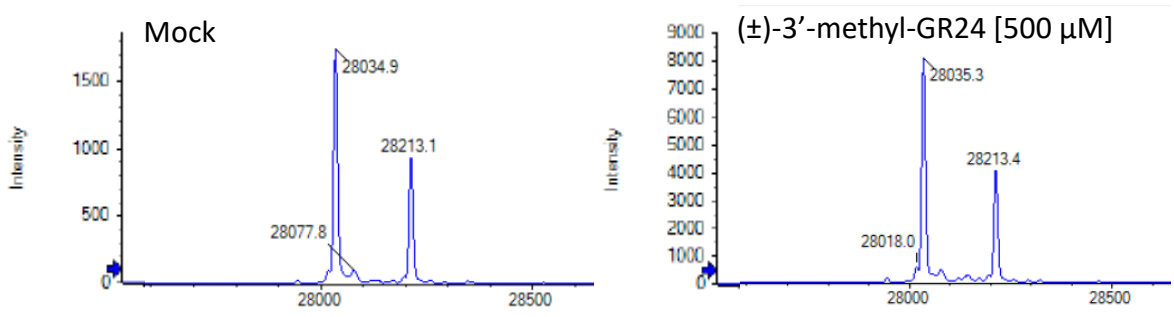

Figure 42. BJ318 does not covalently bind (±)-3'-methyl-GR24

Deconvoluted electrospray mass spectra of the BJ318 protein in the absence (left panel) or presence (right panel) of (±)-3'-methyl-GR24.

we could not observe a covalent linkage of BJ318 to (±)-3'-methyl-GR24 using mass spectrometry under denaturing conditions (Fig. 42).

III-6) Expression profiles of the candidate genes

To further characterize the candidate genes, we examined their expression profiles under different conditions (Fig. 43) using the RhiirExpress RNA-Seq platform. (http://rhiirexpress.gbfwebtools.fr/) (Zouine et al., 2017). First, the expression of the candidate genes was examined in germinating spores grown *in vitro* in the absence of a host plant, treated or not with GR24. Overall, their expression was not regulated by GR24 and did not show important variations along the germination process. Among the candidates, *BJ309*, *BJ311*, *BJ313* and *BJ315* were the least expressed in this fungal material. Gene expression was also examined in intra-radical mycelium with different host plants including SL-deficient plants.

With the exception of *BJ311*, the expression of the candidate genes under symbiotic conditions was quite similar to their expression in germinating spores. In contrast, *BJ311* was preferentially expressed under symbiotic conditions. The absence of SLs in *Psccd8* plants did not influence the expression of the candidate genes. Finally, we examined gene expression in extracellular hyphae obtained on carrot hairy roots grown *in vitro*. Only *BJ311* was highly expressed in these hyphae. In conclusion, all candidate genes were expressed in germinating spore and during symbiosis. We did not observe any particular expression profile that would lead us to focus on one candidate in particular.

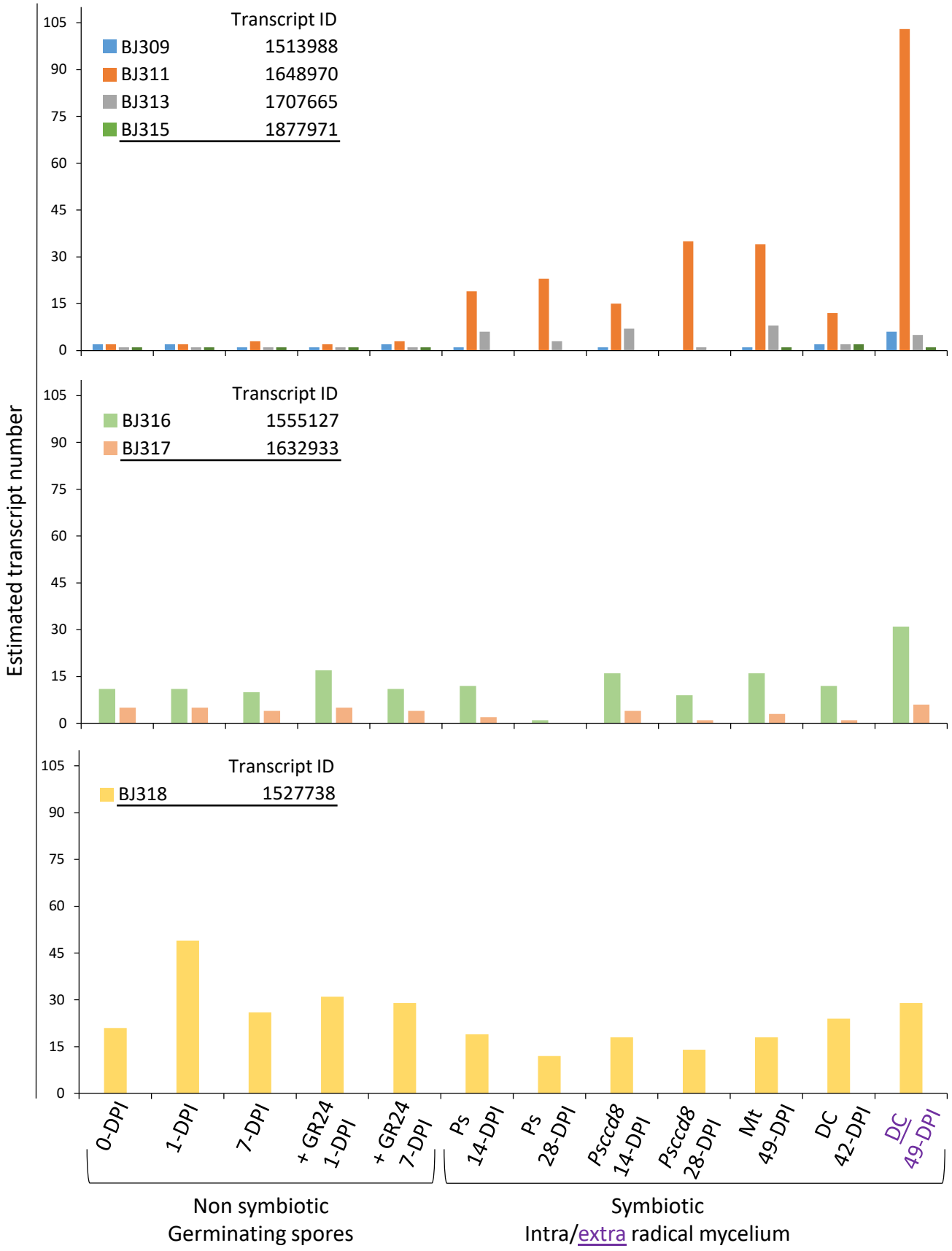

Figure 43. Gene expression of *R. irregularis* candidate genes under different conditions

Gene expression in germinating spores, intra- or extra- radical mycelium. DPI: days post inoculation, GR24 treatment at 100 nM, Mt: *Medicago truncatula*; Ps: *Pisum Sativum*, *Psccd8*: SL-deficient plants, DC: *Daucus carota* (hairy roots). Data were extracted from The RhiirExpress RNA-Seq platform (http://rhiirexpress.gbfwebtools.fr/) (Zouine et al., 2017).

Discussion

The branching inhibition caused by TFA (Taulera et al. (*in prep*) – Fig. 2) cannot be attributed to toxicity because treatment with a mix of (±)-GR24 and TFA was still able to restore symbiosis in *Mtccd8* roots. The addition of TFA suppresses the induction of higher-order branches triggered by KAR2, suggesting that KAR2 perception by *R. irregularis* may involve ABH proteins. The fact that TFA was able to suppress the inhibition of spore germination caused by (±)-4'-desmethyl-2'-*epi*-GR24 (Fig. 38) also suggests that perception of this compound by *R. irregularis* involves ABH proteins. This shows consistency with the hypothesis that AM fungi can perceive methylated and unmethylated butenolides through related signaling pathways. KK094 could not suppress the induction of spore germination induced by (±)-GR24. The fact that KK094 could suppress (±)-GR24-induced germ tube elongation (Taulera et al. (*in prep*) – Fig. 2) but not spore germination (Fig. 38) supports that multiple pathways regulate these developmental responses.

Although (±)-3'methyl-GR24 is inactive on hyphal branching, it is perceived by *R. irregularis* to induce spore germination (Fig. 30). BJ318 shows a very low hydrolytic activity towards (±)-3'methyl-GR24 and a strong conformational change was observed. This is reminiscent of the characteristics of plant SL receptors (de Saint Germain et al., 2016) although we did not observe a covalent binding to the protein (Fig. 42). In Taulera et al. (*in prep*), we hypothesized that the high hydrolytic activity of BJ318 towards (±)-GR24 coupled with the absence of conformational change of the protein could correspond to a catabolic activity to regulate the level of SLs in fungal cells. In view of the results obtained with (±)-3'methyl-GR24, we cannot rule out the possibility that a single protein could exhibit a catabolic activity towards one substrate and perceive another ligand to activate the associated signaling pathway.

Chapter 3
Transfer of hormones between plants connected by mycorrhizal fungi

Background

The following work is part of the Mycormones project in which we aimed to investigate the transfer of phytohormones from one plant to another via a mycorrhizal fungus. This question had never been explored in our laboratory, so the associated experimental designs had not been defined. This is why, at the beginning of my thesis, we decided to conduct a few trials to determine if it would be worthwhile to pursue this topic. We set up a culture system to study the transmission of signals between two plants connected through AMF and performed two experiments. The results were not encouraging and we decided not to continue this project during my PhD. Nevertheless, I will present here the outcome of these tests.

Plants are constantly interacting with a multitude of organisms, from microscopic ones such as bacteria and fungi to macroscopic ones such as insects and other plants. Different plant-plant interactions have been described to date: interactions such as cooperation or commensalism are beneficial or neutral for each of the plants involved, while parasitism and competition are detrimental for at least one of the two plants (Subrahmaniam et al., 2018). Plants can sense many aspects of the environment and modulate these interactions. It has been proposed that unfavorable environmental conditions increase the frequency of positive interactions between plants, leading to better survival (hypothesized by Bertness & Callaway, 1994 and debated in Lortie & Callaway, 2006).

Plant behaviors are now acknowledged as surprisingly complex. One of the most striking examples is the observation of plants adjusting their responses based on the identity of surrounding plants. Dudley and File (2007) were first to observe that plants grown with close

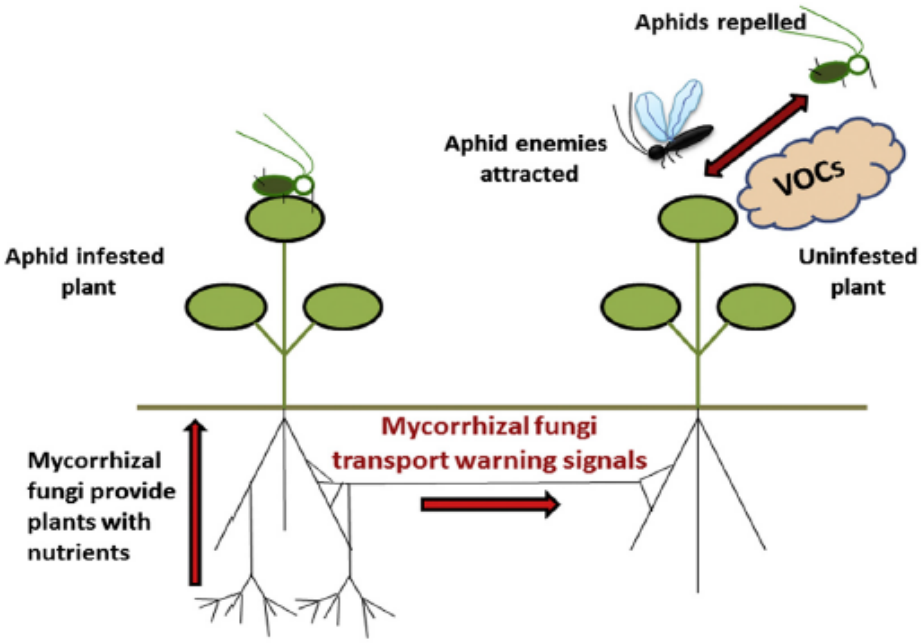

Figure 44. Common mycorhizal networks are able to convey warning signals between plants

A common mycorrhizal network is able to convey plant-generated warning signals in response to aphid attack to unchallenged connected plants, leading the receiver plant to emit VOCs. Natural aphid enemies are then recruited by VOCs, resulting in an improvement of plant survival. Figure from Gilbert & Johnson, 2017.

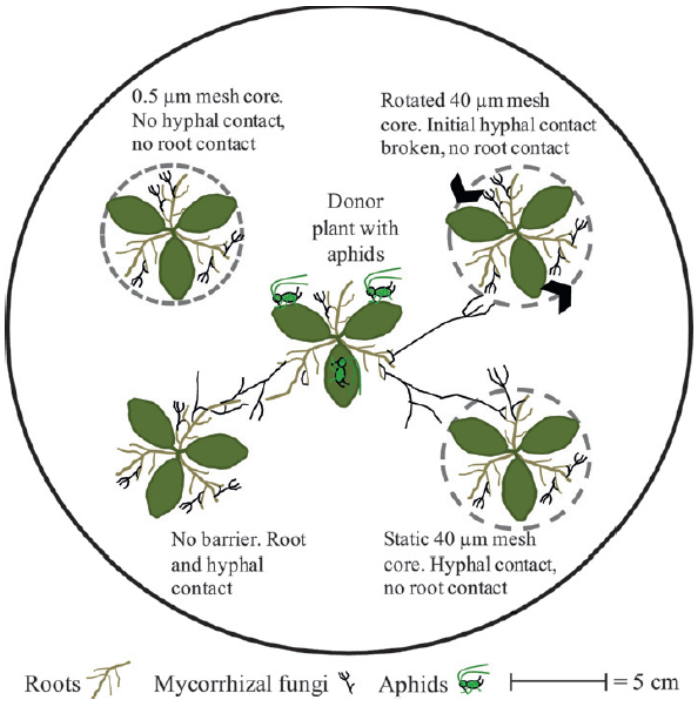

Figure 45. Example of an experimental design used in Babikova et al., 2013

A donor plant, which was colonized by aphids, and four aphid-free receiver plants were grown in a mesocosm. All plants were grown in the mycorrhizal condition. One control plant was prevented from forming mycelial connections to donor plants (0.5 µm mesh). Another was allowed to form connections initially but the connections were snapped after exposure of the donor to aphids (rotated 40 µm mesh). Two test plants were allowed to form shared mycorrhizal fungal networks (non-rotated 40 µm mesh allowing fungal contact only; no barrier allowing fungal and root contact) with the donor plant for the duration of the experiment. Receiver plant responses were analyzed 96 h after addition of aphids to the donor plant. Figure from Babikova et al., 2013.

genetic relatives (kin) allocated less resources to their fine roots than plants growing with genetically unrelated plants. This provided evidence that plants are capable of discriminating between related and unrelated neighbors, which has since been confirmed in several species (reviewed in Bilas et al., 2021).

Perception of neighboring plants can be mediated through both indirect and direct signals. On the one hand, plants detect changes in resource availability such as light (Crepy & Casal, 2015), water (Casper & Jackson, 1997) and nutrients (Schenk, 2006) caused by neighboring plants. On the other hand, plants perceive and communicate with neighboring plants through direct molecular signals occurring above and below- ground.

Aboveground plant communication is essentially mediated by airborne chemicals called volatile organic compounds (VOCs) emitted by plants and perceived by surrounding plants. VOCs have been shown to convey information between plants in several contexts such as pathogen or insect attack (Fig. 44), and are used for kin recognition (for review see Ninkovic et al., 2020).

Root volatile signals have also been described as belowground signals during plant-plant interactions (Schenkel et al., 2015). In addition, significant amounts of primary and specialized metabolites (also referred to as secondary metabolites) are exuded into the rhizosphere by plants, mediating their interactions with surrounding organisms. Perception of root exudates drive root behavior, kin recognition, parasitism and shape interactions between plants and soil (micro-)organisms (for review see Wang et al., 2021a, Rasmann & Turlings, 2016).

In addition to exchanging diffusible signals, plants can also be directly “wired” together by other organisms with which they form intimate physical connections. For example, parasitic plants of the genus *Cuscuta* (known as dodders), are devoid of leaves and roots. They develop multiple stems that twist to find host plants to parasitize. Through a specific organ, called haustorium, dodders penetrate host plants to extract water and nutrients. Unlike other species of parasitic plants, they are able to colonize several host plants simultaneously, thereby interconnecting them together. Such a network has long been known to transfer viruses between connected plants (Hosford, 1967), and more recently to transfer mRNAs (Kim et al., 2014), specialized metabolites (Smith et al., 2016), and proteins (Liu et al., 2020).

The interplant networks that have been best documented are common mycorrhizal networks (CMNs), which consist of two or more plants connected by ectomycorrhizal (EM) or arbuscular mycorrhizal fungi. Common ectomycorrhizal networks (referred to as CeMNs) formed by EM fungi are considered to connect a smaller range of plant species due to high plant host selectivity of EM fungi (Tedersoo et al., 2008) compared to AM fungi, which exhibit low host specificity (Klironomos et al., 2000). CMNs have been shown to influence their ecosystem by driving plant establishment, growth, defense (for review see Simard et al., 2012), and plant-plant communication through the transfer of molecules between connected plants. Flows through arbuscular and ectomycorrhizal mycorrhizal networks have been found to transfer nutrients such as carbon, nitrogen, phosphorus, and water (for review see Simard et al., 2015). In addition, specialized metabolites can be transported along CMNs, for instance to expand the bioactive zone of allelochemicals released by one plant to reduce the growth of neighboring plants (Barto et al., 2011).

The discoveries of the ability of ectomycorrhizal (Song et al., 2015), arbuscular mycorrhizal (Song et al., 2015), and endophytic (Vahabi et al., 2018) fungi to convey plant-generated warning signals in response to herbivore or pathogen attack to unchallenged connected plants have been major breakthroughs in plant ecology (Fig. 44) (for review, see Gilbert & Johnson, 2017). I will focus here only on signal transfers through CMNs formed by arbuscular mycorrhizal fungi, referred to as CaMNs.

To ensure that there is no confusion in observing true CaMN-mediated transfer, as opposed to diffusion of root exudates through the soil, multiple experimental controls were used in different studies as illustrated in Fig. 45. To summarize the different experimental designs, two plants were grown separated by a membrane, which prevents root passage but allows fungal hyphae to pass through allowing CaMNs to connect plants. This CaMN was either left intact (test plants) or mechanically disrupted (control plants). Then, one of the two plants (named donor plant) was challenged with either a herbivore or a pathogen. Physiological responses, gene expression, modulation of protein activity or specialized metabolite production were analyzed in the receiver plants. Using this experimental design, transfer of warning signals between CaMNs-connected plants were shown by different teams.

Song and his co-workers (2010) demonstrated that the connection by CaMNs between a donor plant challenged with the fungus *Alternaria solani* and a receiver plant, increased defense-related gene expression and activated putative defense enzymes in the receiver plants, increasing plant resistance. This study established for the first time the physiological relevance of CaMN-mediated signaling, in "priming" receiver plants prior to a potential pest attack. Zhang and co-workers observed an increase in salicylic acid (SA) content and the activation of the SA signaling pathway in an un-challenged citrus plant connected by AMF to a donor plant challenged with the bacterium *Xanthomonas axonopodi* (Zhang et al., 2019). Using an *in vitro* experimental setup, Alaux et al. (2020) measured an enhanced expression of four defense genes belonging to the JA and ethylene signaling pathways, in un-challenged potato plants connected by a CaMN to donor plants infected by the oomycete *Phytophtora infestans*. Last, using donor tomato plants challenged with caterpillars, Song et al., (2014) revealed an increase of insect resistance in un-challenged plants, mediated by the activation of the JA signaling pathway (Song et al., 2014). Donor plants mutated in the JA biosynthesis pathway were no longer able to trigger defense induction in the receiver plants. This led the authors to hypothesize that JA moved from roots of one plant to another via CaMNs. However, no biochemical evidence for a transfer of JA or other phytohormones between plants connected by a CaMN has yet been published.

Both JA and SA can be modified to produce methylated volatile forms. This makes the analysis of direct transfer of these hormones challenging. It also requires additional experimental controls to rule out any air-borne transport of volatile forms from donor to receiver plants. We thus decided not to study JA or SA. Rather, we attempted to obtain evidence for a putative transfer of other phytohormones (auxin, strigolactones, cytokinins, brassinosteroids and gibberellins) between plants connected by a CaMN. To this end, a set of analogs or labelled phytohormones were injected into a donor plant, and the presence of these hormones in receiver plants connected by CaMNs was assessed by mass spectrometry. In parallel, the transfer of endogenous phytohormones from one plant to another was investigated by studying the ability of wild-type plants to complement the developmental phenotype of hormone-deficient mutants.

Materials and Methods

Biological materials

The experiments were carried out on *Medicago truncatula* A17-Jemalong, or tomato (*Solanum lycopersicum L.)* cultivars Marmande and Micro-Tom. *Rhizophagus irregularis* spores (strain DAOM197198) were purchased from Agronutrition (France). They were rinsed from their storage buffer using a 40 µM nylon mesh with 750 mL sterile UHQ water. Spores were resuspended in sterile UHQ water and stored at 4 °C for 48 h before use.

Chemicals

(±)-GR24 was purchased from Chiralix (The Netherlands). Naphtalene acetic acid (NAA), 2,4-Dichlorophenoxyacetic acid (2,4-D), kinetin and labelled phytohormones: $[^2H_6]N^6$- isopentenyl adenosine ($[^2H_6$-$N^6]$-iPR), $[^{15}N_4$-$N^6]$- isopentenyl adenine ($[^{15}N_4$-$N^6]$-iP), $[^{13}C_6]$- indole-3-acetic acid ($[^{13}C_6]$-IAA) were purchased from Olchemim. All phytohormone stock solutions were prepared at 10 mM and stored at – 20 °C. (±)-GR24 was dissolved in acetone, NAA, 2,4-D, kinetin in NaOH and $[^2H_6$-$N^6]$-iPR, $[^{15}N_4$-$N^6]$-iP and $[^{13}C_6]$-IAA in ethanol.

Seed sterilization and germination

Medicago truncatula seeds were chemically scarified using a 7-minute treatment with 98% sulfuric acid (Sigma-Aldrich) followed by three washes in sterile water. They were then surface-sterilized for 2 minutes in 2.4% active chlorine. After five washes in sterile water, and 10 minutes of soaking, the seeds were transferred to 1.5% agar-water plates and incubated at 4 °C in the dark for 72 h. They were then left to germinate overnight at room temperature in the dark.

Tomato seeds were surface-sterilized for 10 minutes in 2.4% active chlorine. After five washes in sterile water, and 30 minutes of soaking, the seeds were transferred to 1.5% agar-water plates and incubated at 4 °C in the dark for 72 h. They were then left to germinate for five days at room temperature in the dark, then under daylight for 3 to 5 days.

Experimental set-up – *Medicago truncatula*

Each system was composed of a rectangular plastic container (length/height/width 16/11/5 cm) filled with about 0.8 L of sterilized substrate (zeolite:sand 1:1 v:v) inoculated with 400 spores of *R. irregularis.* Two *Medicago truncatula* plants grown individually in two modified circular pots (diameter 5 cm, height 7 cm) were positioned at opposite sides of the container.

A circular slot (3 cm diameter) was cut in each pot and a metal mesh (pore diameter 30 µM) was externally soldered, preventing direct root contact but allowing AMF hyphae to grow freely in the container. The pots were filled with 0.2 L of sterilized substrate (zeolite:sand 1:1 v:v) inoculated with 400 spores of *R. irregularis* (Fig. 46). Plants were grown for eight weeks in a growth chamber under a 16 h photoperiod (light intensity 300 µmol $m^{-2}.s^{-1}$). The temperature was set to 22 °C day and 20 °C night, with 70% humidity. Plants were watered with a modified half-strength low-phosphate and low-nitrogen Long Ashton solution (Hewitt, 1966), containing 7.5 µM Na_2HPO_4, 750 µM KNO_3 , 400 µM $Ca(NO_3)_2$, 200 mg/L MES buffer, pH 6.5. Two conditions were used (Fig. 46): (a) intact CaMNs and (b) CaMNs severed by rotation of the pots. Two solutions were freshly prepared in water: a mix of phytohormones containing 10 µM each of of 2,4-D, NAA, kinetin and (±)-GR24, or the corresponding volume of solvents for the mock treatment. One plant per system was treated with either the hormone mix or the mock solution. Ten droplets of 20 µL of solution supplemented with 0.05% tween20 were dispatched to several secondary apical meristems. Additionally, a cotton thread immersed in 500 µL of solution was passed through the stem with a needle over the root crown, in order to directly feed the vascular system. Plants that received treatments were referred as donor plants, and untreated plants were termed receiver plants. Roots and aerial parts of donor and receiver plants were harvested 24 h after treatment. After several washes in water, the plant material was chopped in small parts and approximately 1 g was randomly sampled and ground in liquid nitrogen. Two donor and two receiver plants were analyzed for the hormone treatment, and one of each for the mock treatment.

Experimental set-up - Tomato

Tomato plants of cultivars Marmande (Mm) and Micro-Tom (MT) were grown in pairs in plastic pots (volume 0.3 L) containing substrate composed of black peat: blond peat: clay (49.5:49.5:1 v:v:v) for seven weeks in a greenhouse. Plants were watered with a modified half-strength low-phosphate and low-nitrogen Long Ashton solution (Hewitt, 1966) as described above. Three different combinations were used: (a) one MT plant was grown together with one Mm plant without a mycorrhizal fungus, (b) 500 spores of *R. irregularis* were inoculated to one MT plant grown with one Mm plant, (c) 500 spores of *R. irregularis* were inoculated to two MT plants grown in the same pot (Fig. 47). Ten pots were used for each combination. The height of each MT plant was measured at various time points (20, 28, 35 and 50 days after germination). At the end of the experiment (50 days post germination), Mm donor plants were

treated with one of the following mixes: (I) 10 µM of kinetin, 2,4-D and (±)-GR24; (II) 10 µM of [$^{2}H_{6}$-N^{6}]-iPR and [$^{15}N_{4}$-N^{6}]-iP; or (III) H_2O. MT donor plants were treated with 10 µM [$^{13}C_{6}$]-IAA. Solutions were applied to the vascular system using a cotton thread immersed in 2 mL of hormonal mix, as described above for *Medicago* plants. After 24 h, a part of the root system located near the root crown and a fraction of the aerial part of one donor and one receiver plant per treatment were harvested. The sampled fraction of the aerial part was composed of approximately five cm of stem and ten leaflets collected at several levels. The plant material was washed with water then chopped in small parts and approximately 1 g was randomly sampled and ground in liquid nitrogen.

Staining and observation of mycorrhizal structures

To verify that the plants were mycorrhized, a small part of the root system was stained to observe mycorrhizal structures. Roots were cleared in 10% KOH (w:v) for three days at room temperature and stained with Schaeffer black ink (Vierheilig et al., 1998) for eight minutes at 95 °C. The mycorrhizal structures were examined under a Leica RZ75 stereomicroscope.

Phytohormone extraction

The protocol of phytohormone extraction and separation by Solid Phase Extraction (SPE) was adapted from Kojima et al., (2009) as follows: 100mg of plant material was hand-ground in liquid nitrogen with a mortar and pestle, then resuspended in 1 mL of cold modified Bieleski's solvent (methanol/water/formic acid 75:20:5, v:v:v) and left overnight at -20°C to achieve complete extraction. The crude extracts were centrifuged for 15 min at 10,000 x *g*, at 4°C. The pellet was reextracted in 200 µL modified Bieleski's solvent for 30 min at -20°C, centrifuged 15 min at 10,000 x *g*, and the supernatant was pooled with the first one. Extracts were pre-purified on SPE Oasis HBL cartridges (1 mL per 30 mg, Waters). Cartridges were conditioned in 1 mL methanol and equilibrated in 1 mL of 1 M formic acid. Samples were loaded and eluted with 1 mL modified Bieleski's solvent. Eluates containing phytohormones were dried under nitrogen stream and were reconstituted in 100 µL 1 M formic acid and then analyzed by LC-MS.

LC-MS analysis of phytohormones

A UHPLC system (Dionex Ultimate 3000, Thermo Scientific) was equipped with a phase column (Kinetex C18, 100 x 2.1mm, 2.6 µm, 100 Å, Phenomenex) heated at 45°C. Five-µL samples were injected. Separation was performed at a constant flow rate of 0.3 $mL.min^{-1}$, in a gradient of solvent A (water + 0.05% formic acid) and solvent B (acetonitrile + 0.05% formic acid): 1 min

5% B; 8 min 5% to 96% B; 1 min 96% B, and re-equilibration to the initial conditions in 3 min. A Q-Trap 4500 mass spectrometer (AB Sciex) was used with an electro-spray ionization source in the positive and negative ion mode. Curtain gas was set to 30 psi, nebulizer to 40 psi and turbo gas to 60 psi. Capillary voltage was set to 5.5 kV (positive mode) or -3.5 kV (negative mode) on Electrospray Ionization (ESI) source (600°C). Data were analyzed using Skyline software.

A

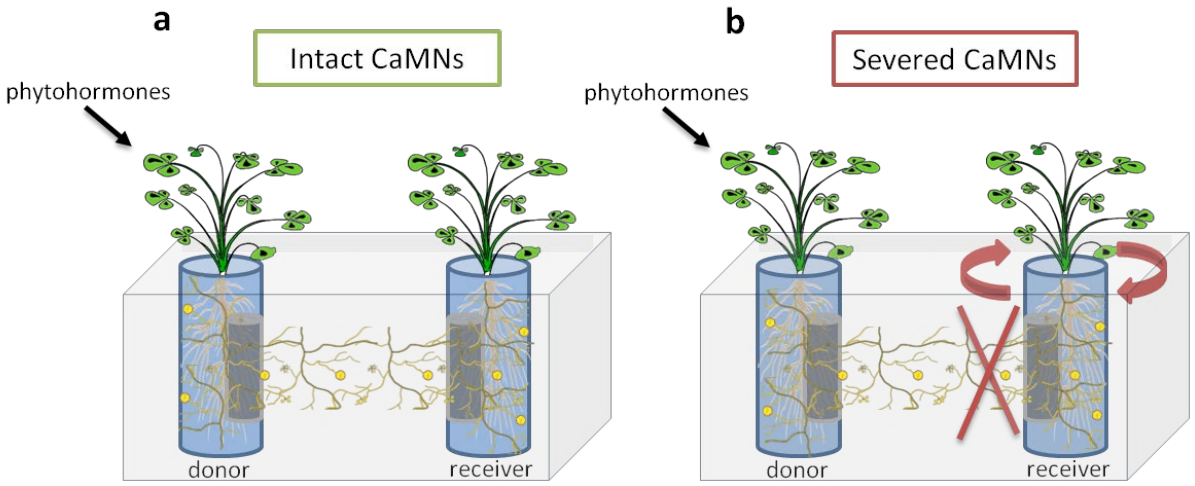

B

			Roots		Aerial parts	
			Donor	Receiver	Donor	Receiver
kinetin	Mock	CaMNs				
		Severed CaMNs				
	Mix	CaMNs				
		Severed CaMNs				
2,4-D	Mock	CaMNs				
		Severed CaMNs				
	Mix	CaMNs				
		Severed CaMNs				

presence absence

Figure 46. Transfer of phytohormones between *Medicago* plants connected via a CaMN

(A) Experimental design. Two *Medicago truncatula* plants were grown in two modified circular pots placed on either side of a rectangular container. A mesh was soldered on each pot, preventing direct root contact between plants but allowing the establishment of CaMNs. CaMNs were (a) left intact or (b) severed by rotating the pots, prior to hormone application. A mix of hormones or a mock treatment were supplied to the donor plant. Roots and aerial parts of each plant were harvested 24 h after treatment.

(B) The presence (green) and the absence (red) of these phytohormones were analyzed by mass spectrometry. Two donor and receiver plants per conditions were analyzed. The experiment was performed once.

Results

I) Transfer of phytohormones in *Medicago truncatula*

The first experiment was carried out with *Medicago truncatula* plants. Two plants were grown in two modified circular pots placed on either side of a rectangular container filled with substrate. The substrate in both pots and in the rest of the container was inoculated with AM fungi. A circular slot was cut in each pot and a metal mesh was externally soldered, preventing direct root contact but allowing AMF hyphae to establish CaMNs (Fig. 46). For the purpose of distinguishing between true CaMN-mediated transfer and soil diffusion of root exudates, two conditions were used: (a) CaMN left intact and (b) CaMN disrupted by rotation of the pots. In order to verify that the plants were mycorrhized, a small part of the root system was harvested and stained to observe mycorrhizal structures. All inoculated plants exhibited high levels of mycorrhization, and hyphae of AM fungi were observed throughout the mesh (data not shown). To distinguish applied chemicals from endogenous plant hormones, synthetic analogs (2,4-D, NAA, (±)-GR24 and kinetin) were injected into one of the two plants, named donor plant. The presence of these phytohormones was analyzed by mass spectrometry in the other plant, termed receiver plant. A first problem during sample analysis was that small amounts of (±)-GR24 and NAA were detected in blank samples, indicating that the mass spectrometry source was contaminated. The results were thus un-interpretable (data not shown). Secondly, a signal corresponding to kinetin was found in the aerial parts of the plant treated with the mock solution (Fig. 46). Finally, 2,4-D was detected in the roots and aerial parts of the donor plant but not in the receiver plant, connected or not with a CaMN (Fig. 46).

II) Transfer of phytohormones in tomato

As an alternative approach, the putative transfer of endogenous phytohormones from one plant to another by a CaMN was investigated by studying the ability of a wild-type plant to complement the phenotype of a dwarf plant. The dwarf tomato cultivar Micro-Tom (MT) contains a mutation in the brassinosteroid (BR) biosynthesis pathway that is partly responsible for its dwarf phenotype. BR acts synergistically with gibberellins (GA), as co-application of GA and BR on MT leaves results in an increase of internode length compared to the single

A

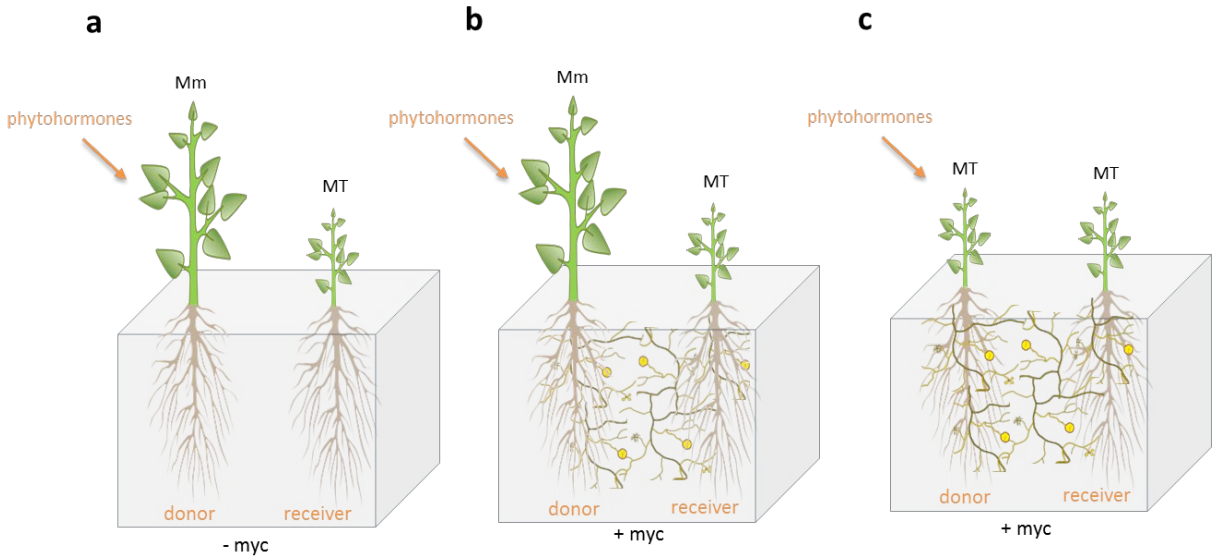

B

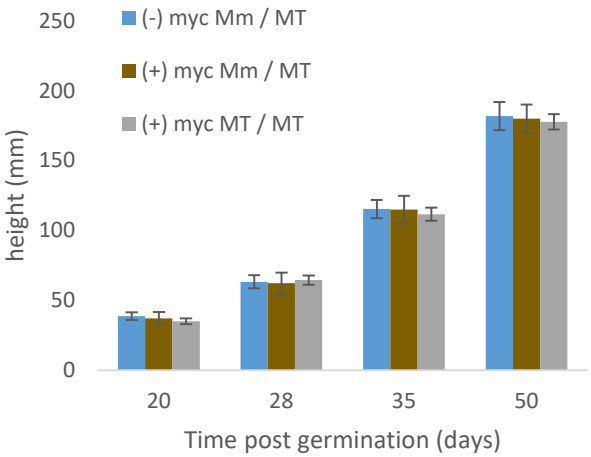

C

		Roots		Aerial parts	
		Donor	Receiver	Donor	Receiver
2,4-D	(+) myc				
	(-) myc				
GR24	(+) myc				
	(-) myc				
[$^{2}H_{6}$-N^{6}]-iPR	(+) myc				
	(-) myc				
[$^{15}N_{4}$-N^{6}].iP	(+) myc				
	(-) myc				
[$^{13}C_{6}$]-IAA	(+) myc				
	(-) myc				

presence absence

Figure 47. Transfer of phytohormones between tomato plants connected by a CaMN

(A) Experimental design. Three combinations were used: (a) one MT was grown in pair with one Mm without AM fungi, (b) one MT was grown with one Mm and inoculated with AM fungi (c) two Mt were grown together and inoculated with AM fungi.

(B) Growth of MT plants in the three combinations. The height of each MT plant was measured at different time points. Ten pots were used for each condition.

(C) Donor plants were treated with phytohormones or water. Roots and aerial parts were harvested 24h after treatment. The presence (green) and the absence (red) of these phytohormones was analyzed by mass spectrometry. One donor and receiver plants per condition were analyzed. The experiment was performed once.

application of BR (Martí et al., 2006). This also shows that exogenous application of both hormones on leaves is efficient to complement the dwarf phenotype of MT.

Preliminary results in our group have shown that BR application to MT roots is also able to increase MT plant height. Similar results have been observed for GA, which when applied to roots increases the height of a pea GA biosynthesis mutant (data not shown). These findings indicate that BR and GA can be taken up by roots and lead to increase shoot elongation. Therefore, to investigate the ability of AM fungi to transfer endogenous phytohormones (*i.e*. GA and BR), we attempted to complement the dwarf phenotype of MT plant grown with a wild-type tomato plant (cultivar Marmande (Mm)), in the presence or absence of CaMNs. In a preliminary experiment, which did not include all necessary controls, three conditions were used (Fig. 47): (a) one MT plant was grown together with one Mm plant without mycorrhizal fungi, (b) one MT plant was connected to one Mm plant by a CaMN (c) two MT plants were connected together by a CaMN. A small part of the root system was harvested before grinding and stained to observe mycorrhizal structures. No fungal structures (spores, hyphae and arbuscules) were observed in the un-inoculated controls compared to inoculated plants, which exhibited high levels of mycorrhization (data not shown). To monitor the growth phenotype of MT plants, their height was measured at various timepoints (20 to 50 days after germination). No differences were observed between the different conditions for each timepoint (Fig. 47). Last, using the same tomato plants, the transfer of phytohormone analogs and labelled phytohormones between plants connected by a CaMN was investigated. After the last measurement of plant height (50 days after germination), donor tomato plants were infiltrated with one of the following mixes: (i) synthetic analogs containing: 2,4-D, (±)-GR24 and kinetin, (ii) labelled phytohormones containing: [$^{2}H_{6}$-N^{6}]-iPR and [$^{15}N_{4}$-N^{6}]-iP or (iii) [$^{13}C_{6}$]-IAA. Water was infiltrated for mock treatments. The presence of these hormones was analyzed in the receiver plant by mass spectrometry (Fig. 47). [$^{13}C_{6}$]-IAA was not detected in any sample. Overall, the main observation was that no differences in the presence or absence of these hormones were found between plants connected or not by a CaMN. A signal corresponding to kinetin was found in the roots of plants treated with water and in both parts of the corresponding receiver plant (Fig. 47). (±)-GR24 was detected in the roots of donor plants and in both parts of receiver plants. Last, [$^{2}H_{6}$-N^{6}]-iPR, [$^{15}N_{4}$-N^{6}]-iP and 2,4-D were detected in the roots of donor plants but not in the receiver plants.

Discussion

Establishment of a common mycorrhizal network

In the present work, we aimed to obtain evidence for the putative transfer of phytohormones between plants connected by AM fungi. CaMNs can be formed from an individual fungus which simultaneously interacts with two plants, connecting them to each other. Alternatively, CaMNs can be formed by fusion of existing mycelial networks through the formation of fusion structures named anastomoses (Giovannetti et al., 1999). The formation of anastomoses was found to be very frequent, approximately every two mm of hyphae (Giovannetti et al., 2001). The establishment of CaMNs by inoculating both plants with spores of AM fungi was confirmed by different studies. Thus, CaMNs are expected to have been established in our experiments. In future experiments, this could be confirmed by evaluating the induction of defense genes in the receiver plant after elicitation of the donor plant (as performed in Song et al., 2010).

Phytohormones are not transferred between plants connected by a CaMN

We failed to obtain biochemical evidence for the transfer of phytohormones between plants connected by a CaMN. Five hypotheses can be considered to explain these results. The first hypothesis is that the phytohormones used in this work are not transported between two plants connected by a CaMN. Several forms of each class of hormones exist, for instance there are more than 130 GAs identified to date (Hedden & Sponsel, 2015). These different forms differ in their specificity of action, localization and activity. The forms of phytohormones used in these experiments represent only a fraction of the existing panel of phytohormones and might not be the one transferred between two plants connected by a CaMN.

Alternatively, AMF may convey hormonal information by other means than direct phytohormone transport. They could perceive phytohormones taken up from the donor plant, and respond by producing new molecular signals. These newly synthesized compounds could be perceived by the receiver plant to trigger physiological responses.

The third possibility is that to observe fungus-mediated hormone transfers, the donor plant must be exposed to specific environmental conditions. The involvement of JA, ethylene, and SA during CaMN-mediated signaling has been demonstrated after elicitation of the donor plant by herbivore or pathogen attacks. Their involvement was suspected as these hormones are known to be recruited in response to such stimuli. Therefore, depending of the hormone

used, it may be necessary to expose the donor plant to particular growth conditions to observe transfers.

Another possibility is that infiltrated hormones have undergone modifications before or during transfer. Hormones can be modified in plants by acetylation, glycosylation or esterification (Piotrowska & Bajguz, 2011). Modified hormones could be the preferred form for transport by a CaMN. Since only the injected hormones were screened by mass spectrometry, we could not detect modified forms.

The last hypothesis is more of a technical issue. Assuming that a transfer of hormones occurred, the amount of hormones transferred might be too low and could escape detection by mass spectrometry. Plant hormones are known to be present and active in plants at low concentrations. During putative transfers, infiltrated hormones are first diluted in the donor plant (aerial and root parts), then transferred to the fungus, and again a portion only could reach the receiver plant and spread through its different parts. In addition, only a small fraction of the receiver plant was sampled. Therefore, it is possible that we were falling below the detection threshold of mass spectrometry. The fact that we were not able to detect [$^{13}C_6$]-IAA in the infiltrated donor plant indicates that dilution or modification of these hormones in the donor plant was sufficient to prevent detection.

The presence of (±)-GR24 in the unconnected receiver plant indicates that there was an uptake of (±)-GR24 by receiver tomato plants. Two possibilities exist: (i) (±)-GR24 was taken up from the soil by the receiver plant, or (ii) (±)-GR24 was transferred through root contacts between donor and receiver plant. In the case of connected plants, this does not exclude an additional transport by CaMNs. In future experiments, to eliminate any possibility of soil diffusion or root exchanges, it would be necessary to include additional controls. Two plants could be grown separated by a mesh in a two-compartment container separated by a small air gap (0.5 cm), allowing the fungus to pass through but not the molecules to diffuse. In one condition, the fungus would be left untouched whereas in the second condition, the fungus would be removed from the air gap.

The results presented in this study have to be carefully interpreted. Only two donor and receiver plants for the *Medicago* experiment and one of each for the Tomato experiment were analyzed. Furthermore, we have encountered several technical issues. First, a signal corresponding to kinetin was found in the aerial parts of the donor and receiver plant

infiltrated with water in both experiments. It is possible that an endogenous molecule present in the aerial parts of *Medicago* and Tomato plants displays the same mass spectrometry signal as kinetin. In addition, during *Medicago* sample analysis, (±)-GR24 and NAA were detected in blank samples indicating that the mass spectrometry source was contaminated. Last, we evaluated if the dwarf phenotype of MT tomato plants could be partly rescued by a CaMN-connected wild-type tomato plant supplying its own hormones or signals. We did not observe such complementation in this experiment. Insufficient BR or GA could have reached the MT plant and failed to rescue its shoot elongation phenotype.

Perspectives

To conclude, we were not able to observe true CaMN-mediated hormone transfer between connected plants. The results obtained were not encouraging and we decided not to continue this project during my PhD. Nevertheless, an experimental design composed of double compartment Petri dishes was set up by another person in the laboratory to pursue the investigation of hormone transfers between plant roots and AM fungi. One of the compartments contained roots colonized by AM fungi, which were able to grow in the second, root-free compartment. Analogues or labelled phytohormones were applied to one of the compartments, and searched in the other by mass spectrometry. This experimental design offers several advantages. It provides the opportunity to investigate the putative transfer of hormones from the roots to the fungus or vice versa. Mass spectrometry signals are enhanced in this experimental design because it allows for lower dilutions of infiltrated hormones compared to experiments on whole plants grown in soil. Last, a larger number of biological replicates can be obtained and more hormones mixes or single hormone applications could be tested. In the future, results obtained with this *in vitro* system could guide further experiments on whole plants.

General discussion

In the first chapter, we showed that *R. irregularis* responded to unmethylated SL analogs. (±)-4'-desmethyl-2'-*epi*-GR24 inhibited hyphal branching while retaining the ability to restore symbiosis in SL-deficient plants. In the second chapter, we have gathered indirect evidence regarding the nature of SL and unmethylated butenolide receptors in AMF, which likely include ABH proteins. Our results suggest the existence in AMF of several signaling pathways regulating the response to methylated and unmethylated butenolides. This points to an interesting parallel with the activation of homologous, yet distinct pathways by SLs and unmethyl butenolides in plants. In plants, unmethylated butenolides mimic the unidentified KL (Yao et al., 2018, 2021), an endogenous plant signal regulating several developmental processes. A growing amount of evidence links the KAI2/KL pathway to mycorrhizal symbiosis. First, Gutjahr et al. 2015 reported that the symbiotic interaction was completely abolished in rice *Oskai2* mutants. Later, this phenotype was confirmed in *Petunia* (Liu et al., 2019) and *Brachypodium distachyon* (Meng et al., 2022). In addition, mutation of Os*SMAX1* fully suppressed the symbiotic phenotypes of Os*kai2* and Os*d3* mutants indicating that OsSMAX1 is a negative regulator of AM symbiosis (Choi et al., 2020). In view of these observations it has been proposed that the KAI2 signaling pathway mediates AM symbiosis by conditioning plant roots for fungal infection (Hull et al., 2021).

Evolutionary origin of SL and KAR receptors

To assess the taxonomic distribution of the *D14/KAI2* gene family, Wang et al. (2021b) conducted a BLAST analysis using plant D14/KAI2 sequences as query. They identified homologs in bacteria and streptophytes, annotated as RsbQ (Wang et al., 2021b). RsbQ proteins share structural features with D14/KAI2 proteins. Phylogenetic analysis suggests that the plant *D14/KAI2* gene family was acquired from proteobacteria through horizontal gene transfer, likely before the emergence of streptophytes. In the fungal kingdom, no significant RsbQ homologs were identified. The authors suggested that AM fungi possess distinct SL receptors that differ from RsbQ (Wang et al., 2021b). The enzymatic function of ABH proteins

is tightly linked to their three-dimensional core architecture rather than to sequence identity. In Taulera et al. (*in prep*), we showed that two inhibitors known to target plant SL receptors could also inhibit *R. irregularis* responses to SLs, and could inhibit the SL-hydrolytic activity of at least two fungal ABHs. This suggests that SLs receptor(s) in AMF and plants converged towards similar structural features and that fungal SL receptors could have arisen from the neofunctionalization of existing fungal ABH protein(s), independent of RsbQ.

Putative functions of secreted fungal ABH proteins with hydrolytic activity towards SLs

Among the candidate proteins identified in *R. irregularis*, a family of ABH proteins possessing a signal peptide has expanded in the Glomeromycota subphylum. *In vitro*, some of these proteins cleave (±)-GR24 (Taulera et al., *in prep* - Fig. 7). Their secretion outside the fungal cells needs to be confirmed. If it does occur, it is difficult to conceive that these proteins act as receptors. They might instead exert a function associated with the degradation of SLs. A first possibility is that these proteins reduce the pool of active SLs in the extracellular environment in order to prevent an excessive response to SLs. This could mirror the situation in plants, where catabolism of SLs by a carboxylesterase has been recently proposed to regulate SL contents (Xu et al., 2021). A second possibility is that a degradation of SLs in the soil decreases the competition between different species of AM fungi. Such competition has been described many times and *R. irregularis* is known to be particularly efficient in competing for plant colonization (Engelmoer et al., 2014; Symanczik et al., 2015). A fungus that has already colonized a host plant could degrade SLs in the soil to avoid the stimulation of other AM fungi. A final possibility is that these putative secreted proteins are involved in the regulation of SL content in host cells during symbiosis, for example by being secreted into the peri-arbuscular space. In this respect, it is worth remembering that the candidate proteins identified in this work exhibit hydrolytic activity towards the unmethylated butenolide (±)-desmethyl-GR24 (Taulera et al., *in prep* – Fig. 5). Such hydrolytic activity raises questions about their putative capacity to cleave the KL *in planta*.

Activity of unmethylated butenolides during AM symbiosis

We showed that (±)-4'-desmethyl-2'-*epi*-GR24 is able to restore symbiosis in SL-deficient mutants. This suggests that in a context of symbiosis, (±)-4'-desmethyl-2'-*epi*-GR24 makes the SL pathway dispensable. This activity could reflect the effects of (±)-4'-desmethyl-2'-*epi*-GR24 on the fungus, on the plant or both.

From a fungal perspective, we observed that *in vitro*, (±)-4'-desmethyl-2'-*epi*-GR24 stimulated elongation of the germ tube and inhibited the formation of new hyphal branches. This raises questions about the ability of *R. irregularis* to perceive the KL. In contrast to plants, the fungus exhibited distinct responses toward the KL mimics: (±)-4'-desmethyl-2'-*epi*-GR24, KAR2 and (-)-GR24 (Fig. 25, 26, 27) suggesting different mechanisms of perception in AMF compared to plants for these compounds. It also indicates the existence of several receptors to perceive unmethylated butenolides in AMF.

In plants, several compounds mimic the KL through the KAI2 signaling pathway (Yao et al., 2018, 2021). However, under certain circumstances, these compounds can trigger responses through both KAI2 and D14 signaling pathways. For example, although (-)-GR24 exhibits strong KAR-like activity, residual D14-dependent activity has been reported in *A. thaliana* (Wang et al., 2020c). Likewise, in hypocotyl elongation assays, *kai2 Atd14* double mutants were insensitive to desmethyl-YLG while both single mutants showed responses to high concentrations of desmethyl-YLG (Yao et al., 2018). In AM fungi, we have shown that the symbiotic capacity of the fungus is independent of hyphal branching. We hypothesized that the 4'-desmethyl-GR24-related pathway was distinct from the SL signaling pathway. However, we cannot exclude that unmethylated butenolides and SLs activate the same pathway to stimulate the symbiotic capacity of the fungus, while regulating two distinct pathways to control hyphal branching.

From the plant point of view, it seems likely that (±)-4'-desmethyl-2'-*epi*-GR24 activates the KAI2 signaling pathway and creates a permissive state for fungal colonization (Hull et al., 2021). However, the KL mimics (-)-GR24 and KAR2 were unable to to restore symbiosis in SL-deficient plants (Taulera et al., 2020; data not shown), indicating that activation of a permissive state in plant roots through KAI2 is not sufficient to allow AM root colonization in the absence of SLs. To confirm this, it would be of interest to test the symbiotic capacity of *ccd8/smax1* double mutants in which the plants are in a constitutive permissive state (Choi et al., 2020) but the fungus is not stimulated (absence of SLs). Furthermore, AM fungi can successfully colonize *Marchantia paleacea kai2* mutants. To study the effects of (±)-4'-desmethyl-2'-*epi*-GR24 on the fungus in a symbiotic context independently of their effects on the plant, it would be interesting to assess the capacity of (±)-4'-desmethyl-2'-*epi*-GR24 to restore symbiosis in *Mpccd8 kai2* double mutants.

Do AM fungi produce KL-like compounds?

The identification of KL is one of the challenges that animates the scientific community. KL can be mimicked by other signals such as karrikins, and KL is thought to be an unmethylated butenolide (J. Yao et al., 2021b). In addition to KAR2, other natural unmethylated butenolides are found in the soil. For example, N-acyl-homoserine lactones (AHLs) have been characterized to mediate bacterial quorum sensing (Kitani et al., 2011; Klapper et al., 2020; Nguyen et al., 2018). Interestingly, indirect evidence shows that bacterial endosymbionts of AMF (although absent in *R. irregularis*) can produce N-acyl-homoserine lactones (Palla et al., 2018). Furthermore, the endophytic fungus *Aspergillus terreus* was reported to produce butenolide compounds (Guo et al., 2016). It is possible that mycorrhizal fungi produce KL mimics to stimulate the plant prior to colonisation. In line, *Oskai2* mutants no longer respond to *R. irregularis* germinating spore exudates (GSE) (Gutjahr et al., 2015). This supports that AM fungi may produce KL-like compounds perceived by KAI2, although we cannot exclude that the plant responds to other fungal signals in a KAI2-dependent manner. It would be interesting to apply fractions of GSE and evaluate the activation of the KAI2 pathway using marker genes to identify the associated fungal compound(s).

Recruitment of the KAI2 signaling pathway in AM symbiosis

As described earlier in this work, different studies have highlighted the ancestral function of SLs as rhizosphere signals to AM fungi before they acquired a function as endogenous plant hormones. That *kai2* mutants of several flowering plant species are defective in colonization by the AM fungus (Gutjahr et al., 2015; Liu et al., 2019; Meng et al., 2021) but not *Mpkai2* mutants (Kodama et al., 2021) suggests that the ancestral function of the KAI2 pathway was endogenous to plants and was later recruited as a signaling component in AM symbiosis, likely in vascular plant lineages (Kodama et al., 2021).

Genetic analysis failed to identify the KL. One of the hypotheses put forward is the existence of functional redundancy in the biosynthesis of KL. The high degree of flexibility of the KAI2 receptor to recognize different substrates may reflect the existence of multiple structures of the KL. This is reminiscent of the wide variety of SL structures. The different KLs may have distinct functions, as endogenous plant signals and possibly as rhizospheric signals.

References

Abe, S., Sado, A., Tanaka, K., Kisugi, T., Asami, K., Ota, S., Il Kim, H., Yoneyama, K., Xie, X., Ohnishi, T., Seto, Y., Yamaguchi, S., Akiyama, K., Yoneyama, K., & Nomura, T. (2014). Carlactone is converted to carlactonoic acid by MAX1 in *Arabidopsis* and its methyl ester can directly interact with AtD14 *in vitro*. *Proceedings of the National Academy of Sciences of the United States of America*, *111*(50), 18084–18089. https://doi.org/10.1073/pnas.1410801111

Ablazov, A., Mi, J., Jamil, M., Jia, K.-P., Wang, J. Y., Feng, Q., & Al-Babili, S. (2020). The apocarotenoid zaxinone is a positive regulator of strigolactone and abscisic acid biosynthesis in A*rabidopsis* roots. *Frontiers in Plant Science*, *11*, 578. https://doi.org/10.3389/fpls.2020.00578

Agusti, J., Herold, S., Schwarz, M., Sanchez, P., Ljung, K., Dun, E. A., Brewer, P. B., Beveridge, C. A., Sieberer, T., Sehr, E. M., & Greb, T. (2011). Strigolactone signaling is required for auxin-dependent stimulation of secondary growth in plants. *Proceedings of the National Academy of Sciences of the United States of America*, *108*(50), 20242–20247. https://doi.org/10.1073/pnas.1111902108

Akiyama, K., Matsuzaki, K. I., & Hayashi, H. (2005). Plant sesquiterpenes induce hyphal branching in arbuscular mycorrhizal fungi. *Nature*, *435*(7043), 824–827. https://doi.org/10.1038/nature03608

Akiyama, K., Ogasawara, S., Ito, S., & Hayashi, H. (2010). Structural requirements of strigolactones for hyphal branching in AM fungi. *Plant and Cell Physiology*, *51*(7), 1104–1117. https://doi.org/10.1093/pcp/pcq058

Alaux, P., Zhang, Y., Gilbert, L., & Johnson, D. (2021). Can common mycorrhizal fungal networks be managed to enhance ecosystem functionality? *Plants, People, Planet*. https://doi.org/10.1002/ppp3.10178

Alder, A., Jamil, M., Marzorati, M., Bruno, M., Vermathen, M., Bigler, P., Ghisla, S., Bouwmeester, H., Beyer, P., & Al-Babili, S. (2012). The path from -carotene to carlactone, a strigolactone-like plant hormone. *Science*, *335*(6074), 1348–1351. https://doi.org/10.1126/science.1218094

Alder, Adrian, Jamil, M., Marzorati, M., Bruno, M., Vermathen, M., Bigler, P., Ghisla, S., Bouwmeester, H., Beyer, P., & Al-Babili, S. (2012). The path from β-carotene to carlactone, a strigolactone-like plant hormone. *Science*, *335*(6074), 1348–1351. https://doi.org/10.1126/science.1218094

Almagro Armenteros, J. J., Tsirigos, K. D., Sønderby, C. K., Petersen, T. N., Winther, O., Brunak, S., von Heijne, G., & Nielsen, H. (2019). SignalP 5.0 improves signal peptide predictions using deep neural networks. *Nature Biotechnology*, *37*(4), 420–423. https://doi.org/10.1038/s41587-019-0036-z

Andreo-Jimenez, B., Ruyter-Spira, C., Bouwmeester, H. J., & Lopez-Raez, J. A. (2015). Ecological relevance of strigolactones in nutrient uptake and other abiotic stresses, and in plant-microbe interactions below-ground. *Plant and Soil* (Vol. 394, Issues 1–2, pp. 1–19). https://doi.org/10.1007/s11104-015-2544-z

Arite, T., Iwata, H., Ohshima, K., Maekawa, M., Nakajima, M., Kojima, M., Sakakibara, H., & Kyozuka, J. (2007). DWARF10, an RMS1/MAX4/DAD1 ortholog, controls lateral bud outgrowth in rice. *Plant Journal*, *51*(6), 1019–1029. https://doi.org/10.1111/j.1365-313X.2007.03210.x

Arite, T., Umehara, M., Ishikawa, S., Hanada, A., Maekawa, M., Yamaguchi, S., & Kyozuka, J. (2009). D14, a strigolactone-Insensitive mutant of rice, shows an accelerated outgrowth of tillers. *Plant and Cell Physiology*, *50*(8), 1416–1424. https://doi.org/10.1093/pcp/pcp091

Bago, B., Azcon-Aguilar, C., Goulet, A., & Piche, Y. (1998). Branched absorbing structures (BAS): a feature of the extraradical mycelium of symbiotic arbuscular mycorrhizal fungi. *New Phytologist*, *139*(2), 375–388. https://doi.org/10.1046/j.1469-8137.1998.00199.x

Balzergue, C., Puech-Pagès, V., Bécard, G., & Rochange, S. F. (2011). The regulation of arbuscular mycorrhizal symbiosis by phosphate in pea involves early and systemic signalling events. *Journal of Experimental Botany*, *62*(3), 1049–1060. https://doi.org/10.1093/jxb/erq335

Banasiak, J., Borghi, L., Stec, N., Martinoia, E., & Jasiński, M. (2020). The full-size abcg transporter of M*edicago truncatula* is involved in strigolactone secretion, affecting arbuscular mycorrhiza. *Frontiers in Plant Science*, *11*, 18. https://doi.org/10.3389/fpls.2020.00018

Banasiak, J., Jamruszka, T., Murray, J. D., & Jasiński, M. (2021). A roadmap of plant membrane transporters in arbuscular mycorrhizal and legume–rhizobium symbioses. *Plant Physiology*. https://doi.org/10.1093/plphys/kiab280

Bao, Y. Z., Yao, Z. Q., Cao, X. L., Peng, J. F., Xu, Y., Chen, M. X., & Zhao, S. F. (2017). Transcriptome analysis of *Phelipanche* aegyptiaca seed germination mechanisms stimulated by fluridone, TIS108, and GR24. *PLoS ONE*, *12*(11). https://doi.org/10.1371/journal.pone.0187539

Barbier, F., Dun, E. A., Kerr, S. C., Chabikwa, T. G., & Beveridge, C. A. (2019). An update on the signals controlling shoot branching. *Trends in Plant Science* (Vol. 24, Issue 3, pp. 220–236). https://doi.org/10.1016/j.tplants.2018.12.001

Barea, J. M., & Azcón-Aguilar, C. (1982). Production of plant growth-regulating substances by the vesicular-arbuscular mycorrhizal fungus *Glomus mosseae* . *Applied and Environmental Microbiology*, *43*(4), 810–813. https://doi.org/10.1128/aem.43.4.810-813.1982

Barto, E. K., Hilker, M., Müller, F., Mohney, B. K., Weidenhamer, J. D., & Rillig, M. C. (2011). The fungal fast lane: Common mycorrhizal networks extend bioactive zones of allelochemicals in soils. *Plos One*, *6*(11), e27195. https://doi.org/10.1371/journal.pone.0027195

Bárzana, G., Aroca, R., Bienert, G. P., Chaumont, F., & Ruiz-Lozano, J. M. (2014). New insights into the regulation of aquaporins by the arbuscular mycorrhizal symbiosis in maize plants under drought stress and possible implications for plant performance. *Molecular Plant-Microbe Interactions*, *27*(4), 349–363. https://doi.org/10.1094/MPMI-09-13-0268-R

Bécard, G., & Fortin, J. A. (1988). Early events of vesicular–arbuscular mycorrhiza formation on Ri T-DNA transformed roots. *New Phytologist*, *108*(2), 211–218. https://doi.org/10.1111/j.1469-8137.1988.tb03698.x

Bécard, G., & Piché, Y. (1989). Fungal growth stimulation by co 2 and root exudates in vesicular-arbuscular mycorrhizal symbiosis . *Applied and Environmental Microbiology*, *55*(9), 2320–2325. https://doi.org/10.1128/aem.55.9.2320-2325.1989

Bécard, G., Taylor, L. P., Douds, D., Pfeffer, P. E., & Doner, L. W. (1995). Flavonoids are not necessary plant signal compounds in arbuscular mycorrhizal symbioses. *Molecular Plant-Microbe Interactions*, *8*(2), 252–258. https://doi.org/10.1094/MPMI-8-0252

Bedini, A., Mercy, L., Schneider, C., Franken, P., & Lucic-Mercy, E. (2018). Unraveling the initial plant hormone signaling, metabolic mechanisms and plant defense triggering the endomycorrhizal symbiosis behavior. *Frontiers in Plant Science* (Vol. 871, p. 1800). https://doi.org/10.3389/fpls.2018.01800

Belmondo, S., Marschall, R., Tudzynski, P., López Ráez, J. A., Artuso, E., Prandi, C., & Lanfranco, L. (2017). Identification of genes involved in fungal responses to strigolactones using mutants from fungal pathogens. *Current Genetics*, *63*(2), 201–213. https://doi.org/10.1007/s00294-016-0626-y

Bertheloot, J., Barbier, F., Boudon, F., Perez-Garcia, M. D., Péron, T., Citerne, S., Dun, E., Beveridge, C., Godin, C., & Sakr, S. (2020). Sugar availability suppresses the auxin-induced strigolactone pathway to promote bud outgrowth. *New Phytologist*, *225*(2), 866–879. https://doi.org/10.1111/nph.16201

Bertness, M. D., & Callaway, R. (1994). Positive interactions in communities. *Trends in Ecology and Evolution* (Vol. 9, Issue 5, pp. 191–193). https://doi.org/10.1016/0169-5347(94)90088-4

Besserer, A., Bécard, G., Jauneau, A., Roux, C., Séjalon-Delmas, N., Bécard, G., Jauneau, A., Roux, C., & Séjalon-Delmas, N. (2008). GR24, a synthetic analog of strigolactones, stimulates the mitosis and growth of the

arbuscular mycorrhizal fungus Gigaspora rosea by boosting its energy metabolism. *Plant Physiology*, *148*(1), 402–413. https://doi.org/10.1104/pp.108.121400

Besserer, A., Bécard, G., Roux, C., Séjalon-Delmas, N., Becard, G., Roux, C., & Séjalon-Delmas, N. (2009). Role of mitochondria in the response of arbuscular mycorrhizal fungi to strigolactones. *Plant Signaling and Behavior*, *4*(1), 75–77. https://doi.org/10.4161/psb.4.1.7419

Besserer, A., Puech-Pagès, V., Kiefer, P., Gomez-Roldan, V., Jauneau, A., Roy, S., Portais, J. C., Roux, C., Bécard, G., & Séjalon-Delmas, N. (2006). Strigolactones stimulate arbuscular mycorrhizal fungi by activating mitochondria. *Plos Biology*, *4*(7), 1239–1247. https://doi.org/10.1371/journal.pbio.0040226

Beveridge, C. A. (2006). Axillary bud outgrowth: Sending a message. *Current Opinion in Plant Biology* (Vol. 9, Issue 1, pp. 35–40). https://doi.org/10.1016/j.pbi.2005.11.006

Beveridge, C. A., Symons, G. M., Murfet, I. C., Ross, J. J., & Rameau, C. (1997). The *rms1* mutant of pea has elevated indole-3-acetic acid levels and reduced root-sap zeatin riboside content but increased branching controlled by graft-transmissible signal(s). *Plant Physiology*, *115*(3), 1251–1258. https://doi.org/10.1104/pp.115.3.1251

Beveridge, C. A., Symons, G. M., & Turnbull, C. G. N. (2000). Auxin inhibition of decapitation-induced branching is dependent on graft-transmissible signals regulated by genes *rms1* and *rms2*. *Plant Physiology*, *123*(2), 689–698. https://doi.org/10.1104/pp.123.2.689

Bhatt, M. D., & Bhatt, D. (2020). Strigolactones in overcoming environmental stresses. *Protective chemical agents in the amelioration of plant abiotic stress* (pp. 327–341). https://doi.org/10.1002/9781119552154.ch16

Biermann, B., & Linderman, R. G. (1983). Use of vesicular-arbuscular mycorrhizal roots, intraradical vesicles and extraradical vesicles as inoculum. *New Phytologist*, *95*(1), 97–105. https://doi.org/10.1111/j.1469-8137.1983.tb03472.x

Bilas, R. D., Bretman, A., & Bennett, T. (2021). Friends, neighbours and enemies: an overview of the communal and social biology of plants. *Plant, Cell & Environment*, *44*(4), 997–1013. https://doi.org/10.1111/pce.13965

Blilou, I., Ocampo, J. A., & García-Garrido, J. M. (2000). Induction of LTP (lipid transfer protein) and Pal (phenylalanine ammonia-lyase) gene expression in rice roots colonized by the arbuscular mycorrhizal fungus *Glomus mosseae*. *Journal of Experimental Botany*, *51*(353), 1969–1977. https://doi.org/10.1093/jexbot/51.353.1969

Boari, A., Ciasca, B., Pineda-Martos, R., Lattanzio, V. M., Yoneyama, K., & Vurro, M. (2016). Parasitic weed management by using strigolactone-degrading fungi. *Pest Management Science*, *72*(11), 2043–2047. https://doi.org/10.1002/ps.4226

Bonfante, P., & Genre, A. (2010). Mechanisms underlying beneficial plant - Fungus interactions in mycorrhizal symbiosis. *Nature Communications* (Vol. 1, Issue 4, pp. 1–11). https://doi.org/10.1038/ncomms1046

Booker, J., Auldridge, M., Wills, S., McCarty, D., Klee, H., & Leyser, O. (2004). MAX3/CCD7 is a carotenoid cleavage dioxygenase required for the synthesis of a novel plant signaling molecule. *Current Biology*, *14*(14), 1232–1238. https://doi.org/10.1016/j.cub.2004.06.061

Booker, J., Sieberer, T., Wright, W., Williamson, L., Willett, B., Stirnberg, P., Turnbull, C., Srinivasan, M., Goddard, P., & Leyser, O. (2005). MAX1 encodes a cytochrome P450 family member that acts downstream of MAX3/4 to produce a carotenoid-derived branch-inhibiting hormone. *Developmental Cell*, *8*(3), 443–449. https://doi.org/10.1016/j.devcel.2005.01.009

Borghi, L., Screpanti, C., Lumbroso, A., Lachia, M., Gübeli, C., & De Mesmaeker, A. (2021). Efficiency and bioavailability of new synthetic strigolactone mimics with potential for sustainable agronomical applications. *Plant and Soil*, *465*(1–2), 109–123. https://doi.org/10.1007/s11104-021-04943-8

Bouwmeester, H., Li, C., Thiombiano, B., Rahimi, M., & Dong, L. (2021). Adaptation of the parasitic plant lifecycle: Germination is controlled by essential host signaling molecules. *Plant Physiology* (Vol. 185, Issue

4, pp. 1292–1308). https://doi.org/10.1093/plphys/kiaa066

Boyer, F.-D., de Saint Germain, A., Pillot, J.-P., Pouvreau, J.-B., Chen, V. X., Ramos, S., Stévenin, A., Simier, P., Delavault, P., Beau, J.-M., & Rameau, C. (2012). Structure-activity relationship studies of strigolactone-related molecules for branching inhibition in garden pea: molecule design for shoot branching. *Plant Physiology*. https://doi.org/10.1104/pp.112.195826

Boyer, F.-D., de Saint Germain, A., Pouvreau, J. B., Clavé, G., Pillot, J. P., Roux, A., Rasmussen, A., Depuydt, S., Lauressergues, D., Frei Dit Frey, N., Heugebaert, T. S. A., Stevens, C. V., Geelen, D., Goormachtig, S., & Rameau, C. (2014). New strigolactone analogs as plant hormones with low activities in the rhizosphere. *Molecular Plant*, *7*(4), 675–690. https://doi.org/10.1093/mp/sst163

Breuillin-Sessoms, F., Floss, D. S., Gomez, S. K., Pumplin, N., Ding, Y., Levesque-Tremblay, V., Noar, R. D., Daniels, D. A., Bravo, A., Eaglesham, J. B., Benedito, V. A., Udvardi, M. K., & Harrison, M. J. (2015). Suppression of Arbuscule Degeneration in *Medicago truncatula phosphate transporter4* Mutants Is Dependent on the Ammonium Transporter 2 Family Protein AMT2;3. *The Plant Cell*, *27*(4), 1352–1366. https://doi.org/10.1105/tpc.114.131144

Brewer, P. B., Dun, E. A., Gui, R., Mason, M. G., & Beveridge, C. A. (2015). Strigolactone inhibition of branching independent of polar auxin transport. *Plant Physiology*, *168*(4), 1820–1829. https://doi.org/10.1104/pp.15.00014

Brewer, P. B., Yoneyama, K., Filardo, F., Meyers, E., Scaffidi, A., Frickey, T., Akiyama, K., Seto, Y., Dun, E. A., Cremer, J. E., Kerr, S. C., Waters, M. T., Flematti, G. R., Mason, M. G., Weiller, G., Yamaguchi, S., Nomura, T., Smith, S. M., Yoneyama, K., & Beveridge, C. A. (2016). Lateral branching oxidoreductase acts in the final stages of strigolactone biosynthesis in *Arabidopsis*. *Proceedings of the National Academy of Sciences of the United States of America*, *113*(22), 6301–6306. https://doi.org/10.1073/pnas.1601729113

Brooks, D. W., Bevinakatti, H. S., & Powell, D. R. (1985). The absolute structure of (+)-Strigol. *Journal of Organic Chemistry*, *50*(20), 3779–3781. https://doi.org/10.1021/jo00220a020

Brooks HB, Geeganage S, Kahl SD, Montrose C, Sittampalam S, Smith MC, Weidner JR (2012). Basics of Enzymatic Assays for HTS. Assay Guidance Manual [Internet]. Bethesda (MD): Eli Lilly & Company and the National Center for Advancing Translational Sciences; 2004–. PMID: 22553875.

Brundrett, M. C., Walker, C., Harper, C. J., & Krings, M. (2018). Fossils of arbuscular mycorrhizal fungi give insights into the history of a successful partnership with plants. *Transformative Paleobotany* (pp. 461–480). https://doi.org/10.1016/b978-0-12-813012-4.00019-x

Buée, M., Rossignol, M., Jauneau, A., Ranjeva, R., & Bécard, G. (2000). The pre-symbiotic growth of arbuscular mycorrhizal fungi is induced by a branching factor partially purified from plant root exudates. *MPMI* (Vol. 13, Issue 6).

Bunsick, M., Toh, S., Wong, C., Xu, Z., Ly, G., McErlean, C. S. P., Pescetto, G., Nemrish, K. E., Sung, P., Li, J. D., Scholes, J. D., & Lumba, S. (2020). SMAX1-dependent seed germination bypasses GA signalling in *Arabidopsis* and *Striga*. *Nature Plants*, *6*(6), 646–652. https://doi.org/10.1038/s41477-020-0653-z

Bürger, M., & Chory, J. (2020a). The many models of strigolactone signaling. *Trends in Plant Science* (Vol. 25, Issue 4, pp. 395–405). https://doi.org/10.1016/j.tplants.2019.12.009

Bürger, M., & Chory, J. (2020b). In-silico analysis of the strigolactone ligand-receptor system. *Plant Direct*, *4*(9), e00263. https://doi.org/10.1002/pld3.263

Bürger, M., Mashiguchi, K., Lee, H. J., Nakano, M., Takemoto, K., Seto, Y., Yamaguchi, S., & Chory, J. (2019). Structural basis of karrikin and non-natural strigolactone perception in *Physcomitrella patens*. *Cell Reports*, *26*(4), 855-865.e5. https://doi.org/10.1016/j.celrep.2019.01.003

Bythell-Douglas, R., Rothfels, C. J., Stevenson, D. W. D., Graham, S. W., Wong, G. K. S., Nelson, D. C., & Bennett, T. (2017). Evolution of strigolactone receptors by gradual neo-functionalization of KAI2 paralogues. *BMC Biology*, *15*(1), 52. https://doi.org/10.1186/s12915-017-0397-z

Calabrese, S., Pérez-Tienda, J., Ellerbeck, M., Arnould, C., Chatagnier, O., Boller, T., Schüßler, A., Brachmann, A.,

Wipf, D., Ferrol, N., & Courty, P. E. (2016). GintAMT3-a low-affinity ammonium transporter of the arbuscular mycorrhizal *Rhizophagus irregularis*. *Frontiers in Plant Science*, *7*(MAY2016). https://doi.org/10.3389/fpls.2016.00679

Carbonnel, S., Torabi, S., & Gutjahr, C. (2021). MAX2-independent transcriptional responses to rac-GR24 in Lotus japonicus roots. *Plant Signaling and Behavior*, *16*(1). https://doi.org/10.1080/15592324.2020.1840852

Carlsson, G. H., Hasse, D., Cardinale, F., Prandi, C., & Andersson, I. (2018). The elusive ligand complexes of the DWARF14 strigolactone receptor. *Journal of Experimental Botany*, *69*(9), 2345–2354. https://doi.org/10.1093/jxb/ery036

Casper, B. B., & Jackson, R. B. (1997). Plant competition underground. *Annual Review of Ecology and Systematics* (Vol. 28, pp. 545–570). https://doi.org/10.1146/annurev.ecolsys.28.1.545

Cavagnaro, T. R., Gao, L., Smith, F. A., & Smith, S. E. (2001). Morphology of arbuscular mycorrhizas is influenced by fungal identity. *New Phytologist*, *151*(2), 469–475. https://doi.org/10.1046/j.0028-646X.2001.00191.x

Chabaud, M., Genre, A., Sieberer, B. J., Faccio, A., Fournier, J., Novero, M., Barker, D. G., & Bonfante, P. (2011). Arbuscular mycorrhizal hyphopodia and germinated spore exudates trigger Ca^{2+} spiking in the legume and nonlegume root epidermis. *New Phytologist*, *189*(1), 347–355. https://doi.org/10.1111/j.1469-8137.2010.03464.x

Chabot, S., Bel-Rhlid, R., Chenevert, R., & Piche, Y. (1992). Hyphal growth promotion *in vitro* of the VA mycorrhizal fungus, *Gigaspora margarita* Becker & Hall, by the activity of structurally specific flavonoid compounds under CO2-enriched conditions. *New Phytologist*, *122*(3), 461–467. https://doi.org/10.1111/j.1469-8137.1992.tb00074.x

Chanclud, E., & Morel, J. B. (2016). Plant hormones: a fungal point of view. *Molecular plant pathology* (Vol. 17, Issue 8, pp. 1289–1297). https://doi.org/10.1111/mpp.12393

Chen, M., Arato, M., Borghi, L., Nouri, E., & Reinhardt, D. (2018). Beneficial services of arbuscular mycorrhizal fungi – from ecology to application. In *Frontiers in Plant Science* (Vol. 9). https://doi.org/10.3389/fpls.2018.01270

Cheng, S., Zou, Y. N., Kuča, K., Hashem, A., Abd-Allah, E. F., & Wu, Q. S. (2021). Elucidating the mechanisms underlying enhanced drought tolerance in plants mediated by arbuscular mycorrhizal fungi. *Frontiers in Microbiology* (Vol. 12, p. 4029). Https://doi.org/10.3389/fmicb.2021.809473

Chevalier, F., Nieminen, K., Sánchez-Ferrero, J. C., Rodríguez, M. L., Chagoyen, M., Hardtke, C. S., & Cubas, P. (2014). Strigolactone promotes degradation of DWARF14, an α/β hydrolase essential for strigolactone signaling in *Arabidopsis*. *Plant Cell*, *26*(3), 1134–1150. https://doi.org/10.1105/tpc.114.122903

Choi, J., Lee, T., Cho, J., Servante, E. K., Pucker, B., Summers, W., Bowden, S., Rahimi, M., An, K., An, G., Bouwmeester, H. J., Wallington, E. J., Oldroyd, G., & Paszkowski, U. (2020). The negative regulator SMAX1 controls mycorrhizal symbiosis and strigolactone biosynthesis in rice. *Nature Communications*, *11*(1), 2114. https://doi.org/10.1038/s41467-020-16021-1

Conn, C. E., Bythell-Douglas, R., Neumann, D., Yoshida, S., Whittington, B., Westwood, J. H., Shirasu, K., Bond, C. S., Dyer, K. A., & Nelson, D. C. (2015). Convergent evolution of strigolactone perception enabled host detection in parasitic plants. *Science*, *349*(6247), 540–543. https://doi.org/10.1126/science.aab1140

Conn, C. E., & Nelson, D. C. (2016). Evidence that KARRIKIN-INSENSITIVE2 (KAI2) receptors may perceive an unknown signal that is not karrikin or strigolactone. *Frontiers in Plant Science*, *6*(JAN2016). https://doi.org/10.3389/fpls.2015.01219

Cook, C. E., Whichard, L. P., Turner, B., Wall, M. E., & Egley, G. H. (1966). Germination of witchweed (*Striga* lutea lour.): Isolation and properties of a potent stimulant. *Science*, *154*(3753), 1189–1190. https://doi.org/10.1126/science.154.3753.1189

Cook, C. E., Whichard, L. P., Wall, M. E., Egley, G. H., Coggon, P., Luhan, P. A., & Mcphail, A. T. (1972). Germination Stimulants. II. The structure of strigol–a potent seed germination stimulant for witchweed

(*Striga* lutea Lour.)1,2. *Journal of the American Chemical Society*, *94*(17), 6198–6199. https://doi.org/10.1021/ja00772a048

Cosme, M., Ramireddy, E., Franken, P., Schmülling, T., & Wurst, S. (2016). Shoot- and root-borne cytokinin influences arbuscular mycorrhizal symbiosis. *Mycorrhiza*, *26*(7), 709–720. https://doi.org/10.1007/s00572-016-0706-3

Coudert, Y., Palubicki, W., Ljung, K., Novak, O., Leyser, O., & Jill Harrison, C. (2015). Three ancient hormonal cues co-ordinate shoot branching in a moss. *ELife*, *2015*(4). https://doi.org/10.7554/eLife.06808.001

Crepy, M. A., & Casal, J. J. (2015). Photoreceptor-mediated kin recognition in plants. *New Phytologist*, *205*(1), 329–338. https://doi.org/10.1111/nph.13040

Das, D., & Gutjahr, C. (2019). Role of phytohormones in arbuscular mycorrhiza development. *The Model Legume Medicago truncatula* (pp. 485–500). https://doi.org/10.1002/9781119409144.ch61

Das, M., Fernández-Aparicio, M., Yang, Z., Huang, K., Wickett, N. J., Alford, S., Wafula, E. K., DePamphilis, C., Bouwmeester, H., Timko, M. P., Yoder, J. I., & Westwood, J. H. (2015). Parasitic plants *striga* and *phelipanche* dependent upon exogenous strigolactones for germination have retained genes for strigolactone biosynthesis. *American Journal of Plant Sciences*, *06*(08), 1151–1166. https://doi.org/10.4236/ajps.2015.68120

Davière, J. M., & Achard, P. (2013). Gibberellin signaling in plants. *Development (Cambridge)*, *140*(6), 1147–1151. https://doi.org/10.1242/dev.087650

De Cuyper, C., Fromentin, J., Yocgo, R. E., De Keyser, A., Guillotin, B., Kunert, K., Boyer, F.-D., & Goormachtig, S. (2015). From lateral root density to nodule number, the strigolactone analogue GR24 shapes the root architecture of *Medicago truncatula*. *Journal of Experimental Botany*, *66*(1), 137–146. https://doi.org/10.1093/jxb/eru404

De Cuyper, C., Struk, S., Braem, L., Gevaert, K., De Jaeger, G., & Goormachtig, S. (2017). Strigolactones, karrikins and beyond. *Plant, Cell & Environment*, *40*(9), 1691–1703. https://doi.org/10.1111/pce.12996

de Saint Germain, A., Clavé, G., Badet-Denisot, M. A., Pillot, J. P., Cornu, D., Le Caer, J. P., Burger, M., Pelissier, F., Retailleau, P., Turnbull, C., Bonhomme, S., Chory, J., Rameau, C., & Boyer, F. D. (2016). An histidine covalent receptor and butenolide complex mediates strigolactone perception. *Nature Chemical Biology*, *12*(10), 787–794. https://doi.org/10.1038/nchembio.2147

de Saint Germain, A., Jacobs, A., Brun, G., Pouvreau, J. B., Braem, L., Cornu, D., Clavé, G., Baudu, E., Steinmetz, V., Servajean, V., Wicke, S., Gevaert, K., Simier, P., Goormachtig, S., Delavault, P., & Boyer, F. D. (2021). A *Phelipanche ramosa* KAI2 protein perceives strigolactones and isothiocyanates enzymatically. *Plant Communications*, *2*(5), 100166. https://doi.org/10.1016/j.xplc.2021.100166

de Saint Germain, A., Ligerot, Y., Dun, E. A., Pillot, J. P., Ross, J. J., Beveridge, C. A., & Rameau, C. (2013). Strigolactones stimulate internode elongation independently of gibberellins. *Plant Physiology*, *163*(2), 1012–1025. https://doi.org/10.1104/pp.113.220541

de Saint Germain, A., Retailleau, P., Norsikian, S., Servajean, V., Pelissier, F., Steinmetz, V., Pillot, J. P., Rochange, S., Pouvreau, J. B., & Boyer, F. D. (2019). Contalactone, a contaminant formed during chemical synthesis of the strigolactone reference GR24 is also a strigolactone mimic. *Phytochemistry*, *168*, 112112. https://doi.org/10.1016/j.phytochem.2019.112112

Decker, E. L., Alder, A., Hunn, S., Ferguson, J., Lehtonen, M. T., Scheler, B., Kerres, K. L., Wiedemann, G., Safavi-Rizi, V., Nordzieke, S., Balakrishna, A., Baz, L., Avalos, J., Valkonen, J. P. T., Reski, R., & Al-Babili, S. (2017). Strigolactone biosynthesis is evolutionarily conserved, regulated by phosphate starvation and contributes to resistance against phytopathogenic fungi in a moss, *Physcomitrella patens*. *New Phytologist*, *216*(2), 455–468. https://doi.org/10.1111/nph.14506

Delaux, P.-M., Radhakrishnan, G. V., Jayaraman, D., Cheema, J., Malbreil, M., Volkening, J. D., Sekimoto, H., Nishiyama, T., Melkonian, M., Pokorny, L., Rothfels, C. J., Sederoff, H. W., Stevenson, D. W., Surek, B., Zhang, Y., Sussman, M. R., Dunand, C., Morris, R. J., Roux, C., … Ane, J. M. (2015). Algal ancestor of land plants was preadapted for symbiosis. *Proc. Natl Acad. Sci. USA*, *112*(43), 13390–13395.

https://doi.org/10.1073/pnas.1515426112

Delaux, P.-M., Xie, X., Timme, R. E., Puech-Pages, V., Dunand, C., Lecompte, E., Delwiche, C. F., Yoneyama, K., Bécard, G., & Séjalon-Delmas, N. (2012). Origin of strigolactones in the green lineage. *New Phytologist*, *195*(4), 857–871. https://doi.org/10.1111/j.1469-8137.2012.04209.x

Dudley, S. A., & File, A. L. (2007). Kin recognition in an annual plant. *Biology Letters*, *3*(4), 435–438. https://doi.org/10.1098/rsbl.2007.0232

Dutra, P. V., Abad, M., Almela, V., & Agustí, M. (1996). Auxin interaction with the vesicular-arbuscular mycorrhizal fungus *Glomus intraradices* Schenck and Smith improves vegetative growth of two citrus rootstocks. *Scientia Horticulturae*, *66*(1–2), 77–83. https://doi.org/10.1016/0304-4238(96)00887-4

Egamberdieva, D., Wirth, S. J., Alqarawi, A. A., Abd-Allah, E. F., & Hashem, A. (2017). Phytohormones and beneficial microbes: Essential components for plants to balance stress and fitness. *Frontiers in Microbiology* (Vol. 8, Issue OCT, p. 2104). https://doi.org/10.3389/fmicb.2017.02104

Elias, K. S., & Safir, G. R. (1987). Hyphal elongation of *Glomus fasciculatus* in response to root exudates . *Applied and Environmental Microbiology*, *53*(8), 1928–1933. https://doi.org/10.1128/aem.53.8.1928-1933.1987

Engelmoer, D. J. P., Behm, J. E., & Toby Kiers, E. (2014). Intense competition between arbuscular mycorrhizal mutualists in an *in vitro* root microbiome negatively affects total fungal abundance. *Molecular Ecology*, *23*(6), 1584–1593. https://doi.org/10.1111/mec.12451

Esch, H., Hundeshagen, B., Schneider-Poetsch, H., & Bothe, H. (1994). Demonstration of abscisic acid in spores and hyphae of the arbuscular-mycorrhizal fungus Glomus and in the N2-fixing cyanobacterium Anabaena variabilis. *Plant Science*, *99*(1), 9–16. https://doi.org/10.1016/0168-9452(94)90115-5

Etemadi, M., Gutjahr, C., Couzigou, J. M., Zouine, M., Lauressergues, D., Timmers, A., Audran, C., Bouzayen, M., Bécard, G., & Combier, J. P. (2014). Auxin perception is required for arbuscule development in arbuscular mycorrhizal symbiosis. *Plant Physiology*, *166*(1), 281–292. https://doi.org/10.1104/pp.114.246595

Feng, F., Sun, J., Radhakrishnan, G. V., Lee, T., Bozsóki, Z., Fort, S., Gavrin, A., Gysel, K., Thygesen, M. B., Andersen, K. R., Radutoiu, S., Stougaard, J., & Oldroyd, G. E. D. (2019). A combination of chitooligosaccharide and lipochitooligosaccharide recognition promotes arbuscular mycorrhizal associations in *Medicago truncatula*. *Nature Communications*, *10*(1), 1–12. https://doi.org/10.1038/s41467-019-12999-5

Fernández-Aparicio, M., Yoneyama, K., & Rubiales, D. (2011). The role of strigolactones in host specificity of *Orobanche* and *Phelipanche* seed germination. *Seed Science Research*, *21*(1), 55–61. https://doi.org/10.1017/S0960258510000371

Fiorilli, V., Forgia, M., de Saint Germain, A., D'Arrigo, G., Cornu, D., Le Bris, P., Al-Babili, S., Cardinale, F., Prandi, C., Spyrakis, F., Boyer, F., Turina, M., & Lanfranco, L. (2022). A structural homologue of the plant receptor D14 mediates responses to strigolactones in the fungal phytopathogen *Cryphonectria parasitica*. *New Phytologist*. https://doi.org/10.1111/nph.18013

Fiorilli, V., Vallino, M., Biselli, C., Faccio, A., Bagnaresi, P., & Bonfante, P. (2015). Host and non-host roots in rice: cellular and molecular approaches reveal differential responses to arbuscular mycorrhizal fungi. *Frontiers in Plant Science*, *6*(AUG), 636. https://doi.org/10.3389/fpls.2015.00636

Flematti, G. R., Ghisalberti, E. L., Dixon, K. W., & Trengove, R. D. (2004). A compound from smoke that promotes seed germination. *Science*, *305*(5686), 977. https://doi.org/10.1126/science.1099944

Foo, E. (2013). Something old, something new: Auxin and strigolactone interact in the ancient mycorrhizal symbiosis. *Plant Signaling and Behavior*, *8*(4). https://doi.org/10.4161/psb.23656

Foo, E., & Davies, N. W. (2011). Strigolactones promote nodulation in pea. *Planta*, *234*(5), 1073–1081. https://doi.org/10.1007/s00425-011-1516-7

Foo, E., Ross, J., Jones, W. T., & Reid, J. B. (2013). Plant hormones in arbuscular mycorrhizal symbioses: an

emerging role for gibberellins. *Annals of Botany*, *111*(5), 769–779. https://doi.org/10.1093/aob/mct041

Foo, E., Turnbull, C. G. N., & Beveridge, C. A. (2001). Long-distance signaling and the control of branching in the *rms1* mutant of Pea. *Plant Physiology*, *126*(1), 203–209. https://doi.org/10.1104/pp.126.1.203

Foo, E., Yoneyama, K., Hugill, C. J., Quittenden, L. J., & Reid, J. B. (2013). Strigolactones and the regulation of pea symbioses in response to nitrate and phosphate deficiency. *Molecular Plant*, *6*(1), 76–87. https://doi.org/10.1093/mp/sss115

Fukui, K., Ito, S., Ueno, K., Yamaguchi, S., Kyozuka, J., & Asami, T. (2011). New branching inhibitors and their potential as strigolactone mimics in rice. *Bioorganic and Medicinal Chemistry Letters*, *21*(16), 4905–4908. https://doi.org/10.1016/j.bmcl.2011.06.019

Gamir, J., Torres-Vera, R., Rial, C., Berrio, E., Souza Campos, P. M., Varela, R. M., Macías, F. A., Pozo, M. J., Flors, V., & López-Ráez, J. A. (2020). Exogenous strigolactones impact metabolic profiles and phosphate starvation signalling in roots. *Plant, Cell & Environment*, *43*(7), 1655–1668. https://doi.org/10.1111/pce.13760

Garcia, K., Doidy, J., Zimmermann, S. D., Wipf, D., & Courty, P. E. (2016). Take a Trip Through the Plant and Fungal Transportome of Mycorrhiza. In *Trends in Plant Science* (Vol. 21, Issue 11, pp. 937–950). https://doi.org/10.1016/j.tplants.2016.07.010

Genre, A., Chabaud, M., Balzergue, C., Puech-Pagès, V., Novero, M., Rey, T., Fournier, J., Rochange, S., Bécard, G., Bonfante, P., & Barker, D. G. (2013). Short-chain chitin oligomers from arbuscular mycorrhizal fungi trigger nuclear Ca2+ spiking in *Medicago truncatula* roots and their production is enhanced by strigolactone. *New Phytologist*, *198*(1), 190–202. https://doi.org/10.1111/nph.12146

Genre, A., Chabaud, M., Faccio, A., Barker, D. G., & Bonfante, P. (2008). Prepenetration apparatus assembly precedes and predicts the colonization patterns of arbuscular mycorrhizal fungi within the root cortex of both *Medicago truncatula* and Daucus carota. *Plant Cell*, *20*(5), 1407–1420. https://doi.org/10.1105/tpc.108.059014

Genre, A., Chabaud, M., Timmers, T., Bonfante, P., & Barker, D. G. (2005). Arbuscular mycorrhizal fungi elicit a novel intracellular apparatus in *Medicago truncatula* root epidermal cells before infection. *Plant Cell*, *17*(12), 3489–3499. https://doi.org/10.1105/tpc.105.035410

Gholamhoseini, M., Ghalavand, A., Dolatabadian, A., Jamshidi, E., & Khodaei-Joghan, A. (2013). Effects of arbuscular mycorrhizal inoculation on growth, yield, nutrient uptake and irrigation water productivity of sunflowers grown under drought stress. *Agricultural Water Management*, *117*, 106–114. https://doi.org/10.1016/j.agwat.2012.11.007

Gilbert, L., & Johnson, D. (2017). Plant–plant communication through common mycorrhizal networks. *Advances in Botanical Research*, *82*, 83–97. https://doi.org/10.1016/bs.abr.2016.09.001

Giovannetti, M. (2000). Spore germination and pre-symbiotic mycelial growth. In *Arbuscular Mycorrhizas: Physiology and Function* (pp. 47–68). https://doi.org/10.1007/978-94-017-0776-3_3

Giovannetti, M., Azzolini, D., & Citernesi, A. S. (1999). Anastomosis formation and nuclear and protoplasmic exchange in arbuscular mycorrhizal fungi. *Applied and Environmental Microbiology*, *65*(12), 5571–5575. https://doi.org/10.1128/aem.65.12.5571-5575.1999

Giovannetti, M., Fortuna, P., Citernesi, A. S., Morini, S., & Nuti, M. P. (2001). The occurrence of anastomosis formation and nuclear exchange in intact arbuscular mycorrhizal networks. *New Phytologist*, *151*(3), 717–724. https://doi.org/10.1046/j.0028-646x.2001.00216.x

Giovannetti, Sbrana, C., Avio, L., Citernesi, A. S., & Logi, C. (1993). Differential hyphal morphogenesis in arbuscular mycorrhizal fungi during pre-infection stages. *New Phytologist*, *125*(3), 587–593. https://doi.org/10.1111/j.1469-8137.1993.tb03907.x

Goldwasser, Y., Yoneyama, K., Xie, X., & Yoneyama, K. (2008). Production of strigolactones by *Arabidopsis* thaliana responsible for Orobanche aegyptiaca seed germination. *Plant Growth Regulation*, *55*(1), 21–28. https://doi.org/10.1007/s10725-008-9253-z

Gomez-Roldan, V., Fermas, S., Brewer, P. B., Puech-Pagès, V., Dun, E. A., Pillot, J. P., Letisse, F., Matusova, R., Danoun, S., Portais, J. C., Bouwmeester, H., Bécard, G., Beveridge, C. A., Rameau, C., & Rochange, S. (2008). Strigolactone inhibition of shoot branching. *Nature*, *455*(7210), 189–194. https://doi.org/10.1038/nature07271

Guether, M., Neuhäuser, B., Balestrini, R., Dynowski, M., Ludewig, U., Bonfante, P., Neuhäuser, B., Balestrini, R., Dynowski, M., Ludewig, U., & Bonfante, P. (2009). A mycorrhizal-specific ammonium transporter from lotus japonicus acquires nitrogen released by Arbuscular Mycorrhizal Fungi. *Plant Physiology*, *150*(1), 73–83. https://doi.org/10.1104/pp.109.136390

Guillory, A., & Bonhomme, S. (2021). Phytohormone biosynthesis and signaling pathways of mosses. *Plant Molecular Biology*, 1–33. https://doi.org/10.1007/s11103-021-01172-6

Guillotin, B., Etemadi, M., Audran, C., Bouzayen, M., Bécard, G., & Combier, J. P. (2017). Sl-IAA27 regulates strigolactone biosynthesis and mycorrhization in tomato (var. MicroTom). *New Phytologist*, *213*(3), 1124–1132. https://doi.org/10.1111/nph.14246

Guo, Y., Zheng, Z., La Clair, J. J., Chory, J., & Noel, J. P. (2013). Smoke-derived karrikin perception by the α/β-hydrolase KAI2 from *Arabidopsis*. *Proceedings of the National Academy of Sciences of the United States of America*, *110*(20), 8284–8289. https://doi.org/10.1073/pnas.1306265110

Gutjahr, C., Gobbato, E., Choi, J., Riemann, M., Johnston, M. G., Summers, W., Carbonnel, S., Mansfield, C., Yang, S. Y., Nadal, M., Acosta, I., Takano, M., Jiao, W. B., Schneeberger, K., Kelly, K. A., & Paszkowski, U. (2015). Rice perception of symbiotic arbuscular mycorrhizal fungi requires the karrikin receptor complex. *Science*, *350*(6267), 1521–1524. https://doi.org/10.1126/science.aac9715

Gutjahr, C., Sawers, R. J. H., Marti, G., Andrés-Hernández, L., Yang, S. Y., Casieri, L., Angliker, H., Oakeley, E. J., Wolfender, J. L., Abreu-Goodger, C., & Paszkowski, U. (2015). Transcriptome diversity among rice root types during asymbiosis and interaction with arbuscular mycorrhizal fungi. *Proceedings of the National Academy of Sciences of the United States of America*, *112*(21), 6754–6759. https://doi.org/10.1073/pnas.1504142112

Haider, I., Andreo-Jimenez, B., Bruno, M., Bimbo, A., Floková, K., Abuauf, H., Ntui, V. O., Guo, X., Charnikhova, T., Al-Babili, S., Bouwmeester, H. J., & Ruyter-Spira1, C. (2018). The interaction of strigolactones with abscisic acid during the drought response in rice. *Journal of Experimental Botany*, *69*(9), 2403–2414. https://doi.org/10.1093/jxb/ery089

Hamiaux, C., Drummond, R. S. M., Janssen, B. J., Ledger, S. E., Cooney, J. M., Newcomb, R. D., & Snowden, K. C. (2012). DAD2 is an α/β hydrolase likely to be involved in the perception of the plant branching hormone, strigolactone. *Current Biology*, *22*(21), 2032–2036. https://doi.org/10.1016/j.cub.2012.08.007

Hamiaux, C., Drummond, R. S. M., Luo, Z., Lee, H. W., Sharma, P., Janssen, B. J., Perry, N. B., Denny, W. A., & Snowden, K. C. (2018). Inhibition of strigolactone receptors by N-phenylanthranilic acid derivatives: Structural and functional insights. *Journal of Biological Chemistry*, *293*(17), 6530–6543. https://doi.org/10.1074/jbc.RA117.001154

Hamiaux, C., Janssen, B.J., Snowden, K.C. (2021). The Use of Differential Scanning Fluorimetry to Assess Strigolactone Receptor Function. Strigolactones. Methods in Molecular Biology, vol 2309. https://doi.org/10.1007/978-1-0716-1429-7_18

Harrison, M. J. (2012). Cellular programs for arbuscular mycorrhizal symbiosis. *Current Opinion in Plant Biology* (Vol. 15, Issue 6, pp. 691–698). https://doi.org/10.1016/j.pbi.2012.08.010

Harrison, M. J., Dewbre, G. R., & Liu, J. (2002). A phosphate transporter from *Medicago truncatula* involved in the acquisition of phosphate released by arbuscular mycorrhizal fungi. *Plant Cell*, *14*(10), 2413–2429. https://doi.org/10.1105/tpc.004861

Hauck, C., Müller, S., & Schildknecht, H. (1992). A Germination Stimulant for Parasitic Flowering Plants from Sorghum bicolor, a Genuine Host Plant. *Journal of Plant Physiology*, *139*(4), 474–478. https://doi.org/10.1016/S0176-1617(11)80497-9

Hedden, P., & Sponsel, V. (2015). A Century of Gibberellin Research. In *Journal of Plant Growth Regulation* (Vol.

34, Issue 4, pp. 740–760). https://doi.org/10.1007/s00344-015-9546-1

Heide-Jørgensen, H. S. (2008). Parasitic flowering plants. In *Parasitic Flowering Plants*. Brill. https://doi.org/10.1163/ej.9789004167506.i-438

Helber, N., Wippel, K., Sauer, N., Schaarschmidt, S., Hause, B., & Requena, N. (2011). a versatile monosaccharide transporter that operates in the arbuscular mycorrhizal fungus *Glomus* sp Is crucial for the symbiotic relationship with plants . *The Plant Cell*, *23*(10), 3812–3823. https://doi.org/10.1105/tpc.111.089813

Hérivaux, A., De Bernonville, T. D., Roux, C., Clastre, M., Courdavault, V., Gastebois, A., Bouchara, J. P., James, T. Y., Latgé, J. P., Martin, F., & Papon, N. (2017). The identification of phytohormone receptor homologs in early diverging fungi suggests a role for plant sensing in land colonization by fungi. *MBio*, *8*(1). https://doi.org/10.1128/mBio.01739-16

Ho-Plágaro, T., Morcillo, R. J. L., Tamayo-Navarrete, M. I., Huertas, R., Molinero-Rosales, N., López-Ráez, J. A., Macho, A. P., & García-Garrido, J. M. (2021). DLK2 regulates arbuscule hyphal branching during arbuscular mycorrhizal symbiosis. *New Phytologist*, *229*(1), 548–562. https://doi.org/10.1111/nph.16938

Hoffmann, B., Proust, H., Belcram, K., Labrune, C., Boyer, F. D., Rameau, C., & Bonhomme, S. (2014). Strigolactones inhibit caulonema elongation and cell division in the moss *Physcomitrella patens*. *Plos One*, *9*(6). https://doi.org/10.1371/journal.pone.0099206

Hohnjec, N., Czaja-Hasse, L. F., Hogekamp, C., & Küster, H. (2015). Pre-announcement of symbiotic guests: Transcriptional reprogramming by mycorrhizal lipochitooligosaccharides shows a strict co-dependency on the GRAS transcription factors NSP1 and RAM1. *BMC Genomics*, *16*(1), 994. https://doi.org/10.1186/s12864-015-2224-7

Holmquist, M. (2005). Alpha beta-hydrolase fold enzymes structures, functions and mechanisms. *Current Protein and Peptide Science*, *1*(2), 209–235. https://doi.org/10.2174/1389203003381405

Hong, J., Park, Y. S., Bravo, A., Bhattarai, K. K., Daniels, D. A., & Harrison, M. J. (2012). Diversity of morphology and function in arbuscular mycorrhizal symbioses in Brachypodium distachyon. *Planta*, *236*(3), 851–865. https://doi.org/10.1007/s00425-012-1677-z

Hosford, R. M. (1967). Transmission of plant viruses by dodder. *The Botanical Review*, *33*(4), 387–406. https://doi.org/10.1007/BF02858742

Hosny, M., Gianinazzi-Pearson, V., & Dulieu, H. (1998). Nuclear DNA content of 11 fungal species in Glomales. *Genome*, *41*(3), 422–428. https://doi.org/10.1139/g98-038

Hull, R., Choi, J., & Paszkowski, U. (2021). Conditioning plants for arbuscular mycorrhizal symbiosis through DWARF14-LIKE signalling. *Current opinion in plant biology* (Vol. 62, p. 102071). https://doi.org/10.1016/j.pbi.2021.102071

Humphreys, C. P. C., Franks, P. J., Rees, M., Bidartondo, M. I., Leake, J. R., & Beerling, D. J. (2010). Mutualistic mycorrhiza-like symbiosis in the most ancient group of land plants. *Nature Communications*, *1*(8). https://doi.org/10.1038/ncomms1105

Ishii, T., Shrestha, Y. H., Matsumoto, I., & Kadoya, K. (1996). Effect of ethylene on the growth of vesicular-arbuscular mycorrhizal fungi and on the mycorrhizal formation of trifoliate orange roots. *Journal of the Japanese Society for Horticultural Science*, *65*(3), 525–529. https://doi.org/10.2503/jjshs.65.525

Ishikawa, S., Maekawa, M., Arite, T., Onishi, K., Takamure, I., & Kyozuka, J. (2005). Suppression of tiller bud activity in tillering dwarf mutants of rice. *Plant and Cell Physiology*, *46*(1), 79–86. https://doi.org/10.1093/pcp/pci022

Ito, S., Yamagami, D., Umehara, M., Hanada, A., Yoshida, S., Sasaki, Y., Yajima, S., Kyozuka, J., Ueguchi-Tanaka, M., Matsuoka, M., Shirasu, K., Yamaguchi, S., & Asami, T. (2017). Regulation of strigolactone biosynthesis by gibberellin signaling. *Plant Physiology*, *174*(2), 1250–1259. https://doi.org/10.1104/pp.17.00301

Janssen, B. J., & Snowden, K. C. (2012). Strigolactone and karrikin signal perception: Receptors, enzymes, or

both. In *Frontiers in Plant Science* (Vol. 3, Issue DEC, p. 296). Frontiers Research Foundation. https://doi.org/10.3389/fpls.2012.00296

Jany, J. L., & Pawlowska, T. E. (2010). Multinucleate spores contribute to evolutionary longevity of asexual glomeromycota. *American Naturalist*, *175*(4), 424–435. https://doi.org/10.1086/650725

Javot, H., Penmetsa, R. V., Breuillin, F., Bhattarai, K. K., Noar, R. D., Gomez, S. K., Zhang, Q., Cook, D. R., & Harrison, M. J. (2011). *Medicago truncatula* mtpt4 mutants reveal a role for nitrogen in the regulation of arbuscule degeneration in arbuscular mycorrhizal symbiosis. *Plant Journal*, *68*(6), 954–965. https://doi.org/10.1111/j.1365-313X.2011.04746.x

Jia, K.-P., Li, C., Bouwmeester, H. J., & Al-Babili, S. (2019). Strigolactone biosynthesis and signal transduction. *Strigolactones - Biology and Applications* (pp. 1–45). https://doi.org/10.1007/978-3-030-12153-2_1

Jia, K. P., Baz, L., & Al-Babili, S. (2018). From carotenoids to strigolactones. *Journal of Experimental Botany* (Vol. 69, Issue 9, pp. 2189–2204). https://doi.org/10.1093/jxb/erx476

Jiang, Liu, X., Xiong, G., Liu, H., Chen, F., Wang, L., Meng, X., Liu, G., Yu, H., Yuan, Y., Yi, W., Zhao, L., Ma, H., He, Y., Wu, Z., Melcher, K., Qian, Q., Xu, H. E., Wang, Y., & Li, J. (2013). DWARF 53 acts as a repressor of strigolactone signalling in rice. *Nature*, *504*(7480), 401–405. https://doi.org/10.1038/nature12870

Jiang, Y., Wang, W., Xie, Q., Liu, N., Liu, L., Wang, D., Zhang, X., Yang, C., Chen, X., Tang, D., & Wang, E. (2017). Plants transfer lipids to sustain colonization by mutualistic mycorrhizal and parasitic fungi. *Science*, *356*(6343), 1172–1173. https://doi.org/10.1126/science.aam9970

Joel, D. M., Gressel, J., & Musselman, L. J. (2013). Parasitic Orobanchaceae: Parasitic mechanisms and control strategies. *Parasitic Orobanchaceae: Parasitic Mechanisms and Control Strategies* (Vol. 9783642381461). https://doi.org/10.1007/978-3-642-38146-1

Johnson, X., Brcich, T., Dun, E. A., Goussot, M., Haurogné, K., Beveridge, C. A., & Rameau, C. (2006). Branching genes are conserved across species. genes controlling a novel signal in pea are coregulated by other long-distance signals. *Plant Physiology*, *142*(3), 1014–1026. https://doi.org/10.1104/pp.106.087676

Kagiyama, M., Hirano, Y., Mori, T., Kim, S.-Y., Kyozuka, J., Seto, Y., Yamaguchi, S., & Hakoshima, T. (2013). Structures of D14 and D14L in the strigolactone and karrikin signaling pathways. *Genes to Cells*, *18*(2), 147–160. https://doi.org/10.1111/gtc.12025

Kamel, L., Keller-Pearson, M., Roux, C., & Ané, J. (2017). Biology and evolution of arbuscular mycorrhizal symbiosis in the light of genomics. *New Phytologist*, *213*(2), 531–536. https://doi.org/10.1111/nph.14263

Kamel, L., Tang, N., Malbreil, M., San Clemente, H., Le Marquer, M., Roux, C., & dit Frey, N. F. (2017). The comparison of expressed candidate secreted proteins from two arbuscular mycorrhizal fungi unravels common and specific molecular tools to invade different host plants. *Frontiers in Plant Science*, *8*(FEBRUARY), 124. https://doi.org/10.3389/fpls.2017.00124

Kameoka, H., & Kyozuka, J. (2018). Spatial regulation of strigolactone function. *Journal of Experimental Botany*, *69*(9), 2255–2264. https://doi.org/10.1093/jxb/erx434

Kameoka, H., Tsutsui, I., Saito, K., Kikuchi, Y., Handa, Y., Ezawa, T., Hayashi, H., Kawaguchi, M., & Akiyama, K. (2019). Stimulation of asymbiotic sporulation in arbuscular mycorrhizal fungi by fatty acids. *Nature Microbiology* (Vol. 4, Issue 10, pp. 1654–1660). https://doi.org/10.1038/s41564-019-0485-7

Kerr, S. C., Patil, S., de Saint Germain, A., Pillot, J., Saffar, J., Ligerot, Y., Aubert, G., Citerne, S., Bellec, Y., Dun, E. A., Beveridge, C. A., & Rameau, C. (2021). Integration of the SMXL/D53 strigolactone signalling repressors in the model of shoot branching regulation in *Pisum sativum*. *The Plant Journal*, tpj.15415. https://doi.org/10.1111/tpj.15415

Keymer, A., Pimprikar, P., Wewer, V., Huber, C., Brands, M., Bucerius, S. L., Delaux, P. M., Klingl, V., von Röpenack-Lahaye, E., Wang, T. L., Eisenreich, W., Dörmann, P., Parniske, M., & Gutjahr, C. (2017). Lipid transfer from plants to arbuscular mycorrhiza fungi. *ELife*, *6*, e29107. https://doi.org/10.7554/eLife.29107

Kim, G., LeBlanc, M. L., Wafula, E. K., DePamphilis, C. W., & Westwood, J. H. (2014). Genomic-scale exchange of mRNA between a parasitic plant and its hosts. *Science*, *345*(6198), 808–811. https://doi.org/10.1126/science.1253122

Kitani, S., Miyamoto, K. T., Takamatsu, S., Herawati, E., Iguchi, H., Nishitomi, K., Uchida, M., Nagamitsu, T., Omura, S., Ikeda, H., & Nihira, T. (2011). Avenolide, a Streptomyces hormone controlling antibiotic production in Streptomyces avermitilis. *Proceedings of the National Academy of Sciences of the United States of America*, *108*(39), 16410–16415. https://doi.org/10.1073/pnas.1113908108

Klapper, M., Schlabach, K., Paschold, A., Zhang, S., Chowdhury, S., Menzel, K. D., Rosenbaum, M. A., & Stallforth, P. (2020). Biosynthesis of *Pseudomonas*-derived butenolides. *Angewandte Chemie - International Edition*, *59*(14), 5607–5610. https://doi.org/10.1002/anie.201914154

Klironomos, J., McCune, J., Hart, M., & Neville, J. (2000). The influence of arbuscular mycorrhizae on the relationship between plant diversity and productivity. *Ecology Letters*, *3*(2), 137–141. https://doi.org/10.1046/j.1461-0248.2000.00131.x

Klironomos, J. N., & Hart, M. M. (2002). Colonization of roots by arbuscular mycorrhizal fungi using different sources of inoculum. *Mycorrhiza*, *12*(4), 181–184. https://doi.org/10.1007/s00572-002-0169-6

Kobae, Y. (2019). The infection unit: an overlooked conceptual unit for arbuscular mycorrhizal function. *Root Biology - Growth, Physiology, and Functions*. https://doi.org/10.5772/intechopen.86996

Kobae, Y., & Hata, S. (2010). Dynamics of periarbuscular membranes visualized with a fluorescent phosphate transporter in arbuscular mycorrhizal roots of rice. *Plant and Cell Physiology*, *51*(3), 341–353. https://doi.org/10.1093/pcp/pcq013

Kobae, Y., Kameoka, H., Sugimura, Y., Saito, K., Ohtomo, R., Fujiwara, T., & Kyozuka, J. (2018). Strigolactone biosynthesis genes of rice are required for the punctual entry of arbuscular mycorrhizal fungi into the roots. *Plant and Cell Physiology*, *59*(3), 544–553.

Kobae, Y., Tamura, Y., Takai, S., Banba, M., & Hata, S. (2010). Localized expression of arbuscular mycorrhiza-inducible ammonium transporters in soybean. *Plant and Cell Physiology*, *51*(9), 1411–1415. https://doi.org/10.1093/pcp/pcq099

Kodama, K., Rich, M. K., Yoda, A., Shimazaki, S., Xie, X., Akiyama, K., Mizuno, Y., Komatsu, A., Luo, Y., Suzuki, H., Kameoka, H., Libourel, C., Keller, J., Sakakibara, K., Nishiyama, T., Nakagawa, T., Mashiguchi, K., Uchida, K., Yoneyama, K., … Kyozuka, J. (2021). An ancestral function of strigolactones as symbiotic rhizosphere signals. *BioRxiv*, 2021.08.20.457034. https://doi.org/10.1101/2021.08.20.457034

Kohlen, W., Charnikhova, T., Liu, Q., Bours, R., Domagalska, M. A., Beguerie, S., Verstappen, F., Leyser, O., Bouwmeester, H., & Ruyter-Spira, C. (2011). Strigolactones are transported through the xylem and play a key role in shoot architectural response to phosphate deficiency in nonarbuscular mycorrhizal host *Arabidopsis*. *Plant Physiology*, *155*(2), 974–987. https://doi.org/10.1104/pp.110.164640

Kojima, M., Kamada-Nobusada, T., Komatsu, H., Takei, K., Kuroha, T., Mizutani, M., Ashikari, M., Ueguchi-Tanaka, M., Matsuoka, M., Suzuki, K., & Sakakibara, H. (2009). Highly sensitive and high-throughput analysis of plant hormones using ms-probe modification and liquid chromatography–tandem mass spectrometry: an application for hormone profiling in oryza sativa. *Plant and Cell Physiology*, *50*(7), 1201–1214. https://doi.org/10.1093/pcp/pcp057

Kosuta, S., Chabaud, M., Lougnon, G., Gough, C., Dénarié, J., Barker, D. G., & Bécard, G. (2003). A diffusible factor from arbuscular mycorrhizal fungi induces symbiosis-specific MtENOD11 expression in roots of *Medicago truncatula*. *Plant Physiology*, *131*(3), 952–962. https://doi.org/10.1104/pp.011882

Kretzschmar, T., Kohlen, W., Sasse, J., Borghi, L., Schlegel, M., Bachelier, J. B., Reinhardt, D., Bours, R., Bouwmeester, H. J., & Martinoia, E. (2012). A petunia ABC protein controls strigolactone-dependent symbiotic signalling and branching. *Nature*, *483*(7389), 341–344. https://doi.org/10.1038/nature10873

Lanfranco, L. ., Fiorilli, V., Venice, F., & Bonfante, P. (2018). Strigolactones cross the kingdoms: Plants, fungi, and bacteria in the arbuscular mycorrhizal symbiosis. *Journal of Experimental Botany* (Vol. 69, Issue 9, pp. 2175–2188). https://doi.org/10.1093/jxb/erx432

Lanfranco, L., Fiorilli, V., & Gutjahr, C. (2018). Partner communication and role of nutrients in the arbuscular mycorrhizal symbiosis. In *New Phytologist* (Vol. 220, Issue 4, pp. 1031–1046). https://doi.org/10.1111/nph.15230

Lauressergues, D., Andre, O., Peng, J., Wen, J., Chen, R., Ratet, P., Tadege, M., Mysore, K. S., & Rochange, S. F. (2015). Strigolactones contribute to shoot elongation and to the formation of leaf margin serrations in *Medicago truncatula* R108. *Journal of Experimental Botany*, *66*(5), 1237–1244. https://doi.org/10.1093/jxb/eru471

Lauressergues, Dominique, André, O., Peng, J., Wen, J., Chen, R., Ratet, P., Tadege, M., Mysore, K. S., & Rochange, S. F. (2015). Strigolactones contribute to shoot elongation and to the formation of leaf margin serrations in *Medicago truncatula* R108. *Journal of Experimental Botany*, *66*(5), 1237–1244. https://doi.org/10.1093/jxb/eru471

Lechat, M.-M., Pouvreau, J.-B., Peron, T., Gauthier, M., Montiel, G., Veronesi, C., Todoroki, Y., Le Bizec, B., Monteau, F., Macherel, D., Simier, P., Thoiron, S., & Delavault, P. (2012). PrCYP707A1, an ABA catabolic gene, is a key component of *Phelipanche ramosa* seed germination in response to the strigolactone analogue GR24. *Journal of Experimental Botany*, *63*(14), 5311–5322. https://doi.org/10.1093/jxb/ers189

Lee, H. W., Sharma, P., Janssen, B. J., Drummond, R. S. M., Luo, Z., Hamiaux, C., Collier, T., Allison, J. R., Newcomb, R. D., & Snowden, K. C. (2020). Flexibility of the petunia strigolactone receptor DAD2 promotes its interaction with signaling partners. *Journal of Biological Chemistry*, *295*(13), 4181–4193. https://doi.org/10.1074/jbc.RA119.011509

Li, W., Nguyen, K. H., Chu, H. D., Ha, C. Van, Watanabe, Y., Osakabe, Y., Leyva-González, M. A., Sato, M., Toyooka, K., Voges, L., Tanaka, M., Mostofa, M. G., Seki, M., Seo, M., Yamaguchi, S., Nelson, D. C., Tian, C., Herrera-Estrella, L., & Tran, L.-S. P. (2017). The karrikin receptor KAI2 promotes drought resistance in *Arabidopsis* thaliana. *PLOS Genetics*, *13*(11), e1007076. https://doi.org/10.1371/journal.pgen.1007076

Liu, J., Cheng, X., Liu, P., & Sun, J. (2017). miR156-targeted SBP-box transcription factors interact with DWARF53 to regulate teosinte branched1 and barren STALK1 expression in bread wheat. *Plant Physiology*, *174*(3), 1931–1948. https://doi.org/10.1104/pp.17.00445

Liu, N., Shen, G., Xu, Y., Liu, H., Zhang, J., Li, S., Li, J., Zhang, C., Qi, J., Wang, L., & Wu, J. (2020). Extensive inter-plant protein transfer between Cuscuta parasites and their host plants. *Molecular Plant*, *13*(4), 573–585. https://doi.org/10.1016/j.molp.2019.12.002

Liu, W., Kohlen, W., Lillo, A., den Camp, R. O., Ivanov, S., Hartog, M., Limpens, E., Jamil, M., Smaczniak, C., Kaufmann, K., Yang, W. C., Hooiveld, G. J. E. J., Charnikhova, T., Bouwmeester, H. J., Bisseling, T., & Geurts, R. (2011). Strigolactone biosynthesis in *Medicago truncatula* and rice requires the symbiotic GRAS-type transcription factors NSP1 and NSP2. *Plant Cell*, *23*(10), 3853–3865. https://doi.org/10.1105/tpc.111.089771

Liu, X., Feng, Z., Zhu, H., & Yao, Q. (2019). Exogenous abscisic acid and root volatiles increase sporulation of *Rhizophagus irregularis* DAOM 197198 in asymbiotic and pre-symbiotic status. *Mycorrhiza*, *29*(6), 581–589. https://doi.org/10.1007/s00572-019-00916-z

Logi, C., Sbrana, C., Giovannetti, M., & C Logi, C. S. M. G. (1998). Cellular events involved in survival of individual arbuscular mycorrhizal symbionts growing in the absence of the host. *Applied and Environmental Microbiology*, *64*(9), 3473–3479. https://doi.org/10.1128/aem.64.9.3473-3479.1998

Lopez-Obando, M., Ligerot, Y., Bonhomme, S., Boyer, F.-D., & Rameau, C. (2015). Strigolactone biosynthesis and signaling in plant development. *Development*, *142*(21), 3615–3619. https://doi.org/10.1242/dev.120006

Lopez-Obando, Mauricio, Conn, C. E., Hoffmann, B., Bythell-Douglas, R., Nelson, D. C., Rameau, C., & Bonhomme, S. (2016). Structural modelling and transcriptional responses highlight a clade of *PpKAI2-LIKE* genes as candidate receptors for strigolactones in *Physcomitrella patens*. *Planta*, *243*(6), 1441–1453. https://doi.org/10.1007/s00425-016-2481-y

Lopez-Obando, Mauricio, de Villiers, R., Hoffmann, B., Ma, L., de Saint Germain, A., Kossmann, J., Coudert, Y., Harrison, C. J., Rameau, C., Hills, P., & Bonhomme, S. (2018). *Physcomitrella patens* MAX2

characterization suggests an ancient role for this F-box protein in photomorphogenesis rather than strigolactone signalling. *New Phytologist*, *219*(2), 743–756. https://doi.org/10.1111/nph.15214

Lopez-Obando, Mauricio, Guillory, A., Boyer, F.-D., Cornu, D., Hoffmann, B., Le Bris, P., Pouvreau, J.-B., Delavault, P., Rameau, C., de Saint Germain, A., & Bonhomme, S. (2021). The *Physcomitrium* (*Physcomitrella*) *patens* PpKAI2L receptors for strigolactones and related compounds function via MAX2-dependent and -independent pathways. *The Plant Cell*. https://doi.org/10.1093/plcell/koab217

López-Pedrosa, A., González-Guerrero, M., Valderas, A., Azcón-Aguilar, C., & Ferrol, N. (2006). GintAMT1 encodes a functional high-affinity ammonium transporter that is expressed in the extraradical mycelium of *Glomus intraradices*. *Fungal Genetics and Biology*, *43*(2), 102–110. https://doi.org/10.1016/j.fgb.2005.10.005

López-Ráez, J. A., Fernández, I., García, J. M., Berrio, E., Bonfante, P., Walter, M. H., & Pozo, M. J. (2015). Differential spatio-temporal expression of carotenoid cleavage dioxygenases regulates apocarotenoid fluxes during AM symbiosis. *Plant Science*, *230*, 59–69. https://doi.org/10.1016/j.plantsci.2014.10.010

López-Ráez, J. A., Shirasu, K., & Foo, E. (2017). Strigolactones in plant interactions with beneficial and detrimental organisms: the yin and yang. *Trends in Plant Science* (Vol. 22, Issue 6, pp. 527–537). Elsevier Ltd. https://doi.org/10.1016/j.tplants.2017.03.011

López-Ráez, J. A., Kohlen, W., Charnikhova, T., Mulder, P., Undas, A. K., Sergeant, M. J., Verstappen, F., Bugg, T. D. H., Thompson, A. J., Ruyter-Spira, C., & Bouwmeester, H. (2010). Does abscisic acid affect strigolactone biosynthesis? *New Phytologist*, *187*(2), 343–354. https://doi.org/10.1111/j.1469-8137.2010.03291.x

Lortie, C. J., & Callaway, R. M. (2006). Re-analysis of meta-analysis: support for the stress-gradient hypothesis. *Journal of Ecology*, *94*(1), 7–16. https://doi.org/10.1111/j.1365-2745.2005.01066.x

Ludwig-Müller, J. (2010). Hormonal responses in host plants triggered by arbuscular mycorrhizal fungi. In *Arbuscular Mycorrhizas: Physiology and Function* (pp. 169–190). https://doi.org/10.1007/978-90-481-9489-6_8

Ludwig-Müller, J., Kaldorf, M., Sutter, E. G., & Epstein, E. (1997). Indole-3-butyric acid (IBA) is enhanced in young maize (Zea mays L.) roots colonized with the arbuscular mycorrhizal fungus *Glomus intraradices*. *Plant Science*, *125*(2), 153–162. https://doi.org/10.1016/S0168-9452(97)00064-2

Luginbuehl, L. H. L., Menard, G. N., Kurup, S., Van Erp, H., Radhakrishnan, G. V., Breakspear, A., Oldroyd, G. E. D., & Eastmond, P. J. (2017). Fatty acids in arbuscular mycorrhizal fungi are synthesized by the host plant. *Science*, *356*(6343), 1175–1178. https://doi.org/10.1126/science.aan0081

Maclean, A. M., Bravo, A., & Harrison, M. J. (2017). Plant signaling and metabolic pathways enabling arbuscular mycorrhizal symbiosis.*Plant Cell* (Vol. 29, Issue 10, pp. 2319–2335). https://doi.org/10.1105/tpc.17.00555

Maillet, F., Poinsot, V., André, O., Puech-Pagés, V., Haouy, A., Gueunier, M., Cromer, L., Giraudet, D., Formey, D., Niebel, A., Martinez, E. A., Driguez, H., Bécard, G., Dénarié, J., Puech-Pagès, V., Haouy, A., Gueunier, M., Cromer, L., Giraudet, D., … Dénarié, J. (2011). Fungal lipochitooligosaccharide symbiotic signals in arbuscular mycorrhiza. *Nature*, *469*(7328), 58–64. https://doi.org/10.1038/nature09622

Malloch, D. W., Pirozynski, K. A., & Raven, P. H. (1980). Ecological and evolutionary significance of mycorrhizal symbioses in vascular plants (A Review). *Proceedings of the National Academy of Sciences*, *77*(4), 2113–2118. https://doi.org/10.1073/pnas.77.4.2113

Mangnus, E. M., Dommerholt, F. J., de Jong, R. L. P., & Zwanenburg, B. (1992). Improved Synthesis of Strigol Analogue GR24 and Evaluation of the Biological Activity of Its Diastereomers. *Journal of Agricultural and Food Chemistry*, *40*(7), 1230–1235. https://doi.org/10.1021/jf00019a031

Mangnus, E. M., & Zwanenburg, B. (1992). Tentative molecular mechanism for germination stimulation of *Striga* and *Orobanche* seeds by strigol and its synthetic analogues. In *Food Chem* (Vol. 40). https://pubs.acs.org/sharingguidelines

Martín-Rodríguez, J. Á., Ocampo, J. A., Molinero-Rosales, N., Tarkowská, D., Ruíz-Rivero, O., & García-Garrido, J. M. (2015). Role of gibberellins during arbuscular mycorrhizal formation in tomato: New insights revealed

by endogenous quantification and genetic analysis of their metabolism in mycorrhizal roots. *Physiologia Plantarum*, *154*(1), 66–81. https://doi.org/10.1111/ppl.12274

Marzec, M., & Melzer, M. (2018). Regulation of root development and architecture by strigolactones under optimal and nutrient deficiency conditions. In *International Journal of Molecular Sciences* (Vol. 19, Issue 7, p. 1887). MDPI AG. https://doi.org/10.3390/ijms19071887

Mashiguchi, K., Sasaki, E., Shimada, Y., Nagae, M., Ueno, K., Nakano, T., Yoneyama, K., Suzuki, Y., & Asami, T. (2009). Feedback-regulation of strigolactone biosynthetic genes and strigolactone-regulated genes in *Arabidopsis*. *Bioscience, Biotechnology and Biochemistry*, *73*(11), 2460–2465. https://doi.org/10.1271/bbb.90443

Matthys, C., Walton, A., Struk, S., Stes, E., Boyer, F. D., Gevaert, K., & Goormachtig, S. (2016). The Whats, the Wheres and the Hows of strigolactone action in the roots. *Planta* (Vol. 243, Issue 6, pp. 1327–1337). Springer Verlag. https://doi.org/10.1007/s00425-016-2483-9

Matusova, R., Mourik, T. van, & Bouwmeester, H. J. (2004). Changes in the sensitivity of parasitic weed seeds to germination stimulants. *Seed Science Research*, *14*(4), 335–344. https://doi.org/10.1079/ssr2004187

Matusova, R., Rani, K., Verstappen, F. W. A., Franssen, M. C. R., Beale, M. H., & Bouwmeester, H. J. (2005). The strigolactone germination stimulants of the plant-parasitic *Striga* and *Orobanche* spp. are derived from the carotenoid pathway. *Plant Physiology*, *139*(2), 920–934. https://doi.org/10.1104/pp.105.061382

McCourt, P., Lumba, S., & Bunsick, M. (2017). Chemical genetics and strigolactone perception. *F1000Research* (Vol. 6, p. 975). https://doi.org/10.12688/f1000research.11379.1

Meng, Y., Varshney, K., Incze, N., Badics, E., Kamran, M., Davies, S. F., Oppermann, L. M. F., Magne, K., Dalmais, M., Bendahmane, A., Sibout, R., Vogel, J., Laudencia-Chingcuanco, D., Bond, C. S., Soós, V., Gutjahr, C., & Waters, M. T. (2022). *KARRIKIN INSENSITIVE2* regulates leaf development, root system architecture and arbuscular-mycorrhizal symbiosis in Brachypodium distachyon. *The Plant Journal*. https://doi.org/10.1111/tpj.15651

Mindrebo, J. T., Nartey, C. M., Seto, Y., Burkart, M. D., & Noel, J. P. (2016). Unveiling the functional diversity of the alpha/beta hydrolase superfamily in the plant kingdom. *Current Opinion in Structural Biology* (Vol. 41, pp. 233–246). Elsevier Ltd. https://doi.org/10.1016/j.sbi.2016.08.005

Minh, B. Q., Schmidt, H. A., Chernomor, O., Schrempf, D., Woodhams, M. D., von Haeseler, A., & Lanfear, R. (2020). IQ-TREE 2: new models and efficient methods for phylogenetic inference in the genomic era. *Molecular Biology and Evolution*, *37*(5), 1530–1534. https://doi.org/10.1093/molbev/msaa015

Mohemed, N., Charnikhova, T., Bakker, E. J., van Ast, A., Babiker, A. G., & Bouwmeester, H. J. (2016). Evaluation of field resistance to *Striga hermonthica* (Del.) Benth. in *Sorghum bicolor* (L.) Moench. The relationship with strigolactones. *Pest Management Science*, *72*(11), 2082–2090. https://doi.org/10.1002/ps.4426

Mohemed, N., Charnikhova, T., Fradin, E. F., Rienstra, J., Babiker, A. G. T., & Bouwmeester, H. J. (2018). Genetic variation in Sorghum bicolor strigolactones and their role in resistance against *Striga hermonthica*. *Journal of Experimental Botany*, *69*(9), 2415–2430. https://doi.org/10.1093/jxb/ery041

Moreno, J. C., Mi, J., Alagoz, Y., & Al-Babili, S. (2021). Plant apocarotenoids: from retrograde signaling to interspecific communication. *Plant Journal*, *105*(2), 351–375. https://doi.org/10.1111/tpj.15102

Mori, N., Nishiuma, K., Sugiyama, T., Hayashi, H., & Akiyama, K. (2016). Carlactone-type strigolactones and their synthetic analogues as inducers of hyphal branching in arbuscular mycorrhizal fungi. *Phytochemistry*, *130*, 90–98. https://doi.org/10.1016/j.phytochem.2016.05.012

Mori, N., Nomura, T., & Akiyama, K. (2020). Identification of two oxygenase genes involved in the respective biosynthetic pathways of canonical and non-canonical strigolactones in Lotus japonicus. *Planta*, *251*(2), 40. https://doi.org/10.1007/s00425-019-03332-x

Morris, S. E., Turnbull, C. G. N., Murfet, I. C., & Beveridge, C. A. (2001). Mutational Analysis of Branching in Pea. Evidence That *Rms1* and *Rms5* Regulate the Same Novel Signal. *Plant Physiology*, *126*(3), 1205–1213. https://doi.org/10.1104/pp.126.3.1205

Mosse, B. (1988). Some studies relating to “independent” growth of vesicular–arbuscular endophytes. *Canadian Journal of Botany*, *66*(12), 2533–2540. https://doi.org/10.1139/b88-345

Mosse, B., & Hepper, C. (1975). Vesicular-arbuscular mycorrhizal infections in root organ cultures. *Physiological Plant Pathology*, *5*(3), 215–223. https://doi.org/10.1016/0048-4059(75)90088-0

Müller, L. M., Flokova, K., Schnabel, E., Sun, X., Fei, Z., Frugoli, J., Bouwmeester, H. J., & Harrison, M. J. (2019). A CLE–SUNN module regulates strigolactone content and fungal colonization in arbuscular mycorrhiza. *Nature Plants*, *5*(9), 933–939. https://doi.org/10.1038/s41477-019-0501-1

Müller, L. M., & Harrison, M. J. (2019). Phytohormones, miRNAs, and peptide signals integrate plant phosphorus status with arbuscular mycorrhizal symbiosis. *Current Opinion in Plant Biology* (Vol. 50, pp. 132–139). https://doi.org/10.1016/j.pbi.2019.05.004

Nadal, M., Sawers, R., Naseem, S., Bassin, B., Kulicke, C., Sharman, A., An, G., An, K., Ahern, K. R., Romag, A., Brutnell, T. P., Gutjahr, C., Geldner, N., Roux, C., Martinoia, E., Konopka, J. B., & Paszkowski, U. (2017). An N-acetylglucosamine transporter required for arbuscular mycorrhizal symbioses in rice and maize. *Nature Plants*, *3*. https://doi.org/10.1038/nplants.2017.73

Nagahashi, G., & Douds, J. (1999). Rapid and sensitive bioassay to study signals between root exudates and arbuscular mycorrhizal fungi. *Biotechnology Techniques*, *13*(12), 893–897. https://doi.org/10.1023/A:1008938527757

Nagahashi, G., & Douds, J. (2000). Partial separation of root exudate components and their effects upon the growth of germinated spores of AM fungi. *Mycological Research*, *104*(12), 1453–1464. https://doi.org/10.1017/S0953756200002860

Nagahashi, G., & Douds, J. (2011). The effects of hydroxy fatty acids on the hyphal branching of germinated spores of AM fungi. *Fungal Biology*, *115*(4–5), 351–358. https://doi.org/10.1016/j.funbio.2011.01.006

Nagahashi, G., Douds, J., & Abney, G. (1996). Phosphorus amendment inhibits hyphal branching of the VAM fungus *Gigaspora margarita* directly and indirectly through its effect on root exudation. *Mycorrhiza*, *6*(5), 403–408. https://doi.org/10.1007/s005720050139

Nagata, M., Yamamoto, N., Miyamoto, T., Shimomura, A., Arima, S., Hirsch, A. M., & Suzuki, A. (2016). Enhanced hyphal growth of arbuscular mycorrhizae by root exudates derived from high R/FR treated Lotus japonicus. *Plant Signaling and Behavior*, *11*(6). https://doi.org/10.1080/15592324.2016.1187356

Nakamura, H., Hirabayashi, K., Miyakawa, T., Kikuzato, K., Hu, W., Xu, Y., Jiang, K., Takahashi, I., Niiyama, R., Dohmae, N., Tanokura, M., & Asami, T. (2019). Triazole ureas covalently bind to strigolactone receptor and antagonize strigolactone responses. *Molecular Plant*, *12*(1), 44–58. https://doi.org/10.1016/j.molp.2018.10.006

Nakamura, H., Xue, Y. L., Miyakawa, T., Hou, F., Qin, H. M., Fukui, K., Shi, X., Ito, E., Ito, S., Park, S. H., Miyauchi, Y., Asano, A., Totsuka, N., Ueda, T., Tanokura, M., & Asami, T. (2013). Molecular mechanism of strigolactone perception by DWARF14. *Nature Communications*, *4*. https://doi.org/10.1038/ncomms3613

Napoli, C. (1996). Highly branched phenotype of the petunia dad1-1 mutant is reversed by grafting. *Plant Physiology*, *111*(1), 27–37. https://doi.org/10.1104/pp.111.1.27

Nelson, D. C. (2021). The mechanism of host-induced germination in root parasitic plants. *Plant Physiology*, *185*(4), 1353–1373. https://doi.org/10.1093/plphys/kiab043

Nelson, D. C., Flematti, G. R., Ghisalberti, E. L., Dixon, K. W., & Smith, S. M. (2012). Regulation of seed germination and seedling growth by chemical signals from burning vegetation. *Annual Review of Plant Biology* (Vol. 63, pp. 107–130). https://doi.org/10.1146/annurev-arplant-042811-105545

Nelson, D. C., Flematti, G. R., Riseborough, J. A., Ghisalberti, E. L., Dixon, K. W., & Smitha, S. M. (2010). Karrikins enhance light responses during germination and seedling development in *Arabidopsis* thaliana. *Proc. Natl Acad. Sci. USA*, *107*(15), 7095–7100. https://doi.org/10.1073/pnas.0911635107

Nelson, D. C., Riseborough, J. A., Flematti, G. R., Stevens, J., Ghisalberti, E. L., Dixon, K. W., Smith, S. (2009).

Karrikins discovered in smoke trigger *Arabidopsis* seed germination by a mechanism requiring gibberellic acid synthesis and light. *149*(2), 863–873. https://doi.org/10.1104/pp.108.131516

Nelson, D. C., Scaffidi, A., Dun, E. A., Waters, M. T., Flematti, G. R., Dixon, K. W., Beveridge, C. A., Ghisalberti, E. L., & Smith, S. M. (2011). F-box protein MAX2 has dual roles in karrikin and strigolactone signaling in *Arabidopsis thaliana*. *Proceedings of the National Academy of Sciences of the United States of America*, *108*(21), 8897–8902. https://doi.org/10.1073/pnas.1100987108

Nguyen, T. B., Kitani, S., Shimma, S., & Nihira, T. (2018). Butenolides from Streptomyces albus J1074 act as external signals to stimulate avermectin production in Streptomyces avermitilis. *Applied and Environmental Microbiology*, *84*(9). https://doi.org/10.1128/AEM.02791-17

Ninkovic, V., Markovic, D., & Rensing, M. (2020). Plant volatiles as cues and signals in plant communication. In *Plant Cell and Environment* (Vol. 44, Issue 4, pp. 1030–1043). https://doi.org/10.1111/pce.13910

Oláh, D., Feigl, G., Molnár, Á., Ördög, A., & Kolbert, Z. (2020). Strigolactones interact with nitric oxide in regulating root system architecture of *Arabidopsis thaliana*. *Frontiers in Plant Science*, *11*, 1019. https://doi.org/10.3389/fpls.2020.01019

Oldroyd, G. E. D. (2013). Speak, friend, and enter: Signalling systems that promote beneficial symbiotic associations in plants. *Nature Reviews Microbiology* (Vol. 11, Issue 4, pp. 252–263). https://doi.org/10.1038/nrmicro2990

Palla, M., Battini, F., Cristani, C., Giovannetti, M., Squartini, A., & Agnolucci, M. (2018). Quorum sensing in rhizobia isolated from the spores of the mycorrhizal symbiont *Rhizophagus intraradices*. *Mycorrhiza*, *28*(8), 773–778. https://doi.org/10.1007/s00572-018-0847-7

Parniske, M. (2008). Arbuscular mycorrhiza: The mother of plant root endosymbioses. *Nature Reviews Microbiology* (Vol. 6, Issue 10, pp. 763–775). https://doi.org/10.1038/nrmicro1987

Paszkowski, U., Kroken, S., Roux, C., & Briggs, S. P. (2002). Rice phosphate transporters include an evolutionarily divergent gene specifically activated in arbuscular mycorrhizal symbiosis. *Proceedings of the National Academy of Sciences of the United States of America*, *99*(20), 13324–13329. https://doi.org/10.1073/pnas.202474599

Peláez-Vico, M. A., Bernabéu-Roda, L., Kohlen, W., Soto, M. J., & López-Ráez, J. A. (2016). Strigolactones in the Rhizobium-legume symbiosis: Stimulatory effect on bacterial surface motility and down-regulation of their levels in nodulated plants. *Plant Science*, *245*, 119–127. https://doi.org/10.1016/j.plantsci.2016.01.012

Pepe, A., Giovannetti, M., & Sbrana, C. (2018). Lifespan and functionality of mycorrhizal fungal mycelium are uncoupled from host plant lifespan. *Scientific Reports*, *8*(1), 1–10. https://doi.org/10.1038/s41598-018-28354-5

Pérez-Tienda, J., Testillano, P. S., Balestrini, R., Fiorilli, V., Azcón-Aguilar, C., & Ferrol, N. (2011). GintAMT2, a new member of the ammonium transporter family in the arbuscular mycorrhizal fungus *Glomus intraradices*. *Fungal Genetics and Biology*, *48*(11), 1044–1055. https://doi.org/10.1016/j.fgb.2011.08.003

Pimprikar, P., & Gutjahr, C. (2018). Transcriptional regulation of arbuscular mycorrhiza development. *Plant and Cell Physiology* (Vol. 59, Issue 4, pp. 673–690). https://doi.org/10.1093/pcp/pcy024

Piotrowska, A., & Bajguz, A. (2011). Conjugates of abscisic acid, brassinosteroids, ethylene, gibberellins, and jasmonates. In *Phytochemistry* (Vol. 72, Issue 17, pp. 2097–2112). https://doi.org/10.1016/j.phytochem.2011.08.012

Pons, S., Fournier S., Chervin C., Bécard G., Rochange S., Frei Dit Frey N., Puech Pagès V. Phytohormone production by the arbuscular mycorrhizal fungus *Rhizophagus irregularis*, Plos one e0240886 (2020). https://doi.org/10.1371/journal.pone.0240886

Proust, H., Hoffmann, B., Xie, X., Yoneyama, K. K., Schaefer, D. G., Yoneyama, K. K., Nogué, F., & Rameau, C. (2011). Strigolactones regulate protonema branching and act as a quorum sensing-like signal in the moss *Physcomitrella patens*. *Development*, *138*(8), 1531–1539. https://doi.org/10.1242/dev.058495

Radhakrishnan, G. V., Keller, J., Rich, M. K., Vernié, T., Mbadinga Mbadinga, D. L., Vigneron, N., Cottret, L., Clemente, H. S., Libourel, C., Cheema, J., Linde, A. M., Eklund, D. M., Cheng, S., Wong, G. K. S., Lagercrantz, U., Li, F. W., Oldroyd, G. E. D., & Delaux, P. M. (2020). An ancestral signalling pathway is conserved in intracellular symbioses-forming plant lineages. *Nature Plants*, *6*(3), 280–289. https://doi.org/10.1038/s41477-020-0613-7

Rameau, C., Bertheloot, J., Leduc, N., Andrieu, B., Foucher, F., & Sakr, S. (2015). Multiple Pathways Regulate Shoot Branching. *Frontiers in Plant Science*, *5*(JAN), 741. https://doi.org/10.3389/fpls.2014.00741

Rameau, C., Goormachtig, S., Cardinale, F., Bennett, T., & Cubas, P. (2019). Strigolactones as Plant Hormones. *Strigolactones - Biology and Applications* (pp. 47–87). https://doi.org/10.1007/978-3-030-12153-2_2

Rasmann, S., & Turlings, T. C. J. (2016). Root signals that mediate mutualistic interactions in the rhizosphere. *Current Opinion in Plant Biology* (Vol. 32, pp. 62–68). https://doi.org/10.1016/j.pbi.2016.06.017

Raven, J. A. (2018). Evolution and palaeophysiology of the vascular system and other means of long-distance transport. *Philosophical Transactions of the Royal Society B: Biological Sciences* (Vol. 373, Issue 1739). https://doi.org/10.1098/rstb.2016.0497

Redecker, D., Kodner, R., & Graham, L. E. (2000). Glomalean fungi from the Ordovician. *Science*, *289*(5486), 1920–1921. https://doi.org/10.1126/science.289.5486.1920

Remy, W., Taylor, T. N., Hass, H., & Kerp, H. (1994). Four hundred-million-year-old vesicular arbuscular mycorrhizae. *Proceedings of the National Academy of Sciences of the United States of America*, *91*(25), 11841–11843. https://doi.org/10.1073/pnas.91.25.11841

Rich, M. K., Vigneron, N., Liboure, C., Keller, J., Xue, L., Hajheidari, M., Radhakrishnan, G. V., Le Ru, A., Diop, S. I., Potente, G., Conti, E., Duijsings, D., Batut, A., Le Faouder, P., Kodama, K., Kyozuka, J., Sallet, E., Bécard, G., Rodriguez-Franco, M., … Delaux, P. M. (2021). Lipid exchanges drove the evolution of mutualism during plant terrestrialization. *Science*, *372*(6544), 864–868. https://doi.org/10.1126/science.abg0929

Rochange, S., Goormachtig, S., Lopez-Raez, J. A., & Gutjahr, C. (2019). The Role of Strigolactones in Plant–Microbe Interactions. *Strigolactones - Biology and Applications* (pp. 121–142). https://doi.org/10.1007/978-3-030-12153-2_4

Sanchez, E., Artuso, E., Lombardi, C., Visentin, I., Lace, B., Saeed, W., Lolli, M. L., Kobauri, P., Ali, Z., Spyrakis, F., Cubas, P., Cardinale, F., & Prandi, C. (2018). Structure–activity relationships of strigolactones via a novel, quantitative *in planta* bioassay. *Journal of Experimental Botany*, *69*(9), 2333–2343. https://doi.org/10.1093/jxb/ery092

Sancholle, M., Dalpé, Y., & Grandmougin-Ferjani, A. (2001). Lipids of Mycorrhizae. *Fungal Associations* (pp. 63–93). https://doi.org/10.1007/978-3-662-07334-6_5

Sasse, J., Simon, S., Gübeli, C., Liu, G. W., Cheng, X., Friml, J., Bouwmeester, H., Martinoia, E., & Borghi, L. (2015). Asymmetric localizations of the ABC transporter PaPDR1 trace paths of directional strigolactone transport. *Current Biology*, *25*(5), 647–655. https://doi.org/10.1016/j.cub.2015.01.015

Scaffidi, A., Waters, M. T., Sun, Y. K., Skelton, B. W., Dixon, K. W., Ghisalberti, E. L., Flematti, G. R., & Smith, S. M. (2014). Strigolactone hormones and their stereoisomers signal through two related receptor proteins to induce different physiological responses in *Arabidopsis*. *Plant Physiology*, *165*(3), 1221–1232. https://doi.org/10.1104/pp.114.240036

Schalamuk, S., & Cabello, M. (2010). Arbuscular mycorrhizal fungal propagules from tillage and no-tillage systems: Possible effects on Glomeromycota diversity. *Mycologia*, *102*(2), 261–268. https://doi.org/10.3852/08-118

Schenk, H. J. (2006). Root competition: Beyond resource depletion. *Journal of Ecology* (Vol. 94, Issue 4, pp. 725–739). https://doi.org/10.1111/j.1365-2745.2006.01124.x

Schenkel, D., Lemfack, M. C., Piechulla, B., & Splivallo, R. (2015). A meta-analysis approach for assessing the diversity and specificity of belowground root and microbial volatiles. *Frontiers in Plant Science*, *6*(September), 707. https://doi.org/10.3389/fpls.2015.00707

Schmitz, A. M., Pawlowska, T. E., & Harrison, M. J. (2019). A short LysM protein with high molecular diversity from an arbuscular mycorrhizal fungus, *Rhizophagus irregularis*. *Mycoscience*, *60*(1), 63–70. https://doi.org/10.1016/j.myc.2018.09.002

Schwartz, S. H., Qin, X., & Loewen, M. C. (2004). The biochemical characterization of two carotenoid cleavage enzymes from *Arabidopsis* indicates that a carotenoid-derived compound inhibits lateral branching. *Journal of Biological Chemistry*, *279*(45), 46940–46945. https://doi.org/10.1074/jbc.M409004200

Seto, Y., Sado, A., Asami, K., Hanada, A., Umehara, M., Akiyama, K., & Yamaguchi, S. (2014). Carlactone is an endogenous biosynthetic precursor for strigolactones. *Proceedings of the National Academy of Sciences of the United States of America*, *111*(4), 1640–1645. https://doi.org/10.1073/pnas.1314805111

Seto, Y., Yasui, R., Kameoka, H., Tamiru, M., Cao, M., Terauchi, R., Sakurada, A., Hirano, R., Kisugi, T., Hanada, A., Umehara, M., Seo, E., Akiyama, K., Burke, J., Takeda-Kamiya, N., Li, W., Hirano, Y., Hakoshima, T., Mashiguchi, K., … Yamaguchi, S. (2019). Strigolactone perception and deactivation by a hydrolase receptor DWARF14. *Nature Communications*, *10*(1). https://doi.org/10.1038/s41467-018-08124-7

Shabek, N., Ticchiarelli, F., Mao, H., Hinds, T. R., Leyser, O., & Zheng, N. (2018). Structural plasticity of D3–D14 ubiquitin ligase in strigolactone signalling. *Nature*, *563*(7733), 652–656. https://doi.org/10.1038/s41586-018-0743-5

Sharda, J. N., & Koide, R. T. (2008). Can hypodermal passage cell distribution limit root penetration by mycorrhizal fungi? *New Phytologist*, *180*(3), 696–701. https://doi.org/10.1111/j.1469-8137.2008.02600.x

Shindo, M., Yamamoto, S., Shimomura, K., & Umehara, M. (2020). Strigolactones decrease leaf angle in response to nutrient deficiencies in rice. *Frontiers in Plant Science*, *11*, 135. https://doi.org/10.3389/fpls.2020.00135

Shinohara, N., Taylor, C., & Leyser, O. (2013). Strigolactone Can Promote or Inhibit Shoot Branching by Triggering Rapid Depletion of the Auxin Efflux Protein PIN1 from the Plasma Membrane. *Plos Biology*, *11*(1), e1001474. https://doi.org/10.1371/journal.pbio.1001474

Simard, S., Asay, A., Beiler, K., Bingham, M., Deslippe, J., He, X., Philip, L., Song, Y., & Teste, F. (2015). *Resource Transfer Between Plants Through Ectomycorrhizal Fungal Networks* (pp. 133–176). https://doi.org/10.1007/978-94-017-7395-9_5

Simard, S. W., Beiler, K. J., Bingham, M. A., Deslippe, J. R., Philip, L. J., & Teste, F. P. (2012). Mycorrhizal networks: Mechanisms, ecology and modelling. *Fungal Biology Reviews* (Vol. 26, Issue 1, pp. 39–60). https://doi.org/10.1016/j.fbr.2012.01.001

Simons, J. L., Napoli, C. A., Janssen, B. J., Plummer, K. M., & Snowden, K. C. (2007). Analysis of the DECREASED APICAL DOMINANCE genes of petunia in the control of axillary branching. *Plant Physiology*, *143*(2), 697–706. https://doi.org/10.1104/pp.106.087957

Siqueira, J. O., Safir, G. R., & Nair, M. G. (1991). Stimulation of vesicular-arbuscular mycorrhiza formation and growth of white clover by flavonoid compounds. *New Phytologist*, *118*(1), 87–93. https://doi.org/10.1111/j.1469-8137.1991.tb00568.x

Smith, F. A., & Smith, S. E. (1997). Structural diversity in (vesicular)-arbuscular mycorrhizal symbioses. *New Phytologist* (Vol. 137, Issue 3, pp. 373–388). https://doi.org/10.1046/j.1469-8137.1997.00848.x

Smith, J. D., Woldemariam, M. G., Mescher, M. C., Jander, G., & de Moraes, C. M. (2016). Glucosinolates from host plants influence growth of the parasitic plant *Cuscuta gronovii* and its susceptibilityto aphid feeding. *Plant Physiology*, *172*(1), 181–197. https://doi.org/10.1104/pp.16.00613

Smith, S., & Read, D. (2008). Mycorrhizal Symbiosis. In *Mycorrhizal Symbiosis* (3rd ed.). https://doi.org/10.1016/B978-0-12-370526-6.X5001-6

Song, Wang, M., Zeng, R., Groten, K., & Baldwin, I. T. (2019). Priming and filtering of antiherbivore defences among Nicotiana attenuata plants connected by mycorrhizal networks. *Plant Cell and Environment*, *42*(11), 2945–2961. https://doi.org/10.1111/pce.13626

Song, X., Lu, Z., Yu, H., Shao, G., Xiong, J., Meng, X., Jing, Y., Liu, G., Xiong, G., Duan, J., Yao, X. F., Liu, C. M., Li, H., Wang, Y., & Li, J. (2017). IPA1 functions as a downstream transcription factor repressed by D53 in strigolactone signaling in rice. *27*(9), 1128–1141. https://doi.org/10.1038/cr.2017.102

Song, Y. Y., Simard, S. W., Carroll, A., Mohn, W. W., & Zeng, R. Sen. (2015). Defoliation of interior Douglas-fir elicits carbon transfer and stress signalling to ponderosa pine neighbors through ectomycorrhizal networks. *Scientific Reports*, *5*. https://doi.org/10.1038/srep08495

Song, Y. Y., Ye, M., Li, C., He, X., Zhu-Salzman, K., Wang, R. L., Su, Y. J., Luo, S. M., & Zeng, R. Sen. (2014). Hijacking common mycorrhizal networks for herbivore-induced defence signal transfer between tomato plants. *Scientific Reports*, *4*(1), 1–8. https://doi.org/10.1038/srep03915

Song, Y. Y., Zeng, R. Sen, Xu, J. F., Li, J., Shen, X., & Yihdego, W. G. (2010). Interplant communication of tomato plants through underground common mycorrhizal networks. *PLos one*, *5*(10), e13324. https://doi.org/10.1371/journal.pone.0013324

Sorefan, K., Booker, J., Haurogné, K., Goussot, M., Bainbridge, K., Foo, E., Chatfield, S., Ward, S., Beveridge, C., Rameau, C., & Leyser, O. (2003). MAX4 and RMS1 are orthologsgous dioxygenase-like genes that regulate shoot branching in *Arabidopsis* and pea. *Genes and Development*, *17*(12), 1469–1474. https://doi.org/10.1101/gad.256603

Soto, M. J., Fernández-Aparicio, M., Castellanos-Morales, V., García-Garrido, J. M., Ocampo, J. A., Delgado, M. J., & Vierheilig, H. (2010). First indications for the involvement of strigolactones on nodule formation in alfalfa (*Medicago sativa*). *Soil Biology and Biochemistry*, *42*(2), 383–385. https://doi.org/10.1016/j.soilbio.2009.11.007

Soundappan, I., Bennett, T., Morffy, N., Liang, Y., Stanga, J. P., Abbas, A., Leyser, O., Nelsona, D. C., & Nelson, D. C. (2015). SMAX1-LIKE/D53 family members enable distinct MAX2-dependent responses to strigolactones and karrikins in *Arabidopsis*. *Plant Cell*, *27*(11), 3143–3159. https://doi.org/10.1105/tpc.15.00562

Souza, T. (2015). AMF's Main Structures. *Handbook of Arbuscular Mycorrhizal Fungi* (pp. 43–63). https://doi.org/10.1007/978-3-319-24850-9_3

St-Arnaud, M., Hamel, C., Vimard, B., Caron, M., & Fortin, J. A. (1996). Enhanced hyphal growth and spore production of the arbuscular mycorrhizal fungus Glomus intraradices in an *in vitro* system in the absence of host roots. *Mycological Research*, *100*(3), 328–332. https://doi.org/10.1016/S0953-7562(96)80164-X

Stanga, J. P., Morffy, N., & Nelson, D. C. (2016). Functional redundancy in the control of seedling growth by the karrikin signaling pathway. *Planta*, *243*(6), 1397–1406. https://doi.org/10.1007/s00425-015-2458-2

Stanga, J. P., Smith, S. M., Briggs, W. R., & Nelson, D. C. (2013). SUPPRESSOR OF MORE AXILLARY GROWTH2 1 controls seed germination and seedling development in *Arabidopsis*. *Plant Physiology*, *163*(1), 318–330. https://doi.org/10.1104/pp.113.221259

Stirnberg, P., Furner, I. J., & Ottoline Leyser, H. M. (2007). MAX2 participates in an SCF complex which acts locally at the node to suppress shoot branching. *Plant Journal*, *50*(1), 80–94. https://doi.org/10.1111/j.1365-313X.2007.03032.x

Stirnberg, P., van de Sande, K., & Leyser, H. M. O. (2002). MAX1 and MAX2 control shoot lateral branching in *Arabidopsis. Development*, *129*(5), 1131–1141. https://doi.org/10.1242/dev.129.5.1131

Subrahmaniam, H. J., Libourel, C., Journet, E.-P., Morel, J.-B., Muños, S., Niebel, A., Raffaele, S., & Roux, F. (2018). The genetics underlying natural variation of plant-plant interactions, a beloved but forgotten member of the family of biotic interactions. *The Plant Journal*, *93*(4), 747–770. https://doi.org/10.1111/tpj.13799

Sugiura, Y., Akiyama, R., Tanaka, S., Yano, K., Kameoka, H., Marui, S., Saito, M., Kawaguchi, M., Akiyama, K., & Saito, K. (2020). Myristate can be used as a carbon and energy source for the asymbiotic growth of arbuscular mycorrhizal fungi. *Proceedings of the National Academy of Sciences of the United States of America*, *117*(41), 25779–25788. https://doi.org/10.1073/pnas.2006948117

Sun, J., Miller, J. B., Granqvist, E., Wiley-Kalil, A., Gobbato, E., Maillet, F., Cottaz, S., Samain, E.,

Venkateshwaran, M., Fort, S., Morris, R. J., Ané, J. M., Dénarié, J., & Oldroyd, G. E. D. (2015). Activation of symbiosis signaling by arbuscular mycorrhizal fungi in legumes and riceopen. *Plant Cell*, *27*(3), 823–838. https://doi.org/10.1105/tpc.114.131326

Swarbreck, S. M., Guerringue, Y., Matthus, E., Jamieson, F. J. C., & Davies, J. M. (2019). Impairment in karrikin but not strigolactone sensing enhances root skewing in *Arabidopsis thaliana*. *Plant Journal*, *98*(4), 607–621. https://doi.org/10.1111/tpj.14233

Symanczik, S., Courty, P. E., Boller, T., Wiemken, A., & Al-Yahya'ei, M. N. (2015). Impact of water regimes on an experimental community of four desert arbuscular mycorrhizal fungal (AMF) species, as affected by the introduction of a non-native AMF species. *Mycorrhiza*, *25*(8), 639–647. https://doi.org/10.1007/s00572-015-0638-3

Takahashi, I., & Asami, T. (2018). Target-based selectivity of strigolactone agonists and antagonists in plants and their potential use in agriculture. *Journal of Experimental Botany* (Vol. 69, Issue 9, pp. 2241–2254). Oxford University Press. https://doi.org/10.1093/jxb/ery126

Takahashi, I., Jiang, K., & Asami, T. (2021). Counteractive Effects of Sugar and Strigolactone on Leaf Senescence of Rice in Darkness. *Agronomy*, *11*(6), 1044. https://doi.org/10.3390/agronomy11061044

Tamasloukht, M., Séjalon-Delmas, N., Kluever, A., Jauneau, A., Roux, C., Bécard, G., & Franken, P. (2003). Root factors induce mitochondrial-related gene expression and fungal respiration during the developmental switch from asymbiosis to presymbiosis in the arbuscular mycorrhizal fungus *Gigaspora rosea* . *Plant Physiology*, *131*(3), 1468–1478. https://doi.org/10.1104/pp.012898

Tambalo, D. D., Vanderlinde, E. M., Robinson, S., Halmillawewa, A., Hynes, M. F., & Yost, C. K. (2014). Legume seed exudates and *Physcomitrella patens* extracts influence swarming behavior in *Rhizobium leguminosarum*. *Canadian Journal of Microbiology*, *60*(1), 15–24. https://doi.org/10.1139/cjm-2013-0723

Tanaka, S., Hashimoto, K., Kobayashi, Y., Yano, K., Maeda, T., Kameoka, H., Ezawa, T., Saito, K., Akiyama, K., & Kawaguchi, M. (2022). Asymbiotic mass production of the arbuscular mycorrhizal fungus *Rhizophagus clarus*. *Communications Biology*, *5*(1), 1–9. https://doi.org/10.1038/s42003-021-02967-5

Taulera, Q., Lauressergues, D., Martin, K., Cadoret, M., Servajean, V., Boyer, F. D., & Rochange, S. (2020). Initiation of arbuscular mycorrhizal symbiosis involves a novel pathway independent from hyphal branching. *Mycorrhiza*, *30*(4), 491–501. https://doi.org/10.1007/s00572-020-00965-9

Tedersoo, L., Jairus, T., Horton, B. M., Abarenkov, K., Suvi, T., Saar, I., & Kõljalg, U. (2008). Strong host preference of ectomycorrhizal fungi in a Tasmanian wet sclerophyll forest as revealed by DNA barcoding and taxon-specific primers. *New Phytologist*, *180*(2), 479–490. https://doi.org/10.1111/j.1469-8137.2008.02561.x

Thuring, J. W. J. F., Keltjens, R., Nefkens, G. H. L., & Zwanenburg, B. (1997). Synthesis and biological evaluation of potential substrates for the isolation of the strigol receptor. *Journal of the Chemical Society - 1*, *0*(5), 759–765. https://doi.org/10.1039/a604685a

Toh, S., Holbrook-Smith, D., Stogios, P. J., Onopriyenko, O., Lumba, S., Tsuchiya, Y., Savchenko, A., & McCourt, P. (2015). *Science*, *350*(6257), 203–207. https://doi.org/10.1126/science.aac9476

Toh, S., Holbrook-Smith, D., Stokes, M. E., Tsuchiya, Y., & McCourt, P. (2014). Detection of parasitic plant suicide germination compounds using a high-throughput *Arabidopsis* HTL/KAI2 strigolactone perception system. *Chemistry & Biology*, *21*(8), 988–998. https://doi.org/10.1016/j.chembiol.2014.07.005

Toh, S., Kamiya, Y., Kawakami, N., Nambara, E., McCourt, P., & Tsuchiya, Y. (2012). Thermoinhibition uncovers a role for strigolactones in A*rabidopsis* seed germination. *Plant and Cell Physiology*, *53*(1), 107–117. https://doi.org/10.1093/pcp/pcr176

Tokunaga, T., Hayashi, H., & Akiyama, K. (2015). Medicaol, a strigolactone identified as a putative didehydro-orobanchol isomer, from *Medicago truncatula*. *Phytochemistry*, *111*, 91–97. https://doi.org/10.1016/j.phytochem.2014.12.024

Torres-Vera, R., García, J. M., Pozo, M. J., & López-Ráez, J. A. (2014). Do strigolactones contribute to plant

defence? *Molecular Plant Pathology*, *15*(2), 211–216. https://doi.org/10.1111/mpp.12074

Tsuchiya, Y., Yoshimura, M., Sato, Y., Kuwata, K., Toh, S., Holbrook-Smith, D., Zhang, H., McCourt, P., Itami, K., Kinoshita, T., & Hagihara, S. (2015). Probing strigolactone receptors in *Striga hermonthica* with fluorescence. *Science*, *349*(6250), 864–868. https://doi.org/10.1126/science.aab3831

Ueda, H., & Kusaba, M. (2015). Strigolactone regulates leaf senescence in concert with ethylene in *Arabidopsis*. *Plant Physiology*, *169*(1), 138–147. https://doi.org/10.1104/pp.15.00325

Ueguchi-Tanaka, M., Ashikari, M., Nakajima, M., Itoh, H., Katoh, E., Kobayashi, M., Chow, T. Y., Hsing, Y. I. C., Kitano, H., Yamaguchi, I., & Matsuoka, M. (2005). GIBBERELLIN INSENSITIVE DWARF1 encodes a soluble receptor for gibberellin. *Nature*, *437*(7059), 693–698. https://doi.org/10.1038/nature04028

Umehara, M., Cao, M., Akiyama, K., Akatsu, T., Seto, Y., Hanada, A., Li, W., Takeda-Kamiya, N., Morimoto, Y., & Yamaguchi, S. (2015). Structural requirements of strigolactones for shoot branching inhibition in rice and *Arabidopsis*. *Plant and Cell Physiology*, *56*(6), 1059–1072. https://doi.org/10.1093/pcp/pcv028

Umehara, M., Hanada, A., Magome, H., Takeda-Kamiya, N., & Yamaguchi, S. (2010). Contribution of strigolactones to the inhibition of tiller bud outgrowth under phosphate deficiency in rice. *Plant and Cell Physiology*, *51*(7), 1118–1126. https://doi.org/10.1093/pcp/pcq084

Umehara, M., Hanada, A., Yoshida, S., Akiyama, K., Arite, T., Takeda-Kamiya, N., Magome, H., Kamiya, Y., Shirasu, K., Yoneyama, K., Kyozuka, J., & Yamaguchi, S. (2008). Inhibition of shoot branching by new terpenoid plant hormones. *Nature*, *455*(7210), 195–200. https://doi.org/10.1038/nature07272

Vahabi, K., Reichelt, M., Scholz, S. S., Furch, A. C. U., Matsuo, M., Johnson, J. M., Sherameti, I., Gershenzon, J., & Oelmüller, R. (2018). *Alternaria Brassicae* induces systemic jasmonate responses in *Arabidopsis* which travel to neighboring plants via a *Piriformsopora indica* hyphal network and activate abscisic acid responses. *Frontiers in Plant Science*, *9*, 626. https://doi.org/10.3389/fpls.2018.00626

van der Heijden, M. G. A., Martin, F. M., Selosse, M. A., & Sanders, I. R. (2015). Mycorrhizal ecology and evolution: The past, the present, and the future. *New Phytologist* (Vol. 205, Issue 4, pp. 1406–1423). https://doi.org/10.1111/nph.13288

van Rongen, M., T Bennett, F Ticchiarelli, O. L., van Rongen, M., Bennett, T., Ticchiarelli, F., & Leyser, O. (2019). Connective auxin transport contributes to strigolactone-mediated shoot branching control independent of the transcription factor BRC1. *PLOS Genetics*, *15*(3), e1008023. https://doi.org/10.1371/journal.pgen.1008023

Vesty, E. F., Saidi, Y., Moody, L. A., Holloway, D., Whitbread, A., Needs, S., Choudhary, A., Burns, B., McLeod, D., Bradshaw, S. J., Bae, H., King, B. C., Bassel, G. W., Simonsen, H. T., & Coates, J. C. (2016). The decision to germinate is regulated by divergent molecular networks in spores and seeds. *New Phytologist*, *211*(3), 952–966. https://doi.org/10.1111/nph.14018

Vierheilig, H., Coughlan, A. P., Wyss, U., & Piché, Y. (1998). Ink and vinegar, a simple staining technique for arbuscular-mycorrhizal fungi. *Applied and Environmental Microbiology*, *64*(12), 5004–5007. https://doi.org/10.1128/aem.64.12.5004-5007.1998

Vierheilig, H., & Piché, Y. (2002). Signalling in arbuscular mycorrhiza: Facts and hypotheses. *Advances in Experimental Medicine and Biology*, *505*, 23–39. https://doi.org/10.1007/978-1-4757-5235-9_3

Villaécija-Aguilar, J. (2019). SMAX1/SMXL2 regulate root and root hair development downstream of KAI2-mediated signalling in *Arabidopsis*. *PLoS Genet.*, *15*, e1008327.

Vogel, J. T., Walter, M. H., Giavalisco, P., Lytovchenko, A., Kohlen, W., Charnikhova, T., Simkin, A. J., Goulet, C., Strack, D., Bouwmeester, H. J., Fernie, A. R., & Klee, H. J. (2010). SlCCD7 controls strigolactone biosynthesis, shoot branching and mycorrhiza-induced apocarotenoid formation in tomato. *Plant Journal*, *61*(2), 300–311. https://doi.org/10.1111/j.1365-313X.2009.04056.x

Wakabayashi, T., Hamana, M., Mori, A., Akiyama, R., Ueno, K., Osakabe, K., Osakabe, Y., Suzuki, H., Takikawa, H., Mizutani, M., & Sugimoto, Y. (2019). Direct conversion of carlactonoic acid to orobanchol by cytochrome P450 CYP722C in strigolactone biosynthesis. *Science Advances*, *5*(12), 9067–9085.

https://doi.org/10.1126/sciadv.aax9067

Wakabayashi, T., Ishiwa, S., Shida, K., Motonami, N., Suzuki, H., Takikawa, H., Mizutani, M., & Sugimoto, Y. (2021). Identification and characterization of sorgomol synthase in sorghum strigolactone biosynthesis. *Plant Physiology*, *185*(3), 902–913. https://academic.oup.com/plphys/article/185/3/902/6094724

Wakabayashi, T., Shida, K., Kitano, Y., Takikawa, H., Mizutani, M., & Sugimoto, Y. (2020). CYP722C from Gossypium arboreum catalyzes the conversion of carlactonoic acid to 5-deoxystrigol. *Planta*, *251*(5), 3. https://doi.org/10.1007/s00425-020-03390-6

Wakabayashi, T., Shinde, H., Shiotani, N., Yamamoto, S., Mizutani, M., Takikawa, H., & Sugimoto, Y. (2020). Conversion of methyl carlactonoate to heliolactone in sunflower. *Natural Product Research*. https://doi.org/10.1080/14786419.2020.1826477

Walker, C. H., Siu-Ting, K., Taylor, A., O'Connell, M. J., & Bennett, T. (2019). Strigolactone synthesis is ancestral in land plants, but canonical strigolactone signalling is a flowering plant innovation. *BMC Biology*, *17*(1), 70. https://doi.org/10.1186/s12915-019-0689-6

Wallner, E. S., López-Salmerón, V., Belevich, I., Poschet, G., Jung, I., Grünwald, K., Sevilem, I., Jokitalo, E., Hell, R., Helariutta, Y., Agustí, J., Lebovka, I., & Greb, T. (2017). Strigolactone- and karrikin-independent smxl proteins are central regulators of phloem formation. *Current Biology*, *27*(8), 1241–1247. https://doi.org/10.1016/j.cub.2017.03.014

Walter, M. H., Floß, D. S., Hans, J., Fester, T., & Strack, D. (2007). Apocarotenoid biosynthesis in arbuscular mycorrhizal roots: Contributions from methylerythritol phosphate pathway isogenes and tools for its manipulation. *Phytochemistry* (Vol. 68, Issue 1, pp. 130–138). Pergamon. https://doi.org/10.1016/j.phytochem.2006.09.032

Wang, F., Han, T., Song, Q., Ye, W., Song, X., Chu, J., Li, J., & Chen, Z. J. (2020a). The rice circadian clock regulates tiller growth and panicle development through strigolactone signaling and sugar sensing. *The Plant Cell*, *32*(10), 3124–3138. https://doi.org/10.1105/tpc.20.00289

Wang, J. Y., Haider, I., Jamil, M., Fiorilli, V., Saito, Y., Mi, J., Baz, L., Kountche, B. A., Jia, K. P., Guo, X., Balakrishna, A., Ntui, V. O., Reinke, B., Volpe, V., Gojobori, T., Blilou, I., Lanfranco, L., Bonfante, P., & Al-Babili, S. (2019). The apocarotenoid metabolite zaxinone regulates growth and strigolactone biosynthesis in rice. *Nature Communications*, *10*(1), 1–9. https://doi.org/10.1038/s41467-019-08461-1

Wang, L., Wang, B., Jiang, L., Liu, X., Li, X., Lu, Z., Meng, X., Wang, Y., Smith, S. M., Lia, J., & Li, J. (2015). Strigolactone signaling in *Arabidopsis* regulates shoot development by targeting D53-like SMXL repressor proteins for ubiquitination and degradation. *Plant Cell*, *27*(11), 3128–3142. https://doi.org/10.1105/tpc.15.00605

Wang, L., Wang, B., Yu, H., Guo, H., Lin, T., Kou, L., Wang, A., Shao, N., Ma, H., Xiong, G., Li, X., Yang, J., Chu, J., & Li, J. (2020b). Transcriptional regulation of strigolactone signalling in *Arabidopsis*. *Nature*, *583*(7815), 277–281. https://doi.org/10.1038/s41586-020-2382-x

Wang, L., Xu, Q., Yu, H., Ma, H., Li, X., Yang, J., Chu, J., Xie, Q., Wang, Y., Smith, S. M., Li, J., Xiong, G., & Wang, B. (2020c). Strigolactone and karrikin signaling pathways elicit ubiquitination and proteolysis of SMXL2 to regulate hypocotyl elongation in *Arabidopsis*. *The Plant Cell*, *32*(7), 2251–2270. https://doi.org/10.1105/tpc.20.00140

Wang, N. Q., Kong, C. H., Wang, P., & Meiners, S. J. (2021a). Root exudate signals in plant–plant interactions. *Plant Cell and Environment* (Vol. 44, Issue 4, pp. 1044–1058). https://doi.org/10.1111/pce.13892

Wang, Q., Smith, S. M., & Huang, J. (2021b). Origins of strigolactone and karrikin signaling in plants. *Trends in Plant Science*. https://doi.org/10.1016/j.tplants.2021.11.009

Wang, S., Chen, A., Xie, K., Yang, X., Luo, Z., Chen, J., Zeng, D., Ren, Y., Yang, C., Wang, L., Feng, H., López-Arredondo, D. L., Herrera-Estrella, L. R., & Xu, G. (2020d). Functional analysis of the OsNPF4.5 nitrate transporter reveals a conserved mycorrhizal pathway of nitrogen acquisition in plants. *Proceedings of the National Academy of Sciences of the United States of America*, *117*(28), 16649–16659. https://doi.org/10.1073/pnas.2000926117

Wang, Y., Yao, R., Du, X., Guo, L., Chen, L., Xie, D., & Smith, S. M. (2021c). Molecular basis for high ligand sensitivity and selectivity of strigolactone receptors in *Striga*. *Plant Physiology*, *185*(4), 1411–1428. https://doi.org/10.1093/plphys/kiaa048

Waters, M. T., Brewer, P. B., Bussell, J. D., Smith, S. M., & Beveridge, C. A. (2012). The *Arabidopsis* ortholog of rice DWARF27 acts upstream of MAX1 in the control of plant development by Strigolactones. *Plant Physiology*, *159*(3), 1073–1085. https://doi.org/10.1104/pp.112.196253

Waters, M. T., Gutjahr, C., Bennett, T., & Nelson, D. C. (2017). Strigolactone Signaling and Evolution. *Annual Review of Plant Biology* (Vol. 68, pp. 291–322). Annual Reviews Inc. https://doi.org/10.1146/annurev-arplant-042916-040925

Waters, M. T., Nelson, D. C., Scaffidi, A., Flematti, G. R., Sun, Y. K., Dixon, K. W., & Smith, S. M. (2012). Specialisation within the DWARF14 protein family confers distinct responses to karrikins and strigolactones in *Arabidopsis*. *Development*, *139*(7), 1285–1295. https://doi.org/10.1242/dev.074567

Waters, M. T., Smith, S. M., & Nelson, D. C. (2011). Smoke signals and seed dormancy: Where next for MAX2? *Plant Signaling and Behavior*, *6*(9), 1418–1422. https://doi.org/10.4161/psb.6.9.17303

Westwood, J. H. (2013). The physiology of the established parasite-host association. In *Parasitic Orobanchaceae: Parasitic Mechanisms and Control Strategies* (Vol. 9783642381461, pp. 87–114). Springer-Verlag Berlin Heidelberg. https://doi.org/10.1007/978-3-642-38146-1_6

Wewer, V., Brands, M., & Dörmann, P. (2014). Fatty acid synthesis and lipid metabolism in the obligate biotrophic fungus *Rhizophagus irregularis* during mycorrhization of *Lotus japonicus*. *The Plant Journal*, *79*(3), 398–412. https://doi.org/10.1111/tpj.12566

Wilkinson, R. C., Rahman Pour, R., Jamshidi, S., Fülöp, V., & Bugg, T. D. H. (2020). Extracellular alpha/beta-hydrolase from Paenibacillus species shares structural and functional homology to tobacco salicylic acid binding protein 2. *Journal of Structural Biology*, *210*(3), 107496. https://doi.org/10.1016/j.jsb.2020.107496

Wu, H., Li, H., Chen, H., Qi, Q., Ding, Q., Xue, J., Ding, J., Jiang, X., Hou, X., & Li, Y. (2019). Identification and expression analysis of strigolactone biosynthetic and signaling genes reveal strigolactones are involved in fruit development of the woodland strawberry (Fragaria vesca). *BMC Plant Biology*, *19*(1), 73. https://doi.org/10.1186/s12870-019-1673-6

Xie, X., Mori, N., Yoneyama, K., Nomura, T., Uchida, K., Yoneyama, K., & Akiyama, K. (2019). Lotuslactone, a non-canonical strigolactone from Lotus japonicus. *Phytochemistry*, *157*, 200–205. https://doi.org/10.1016/j.phytochem.2018.10.034

Xie, X., Yoneyama, K., Kisugi, T., Nomura, T., Akiyama, K., Asami, T., & Yoneyama, K. (2015). Strigolactones are transported from roots to shoots, although not through the xylem. *J. Pestic. Sci*, *40*(4), 214–216. https://doi.org/10.1584/jpestics.D15-045

Xie, X., Yoneyama, K., Kusumoto, D., Yamada, Y., Takeuchi, Y., Sugimoto, Y., & Yoneyama, K. (2008). Sorgomol, germination stimulant for root parasitic plants, produced by Sorghum bicolor. *Tetrahedron Letters*, *49*(13), 2066–2068. https://doi.org/10.1016/j.tetlet.2008.01.131

Xu, E., Chai, L., Zhang, S., Yu, R., Zhang, X., Xu, C., & Hu, Y. (2021). Catabolism of strigolactones by a carboxylesterase. *Nature Plants*, *7*(11), 1495–1504. https://doi.org/10.1038/s41477-021-01011-y

Xu, Y., Miyakawa, T., Nakamura, H., Nakamura, A., Imamura, Y., Asami, T., & Tanokura, M. (2016). Structural basis of unique ligand specificity of KAI2-like protein from parasitic weed *Striga* hermonthica. *Scientific Reports*, *6*(1), 1–9. https://doi.org/10.1038/srep31386

Xu, Y., Miyakawa, T., Nosaki, S., Nakamura, A., Lyu, Y., Nakamura, H., Ohto, U., Ishida, H., Shimizu, T., Asami, T., & Tanokura, M. (2018). Structural analysis of HTL and D14 proteins reveals the basis for ligand selectivity in *Striga*. *Nature Communications*, *9*(1), 1–11. https://doi.org/10.1038/s41467-018-06452-2

Yamada, Y., Furusawa, S., Nagasaka, S., Shimomura, K., Yamaguchi, S., & Umehara, M. (2014). Strigolactone signaling regulates rice leaf senescence in response to a phosphate deficiency. *Planta*, *240*(2), 399–408.

https://doi.org/10.1007/s00425-014-2096-0

Yamauchi, M., Ueno, K., Furumoto, T., Wakabayashi, T., Mizutani, M., Takikawa, H., & Sugimoto, Y. (2018). Stereospecific reduction of the butenolide in strigolactones in plants. *Bioorganic and Medicinal Chemistry*, *26*(14), 4225–4233. https://doi.org/10.1016/j.bmc.2018.07.016

Yao, J., Mashiguchi, K., Scaffidi, A., Akatsu, T., Melville, K. T., Morita, R., Morimoto, Y., Smith, S. M., Seto, Y., Flematti, G. R., Yamaguchi, S., & Waters, M. T. (2018). An allelic series at the *KARRIKIN INSENSITIVE 2* locus of *Arabidopsis thaliana* decouples ligand hydrolysis and receptor degradation from downstream signalling. *The Plant Journal*, *96*(1), 75–89. https://doi.org/10.1111/tpj.14017

Yao, J., Scaffidi, A., Meng, Y., Melville, K. T., Komatsu, A., Khosla, A., Nelson, D. C., Kyozuka, J., Flematti, G. R., & Waters, M. T. (2021). Desmethyl butenolides are optimal ligands for karrikin receptor proteins. *New Phytologist*, *230*(3), 1003–1016. https://doi.org/10.1111/nph.17224

Yao, Ming, Z., Yan, L., Li, S., Wang, F., Ma, S., Yu, C., Yang, M., Chen, L., Chen, L., Li, Y., Yan, C., Miao, D., Sun, Z., Yan, J., Sun, Y., Wang, L., Chu, J., Fan, S., … Xie, D. (2016). DWARF14 is a non-canonical hormone receptor for strigolactone. *Nature*, *536*(7617), 469–473. https://doi.org/10.1038/nature19073

Yao, R., Wang, F., Ming, Z., Du, X., Chen, L., Wang, Y., Zhang, W., Deng, H., & Xie, D. (2017). ShHTL7 is a non-canonical receptor for strigolactones in root parasitic weeds. *Cell Research* (Vol. 27, Issue 6, pp. 838–841). https://doi.org/10.1038/cr.2017.3

Yokota, T., Sakai, H., Okuno, K., Yoneyama, K., & Takeuchi, Y. (1998). Alectrol and orobanchol, germination stimulants for Orobanche minor, from its host red clover. *Phytochemistry*, *49*(7), 1967–1973. https://doi.org/10.1016/S0031-9422(98)00419-1

Yoneyama, K., Akiyama, K., Brewer, P. B., Mori, N., Kawano-Kawada, M., Haruta, S., Nishiwaki, H., Yamauchi, S., Xie, X., Umehara, M., Beveridge, C. A., Yoneyama, K., & Nomura, T. (2020a). Hydroxyl carlactone derivatives are predominant strigolactones in *Arabidopsis*. *Plant Direct*, *4*(5), e00219. https://doi.org/10.1002/pld3.219

Yoneyama, K., Kisugi, T., Xie, X., Arakawa, R., Ezawa, T., Nomura, T., & Yoneyama, K. (2015). Shoot-derived signals other than auxin are involved in systemic regulation of strigolactone production in roots. *Planta*, *241*(3), 687–698. https://doi.org/10.1007/s00425-014-2208-x

Yoneyama, K., Mori, N., Sato, T., Yoda, A., Xie, X., Okamoto, M., Iwanaga, M., Ohnishi, T., Nishiwaki, H., Asami, T., Yokota, T., Akiyama, K., Yoneyama, K., & Nomura, T. (2018a). Conversion of carlactone to carlactonoic acid is a conserved function of MAX1 homologs in strigolactone biosynthesis. *New Phytologist*, *218*(4), 1522–1533. https://doi.org/10.1111/nph.15055

Yoneyama, K., Xie, X., Kim, H. Il, Kisugi, T., Nomura, T., Sekimoto, H., Yokota, T., & Yoneyama, K. (2012). How do nitrogen and phosphorus deficiencies affect strigolactone production and exudation? *Planta*, *235*(6), 1197–1207. https://doi.org/10.1007/s00425-011-1568-8

Yoneyama, K., Xie, X., Kusumoto, D., Sekimoto, H., Sugimoto, Y., Takeuchi, Y., & Yoneyama, K. (2007). Nitrogen deficiency as well as phosphorus deficiency in sorghum promotes the production and exudation of 5-deoxystrigol, the host recognition signal for arbuscular mycorrhizal fungi and root parasites. *Planta*, *227*(1), 125–132. https://doi.org/10.1007/s00425-007-0600-5

Yoneyama, K., Xie, X., Nomura, T., & Yoneyama, K. (2020b). Do phosphate and cytokinin interact to regulate strigolactone biosynthesis or act independently? *Frontiers in Plant Science*, *11*, 438. https://doi.org/10.3389/fpls.2020.00438

Yoneyama, Xie, X., Yoneyama, K., Kisugi, T., Nomura, T., Nakatani, Y., Akiyama, K., & McErlean, C. S. P. (2018b). Which are the major players, canonical or non-canonical strigolactones? *Journal of Experimental Botany*, *69*(9), 2231–2239. https://doi.org/10.1093/jxb/ery090

Yoshida, S., Kameoka, H., Tempo, M., Akiyama, K., Umehara, M., Yamaguchi, S., Hayashi, H., Kyozuka, J., & Shirasu, K. (2012). The D3 F-box protein is a key component in host strigolactone responses essential for arbuscular mycorrhizal symbiosis. *New Phytologist*, *196*(4), 1208–1216. https://doi.org/10.1111/j.1469-8137.2012.04339.x

Yoshida, S., Kim, S., Wafula, E. K., Tanskanen, J., Kim, Y. M., Honaas, L., Yang, Z., Spallek, T., Conn, C. E., Ichihashi, Y., Cheong, K., Cui, S., Der, J. P., Gundlach, H., Jiao, Y., Hori, C., Ishida, J. K., Kasahara, H., Kiba, T., … Shirasu, K. (2019). Genome Sequence of *Striga* asiatica Provides Insight into the Evolution of Plant Parasitism. *Current Biology*, *29*(18), 3041-3052.e4. https://doi.org/10.1016/j.cub.2019.07.086

Zhang, Y.-C. C., Zou, Y.-N. N., Liu, L.-P. P., & Wu, Q.-S. S. (2019). Common mycorrhizal networks activate salicylic acid defense responses of trifoliate orange (Poncirus trifoliata). *Journal of Integrative Plant Biology*, *61*(10), 1099–1111. https://doi.org/10.1111/jipb.12743

Zhang, Y., van Dijk, A. D. J., Scaffidi, A., Flematti, G. R., Hofmann, M., Charnikhova, T., Verstappen, F., Hepworth, J., van der Krol, S., Leyser, O., Smith, S. M., Zwanenburg, B., Al-Babili, S., Ruyter-Spira, C., & Bouwmeester, H. J. (2014). Rice cytochrome P450 MAX1 homologs catalyze distinct steps in strigolactone biosynthesis. *Nature Chemical Biology*, *10*(12), 1028–1033. https://doi.org/10.1038/nchembio.1660

Zhao, J., Wang, T., Wang, M., Liu, Y., Yuan, S., Gao, Y., Yin, L., Sun, W., Peng, L., Zhang, W., Wan, J., & Li, X. (2014). DWARF3 participates in an SCF complex and associates with DWARF14 to suppress rice shoot branching. *Plant and Cell Physiology*, *55*(6), 1096–1109. https://doi.org/10.1093/pcp/pcu045

Zhao, Li Hua, Edward Zhou, X., Wu, Z. S., Yi, W., Xu, Y., Li, S., Xu, T. H., Liu, Y., Chen, R. Z., Kovach, A., Kang, Y., Hou, L., He, Y., Xie, C., Song, W., Zhong, D., Xu, Y., Wang, Y., … Eric Xu, H. (2013). Crystal structures of two phytohormone signal-transducing α/β hydrolases: Karrikin-signaling KAI2 and strigolactone-signaling DWARF14. *Cell Research* (Vol. 23, Issue 3, pp. 436–439). https://doi.org/10.1038/cr.2013.19

Zheng, J., Hong, K., Zeng, L., Wang, L., Kang, S., Qu, M., Dai, J., Zou, L., Zhu, L., Tang, Z., Meng, X., Wang, B., Hu, J., Zeng, D., Zhao, Y., Cui, P., Wang, Q., Qian, Q., Wang, Y., … Xiong, G. (2020). Karrikin signaling acts parallel to and additively with strigolactone signaling to regulate rice mesocotyl elongation in darkness. *The Plant Cell*, *32*(9), 2780–2805. https://doi.org/10.1105/tpc.20.00123

Zhou, F., Lin, Q., Zhu, L., Ren, Y., Zhou, K., Shabek, N., Wu, F., Mao, H., Dong, W., Gan, L., Ma, W., Gao, H., Chen, J., Yang, C., Wang, D., Tan, J., Zhang, X., Guo, X., Wang, J. J. J., … Wan, J. (2013). D14-SCF D3 -dependent degradation of D53 regulates strigolactone signalling. *Nature*, *504*(7480), 406–410. https://doi.org/10.1038/nature12878

Zou, J., Zhang, S., Zhang, W., Li, G., Chen, Z., Zhai, W., Zhao, X., Pan, X., Xie, Q., & Zhu, L. (2006). The rice HIGH-TILLERING DWARF1 encoding an ortholog of *Arabidopsis* MAX3 is required for negative regulation of the outgrowth of axillary buds. *Plant Journal*, *48*(5), 687–698. https://doi.org/10.1111/j.1365-313X.2006.02916.x

Zouine, M., Maza, E., Djari, A., Lauvernier, M., Frasse, P., Smouni, A., Pirrello, J., & Bouzayen, M. (2017). TomExpress, a unified tomato RNA-Seq platform for visualization of expression data, clustering and correlation networks. *The Plant Journal*, *92*(4), 727–735. https://doi.org/10.1111/tpj.13711

Zwanenburg, B., Mwakaboko, A. S., Reizelman, A., Anilkumar, G., & Sethumadhavan, D. (2009). Structure and function of natural and synthetic signalling molecules in parasitic weed germination. *Pest Management Science*, *65*(5), 478–491. https://doi.org/10.1002/ps.1706

ABSTRACT

The arbuscular mycorrhizal (AM) symbiosis associates the roots of most terrestrial plant species with soil fungi of the Glomeromycotina subphylum. While the fungus provides the plant with water and nutrients, the plant delivers carbon in the form of lipids and carbohydrates to the fungus. The initiation of AM symbiosis involves diffusible molecules secreted by both partners. Strigolactones (SLs) are carotenoid-derived compounds produced by plants and exuded into the soil. They are required at the early stages of symbiosis and trigger in AM fungi cellular, metabolic and developmental responses such as the stimulation of spore germination and hyphal branching. In addition to their bioactivity on AM fungi, SLs induce seed germination of parasitic weeds and act in plants as phytohormones.

The diverse natural SLs identified to date comprise a conserved methylbutenolide D-ring, linked to a more variable tricyclic lactone moiety. The mechanisms of SL perception are well documented in plants: they involve receptors belonging to the alpha/beta-hydrolase fold family of proteins, which have the particularity of cleaving SLs and forming a covalent bond with the D-ring. The main objective of my PhD was to better understand SL perception in AM fungi.

In a first part of my work, I focused on SL analogs bearing a modified D-ring. I tested their impact on the development of the AM fungus *Rhizophagus irregularis* grown *in vitro*, as well as their capacity to favor symbiosis initiation. A striking result was that an SL analog with an unmethylated D-ring could inhibit hyphal branching while enhancing the ability of *R. irregularis* to colonize host roots. This showed for the first time that initiation of AM symbiosis can be uncoupled from hyphal branching.

In the second part of my project, I aimed to gain insight into the nature of SL receptors in AM fungi. I observed that two chemical inhibitors known to target plant SL receptors also suppress responses of *R. irregularis* to SLs. This suggests that fungal SL receptors share structural similarities with those of plants. By using tridimensional modeling, we identified eight fungal alpha/beta-hydrolase fold proteins sharing structural similarities with a plant SL receptor. Phylogenetic analysis revealed an expansion in Glomeromycotina of genes encoding these and related proteins. *In vitro* characterization revealed that two of them were able to cleave synthetic SL analogs. Moreover, both inhibitors of plant SL receptors decreased this enzymatic activity. Taken together, these observations lend support to the hypothesis that like parasitic weeds and mosses, AM fungi evolved the capacity to perceive SLs with great sensitivity through expansion and neo-functionalization of alpha-beta hydrolase fold proteins.

A final objective was to investigate the transfer of phytohormones from one plant to another via common mycorrhizal networks. Experimental setups were designed and implemented, but biochemical analyses failed to provide conclusive evidence for such a transfer. Nevertheless, it remains important to bear in mind the contribution of these networks to plant-fungus and plant-plant interactions in natural environments. My whole PhD project also highlights that molecular signals such as SLs can be perceived, modified or transported by a number of living organisms, and thus can play complex roles in ecosystems beyond their classification as phytohormones.

Keywords : Arbuscular mycorrhiza; Strigolactone; Symbiosis; Receptor; *Rhizophagus*